ΠΑΝΕΠΙΣΤΗΜΙΟ ΚΡΗΤΗΣ

ΣΧΟΛΗ ΕΠΙΣΤΗΜΩΝ ΥΓΕΙΑΣ-ΤΜΗΜΑ ΙΑΤΡΙΚΗΣ

ΤΟΜΕΑΣ ΒΑΣΙΚΩΝ ΕΠΙΣΤΗΜΩΝ

ΕΡΓΑΣΤΗΡΙΟ ΜΟΡΙΑΚΗΣ ΚΑΙ ΚΥΤΤΑΡΙΚΗΣ ΒΙΟΛΟΓΙΑΣ

Διδακτορική διατριβή

"Ο ΡΟΛΟΣ ΤΗΣ MAP3 ΚΙΝΑΣΗΣ TPL2/COT ΣΕ ΚΥΤΤΑΡΙΚΕΣ ΑΠΟΚΡΙΣΕΙΣ ΠΟΥ ΑΦΟΡΟΥΝ ΣΕ ΦΛΕΓΜΟΝΕΣ ΚΑΙ ΒΛΑΒΗ ΤΟΥ DNA"

Δημήτρης Χ. Κανέλλης

Επιβλέπων καθηγητής: Α. Ηλιόπουλος

Ιούνιος 2014

UNIVERSITY OF CRETE

SCHOOL OF HEALTH SCIENCES-DEPARTMENT OF MEDICINE

DIVISION OF BASIC SCIENCES

LABORATORY OF MOLECULAR AND CELLULAR BIOLOGY

Ph.D. Thesis

"THE ROLE OF MAP3K TPL2/COT IN INFLAMMATORY AND INFLAMMATION-ASSOCIATED CANCER PATHWAYS OF THE CELL".

Dimitris C. Kanellis

Supervisor: Professor A. Eliopoulos

Submitted in fulfillment of the requirements for the PhD degree in the graduate program: "The Molecular Basis of Human Diseases"

June 2014

Στη "διευρυμένη" οικογένεια μου

Στον ανιψιό μου, Γιάννη

"αστειεύθητι μόνον ίσοις σου"

Βίων (ο Βορυσθενίτης)

ΕΥΧΑΡΙΣΤΙΕΣ

Θα ήθελα να ευχαριστήσω όλα τα μέλη της οικογένειάς μου για την υπομονή, την ηθική και υλική τους συμπαράσταση. Τις θερμότερες ευχές μου στέλνω επίσης σε όλους τους φίλους (ανεξαρτήτως γεωγραφικής τους θέσης) που με έκαναν να γελάσω όταν το είχα ανάγκη. Ιδιαίτερο ευχαριστώ οφείλω στα μέλη του εργαστηρίου που ανέχτηκαν τις ιδιαιτερότητες μου, συνεισέφεραν στη διεύρυνση των πνευματικών και μορφωτικών μου οριζόντων και ανέλαβαν συχνά καθήκοντα δεύτερης οικογένειας. Το ίδιο σημαντική και η αλληλεπίδρασή μου με μέλη άλλων εργαστηρίων και ακόμα ακόμα άλλων επιστημονικών πεδίων, τα οποία και ευχαριστώ ξεχωριστά. Αναμφίβολα, ο άνθρωπος που πίστεψε σε μένα και μου πρόσφερε μια θέση στην επιστημονική του ομάδα, ο καθηγητής Άρης Ηλιόπουλος, έδωσε το εναρκτήριο κίνητρο της διατριβής μου και καθοδήγησε έμμετρα όλη τη δουλειά μου μέχρι τέλους. Για την επιστημονική του εγκυρότητα, την οικονομική κάλυψη και την άρτια συνεργασία μας τον ευχαριστώ θερμά.

Εύχομαι σε όλους τους συναδέλφους να επιμείνουν στον επιστημονικό ρομαντισμό, τον ευγενή προβληματισμό και την αριστεία. Η επιτυχία είναι τότε σίγουρη.

Η οικονομική υποστήριξη της διατριβής μου προήλθε από 1) The EU 6th Framework Program Apotherapy 2) The EU 7th Framework Program INFLA-CARE 3) ΓΓΕΤ, πρόγραμμα Unistep Plus 4) Υποτροφίες Κληροδοτήματος «Μαρίας Μιχαήλ Μανασάκη», 5) The European Commission FP7-funded support grant TransPOT.

TABLE OF CONTENTS

ABSTRACT

Tpl2/Cot is a MAP3 kinase (MAP3K8) with a diverse role in signaling pathways governing immune and inflammatory responses as well as carcinogenesis. The present thesis explores the physical and functional interaction between TPL2 and Nucleophosmin (NPM, B23). TPL2 is shown for the first time to reside partially in the nucleoli of rested cells where it interacts with NPM and mediates its basal phosphorylation levels at Thr^{199}. Under genotoxic or ribosomal stress TPL2 guides the partial K48-linked ubiquitination of phosphorylated NPM at lysine Lys^{229}. Subsequently, the unaffected and probably homodimerized non-phosphorylated NPM translocates from the nucleoli to the nucleoplasm where it binds HDM2, the physiological inhibitor of p53. Released p53 unfolds its acting repertoire leading to apoptosis of stressed cells. In a feedback regulatory loop, stress-induced upregulated NPM blocks aberrant TPL2 production transcriptionally in order to preserve fine-tuning of the cell response to DNA damage stress.

In another context of experiments, TPL2 was found to mediate the production of the pro-inflammatory and cancer-related cytokine IL-6 downstream of TNFRI signaling. TPL2 associates with the NF-κB transcription factor family member IKKα in TNF-stimulated cells and regulates IKKα nuclear localization and IKKα-mediated IL-6 transcriptional activation. Furthermore, a microRNA microarray analysis in samples from primary BMDMs of wild type or TPL2 knock out mice treated with TNF revealed a unique molecular signature of de-regulated microRNA expression associated with aberrant expression of their mRNA targets. Specifically, microRNAs mmu-miR 223, mmu-let-7a and mmu-let-7i were found to target IL-6 3'-UTR *in silico* and are postulated to regulate post-transcriptionally IL-6 production following cell stimulation with TNF.

ΠΕΡΙΛΗΨΗ

Η πρωτεΐνη TPL2/Cot είναι μία MAP3 κινάση (MAP3K8) που συντονίζει την κυτταρική σηματοδότηση μονοπατιών σχετιζόμενων με ανοσολογικές αποκρίσεις, φλεγμονή και καρκινογένεση. Το κύριο μέρος της παρούσας διατριβής αφορά τη μελέτη της αλληλεπίδρασης της TPL2 με τη φωσφοπρωτεΐνη Nucleophosmin (NPM, B23). Αρχικά, αποδεικνύεται πειραματικά η μερική παρουσία της TPL2 στον πυρήνα αντίθετα με τη γενική πεποίθηση που υποστηρίζει την αμιγή κυτταροπλασματική της θέση. Έπειτα, παρατίθενται δεδομένα που αποδεικνύουν τη δυνατότητα αλληλεπίδρασης και υποκυτταρικού συνεντοπισμού της TPL2 με την NPM, τόσο σε τεχνητές (*in vitro*) όσο και σε φυσιολογικές συνθήκες (*in vivo*). Συγκεκριμένα, η TPL2 εντοπίζεται μερικώς στον πυρηνίσκο όπου και συνδέεται με την NPM και ελέγχει τα βασικά επίπεδα φωσφορυλίωσης της στη θρεονίνη Thr^{199}, γεγονός που εντάσσει τις MAP3K πρωτεΐνες στην πληθώρα κινασών που επηρεάζουν τη φυσιολογία της NPM μέσω φωσφορυλίωσης.

Υπό την επήρεια γενοτοξικού ή ριβοσωμικού στρες, η TPL2 κατευθύνει την K48-σχετιζόμενη ουβικουϊτίνωση της φωσφορυλιωμένης NPM στη λυσίνη Lys^{229} και την επακόλουθη αποικοδόμηση της στο πρωτεάσωμα αποδεικνύοντας τη δυναμική αλληλεξάρτηση των μετα-μετφραστικών τροποποιήσεων στην κυτταρική σηματοδότηση. Στη συνέχεια, η μη φωσφορυλιωμένη και πιθανά ομοδιμερής NPM εξέρχεται από τον πυρηνίσκο στο πυρηνόπλασμα και προσδένεται στη HDM2 αποδεσμεύοντας την από την p53, την οποία η HDM2 καταστέλλει κάτω από φυσιολογικές συνθήκες οδηγώντας την στο πρωτεάσωμα για αποικοδόμηση. Η ελεύθερη p53 μπορεί εν συνεχεία να ενεργοποιήσει το μεταγραφικό της πρόγραμμα με τελικό σκοπό την κυτταρική απόπτωση ανάλογα με το υφιστάμενο στρες. Μέσω ενός μηχανισμού ανάδρασης, η NPM, τα επίπεδα της οποίας αυξάνονται κάτω από κυτταρικό στρες, σταματά τη μεταγραφή της νεοσυντιθέμενης TPL2 αποτρέποντας πιθανά την υπέρμετρη ενεργοποίηση των σχετιζόμενων με το εν λόγω στρες σηματοδοτικών μονοπατιών.

Παράλληλα, παρουσιάζονται δεδομένα που υποστηρίζουν τη δράση της TPL2 στην παραγωγή της προ-φλεγμονώδους και καρκινογενούς κυτοκίνης IL-6 μέσω δύο οδών. Πιο αναλυτικά, η TPL2 αποδεικνύεται απαραίτητη για τη μεταγραφική ενεργοποίηση του γονιδίου της IL-6, από τον παράγοντα ΙΚΚα έπειτα από ερεθισμό των κυττάρων με τον αποπτοτική κυτοκίνη TNF. Η άμεση αλληλεπίδραση της TPL2 με την ΙΚΚα καθορίζει πιθανά μέσω μετα-μεταφραστικών τροποποιήσεων την επαγόμενη από TNF υποκυτταρική μετατόπιση της ΙΚΚα στον πυρήνα και την επακόλουθη πρόσδεσή της στον υποκινητή του γονιδίου της IL-6.

Ταυτόχρονα, η TPL2 βρέθηκε να ρυθμίζει τα επίπεδα του mRNA της IL-6 μέσω της ενεργοποίησης μιας σειράς μικρών RNA μορίων (miRNAs) που στοχεύουν το άκρο 3'-UTR του εν λόγω mRNA. Ανάλυση έκφρασης μορίων microRNA ευρείας κλίμακας (microarrays) σε πρωτογενή μακροφάγα κύτταρα ποντικών που φέρουν ή όχι το γονίδιο της TPL2 και έχουν ερεθιστεί με TNF έδειξε ότι η TPL2 επηρεάζει την έκφραση διαφόρων microRNAs, ενώ ειδικότερα τα microRNAs mmu-miR 223, mmu-let-7a και mmu-let-7i, που έχουν στόχο το 3'-UTR της IL-6, ελέγχονται από την TPL2 και πιθανά ρυθμίζουν τα επίπεδα της IL-6 σε μετα-μεταγραφικό επίπεδο.

Η παρούσα διατριβή υποστηρίζει το σημαντικό ρόλο που διαδραματίζει η κινάση TPL2 στη ρύθμιση του μικροπεριβάλλοντος μιας καρκινικής οντότητας και προσφέρει επιστημονικά δεδομένα για μελλοντική καταπολέμηση καρκινικών τύπων μέσω φαρμακολογικής αναστολής της TPL2.

INTRODUCTION

TPL2 signaling in inflammation and immune responses

TPL2/Cot (also known as MAP3K8) is a serine/threonine MAP3 kinase that mediates phosphorylation events in molecular pathways implicated in inflammation, immune responses and carcinogenesis[1]. Although it was primary identified as a proto-oncogene, the majority of the data up to date underline its prominent role in immunity and inflammation. Deprivation of elegant molecular tools up to the millennium drove many research groups to study the effects of exogenously expressed TPL2 in various biological systems. Under these conditions, TPL2 was found to activate MEK and ERK kinases in association with Ras and Raf [2,3], and was further implicated in regulation of MEK1 and SEK1 in support of a universal role in all known MAPK pathways [4,5]. TPL2 engagement in inflammatory and immune responses was based on initial findings underlying its role in the production of cytokine IL-12 [6] and TNFα expression in T cells [7] and its impact on NFAT and NF-κB transcriptional activity at the promoter of IL-2 [8,9]. TPL2 was further found to interact with the non-canonical NF-κB pathway components NIK and IKKα and was thus speculated to act as a signaling link between the two main NF-κB pathways, the canonical and non-canonical [10,11]. A common denominator of both branches was later proven to be ERK, since its activation through either CD40L or TNF required TPL2 [12]. A major breakthrough regarding NF-κB regulation by TPL2 was published by Professor S.Ley's group in 1999. Their results supported a physiological role of endogenous TPL2 in proteolysis and downstream activation of NF-κB1 in fibroblasts, HELA and T cells treated with the TLR4 agonist LPS or with the cytokine TNF [13]. The significance of these findings was thereto proven in other studies as well, leading to the general rule that TPL2 normally forms a stable complex with p105, which attenuates TPL2 activation. However, appropriate stimuli can provoke a phosphorylation-dependent interplay between TPL2, p105 and other regulatory molecules such as the ubiquitin ligase A20 leading to activation of TPL2, NF-κB and downstream signaling effector molecules (14-19).

Following the general trend of knocking out genes to study their function, Professor P.Tsichlis' colleagues generated the first TPL2 knock mice (KO)

providing thus a more sophisticated tool to study TPL2 function. In a paper published in 2000 the group showed that TPL2 KO mice were resistant to LPS/D-Galactosamine-induced endotoxin shock due to lower TNF production ascribing thus to TPL2 pro-inflammatory features [20]. However, this notion is up to date debatable since subsequent studies argued not only in favor but also against it, providing evidence that support an anti-inflammatory role for TPL2. For instance, whereas TPL2 is substantial for COX2 expression, an enzyme that catalyzes the synthesis of PGE2 in acute inflammatory syndrome [21,22], it also blocks pro-inflammatory IL-12 production in *Helicobacter Hepaticus*-challenged macrophages [23]. In the same line, TPL2 was found to mediate Crohn's-like IBD pathology in $Tnf^{\Delta ARE}$ mice [24] but also to induce IRAK-M expression and regulate adiponectin-mediated endotoxin tolerance [25]. Even more interestingly, TPL2 can drive a pro-inflammatory response with high IL-12 and low IL-10 production in macrophages challenged with bacterial DNA [26], while it blocks anti-inflammatory IL-10 production in the intestine attenuating thus inflammation-driven mucosal carcinogenesis in Apc^{min} mice [27]. Irrespective of its ambiguous role in inflammation, TPL2 posed an attractive kinase target for the treatment of various diseases throughout the years. In 2005 the Lin group at Wyeth Research Cooperation (MA, USA) discovered a new class of small molecules (carbonitriles) highly effective and specific for blocking TPL2 kinase activity [28]. The same group continued to optimize the formula of a chemical inhibitor for TPL2 and in 2007 they published an article showing the effectiveness of a newly synthesized compound in LPS- and IL-1β-induced ERK/MEK phosphorylation, TNF and IL-12 production and TNF-mediated IL-8 upregulation [29]. The interest towards blocking TPL2 activity led to the discovery of other compounds such as Luteolin, prominent to enter clinical studies as well [30,31].

TPL2 in cancer

TPL2/Cot was firstly discovered as a proto-oncogene coding for two isoforms (52 & 58 KDa) of a serine-threonine kinase [32–34] in a screening of a human thyroid carcinoma cell line for transforming genes [35]. TPL2 C terminus

truncation caused either by proviral DNA integration of MoMuLV [36,37] or MMTV [38] in the last intron of *TPL2* leads to the production of a highly stable and tumorigenic oncogene [39,40]. Although these data pointed out that TPL2 C terminus is essential for its activity, they could not support a global pro-carcinogenic role of TPL2, since its truncated form is not found in spontaneous or acquired cancers observed in the clinic [1]. In fact, opposing data up to date favour either a pro- or anti- carcinogenic role of TPL2 depending mostly in the context of the conducted experiments.

Pro-carcinogenic role of TPL2

TPL2 upregulation has been observed in hepatoma, osteosarcoma, gastric and colonic adenocarcinoma cell lines [33,41], human breast cancer speciments [42,43], EBV-associated malignancies [44] and LGL-PD human T cell neoplasias [45]. However, only one publication to date links *TPL2* mutations to lung cancer [46], whereas a study in diffuse large B lymphomas and myeloid leukemias gave negative feedback on the presence of *TPL2* mutations related to such malignancies [47]. The majority of the publications supporting a pro-carcinogenic role of TPL2 are based on experiments performed in the presence of exogenously expressed TPL2 or its combination with external signals. Thus, overexpressed TPL2 has been found to activate MAPK pathways (MEK/ERK, SAPK) and transcription factors (AP-1, Ets, cJun) related to cell transformation [3,5,48]. Furthermore, TPL2 promotes HTLV- and IL-2-mediated T cell proliferation [6,49], EGF-induced cell proliferation through dephosphorylation of p53 at Ser15 [50] and UVB-associated cell transformation acting *in cis* with H3 to upregulate c-Fos expression [51]. Epigenetic regulation of miR-370 induces TPL2 expression in IL-6-associated cholangiocarcinomas [52] and TPL2 upregulates COX2 levels in arsenite- and UVB-induced skin carcinoma mouse models [53,54]. Pancreatic Adenocarcinoma Upregulated Factor (PAUF) promotes cancer metastasis through the TLR-2/TPL2/MEK/ERK pathway [55], whereas TPL2-mediated ERK activation enhances ALCL $CD30^+$ cell proliferation [56] and tumor cell autonomous and non-autonomous cancer mechanisms in myeloma niches [57]. Kim *et al*. found that IL-17A, normally produced by $CD4^+$ memory T cells, promotes tumor

formation through TPL2-mediated upregulation of ERK, cJun, Stat3 and AP-1 [58].

Under a different perspective, TPL2 was implicated in mechanisms governing cell migration, a feature commonly associated to cancer metastasis. Rodriquez *et al*. found that TPL2 mediates cell migration, adhesion loss and cytoskeletal re-organization trough regulation of ERK1,2-mediated COX-2 production [59], while Professor Tsichlis and colleagues provided solid data supporting re-organization of actin through TPL2-mediated Rac-1 and FAK activation following GpCR stimulation of MEFs and BMDMs [60,61]. In many cases it is known that treatment of cancers with specific drugs turns ineffective after a short period due to the ability of cancer cells to by-pass the targeted pathways. In these cases cancer cells use redundant pathways in order to continue their flourish. To this end, overexpressed TPL2 was found to offer resistance to *cis*-platin treated SHOK cells [62], while its downregulation promotes cell death in cancers driven by KRAS mutations [63]. Moreover, cancer patients carrying BRAF mutations develop immunity against treatment with RAF/MEK inhibitors through activation of alternative signaling pathways related to TPL2 [64,65].

Anti-tumorigenic activity of TPL2.

On the contrary, accumulative data presented throughout the last years underline an anti-tumorigenic activity of TPL2. Tsatsanis *et al*. found that TPL2 cooperated with ERK and CTLA4 to induce a proliferation negative feedback loop in T cells and block the formation of T cell lymphomas [66] counteracting a previous report supporting a positive role of exogenously expressed TPL2 in IL-2-induced T cell proliferation through blocking of p27kip and upregulation of E2f expression [67]. The Wiest lab provided also data indicating that TPL2 can act as an anti-carcinogenic molecule. They found that TPL2 absence mediates production of pro-inflammatory cytokines and tumor infiltration of mast cells and neutrophils which both promote a two stage skin carcinogenesis mouse model [68]. Furthermore, they showed that TPL2 alleviated prostaglandin and prostaglandin receptor expression through COX-2 regulation in TPA-induced transformation of keratinocytes and skin cancer

in mouse models [69]. Delicate work published by Koliaraki *et al*. in 2012 showed that TPL2 ablation promotes cancer formation in a Colitis Associated Colon Cancer (CAC) mouse model through its activity on intestinal myofibroblasts (IMFs) and not in myeloid or intestinal epithelial cells. Focusing at the molecular lever, the team showed that TPL2 suppresses the secretion of HGF and subsequent c-Met expression from IMFs [70]. In another study, it was shown that TPL2 ablation in *Apc^{min}* background mice caused intestinal inflammation and tumorigenesis driven partially from the hematopoietic cell lineage. Down regulation of the anti-inflammatory cytokine IL-10 and limitation in the production of iTregs and Tr-1 cells were found to promote the observed phenotype [27]. Recently, our lab has published work supporting that TPL2 suppresses lung carcinogenesis. More specifically, low TPL2 expression levels due to various genetic and epigenetic mechanisms as seen in human specimens of lung cancer and in a urethane-induced lung carcinogenesis mouse model were associated with defective JNK-NPM-p53 pathway activation providing a possible molecular mechanism of lung cancer progression [71].

NPM

Discovery and general features

B23 (alternative name for NPM) was initially discovered in 1974 in B.Harris' lab during a nucleolar proteomic analysis in cells isolated from Novikoff hepatoma ascites [72]. More than a decade later, the cDNA of rat and human B23 (NPM) was isolated and cloned providing the base for the analysis of the newly identified protein [73–75]. Early studies pointed out that B23 could form highly stable oligomers and possessed the ability to bind nucleic acids [76]. At the beginning of the millennium Hinorani *et al*. managed to define the diverse and important structural features and functions of B23 [77] but it was until 2005 that the first NPM knock-out (KO) mice were produced and it became clear that NPM was vital for cell survival since NPM KO mice died *in utero* [78,79]. Accumulative data [reviewed in [80]] give us today a detailed description of this protein. NPM (Nucleophosmin) is a 37 KDa phosphoprotein with three up to

date known different isoforms [81,82]. Its amino acid sequence translates into a specifically complex structure that is characterized mainly by three major regions: a N terminus bearing a homo-oligomerization domain and a nuclear export signal, a central acidic domain with nuclear localization signals, able to bind core histone proteins and a C terminus tail containing a nucleolar localization signal, RNA binding and hetero-dimerization domains [83]. This elaborate structure renders NPM capable of oligomerization and nucleolar-nuclear-cytoplasmic trafficking and ascribes for a variety of NPM-mediated vital cellular functions.

NPM regulation

Tight regulation of a pleiotropic protein such as NPM requires multi-orientated coordination. At the transcriptional level *Npm* was shown to be regulated by YY1 and AP2a [84,85], while serum-activated Myc binds to NPM promoter to upregulate its expression [86] a fact that is enhanced by Ras activity in malignant bladder cancer cells [87]. Post-translationally, NPM undergoes various modifications that define its activity and turn-over. Although phosphorylation of NPM was early discovered [88] and NPM phosphorylation status was found dynamic in a space and type manner during cell cycle [89] (discussed later in detail) there is only one article up to date that associates NPM phosphorylation to its stability. CDK2 prevents NPM degradation in androgen receptor induced apoptosis of prostatic cells through NPM phosphorylation [90] . However, CDK2 suppresses BRCA1/BARD1 Ubiquitin ligase activity on NPM [91] which was initially shown to promote NPM stability during mitosis through K6-linked poly-ubiquitination [92]. More conflicting data came from studies on the interaction of NPM with the tumor suppressor Arf. The latter was initially found to block NPM ribonuclease activity by promoting NPM poly-ubiquitination and 26S proteasomal degradation [93]. Arf however, induces also Lys^{263} NPM SUMOylation which protects NPM from apoptotic degradation, enhances its binding to Rb and stimulates E2F1-mediated transactivation [94,95]. In the same line of evidence, SUMOylation of NPM at Lys^{263} by nuclear Akt2 promoted NPM stability and NPM- mediated cell cycle progression and survival [96]. Enhanced NPM stability through K48-linked ubiquitination blocking was also induced by EDAG and estrogen in leukemia

and endometrial cancer cells respectively pointing out in both cases the carcinogenic facet of NPM [97,98]. Likewise, Granzyme M produced by Natural Killer cells promoted cancer cell death through NPM cleavage and deregulation [99]. Moreover, dephosphorylation of NPM at $Thr^{199/234/237}$ by PP1β was found to promote NPM binding to Rb and release of E2f1 which subsequently engaged promoters of DNA repair genes and switched them on [100]. A post-transcriptional mechanism of NPM regulation was also proposed by Olanich *et al*.. The group showed that mTOR signaling induced FBP1 binding to NPM 3' UTR leading to NPM translational repression and cell proliferation blocking [101]. The oligomerization capacity of NPM is also associated with its regulation. The ratio of oligomer/monomer NPM was suspected to define NPM preference in binding RNA versus DNA [102], while oligomerization blockage with RNA aptamers led to NPM nucleoplasmic translocation and Arf/p53-induced apoptosis [103]. Cys^{21} was found to be an important residue that supports NPM oligomerization and chaperone activity [104], while the cytoplasmic pool of GTP and ATP is essential for proper NPM nucleolar localization [105–107].

NPM functions

Ribosynthesis

One major function of NPM and the first to be discovered relates the protein to pre-ribosomal particle transportation and ribosome biogenesis. Treatment of cells with antibiotics like Actinomycin D (ActD) and lyzopeptines halts ribosome synthesis while at the same time drives NPM relocalization from nucleoli to nucleoplasm [108,109]. This fact combined with the observation that pre-ribosomal particles reside mainly in nucleoli [110] (where most of NPM is normally located) and the fact that NPM can bind nucleic acids (preferably RNA) [111] raised the general suspicion that NPM was somehow related to rRNA maturation and ribosome synthesis. To this end Herrera *et al*. found that NPM possesses an intrinsic ribonuclease activity that supported its role in rRNA splicing and maturation [112]. More specifically, NPM mediates rRNA splicing between 28s and 18s and can chaperone ribosomal proteins to

translocate between cytoplasm and nucleus in order to complete rRNA maturation [113–115]. NPM binding to rRNA and ribo-nucleoprotein complexes (RNPs) is a dynamic event that can be altered during cell cycle progression mainly through phosphorylation events driven by CDK-cyclin complexes [116,117]. NPM was additionally found to regulate rRNA gene transcription epigenetically through chromatin remodeling of rDNA genomic region [118,119], while it can also mediate rRNA processing indirectly by antagonizing other endonucleases such as APE-1 for rRNA binding [120].

NPM acting as a transcription factor

The ability of NPM to bind nucleic acids is not limited to RNA and multiple lines of evidence support a role of this protein in DNA modulation and transcription regulation. NPM was found to repress transcriptional activity of YY1 and IRF1 [121,122] but also to enhance DNA polα activity either directly or through pRb [123]. Moreover, NPM can bind histones through the acidic central domain and participates in nucleosome assembly and chromatin decondensation events [124]. In this context, NPM blocks AP2a transcription in retinoic acid treated cells through chromatin structure repression and histone deacetylation [85] but at the same time acetylated NPM upregulates transcription of genes, implicated in oral carcinoma development such as TNF [125]. NPM enhances androgen receptor (AR) binding to promoters of genes related to prostate cancers and upregulates MnSOD transcription acting *in cis* with NF-κB p50/p65 [126] but at the same time it inhibits GCN5-mediated free histone and nucleosomal acetylation and transactivation [127]. From the data mentioned here it becomes clear that NPM can act both as a positive and negative regulator of transcription.

Chaperone activities

Closely related to NPM ability to affect rRNA processing is its intrinsic capacity to chaperone other proteins throughout different sub-cellular compartments. Szebeni & Olson found that NPM can bind and protect heat-shock denatured protein aggregates, while simultaneously it mediates their renaturation and activity preservation [128]. It was thus proposed that NPM could facilitate rRNA processing through RNP trafficking which is also

supported by a study showing that NPM promotes nucleolar localization of RPS9 [129]. Furthermore, NPM offers chaperone support in un-naturally occurring proteins in a cell like viral HIV Tat and Rev which were found to interact with NPM [130,131]. A possible mechanism proposed later by the same group identified CK2 as the primary kinase, which mediates subsequent association-dissociation events with NPM substrates [132]. Other essential outcomes of NPM chaperone activities were recently published underlying NPM-mediated USP36 nucleolar localization which can affect global nucleolar ubiquitination events [133], NPM-mediated SENP3 and SENP5 nucleolar accumulation important for ribosome biogenesis [134] and NPM-driven Arf nucleolar localization which is pivotal for stress-induced cellular responses (mentioned later in detail).

NPM shuttling capacity

NPM functions mentioned up to this point rely on its ability to shuttle between nucleolar/nuclear and cytoplasmic compartments of the cell. Early observations underlined NPM localization mainly in the nucleoli [135], further supported by the fact that this protein contains a Nucleolar Localization Signal (NuLoS) defined mainly by the presence of two tryptophans (W286, W288) at the C terminus of the protein [136]. More interestingly, mutations in these tryptophans and their interplay with intrinsic and mutation-gained Nuclear Export Signals (NES) was proved to be important for the mislocalization of this protein reported in many cases of Acute Myeloid Leukemias (AMLs) [137]. Apart from its pivotal role in rRNA biosynthesis, translocation of NPM from nucleoli to nucleoplasm was found to be a global outcome in cells under stress provoked either by anti-cancer drug treatment (i.e. ActD, DOX) or serum starvation [108,138,139], while a small portion of NPM was also found in the cytoplasm [140]. Genotoxic stress induced by UVC irradiation was also shown to mediate NPM translocation to the nucleoplasm. UVC upregulates c-jun expression and concomitant c-jun-NPM interaction driving both proteins out of the nucleoli to the nucleoplasmic compartment with various effects on rRNA processing and cell proliferation [141]. NPM translocation from nucleus to cytoplasm was also enhanced in aspirin-treated cells. This stimulus causes RelA translocation to the nucleolus accompanied by NPM relocalization to the

cytoplasm where it binds BAX and induces apoptosis [142]. In the same context, LPS stimulation of macrophages was shown to mediate NPM exodus from nucleus to the cytoplasm and NPM-mediated upregulation of inflammatory cytokines, enlisting thus NPM in the family of "alarmins" [143]. NPM shuttling was correlated to its oligomer-monomer ratio and was found higher during G1 and G1/S phases of cell cycle [144]. More specifically, a thorough analysis of NPM localization during liver regeneration showed a continuous movement of the protein from nucleoli to nucleoplasm, cytoplasm, mitotic spindles and finally mitotic chromatin supporting a role of NPM also in cell cycle progression discussed herein in detail [145].

Cell cycle regulation-Genome integrity maintenance

One major function of NPM, commonly related to its implication in pathological situations, is maintenance of genomic stability. NPM gets phosphorylated by various kinases throughout cell cycle progression and the phosphorylation status of NPM is essential for normal cell cycle progression. NPM phosphorylation at Thr^{199} by CDK2/cyclin E relates to NPM dissociation from centrosomes and proper centrosome duplication [146]. CDK2/cyclin A-mediated NPM phosphorylation is detected during S to G2 transition, while CDK1/cyclin B phosphorylates NPM at $Thr^{234/237}$ during mitosis [147,148]. PLK2 phosphorylates NPM at Ser^{4} during S phase [149] and PLK1/NEK2A-mediated NPM phosphorylation promotes its residence in duplicated centrioles during G2/M transition and mitosis [150,151]. Moreover, phosphorylation of NPM at Thr^{95} is essential for NPM nuclear export via Ran-Crm1 complex and re-distribution to the centrosomes in G1 [152] . KSHV cyclin was found to associate with cellular CDK6 and the complex promoted NPM phosphorylation at Thr^{199} resulting in viral latency and induction of p53-mediated apoptosis to avoid formation of supernumerary centrosomes often leading to genomic instability and cancer [153,154].

NPM regulates tumor suppressors

NPM is also known to interact with various tumor suppressors or oncogenes and to regulate their turnover and activity. The most well studied partner of NPM among them is p14/Arf. Their interaction [155] affects Arf stability through

abrogation of ULF-mediated Arf ubiquitination [79,156,157]. Moreover, NPM competes Arf for HDM2 binding and inhibits thus Arf-depended p53 activation [158]. At the same time, Arf promotes NPM ubiquitination and degradation and blocks NPM nucleoplasmic localization and association with HDM2 [93,159]. NPM can further affect p53 activation either by competing HDM2 for p53 binding or by direct association with p53 [160,161]. P53 stability, transcription activity and mitochondrial relocalization were shown to be affected by NPM protein expression levels [162,163] and even more interestingly, NPM was shown to set a threshold on p53 activation following DNA damage responses [164]. Xiao *et al*. showed that NPM overexpression promotes p21 ubiquitination and degradation [165] and in another set of experiments it was shown that NPM regulates cMyc nucleolar localization and cMyc-mediated rDNA transcription and subsequent cell proliferation and transformation [166,167]. Furthermore, NPM was shown to promote KRAS membrane localization and KRAS-mediated MAPK activation in baby hamster kidney (BHK) cells [168].

NPM in cellular stress responses

Early studies on NPM indicated that it participates in cellular responses induced under various types of stress. Cytotoxic drugs such as Actinomycin D alter NPM subcellular localization [169], a fact that was correlated to cell survival [170]. Moreover, it was shown that NPM regulates global gene expression, chromatin structure and rDNA transcription in the presence of cytotoxic agents such as Taxol [171]. Treatment of cells with the pro-apoptotic ligand TNF alters NPM oligomer/monomer ratio, while the bacterial endotoxin LPS can cause NPM cytoplasmic relocalization and NPM-mediated production of pro-inflammatory cytokines [143,172]. Retinoic Acid-induced cellular differentiation in leukemic cells decreases NPM mRNA levels, while immortalization of serum deprived Ras-transformed cells was attributed to high NPM stability observed under the circumstances [173,174]. NPM is also shown to mediate radiation-induced DNA damage responses. Following UVC irradiation, NPM mRNA levels are rapidly upregulated promoting thus cell resistance to UVC-induced growth inhibition [175,176]. Moreover, NPM translocates from the nucleus to the nucleoplasm after UVC, a fact that is at least partially mediated by the proteasome activity [177,178]. UVC induces NPM-Chk1 interaction and Chk1-

mediated NPM recruitment to chromatin [179]. NPM2, a C terminus truncated NPM isoform, was found to offer apoptosis resistance to IR-treated cells and NPM phosphorylated at Thr[199] was found to be recruited through RNF8 and RNF168 ubiquitin conjugates in DNA damage nuclear foci after IR irirradiation [180,181]. Furthermore, NPM was found to act as an apoptosis evading protein in UVB-induced hermetic response of hepatoma cells [182].

NPM in disease progression and cancer development.

The importance of NPM function in maintaining cellular homeostasis is underlined by the fact that its deregulation correlates to various diseases with cancer being the most prominent. NPM shows aberrant expression in melanomas, colorectal adenocarcinomas, hepatocellular, ovarian, prostate, lung and breast epithelial adenocarcinomas [80] but it was poorly proven whether this fact associated directly with cancer formation or was a consequence of tumorigenesis. On the contrary, accumulative data on the function of NPM mutants revealed their unique role mainly in the establishment of hematopoietic malignancies. Balanced chromosomal translocations between the gene of NPM and those of ALK, RAR and MLF1 produce chimeric protein products with adopted functions correlated to the development of ALCL, APL and MDS/AML respectively [183–185]. Moreover, NPM carrying deletions or C terminus point mutations (designated as NPM c+) loses its nuclear-nucleolar localization signals and is subsequently detected mainly in the cytoplasm of AML patients. Permanent translocation of NPM to the cytoplasm inhibits its physiological functions that take place mainly in the nucleus as described before and causes malignant transformation of the cells carrying the mutant gene [186]. The clinical significance of NPM is further underlined by the fact that NPM serves as molecular diagnostic marker in ALCLs and AMLs where presence of NPM mutants determines prognosis and treatment of patients [187].

IKKα

The NF-κB signaling system

Nuclear Factor-κB (NF-κB) is a transcription factor implicated in a broad range of biological processes such as cell survival, immune responses, organogenesis and cell maturation. Its proper regulation is thus pivotal for cell homeostasis and is achieved through a complex signaling system that is generally known as the NF-κB pathway. The NF-κB family consists of five members [188] that act as the ultimate effectors in a signaling cascade starting with a proper external stimulus in the cell membrane. The signal is subsequently mediated via IKK complexes to IκBα and finally to NF-κB precursors through various post-translational modifications. Precursor processing leads to the formation of mature NF-κB moieties that can potentially form fifteen homo- and heteroduplexes capable of translocating to the nucleus. There they bind to responsive κB promoter sites of various genes that regulate inflammatory, developmental and survival processes. The NF-κB pathway splits into two branches: the canonical, mainly known to orchestrate immunological and inflammatory responses and the non-canonical, which mediates developmental events. Despite the fact that these branches have separated roles, accumulative data during the last years support their cross-talk under various conditions [189].

IKKα and the NF-κB canonical pathway

By the end of the previous century IκBα was already known to associate with NF-κB complexes and block their activation. Upon its self activation from unknown till then factors it would get degraded releasing at the same time NF-κB which could then perform its determined role [190]. In search of the IκBα activator three groups discovered almost simultaneously a new protein kinase named IKKα which was formerly identified as CHUK. IKKα could form a complex with IKKβ (the "IKK complex" that was later enriched with the IKKγ-NEMO protein) and mediate IL-1 and TNFα-induced NF-κB activation through direct phosphorylation of IκBα at serines Ser^{32} and Ser^{36} and IκBβ at Ser^{19} and Ser^{23}. Moreover, IKKα can associate with other known NF-κB activation mediators such as NIK and TRAF2 [191–195]. Phosphorylation of IKKα at Ser^{176}

by NIK was shown to be essential for its association with MEKK1, TPL2 or HTLV-1 protein Tax during NF-κB activation [11,196–198] . The crosstalk between the IKKα/IKKβ comlex, RIP and TRAF2 was also shown to be pivotal for proper NF-κB induction downstream of TNF through TNFRI receptor and both IKKα and IKKβ-mediated NF-κB activation was essential for HSV-1 replication [199]. Furthermore, TNF-induced TRAF2 phosphorylation by PKC and its subsequent K63-linked ubiquitination were shown to be pivotal for recruitment of both IKKα and IKKβ to the TNFRI receptor and their concomitant activation [74]. IKKα-mediated NF-κB pathway activation and IL-6 production after TNF treatment was blocked by Metformin through PI3K-dependent phosphorylation of AMPK [200]. IKKα was also found to mediate Her2+ breast cancer cell invasion through activation of several cytokines and chemokines regulated by NF-κB [201]. Activation of the canonical NF-κB pathway in TCR-stimulated T cells involves phosphorylation of both IKKα and IKKβ by ADAP [202].

Despite its initial implication in the activation of the canonical NF-κB pathway, IKKα was later assumed redundant to this matter inasmuch as ablation of *IKKα* and IKKα phosphorylation-incompetent mutants would not affect proper NF-κB activation downstream of inflammatory signals [203–205]. Nonetheless, its principal role in the IKK complex was soon to be discovered. Structural differences between IKKα and IKKβ accounted for different catalytic potential and whereas IKKα itself is less potent to promote NF-κB activation than IKKβ, it is however essential for IKKβ phosphorylation and subsequent activation itself. Their interplay was shown to be unidirectional since IKKβ is not able to affect reciprocally IKKα [10,206,207]. Activation of the classical NF-κB pathway though phosphorylation of IκBα would however be achieved even in an *IKKβ-/-* background leading to the conclusion that IKKα and IKKβ show functional redundancy [208].

The controversial role of IKKα in regulation of the NF-κB pathway was furthermore pinpointed in two complementary publications. IKKα (and IKKβ) interacts with ABIN-2 and stabilize it by blocking its K48-linked ubiquitination and proteasomal degradation. Moreover, IKKα phosphorylates ABIN-2 at Ser^{42} and Ser^{146} and causes its activation while through a positive feedback loop, activated ABIN-2 promotes IKKα auto-phosphorylation and IKKα-

mediated NF-κB activation [209]. On the contrary, TNFα and IL-1 stimulation of MEFs causes IKKα-mediated TAX1BP1 phosphorylation at Ser^{593} and Ser^{624}. This event promotes formation of the A20 ubiquitin complex, its recruitment to TRAF2 and TRAF6 and their subsequent degradation that ceases NF-κB activation. As a result, HTLV-1 protein Tax that blocks TAX1BP1 phosphorylation induces constitutive NF-κB signaling [210]. Tax however, induces also a senescence checkpoint in HTLV-1-transduced cells [211] and this is happening through IKKα activation by NIK following interaction of Tax with NEMO. This signaling cascade is supplemented by simultenuous activation of IKKβ by TAK1 showing that Tax-mediated signaling is obscure in the means of canonical or non-canonical NF-κB activation [212].

IKKα role in NF-κB non-canonical pathway

The production of IKKα knock out mice by the late 90's promoted our knowledge regarding its role in organonesis and development of organisms. Loss of *IKKα* correlated with massive skin and skeletal abnormalities, a phenotype that quite surprisingly was not solely ascribed to deregulated NF-κB activation [204,205,213]. This paradox was soon after started to get resolved since IKKα was found to be a major component of a second NF-κB pathway established as "alternative" thereafter. IKKα was initially found to mediate NIK-induced NF-κB2 processing and participated in B cell maturation and secondary lymphoid organ formation [214]. B cell linage commitment was however later shown to be regulated by IKKα via combined canonical and non-canonical NF-κB-mediated regulation of Pax5, a transcription factor known to promote expression of genes that control B cell differentiation [215]. NIK phosphorylates directly IKKα at Ser^{176} [196], while in a negative feedback loop IKKα phosphorylates NIK at $Ser^{809,812,815}$ and destabilizes it, irrespectively of TARF-cIAP activity on NIK, blocking in this way aberrant activation of the alternative NF-κB pathway [216]. In support of a novel role for IKKα, it was shown that it could drive RelB:p52 but not RelA:p50 dimers to specific κB promoter sites of genes implicated in distinct organogenesis processes [217]. Production of RelB:p52 dimers was attributed to IKKα function on p100 processing and the whole process was fine-tuned by Akt [218,219]. Exacerbated IKKα activation was correlated to chondrocyte differentiation and

hypertrophy [220] and in line with this, downregulation of miRNAs 223, 15α and 16 during differentiation of monocytes to macrophages was shown to drive IKKα upregulation and subsequent activation of the alternative NF-κB pathway leading to repression of macrophage hyperactivation and priming to pro-inflammatory stimuli [221].

IKKα regulation and NF-κB irrelevant IKKα activities

Accumulative data over the last years underlined a more universal role of IKKα in refining important biological processes often not related to what was already known as canonical or non-canonical NF-κB pathway and usually based to its intrinsic transcriptional activity. This rationale was initially supported by the fact that IKKα could translocate to the nucleus itself making somehow redundant the need to activate the NF-κB pathway that leads to nuclear accumulation of the NF-κB family transcription factors [222]. TNF-mediated nuclear accumulation of IKKα was shown to affect phosphorylation and acetylation of histone H3 and concomitant transcription of cytokines IL-6 and IL-8 [223,224]. IKKα-driven H3 phosphorylation was NIK-mediated [225] and NIK was further implicated in TLR7/9-driven IKKα phosphorylation and subsequent IRF3/7 activation and IFNα production. Interestingly enough, NIK mediates phosphorylation of IKKα both at Ser^{176} and Ser^{180} showing a positive or negative effect on IRF3/7 activation respectively a fact that underlines the complexity and accuracy of IKKα tight regulation [226].

Nuclear IKKα was also found to affect CBP/p300-mediated iNOS production in Lovastatin-treated cells and to enhance IκBα release from *Hes-1* promoter leading to subsequent Hes-1 upregulation in TNFα-treated cells [227,228]. Production of MMP-9 in LPS-treated cells was shown to be regulated by IKKα, which in association with Akt affects p65-mediated *MMP-9* transcription [229]. Helicobacter pylori infection-associated IKKα nuclear accumulation was correlated to aberrant chemokine production from gastric epithelial cells predisposing to gastric inflammation and cancer [230]. IKKα function was also related to human hematopoietic malignance in an NF-κB-irrelevant cIAP-mediated fashion downstream of oncogenic tyrosine kinase activation [231].

NF-κB irrelevant IKKα functions were also related to cancer biology. Of paramount importance is the association of IKKα with cell cycle progression and cell proliferation. To this end, it was shown that IKKα positively regulates PI3K-mediated and β-catenin/Tcf-associated transcription of cyclin D1 [232], while its direct interaction with cyclin D1 regulates the latter's turnover and subcellular localization [233]. In the same principal, IKKα associates with *cyclin D* and *c-myc* promoters in a complex with ERα and AIB1/SRC-3[234]. IKKα-mediated transition of cells from G1 to S phase was also achieved through transcriptional regulation of p27Kip1 by Skp2 [235]. Implication of IKKα in cell cycle progression was not limited to S phase since it was found that it also regulates cyclin B1 and PLK1 levels and phosphorylation of Aurora A in centrosomes during mitosis [236]. Moreover, *IKKα* loss caused G2/M arrest fail due to Suv39h1-mediated 14-3-3σ hypermethylation and subsequent downregulation [237].

The importance of IKKα in epidermal development was high-lightened by the fact that its loss or mutation-related inactivation drove squamous cell carcinomas in humans and relative chemical-induced cancer models [238–240]. In a molecular level, IKKα abrogates keratinocyte and epidermal differentiation though TGFβ/Smad2-3-mediated transcription of cell proliferation inhibitors such as Mad-1 in a Smad-4-independent manner. Transcriptional regulation of IKKα by p63 was underlined as important for normal keratinocyte differentiation and loss of IKKα was correlated to human ectodermal dysplasias [241]. Moreover, patients with ectodermal dysplacia with immune deficiency (EDI) show low IL-12 levels due to reduced phosphorylation of histone H3 by IKKα and concomitant recruitment of RelA and cRel on *IL-12* promoter [242].

IKKα gets transcriptionally upregulated via TNF-induced USP11 activation and this fact leads to enhanced stability and activation of p53. At the same time however, IKKα phosphorylates CBP at Ser^{1382} and Ser^{1386} and increases its transcriptional activity on *NF-κB* but not *p53* promoter responsive elements favoring in this way cell proliferation versus senescence or apoptosis. In line with this, tumor infiltrating cells expressing RANKL promote IKKα nuclear translocation and subsequent repression of Maspin, a known anti-metastatic

factor [243–246]. Moreover, enhanced survival of Caski cervical carcinoma cells was attributed to the interaction of IKKα with Notch1 and subsequent IKKα-mediated upregulation of survival genes [247]. In fact, IKKα was recruited to ERα target genes through Notch 1 promoting ER-mediated survival of ER+ breast cancer cells [248]. Liu *et al*. found that IKKα phosphorylates FOXA2 at $Ser^{107,11}$ downstream of TNF treatment. FOXA1 was subsequently repressed causing simultaneously reduction of NUMB, a negative regulator of Notch-1 signaling and the concomitant hyperactivation of Notch-1 was correlated to formation of hepatocellular carcinomas [249].

IKKα expression however, was not related to the progression of human colorectal cancer implicating IKKα activity in early stages of cancer formation [250]. On the contrary, high IKKα expression promoted liver cancer formation through metastatic and pro-survival mechanisms [251] and inhibition of IKKα repressed prostate cancer invasion and metastasis [252]. IKKα was also found to protect from UVB-induced skin carcinogenesis and a possible mechanism is based on IKKα-mediated cyclin D1 down-regulation and G0/G1 arrest [253,254]. Pancreas-specific IKKα ablation promotes NF-κB-irrelevant spontaneous pancreatitis in mice that is caused by deregulation of autophagy in acinar cells. More specifically, IKKα was shown to control cell homeostasis through its interaction with autophagy-related ATG16L2 and accumulation of p62-associated substrates [255].

IKKα function was further related to inflammatory and inflammation-associated carcinogenesis mechanisms. IKKα is pivotal for terminal differentiation of keratinocytes and skin inflammation control though induction of Myc antagonists Nod-1 and ovo-like 1 and simultaneous suppression of EGFR, ERK, cJun and Stat-3 signaling and growth factor production [256,257]. Furthermore, IKKα promotes SUMOylation-depended phosphorylation of PIAS at Ser^{90} driving its binding to inflammatory gene promoters and their subsequent repression. Moreover, HCV activates IKKα through DDX3X and drives its nuclear accumulation and IKKα-promoted CBP/p300-mediated transcription of SREBPs which orchestrate lipogenesis and viral assembly. Thus, the virus takes advantage of host NF-κB-unrelated IKKα activity to achieve its cycle and infection [258]. In another context, IKKα kinase dead knock

in mice show an IKKα^{low}K5^{+}p63^{hi}trim29^{hi} phenotype and develop inflammation-associated spontaneous lung squamous cell cancer (SCC) underlying a novel NF-κB-unrelated role in inflammation-mediated carcinogenesis [259].

MiRNAs

Discovery and function

At 1993 the Ambros Lab at Harvard University discovered a small RNA transcript called *lin-4* that was essential for the normal development of the nematode *C.elegans.* Its size was calculated between 20-60 nucleotides (nt) and it was not translated into a protein but would rather bind the 3'-UTR of LIN-14 mRNA in a sense-antisense way and repressed its translation [260]. The first microRNA (named after its short size) had been discovered but it was until the beginning of the next century that the presence of these newly identified molecules was generally established. While studying the heterochronic gene pathway of development in *C.elegans,* Gary Ruvkun (Harvard Medical School) and his colleagues recapitulated the data on lin-4 and discovered a second short RNA transcript named let-7 that was capable of regulating a series of genes implicated in growth not only of the nematode but of various animal species as well in a conserved way [261,262].

MiRNA production and processing

MiRNAs are endogenous non-coding RNAs composed of 19-25 nt. Their genes are transcribed by Pol II into pri-miRNAs that consist of 60-100 nt and fold into stem-loop structures [263,264]. Pri-miRNAs are cleaved in the nucleus by a nuclear RNAse III named Drosha which acts in a complex with DGCR8 [265]. The products which are thereafter called pre-miRNAs, bear 2-nt overhangs at their 3' ends and exert the nucleus through the exportin/5-RanGTP complex [266,267]. In the cytoplasm GTP is hydrolysed and pre-miRNAs are processed by Dicer, a second RNAse III enzyme into mature ~22 nt miRNAS [268]. MiRNAs are then assembled into ribonucleoprotein (RNP) complexes called miRNA-induced silencing complexes (miRISCs). The key

components of miRNPs are proteins of the Argonaute (AGO) family. AGO proteins may regulate both miRNA and small interfering RNA (RNAi) pathways and it was found that in mammals, four AGO proteins (AGO1 to AGO4) function in the miRNA repression machinery [269]. One of the two miRNA strands is chosen based on thermodynamic properties and is driven to its complementary mRNA target. Full complementarity leads to RNAi and mRNA slicing whereas imperfect matching between miRNA and mRNA causes translational repression [270–272]. miRNAs bind to the mRNA 3'-UTR region and since no perfect complementarity is usually required, it was initially speculated and later proved that one miRNA can regulate the translation of many mRNAs [273,274]. Apart from this canonical miRNA biogenesis pathway, new alternative pathways have been discovered over the last years. Short hairpin introns produced by mRNA splicing give rise to miRNAs known as miRtrons that bypass the Drosha-mediated step during their maturation [275]. MiRNAs can be produced also from Box H/ACA- and Box C/D snoRNAs, tRNAs and endogenous shRNA and siRNA pathways while their production may also be Dicer-independent [276]. The diversity of miRNAs is further enhanced post-transcriptionally through adenosine to inosine (A-to-I) RNA editing [277].

MiRNA organization, expression and activity

Proximal miRNAs can be clustered and co-expressed as polycistronic units and intronic miRNAs are generally co-expressed with their host genes [278–280]. When intronic miRNAs are antisense to the apparent host gene, they appear to originate from ill-characterized antisense transcription units. MiRNA precursors can also reside in exons in sense orientation or even in 3'-UTRs of mRNAs and they can behave as mRNAs themselves [263,281,282]. Expression and regulation of miRNAs shows tissue specificity in vertebrates, while intriguingly enough miRNAs and their target mRNAs do not always show the same spatial expression patterns [283–285]. Moreover, exogenous expression of miRNAs, localized primarily in specific tissues, can shift their target mRNA expression profile towards specific tissue differentiation [286]. Equally important,

miRNAs are often found in genomic regions prone to changes related to cancer development [287].

The primary role of miRNAs is mRNA translation inhibition and is achieved through perfect Watson-Crick "seed" matching between nucleotides 2-8 (starting at the 5' end) of the miRNA and the target mRNA 3'-UTR [288]. The location of the central loop in miRNA:MRE (miRNA recognition elements) and the presence of flanking adenosines around the seed region are also important for the efficiency of mRNA regulation [289,290]. Proposed models for miRNA-mediated post-transcriptional gene repression focus on inhibition of translation initiation [291], mRNA degradation following removal of poly-A tails [292] or blocking translation after initiation [293]. Their activity can be blocked by complementary antisense 2'-O-methyl oligoribonucleotides [294] that work with high specificity and were commonly referred as antagomiRs [295]. A variety of algorithms for the prediction of miRNA targets has been developed over the years in an effort to produce software often available online to public. These tools such as TargetScan, PicTar, EIMMo, MiRanda and miRBase [296] provide *in silico* data that offer a platform for further investigation of miRNA:mRNA interactions and their physiological role through a variety of gain- and loss-of function based assays [297].

The role of miRNA in tumorigenesis

Being able to offer a post-transcriptional regulation of protein synthesis, miRNAs have been considered to play a great role in orchestrating the cellular homeostasis. It comes unsurprisingly thus that miRNAs regulate developmental processes, genome integrity maintenance, signaling cascades and other major hallmarks of cell physiology. For the purpose of this thesis, however the literature will be narrowed down to miRNAs related to cancer and inflammation-based carcinogenesis.

The role of miRNAs in the establishment and progression of cancer is extended to all aspects known as the hallmarks of cancer [298]. Kefes *et al.*, showed that reduced expression of miR-7 in glioblastoma cells is correlated to

lower EGFR expression and subsequent Akt activation [299]. Constitutive Ras expression in various cancer cell types was also inhibited by various miRNAs such as let-7 and miR-18a*, while at the same time melanomas expressing mutated B-RAF show a number of deregulated miRNAs underlying that feedback signaling loops coordinated by miRNAs may drive acquisition of self sufficiency in growth factors [300–302]. At the same time, loss of growth inhibitory signals which also drives carcinogenesis is affected by miRNAs. MiR-146b-5p, found upregulated in papillary thyroid carcinomas, inhibits SMAD-4 expression and destructs the anti-proliferative signaling circuit orchestrated by TGFβ [303]. Moreover, miR-215 overexpression in gastric carcinoma patients was found to inhibit RB1 expression leading to excess cell proliferation [304]. Carcinogenesis is also linked to evasion of apoptotic machineries that restrain uncontrolled cell proliferation. Pro-apoptotic Bcl-2 was inhibited by miR-125b and miR-155 in CD40L-stimulated human leukemic B cells [305]. Blocking of Bcl-2 expression which is related to the development of Chronic Lymphocytic Leukemia (CCL) was also attributed to aberrant expression of miR-15a and miR-16-1 in these hematopoietic tumors [306]. In another fashion, miRNAs K12-1, 3, 4-3p expressed by Kaposi's Sarcoma Herpesvirus are found to block host caspase 3 expression, promoting thus unsustained proliferation and carcinogenesis [307]. Limitless replicative potential expressed through aberrant telomerase activity was also found to be regulated by miRNAs. MiR-138 inhibits hTERT expression and this fact is believed to drive development of anaplastic thyroid carcinomas and malignant neuroblastomas [308,309]. Moreover, hTERT is regulated by miR-21 through STAT3 and disruption of this circuit leads to glioblastoma development [310]. Another important feature of cancer is sustained angiogenesis. MiR-503 was found to inhibit FGF2/VEGFA and its downregulation correlates with enhanced angiogenesis in Hepatocellular Carcinomas (HCC) [311]. Ovarian cancer patients gain often resistance to chemotherapy and Vechione *et al*. showed that these patients had low expression levels of miR-484 which in turn was found to be secreted from cancer cells and affected VEGFB and VEGFR2 expression in nearby endothelial cells promoting thus angiogenesis and resistance to the specific treatment scheme [312].

The most dubious trait of cancer progression is the ability of cancer cells to invade the host tissue and migrate to distal organs. A handful of data arise during the last decade implicating that miRNAs play an important role in metastasis of cancer cells. MiR-184 was found downregulated in HHC and re-induction of its expression correlated with elevated E-Cadherin levels and simultaneous abrogation of the Met/Snail signaling pathway that promotes epithelial to mesenchymal transition (EMT) an important characteristic of metastatic cancers [313]. Smad3 was found to mediate gastric cancer EMT independently of TGFβ by regulating the transcription of the miR-200 family. MiRNAs of this family were found to regulate E-Cadherin expression through modulation of its transcription factors ZEB1 and 2 [314]. Moreover, ZEB1 and TGFBR2, which are essential components of the TGF-b signaling pathway, were identified as direct targets of miR-655 in pancreatic cancer cells, suggesting that the activation of the TGF-b-ZEB1-E-cadherin axis by aberrant downregulation of miR-655 may accommodate EMT and accelerate cancer progression [315]. MiRNAs were further implicated in the arising theory of cancer development and maintenance through the presence and activity of cancer stem cells [316]. MiR-218 for example was found to reduce the stem cell like phenotype of glioma cells through inhibition of Bmi1 [317]. Moreover, miR-34a regulates the balance between self renewal and differentiation of colon cancer stem cells through direct association with Notch mRNA [318].

MiRNAs were also implicated in emerging hallmarks of cancer [319]. Accelerated and higher metabolism suffices for cancer cell thriving and fine tuning of the metabolic processes may offer a therapeutic solution. Downregulation of miR-326 in glioblastomas accounts at least partially for the exacerbated expression of Pyruvate Kinase M2 (PKM2) which promotes cancer cell metabolism [320]. Moreover, in renal cell carcinomas with high expression of SLC2A1/GLUT1 it was evidenced that its immediate regulator, miR-1291 was downregulated [321]. Another important driving feature of carcinogenesis is high mutagenesis rate and incapability to regulate genome integrity. Valeri *et al*. showed that miR-155 was downregulated in MSI-related (microsateline instability) tumors with inactivated mismatch repair mechanisms (MMR). MiR-155 expression was directly correlated to that of

hMSH2-5 and hMLH1, proteins involved in MMR and found upregulated in MSI-related cancers [322]. Furthermore, negative regulation of tumor suppressor p53 is partially achieved through miR-125b and thus miR-125b regulates cell DNA Damage Response (DDR) and cell fate [323].

Deregulation of miRNA activity may also block the development of a proper immune response and amplify inflammation and inflammation-associated carcinogenesis which compose the remaining hallmarks of cancer observed up to date. MiRNAs are implicated both in innate and adaptive immunity [324,325], the two main branches of the immune system. A major transcription factor that links inflammation to carcinogenesis is NF-κB. NF-κB gets activated during inflammatory responses and subsequently regulates a number of genes linked to tumorigenesis (previously mentioned). MiR-146a/b was found to inhibit NF-κB and NF-κB-mediated gene transcription of IL-8, IL-6 and MMP9 lowering thus the capacity of breast cancer cells to metastasize [326]. In a seminal article published in Cell at 2009, Iliopoulos and colleagues showed that transformation of breast epithelial cells was achieved through a signaling cascade starting with Src activation. Src enhances NF-κB activity, which in turn triggers LIN-28 upregulation. LIN-28 blocks Let-7 expression and causes IL-6 upregulation. The final outcome is up-regulation of Stat-3 that triggers numerous carcinogenic molecular circuits [327]. Following work from the same group showed that Stat-3 regulates a positive feedback loop on NF-κB activation through miR-181b-1 and miR-21 upregulation [328]. Stat-3-mediated miR-21 upregulation downstream of IL-6 was also found to mediate survival of multiple myeloma cells [329]. Of note, the axis Let-7-IL-6-Stat3 was also shown to mediate survival of human malignant cholangiocytes [330], while blocking of Stat-3 by miR-124 suppressed growth of human colorectal cancer cells [331]. The presence of reactive oxygen species (ROS) in an inflammatory milieu is also implicated in carcinogenesis. Zhang *et al*. found that miR-21 reduces the conversion rate of superoxide to hydrogen peroxide through inhibition of SOD-2 and SOD-3 causing thus production of ROS and cell transformation [332]. MiR-128a and miR-200a were found to upregulate ROS through inhibition of Bmi1 and p38a respectively. In the first case, ROS production caused the entrance of medulloblastoma cancer cells into senescence, while in the

second report ROS over-production rendered ovarian cancer cells prone to antioxidant therapy [333,334].

Colon microbiome plays also a great role in inflammation-mediated carcinogenesis through the production of various metabolites. To this end it was found that the anti-cancer effects of the microbe-derived SCFA butyrate may be mediated in part via changes in miRNA expression. A miRNA microarray study on human colon cancer cells showed decreased expression of the miR-106b family which correlated with low p21 expression and reduced cell proliferation [335]. *H. Pylori* infection often related to gastric cancer development attenuates Let-7 expression through cytotoxin-associated gene A (CagA) and this fact causes elevation of RAS signaling and cancer progression [336]. In another context, macrophages infiltrating IBD (Inflammatory Bowel Disease) and UC (Ulcerative Colitis) lesions associate with high NO· production and NO·-mediated senescence in neighboring epithelia. This fact correlates with high expression of miR-21 which is also found high in pre-cancerous colon adenomas implicating its association in IBD and UC-mediated colon carcinogenesis[337]. Moreover, elevated miR-31 expression following progression of IBD to colon dysplacia inhibits HIF-1 (Hypoxia Inducible Factor-1) which is a negative regulator of VEGF and FGF expression promoting thus neo-vascularization, another hallmark of cancer [338]. Even more strikingly, secreted miR-21 and miR-29a from lung cancer cells are able to trigger a prometastatic inflammatory response through production of IL-6 and TNFα and promote tumor growth and metastasis [339]. Finally, TNF was found to induce apoptosis of endothelial cells through suppression of mir-34α and concomitant overexpression of caspase 7 and STK4 [340].

MATERIALS & METHODS

Expression constructs and Mutagenesis

Full length NPM cDNA (PubMed NM_002520.6) designated as "WT NPM" was PCR-amplified (26 cycles x 94^{o}C 40 sec, 58^{o}C 40 sec, 72^{o}C 100 sec) from a human cDNA library using the following primers: For: 5'-GATTCGATGGACATGGAC-3' and Rev: 5'-TTAAAGAGACTTCCTCCACTG-3'. The amplicon was inserted into pCR®2.1 TOPO vector (Invitrogen) according to the manufacturer's guidelines and then sub-cloned into myc-tagged (MT) pRK5 mammalian expression vector (pRK5-MT-NPM) or pGEX-2TK-GST (C terminal) bacterial expression vector (GE Healthcare) as a BamHI-EcoRI fragment with the utilization of the T4 DNA ligase system (Roche). GST-NPM deletion mutants were constructed with PCR amplification using 10 ng GST-NPM WT as template. The primers used are: aa 1-120 (For: WT, Rev: 5'-TAACTCCACAGCTACTAAGTGCTG-3'), aa 1-188 (For: WT, Rev: 5'-TAATTCTTCAGCTTCCTCATCATC-3'), aa 1-244 (For: WT, Rev: 5'-GTCTTCTACAGAACTAGGTCC-3'). The PCR conditions were similar to those used for WT NPM cDNA amplification. Annealing temperatures were calculated in each case according to the equation: 64.9 + 0.41(%G +%C) – 600/n where n: number of nucleotides/primer. NPM point mutations threonine 199 to alanine (T199A) and lysine 299 to arginine (K299R) were generated using the QuikChange™ Site-Directed Mutagenesis Kit (Stratagene) according to the manufacturer's guidelines. 10 ng MT-NPM or GST-NPM were used as template together with the following primer sets: 5'-AAATCTATACGAGATGCACCAGCCAAAAATGCA-3' and its complementary for T199A and 5'-GGACAAGAATCCTTCCGAAAACAGGAAAAAACT-3' and its complimentary for K229R. pcDNA3-NPM-ALK plasmid DNA was a generous gift from Dr. S. Turner (Department of Pathology, University of Cambridge). Myc-tagged wild type (MT-TPL2) and kinase dead (K167M) TPL2 (MT-TPL2 KD) constructs were a kind gift from A.Weiss (Rosalind Russell Medical Research Center for Arthritis, UCSF, CA, USA). For the generation of pcDNA3-TPL2, TPL2 was subcloned from pRK5-MT (MT-TPL2) to pcDNA3 plasmid vector with BamHI-EcoRI double digestion. All constructs were produced with the Expand High Fidelity PCR System (Roche) and subsequently sequenced (Macrogen Co.) to ensure error proof cloning and/or

mutagenesis. MT-NF-κB1 [341], MT-NF-κB2 [342], GST-IκBα (aa 1-62) and HA-NIK [44], GST-MEK (K207A) [4] and HA-ERK1 [12] were elsewhere described. HA-Ub (ubiquitin) was a kind gift from Dr. A. Malliri (Paterson Institute for Cancer Research, Manchester).

Bacteria-based Molecular Biology Techniques

Transformation of competent *E.coli* bacteria

Plasmid DNA or ligation products were transformed into chemically-competent *E.Coli* bacterial strains DH5α or BL21 (for GST carrying plasmids). The bacteria were transferred from -80°C and thawed on ice. The DNA was added to the cells (approximately 100 ng for plasmid DNA or 10μl of the ligation reaction) and after a 20 min incubation on ice, they were treated by heat shock (42°C for 2 min) followed by a 2 min quick chill on ice. Pre-warmed SOC media [2% (w/v) tryptone, 0.5 % (w/v) yeast extracts, 10 mM NaCl, 2.5 mM KCl, 10 mM $MgCl_2$, 10 mM $MgSO_4$, 20 mM glucose, pH to 7] was added to the bacteria (0.5 ml) and they were incubated for 1 hour at 37°C on a shaking rotor. Bacteria were subsequently plated on LB-agar containing the appropriate antibiotics (mainly 100 μg/ml Ampicillin or 50 μg/ml Kanamycin) and incubated overnight at 37°C.

DNA extraction

Minipreps

Single colonies were selected from the LB agar plates, placed into 5 ml - of LB media - starter cultures of [(0,01% (w/v) tryptone, 0,005% (w/v) yeast extracts, 0,01% (w/v) NaCl] containing the appropriate antibiotic (mainly 100 μg/ml Ampicillin or 50 μg/ml Kanamycin) and grown overnight onto a shaking rotor at 37°C. The liquid cultures were centrifuged at 3500 rpm for 15 min to pellet the bacteria and resuspended in 200μl GTE buffer [25 mM Tris-HCl pH 7.5, 10 mM EDTA pH 8.0, 1% glucose (v/v)] supplemented with RNAse A (250 μg/ml). The bacterial cells were lysed in 400 μl of freshly-made Lysis Buffer [200 mM NaOH, 1% SDS (w/v)] and the mix was neutralized after a 5 min incubation on ice with 300 μl Solution III [3M CH_3COOK in acetic acid]. The DNA was precipitated in ice-cold ethanol for 30 min on ice and pelleted at

13000 rpm for 30 min (4°C). The pellets were washed in 200 µl 70% ethanol, and left to air-dry. The DNA was resuspended in 25-50 µl TE buffer (10 mM Tris-HCl, 1 mM EDTA pH 8.0) and left overnight at 4°C prior to determination of DNA concentration to maximize the yield. The concentration of DNA was measured using NanoDrop ND-1000 Spectrophotometer.

Midipreps and maxipreps

The plasmid DNA was extracted from the bacteria using the Plasmid Midi- or Maxi Prep Kit (Qiagen) or the Macherey-Nagel Kit according to the manufacturer's instructions. The resulting DNA pellet was resuspended in 50-150 µl of TE buffer. The concentration of the DNA was determined using the NanoDrop ND1000 Spectrophotometer and/or gel agarose analysis.

Restriction digestion of DNA plasmids

Plasmids were routinely checked with restriction digestion to verify successful cloning. Briefly, approximately 1 µg of plasmid DNA was cut with the desired restriction enzymes according to the individual restriction map. Roughly 1 unit of each enzyme was used per 1 µg of DNA in a 20 µl reaction. BSA was added if necessary to a final concentration of 100 µg/ml and the reactions were incubated at 37°C for $1^{1/2}$ hour and analyzed by agarose gel electrophoresis.

Detection of nucleic acids

Nucleic acids were mixed with loading buffer [20% Ficoll 400, 0.1 M Na_2EDTA pH 8.0, 1.0% sodium dodecyl sulfate (vol/vol), 0.25% bromophenol blue (w/vol), 0.25% xylene cyanol (v/v)] and run on a 1-2% agarose/ethidium bromide/1xTAE gel. 2-3 µl of λ DNA digested with PstI was run as a standard on a Power 300 Electrophoresis Power Supply (Fisher Scientific).

RNA extraction and qRT-PCR

Total RNA was extracted from cells with 1 ml/60mm cell culture dish Trizol Reagent (Life Technologies). RNA quantity and quantity were calculated with Nanodrop. Following DNAse pre-treatment (Invitrogen), 1 µg of total RNA was transcribed to cDNA with Superscript III Reverse Transriptase (Life

Technologies) using oligo-dT primers. Subsequently, samples were qPCR amplified using Platinum SYBR Green qPCR Super Mix UDG kit (Life Technologies) in a MJ Research Chromo4 Real Time PCR instrument (MJ Research). The primers used are: human TPL2 (For: 5'-GCAAGAGGCTGCTGAGTAGC-3', Rev: 5'-CATATTCAAGCGTTGGTGGT CCC-3'), human/mouse GAPDH (For: 5'-GACCACAGTCCATGCCATCAC-3', Rev: 5'-CAGGGATGATGTTCTGGAGAGC-3'), mouse IL-6 (For: 5'-GTCCTTCAGAGAGATACAG-3', Rev: 5'- TCTTAGGAGAGCATTGG -3'). PCR reaction conditions were arranged according to kit manufacturer's guidelines and the Tm was 60^{o}C in all cases. Data analysis was performed using the standard curve method. A serial of dilutions from untreated cells was used for the construction of the standard curve. GAPDH was used as internal control for the normalization of the detected values. miRNA qRT PCR was performed with Taqman MicroRNA assay kit (Life Technologies) according to the manufacturer's instructions with the utilization of U6 snRNA as internal control.

Cell Culture, Transfection assays and Gene Silencing.

A549 lung epithelial carcinoma cells, MCF7 breast epithelial carcinoma cells, HeLa cervical carcinoma cells, Human Embryonic Kidney (HEK) 293T cells and wild type or IKKα Knock out MEFs (kindly provided by Dr. M. Pasparakis, Institute for Genetics, University of Cologne) were cultured as monolayers in Dulbecco's Modified Eagle Medium (D-MEM), containing GlutaMAX^{TM} and pyruvate supplemented with 10% Fetal Bovine Serum (v/v) (Gibco). Maintenance of wild type (WT), TPL2 knock out (KO) and TPL2 KO MEFs stably expressing HA-TPL2 (*TPL2*$^{-/-}$.HA-TPL2 MEFs) was performed as previously describe [61]. For transfection assays, cells were plated at 40% confluency and 24 hours later they were transfected with the designated quantity from each plasmid using Lipofectamine Reagent (Life Technologies) according to manufacturer's instructions. Cells were collected and lysed 24-36 hours post-transfection in lysis buffer containing 0.5% Triton X-100, 150 mM NaCl, 50 mM Tris-Cl pH 7.4, 1 mM EDTA, 1 mM Na_3VO_4, 10 mM NaF, 20 mM glycerophosphate and protease inhibitor cocktail (Sigma-Aldrich).

Gene silencing was performed using Lipofectamine RNAiMax Reagent (Invitrogen) according to the manufacturer's instructions. TPL2 knock down was efficiently achieved after one or two rounds of siRNA transfection using Dharmacon SMARTpool ON-TARGETplus MAP3K8 siRNA (#L003511, Thermo Scientific) or a combination of three Stealth siRNAs against MAP3K8 from Invitrogen (#HSS102181-182-038). The siRNA duplex sequences used for NPM depletion were designed according to previous published data [161] and were purchased from Dharmacon (Thermo Scientific). Control Luciferase siRNA (sense: 5'-UACGCUGAGUACUUCGATT-3', antisesnse: 5'-UCG AAGUACUCAGCGUAAG-3') was custom-made and purchased from Ambion. Working concentration of each siRNA was 10-20 nM.

Primary cell extraction and manipulation

Two month old female mice were sacrificed and bone marrow was flushed from tibias and femurs with 5 ml BMDM medium (49% DMEM, 20% FCS, 30% LC medium, 1% P/S) using a 26G needle, after excessive removal of muscles from the bones. The cells were pelleted (2 min, 1200 rpm) and red blood cells were removed after resuspension of the pellet in 0,165M NH_4Cl and incubation at 4^oC for 2 min. The remaining cells were plated in 175 cm^2 flasks containing 50 ml BMDM medium (cells from one leg/flask). Seven days later the supernatant was removed and the remaining cells were detached with versene (GIBCO), counted and plated for treatment 24 hours later. For the preparation of LC medium, L929 cells were cultured in 175 cm^2 flasks containing DMEM supplemented with 10% v/v FBS until confluence. The supernatant was collected, filtered through 0,2 μM syringe filters (Santorius Stedim) and saved at -20^oC for future use. Efficient differentiation of bone marrow cells to macrophages (> 80%) was checked with FACS. Briefly, 10^5 cells were washed in 1x PBS pH 7.4, transferred in BD Falcon 12x75 mm tubes (BD Biosciences) and stained with a combination of α-F480-PE and α-CD11b-FITC antibodies (BD Biosciences) for 30 min on ice. The cells were further washed twice in 1x PBS pH 7.4, resuspended in 1x PBS pH 7.4 and analyzed in FACS (FACSCalibur, BD Biosciences). B cell primary cell isolation was performed with the B cell Isolation Kit II from MACS (Miltenyi Biotec) according to the manufacturer's guidelines.

Cell treatment, lysis and fractionation

Cells were irradiated with 20 J/m^2 UVC (Vilber Lourmat) as described before [343]. Alternatively they were treated with *cis*-platin (Sigma-Aldrich) at a final concentration of 25 μM or Actinomycin D (Sigma-Aldrich) at 0.05 μg/ml for the indicated time periods. Recombinant human TNFα (R&D systems) was used at a final concentration of 20 ng/ml and CD40L (Bender) at 1 μg/ml. MG132 (ENZO life sciences) was used at a final concentration of 20μM and was added to the medium one hour prior to stimulation. TPL2 kinase inhibitor (Merck-Millipore) was added at the culture medium one hour prior to stimulation at a final concentration of 20μM. DMSO (Applichem) was used as vehicle control. Following treatment, cells were washed twice with 1x PBS pH 7.4, collected and incubated on ice for 20 min in lysis buffer containing 0.5% Triton X-100, 150 mM NaCl, 50 mM Tris-Cl pH 7.4, 1 mM EDTA, 1 mM Na_3VO_4, 10 mM NaF, 20 mM glycerophosphate and protease inhibitor cocktail (Sigma-Aldrich). Alternatively RIPA lysis buffer was used to ensure efficient lysis of nuclei. Fractionation of cells into cytoplasmic and nuclear compartments was performed in a two-step procedure. Cells were firstly lysed in a hypotonic buffer (20 mM Hepes pH 7.6, 10 mM NaCl, 1.5 mM $MgCl_2$, 0.2 mM EDTA, 0.1% NP-40, 20% glycerol, 1 mM DTT, 1 mM Na_3VO_4 and protease inhibitor cocktail) and incubated on ice for 10 min. Following centrifugation (5 min, 1500 rpm) the supernatant was collected as the cytoplasmic fraction. The remaining pellet was washed twice with hypotonic buffer and then resuspended in hypertonic buffer (composed as the hypotonic with NaCl supplemented to final concentration of 0.5 M) and was incubated on ice for 30 min with agitation. Debris and nuclear remnants were removed with centrifugation (20 min, 13000 rpm) and the supernatant was collected as the nuclear fraction. Isolation of highly pure nucleoli was performed as previously described [344].

Immunoblotting and antibodies

Lysed cells were centrifuged for 20 min at 13000 rpm to remove debris and whole cell lysate (WCL) protein concentration was calculated using the Bradford assay. 10-50 μg protein aliquots were mixed with Laemmli buffer

(containing β-mercaptoethanol), loaded onto a 9-12% polyacrylamide gel and transferred to nitrocellulose membrane (GE Healthcare). After blocking with 5% non-fat milk (Regilait) in TBS/Tween 0.1%, the membranes were incubated overnight at 4ºC with the following antibodies: α-TPL2 (M-20), α-NPM (FC82291), α-myc (A-14), α-Sp1 (PEP-2), α-HA (Y-11), α-Lamin-B (C-20), α-UBF (F-9), α-βtubulin (TU-02), α-ERK2 (C-14), α-PARP1 (H-250), α-ERK 1,2 (H-72), α-NF-κB1 (C-19), α-IKKα (M-280), α-IκBα (C-21), α-NF-κB2 (K-27), α-TRAF3 (C-20) and α-p65 (sc-373x) were purchased from Santa Cruz; α-βactin (clone C4) was purchased from Merck-Millipore, α-pERK (M8159) and α-GAPDH from Sigma-Aldrich; α-Ubiquitin FK2H (ENZO life sciences) was a kind gift from Dr. A. Malliri (Paterson Institute for Cancer Research, Manchester) and α-Lamin A (Cell signaling) was kindly provided by Professor C. Spilianakis (Biology School, University of Crete); α-MEK1/2 $pSer^{217}/Ser^{221}$ (#9154), α-MEK1/2 (#9126) and α-pJNK (#4668) were purchased from Cell Signaling. Anti-SUMO I and II were kindly provided by Professor R. Hay (MRC Dundee). Detection of NPM $pThr^{199}$ was achieved with a cocktail of antibodies pursued by Cell Signaling (#3541) and Abcam (EP1857Y). Human α-p53 (DO-1, pAb1801) and α-HDM2 (4B2, 4B11, 2A9) hybridoma supernatants were kindly provided by Professor M. Oren (Weizmann Institute of Science, Israel). Anti-F480PE and α-CD11b-FITC (BD Biosciences) were a kind gift of Professor D. Boumpas (Medical School, University of Crete). Detection of GST-bound proteins was readily executed by SDS-PAGE gel staining with Ponceau S Solution (Sigma-Aldrich). Membranes were further incubated with HRP-labeled rabbit or mouse secondary antibodies (Sigma-Aldrich) for 1 hour at room temperature. Enhanced chemiluminescence (ECL, Perkin-Elmer) was employed for signal development and assessment on autoradiography films (Fuji Medical X-Ray film 100NIF Super RX) or in a Fujifilm Las-3000. Membrane re-blotting was performed with stripping. The membranes were incubated on a rotor at 50°C for 30 min in stripping Buffer [60 mM Tris-HCl pH 6.8, 0.7% β-mercaptoethanol (v/v), 2% SDS (w/v)] and washed extensively under tap water for 30 min. The stripped membrane was blocked in 5% non-fat milk for 1 hour at room temperature and re-incubated overnight with the desired primary antibody.

Immunoprecipitation and GST-pull down assays

Co-Immunoprecipitation (co-IP assays)

Cells were lysed in a buffer containing 0.5% Triton X-100, 150 mM NaCl, 50 mM Tris pH 7.6, 1% EDTA, 1 mM Na_3VO_4 and protease inhibitor cocktail (Sigma-Aldrich) 48h post-transfection or immediately after cell stimulation (endogenous proteins). Equal protein amounts (0.5-1 mg) were mixed with the appropriate antibody (1 μg Ab/ 1 mg input) for 1 hour at room temperature or O/N at 4ºC by rotation. The complexes were then bound to 10-20 μl (bead bed volume), pre-cleared in lysis buffer, protein G sepharose beads (BD Biosciences) for 60 min at 4ºC (rotation). After excess washing in lysis buffer, bead-bound protein complexes were dissociated from the beads in Laemmli buffer (containing β-mercaptoethanol) and boiled for 10 min at 100ºC to ensure complex destruction. Samples were then loaded on polyacrylamide gels for SDS-PAGE analysis. For the detection of immunoprecipitated (IP) TPL2 a light chain specific secondary α-rabbit antibody was used to avoid heavy chain background (Jackson Laboratories).

For Ubiquitin IP assays, 20 μM MG132 (ENZO life sciences) was added to the cell culture medium for 4-5 hours prior to cell lysis. Cells were then washed in 1x PBS pH 7.4 supplemented with 10 μM MG132 and 10 mM NEM (Sigma-Aldrich) and lysed in 1 ml/100mm dish RIPA buffer (150 mM NaCl, 1% NP-40, 0.5% sodium deoxycolate, 0.1% SDS, 50 mM Tris pH 8.0, protease inhibitor cocktail) containing MG132 and NEM. NPM was immunoprecipitated from 900 μl of whole cell lysates O/N at 4^{o}C and analyzed for ubiquitination status by probing with anti-Ub Ab (FK2H).

In SUMOylation IP assays, cells were lysed in RIPA buffer supplemented with protease inhibitors (Sigma), Na_3VO_4 (1 mM) and iodoacetamide (25 mM), were briefly sonicated (20 sec, 50% amp) and 4mg of total protein was incubated with α-NPM overnight at 4°C. Detection of SUMOylated NPM was achieved with immunoblotting using α-SUMO I or II antibodies.

GST-pulldown assays

BL21 cells were transformed with pGEX-2TK-GST-bound fusion proteins, grown to an optical density of 0.4-0.5 and induced with 0.01 mM isopropyl-β-D-thiogalactopyranoside (IPTG, Sigma) for 3 hours at 37°C or O/N at 18^{o}C, on a shaking rotor. Bacteria were lysed by pulse sonication (6 strokes of 20 sec, 50% amp with 30 sec intervals) in 1x PBS pH 7.4 supplemented with protease inhibitor cocktail (Sigma-Aldrich) and 1 mM Na_3VO_4 followed by incubation for 30 min at 4^{o}C (rotation) with the addition of 1% Triton-X-100 and centrifugation at 10000 rpm for 10 min. Soluble GST-tagged proteins were purified via incubation for 3 hours at 4°C with Glutathione Sepharose beads GE Healthcare) and washed three times with 1x PBS pH 7.4. The resultant beads/GST-tagged proteins were mixed with 0.5 mg HEK 293T cell extracts carrying overexpressed various proteins as indicated in the corresponding figures. Following incubation for 3 hours at 4^{o}C, the beads were washed four times in the corresponding lysis buffer, resuspended in Laemmli buffer and boiled for 10 min at 100^{o}C. GST-bound protein complexes were resolved by 9% SDS-polyacrylamide gel electrophoresis prior to immunoblotting.

Chromatin Immunoprecipitation (ChIP) assay

The protocol was based in previous published data [345]. Briefly, cells were plated at 80% confluence one day prior to treatment (5-10 100mm dishes used/condition). 24 hours later cells were treated according to the experiment specifications and at the end of the stimulation period they were washed twice in 1x PBS pH 7.4. Subsequently, they were treated with 1% formaldehyde for 10 min at room temperature. Cross-linking was stopped by the addition of glycine to a final concentration of 0.125 M. The cells were washed with cold 1x PBS pH 7.4 and swelled on ice for 10 min in a solution containing 25 mM HEPES pH 7.8, 1.5 mM $MgCl_2$, 10 mM KCl, 0.1% NP-40, 1 mM dithiothreitol, and a protease inhibitor cocktail (Sigma-Aldrich). Following Dounce homogenization (20 strokes, pestle A), the nuclei were collected and resuspended in sonication buffer containing 50 mM HEPES pH 7.9, 140 mM NaCl, 1 mM EDTA, 1% Triton X-100, 0.1% sodium deoxycholate, 0.1% SDS,

and protease inhibitors and sonicated (Vibra Cell) on ice to an average DNA fragmentation length of 200 to 1,000 bp (10-15 strokes of 30 sec, 50% amp, 2 min intervals). The samples were centrifuged at 14000 rpm for 15 min at 4^{o}C and precleared with protein G-Sepharose beads (BD Biosciences) in the presence of 2 µg sonicated λ DNA and 1 mg of bovine serum albumin/ml. Twenty-five A260 units of the precleared chromatin was immunoprecipitated with 1 µg α-IKKα antibody, and the immune complexes were collected by adsorption to protein G-Sepharose beads. The beads were washed twice with sonication buffer, twice with sonication buffer containing 500 mM NaCl, twice with 20 mM Tris pH 8.0, 1 mM EDTA, 250 mM LiCl, 0.5% NP-40 and 0.5% sodium deoxycholate, and twice with Tris-EDTA buffer. The immunocomplexes were eluted with 50 mM Tris pH 8.0, 1 mM EDTA, 1% SDS at 65°C for 10 min, adjusted to 200 mM NaCl, and incubated a 65°C for 5 hours to reverse the cross-links. After successive treatments with 10 µg of RNAse A and 20 µg of proteinase K/ml, the samples were extracted with phenol chloroform and precipitated with ethanol. One tenth of the immunoprecipitated DNA and input DNA (from extracts corresponding to 0.025 A260 units) was analyzed by PCR amplification (36 cycles of 94^{o}C for 45 sec, 60^{o}C for 60 sec and 72^{o}C for 60 sec) using primers from sequences surrounding the mouse IL-6 proximal promoter (For: 5'-TGTGTGTGTGTGT ATGTGTGTGTCG-3', Rev: 5'-TCGTTCTTGGTGGGCTCCAG -3') designed according to Anest *et al*., 2003 [224] and the amplicons were checked with electrophoresis in a 2% agarose gel.

In vitro kinase assay

HEK 293T cells transfected with MT-ev or MT-TPL2 were lysed in kinase lysis buffer (KLB) [20 mM Tris pH 7.6, 0.5% Triton X-100, 250 mM NaCl, 3 mM EDTA, 3 mM EGTA, 1 mM Na_3VO_4, 0.5 mM sodium pyrophosphate, 25mM β-glycerolphosphate, 1 mM DTT and protease inhibitor cocktail (Sigma-Aldrich)] and 0.5 mg protein lysate was used to immunoprecipitate TPL2 using 2 µg α-TPL2 (M-20) Ab and G-sepharose beads. The beads were washed twice in kinase lysis buffer (KLB) and three times in kinase reaction buffer (KRB) containing 20 mM MOPS pH 7.2, 5 mM EGTA, 0.1 mM Na_3VO_4, 25 mM β-glycerolphosphate, 1 mM DTT and protease inhibitor cocktail. The

supernatant was removed and the beads were resuspended in a mix of KRB (supplemented with 10 mM $MgCl_2$ and 2 mM freshly made ATP) and 1-2 µg purified (with glutathione beads column) GST-NPM, GST-NPM (T199A) or kinase inactive GST-MEK1 (K207A) as substrate. In vitro kinase reaction was performed for 30 min at 30ºC with agitation. Beads were separated from the supernatant, resuspended in 2x Laemmli buffer and boiled for 5 min at 100^{o}C. Supernatants were mixed with equal volumes of 2x Laemmli buffer and boiled. Phosphorylation was determined by western blotting of bead eluates and probing with α-pThr^{199} NPM or α-pSer^{217}/Ser^{221} MEK1/2. Equal loading of GST-NPM and GST-MEK1 (K207A) protein was confirmed by blotting supernatants with α-NPM or α-MEK1/2 antibody.

Cell Biology techniques

Immunofluorescence

Cells were washed twice with 1x PBS pH 7.4 and fixed in 4% PFA (w/v) for 30 min at room temperature followed by permeabilization with 0,1% Triton X-100. Prior to staining, cells were incubated with 10% Horse Serum (Gibco) in 1x PBS pH 7.4 for minimum of 1 hour at room temperature. The incubation with the primary antibody (diluted 1:100 in 1x PBS pH 7.4) was carried out for 30 min at room temperature followed by 30 min incubation with the secondary antibody in the dark. Subsequently, cells were washed twice with 1x PBS pH 7.4 supplemented with 10% Horse Serum. Samples were mounted with AntiFade Reagent (Life Technologies) and analyzed on a Leica TCS Sp2 Confocal microscope. Images were analyzed with ImageJ software (http://rsb.info.nih.gov/ij/). Alexa Fluor 594 (rabbit) and Alexa Fluor 488 (mouse), purchased by Molecular Probes (Life Technologies), were used as secondary antibodies diluted 1:1000 in 1x PBS pH 7.4. DAPI (Molecular probes) was used for the detection of nuclei.

MTT assays

Cells were seeded in 96 well plates and 24 hours later they were stimulated with 20 J/m^2 UVC for the indicated time periods. Following stimulation, the

medium was supplemented with MTT reagent (Sigma-Aldrich) for 2-4 hours and was subsequently replaced with 0,04N Hcl/Isopropanol. Quantitation of MTT conversion was achieved with a BIORAD 680 Microplate Reader (BIORAD). Values were calculated at 550 nm with a reference reading at 655 nm.

Luciferase assays

Cells were seeded in 12well plates and 24 hours later were transfected as previously described. For NF-κB activation cells were transfected with 60 ng of NF-κB1 and 100 ng Renilla reporter plasmids and various MT-TPL2:MT-NPM plasmid DNA ratios (shown in the corresponding figure). For ERK activation cells were transfected with 500 ng pFR-luci, 25 ng pFA2-Elk1 and 100 ng Renilla reporter plasmids and various MT-TPL2:MT-NPM plasmid DNA ratios. 36 hours later cells were lysed and processed according to the manufacturer's instructions (Dual Luciferase Reporter Assay System, Promega) and luciferase activity was measured in a FB12 Luminometer (MBI). Values were normalized to firefly luciferase activity to ensure equal transfection efficiency.

ELISA

IL-6 secretion in the culture medium was measured with ELISA using the Affymetrix-E Bioscience mouse IL-6 kit. 96 well plates (Corning Costar 9018) were coated with 100 μL/well of capture antibody in 1x Coating Buffer, sealed and incubated overnight at 4°C. Wells were washed 3 times with 100 μL/well wash buffer (1x PBS pH 7.4, 0,1% Triton X-100) and incubated with 200 μL/well of 1x ELISA/ELISPOT Diluent at room temperature for 1 hour for blocking. After 2-3 washes, 100 μL/well of each sample (or controls) were added in the wells and the plate was sealed and incubated for 2 hours at room temperature. The wells were further washed excessively and were subsequently incubated with 100 μL/well of detection antibody (mIL-6) diluted in 1x ELISA/ELISPOT Diluent for 60 min at room temperature. Wells were washed 3-5 times, treated with 100 μL/well 1x TMB Solution for 15 min at room temperature and the reaction was stopped with the addition of 50 μl

Stop Solution to each well. Reactions were read at 450 nm with a BIORAD 680 Microplate Reader (BIORAD, CA, USA).

RESULTS

TPL2 interacts with NPM

A proteomic screen using over-expressed TPL2 [346] as bait (and unpublished data) identified NPM as a putative TPL2-interacting protein. NPM-TPL2 association was validated by GST pull-down and immunoprecipitation assays. Bacterially produced GST-NPM fusion protein or GST empty vector (GST-ev), immobilized on glutathione sepharose beads were incubated with lysates from Human Embryonic Kidney (HEK) 293T cells transfected with pRK5-myc empty vector (MT-ev) or a MT-TPL2. As shown in Figure 1A, over-expressed MT-TPL2 but not MT-ev was found to interact with GST-NPM. Further control experiments showed that MT-TPL2 did not associate with GST-ev or GST-IκBα (Fig. 1B). To determine whether the interaction of TPL2 with NPM also occurs *in vivo*, myc-tagged NPM (MT-NPM) and untagged TPL2 were co-expressed in HEK 293T cells and the lysates were immunoprecipitated using anti-TPL2 antibody and immunoblotted with anti-NPM. The results showed that when overexpressed, MT-NPM and TPL2 co-precipitate (Fig. 1C). More interestingly, utilization of UVC as a genotoxic stress stimulus, known to affect NPM activity [160], led to enhanced NPM:TPL2 interaction shown by co-immunoprecipitation assays performed in irradiated A549 cells (Fig. 1D).

1A.

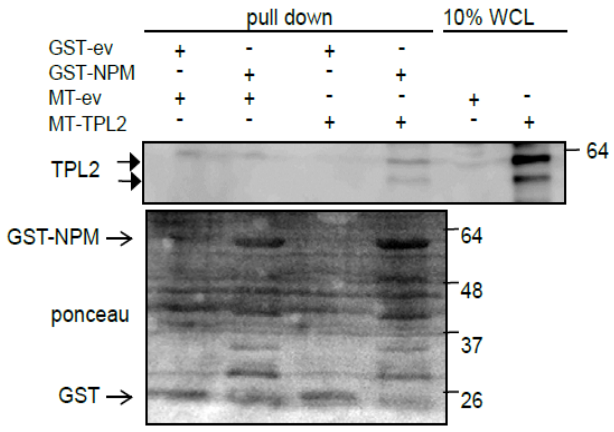

Figure 1 continues overleaf

1B.

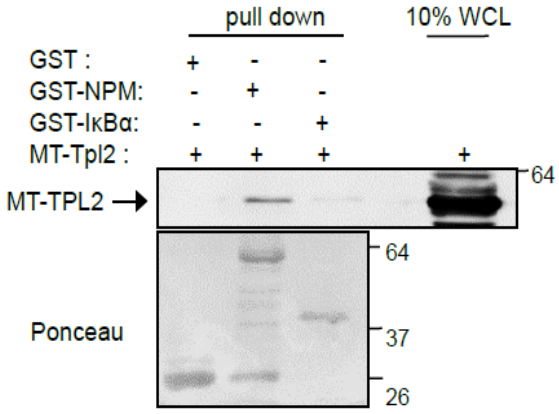

1C.

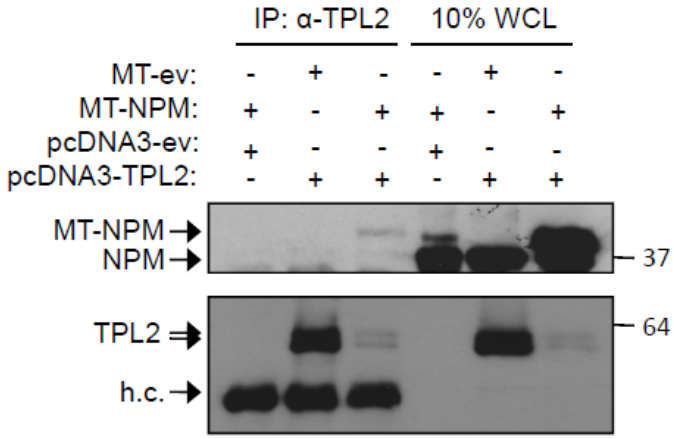

1D.

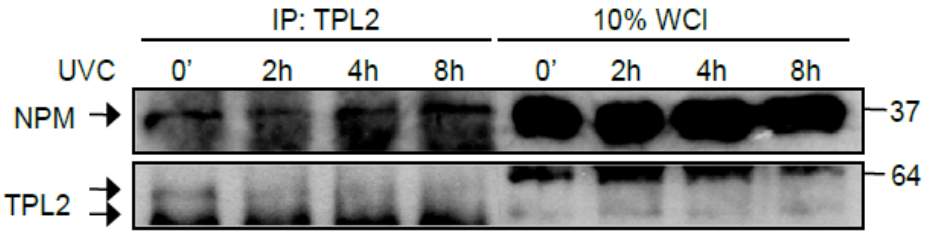

Figure 1. **A**. TPL2 interacts with NPM *in vitro* and *in vivo*. A. GST-pull down of exogenously expressed MT-TPL2 in HEK-293T cells with purified GST-NPM expressed *in vitro* in BL-21 *E.Coli* cells. Ponceau staining was used for detection of GST-bound proteins. MT-ev: pRK5-myc tagged empty vector. **B.**

GST-ev (empty vector) or GST-IκBα do not interact with TPL2 in GST-pull down assay performed as in A. **C**. Co-immunoprecipitation (co-IP) of pcDNA3-TPL2 or -ev with MT-NPM exogenously expressed in HEK-293T cells. **D.** A549 lung ca cells were irradiated with 20J/m^2 UVC for the indicated time points. Co-IP between endogenous TPL2 and NPM shows enhanced interaction following UVC-induced genotoxic stress. 10% of input whole cell lysates (WCL) was used as a loading control in each case.

TPL2 resides both in the cytoplasm and the nucleus.

NPM predominantly resides in the nucleolus and translocates to the nucleoplasm upon cell exposure to DNA damaging agents [347]. In contrast, TPL2 has mostly been studied as a cytoplasmic kinase in the context of cytokine and Toll-like receptor signal transduction [348]. However, recent studies have indicated that TPL2 may also have nuclear functions [51]. The presence of TPL2 has been thus examined in cytoplasmic and nuclear fractions of HEK 293T cells transiently transfected with MT-TPL2. The results of the fractionation experiments showed that over-expressed TPL2 is present both in the cytoplasmic and nuclear extracts from these cells (Fig. 2A). This finding was furthermore supported in MEFs (Fig. 2B) transiently transfected with MT-TPL2 and subjected to immunofluorescence analysis. A possible explanation of the enhanced interaction between TPL2 and NPM following UVC irirradiation of A549 cells (Fig. 1D) would be the increased TPL2 nuclear localization under these conditions. To validate this hypothesis, TPL2 localization was examined in A549 cells treated with UVC and subjected to cytoplasmic versus nuclear fractionation. As shown in Figure 2C, TPL2 is partially located in the nucleus of untreated cells and the nuclear fraction of TPL2 is increased following UVC irradiation. The subcellular localization of TPL2 was also assessed in immortalized fibroblasts from *TPL2*$^{-/-}$ mice stably reconstituted *in vitro* with near-physiological levels of HA-tagged TPL2 [14]. Cells were either exposed to UVC or left untreated and TPL2 localization was monitored by immunofluorescence using α-HA antibody. Staining with α-lamin Ab was used to mark the nuclear envelope. As shown in Figure 2D, TPL2 predominantly localized in the cytoplasm and plasma membrane in untreated

cells but some punctuated staining was also observed in the nucleus. However, significant mobilization of HA-TPL2 to the nucleus was detected following UVC irradiation. This observation is in agreement with a previous study demonstrating nuclear localization of TPL2 following exposure of cells to UVB [51]. A more universal impact of genotoxic stress on TPL2 nuclear relocalization was investigated with the use of the anti-cancer drug *cis*-platin on MCF7 breast epithelial carcinoma cells. Immunofluorescence analysis (Fig. 2E) shows that *cis*-platin can recapitulate the effect of UVC on TPL2 localization and supports a physiological role of TPL2 in the nucleus under genotoxic stress.

2A.

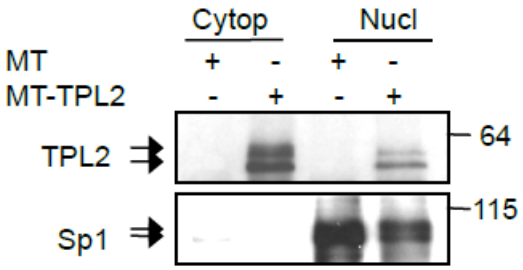

2B.

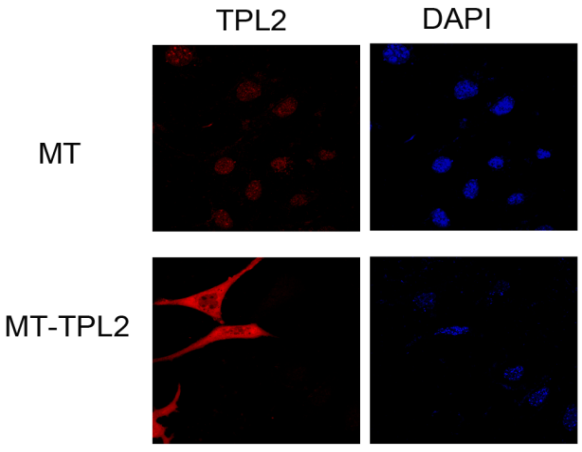

Figure 2 continues overleaf

2C.

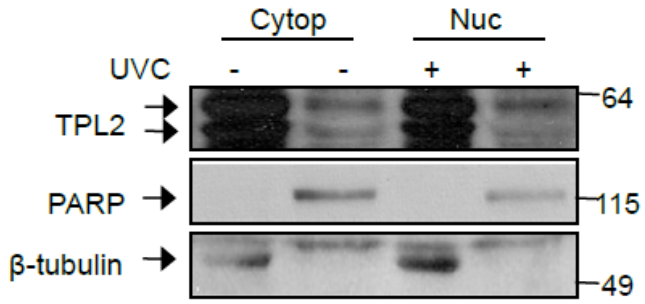

2D.

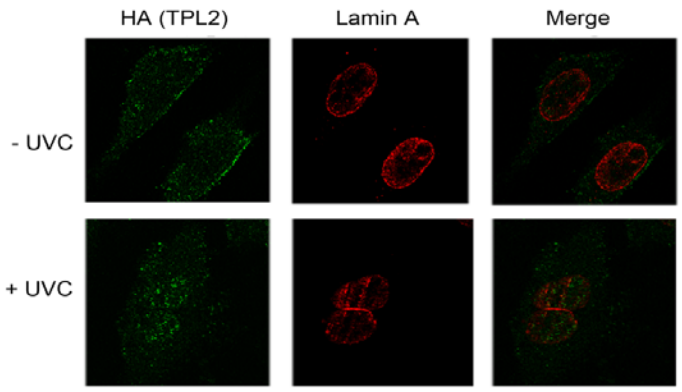

2E.

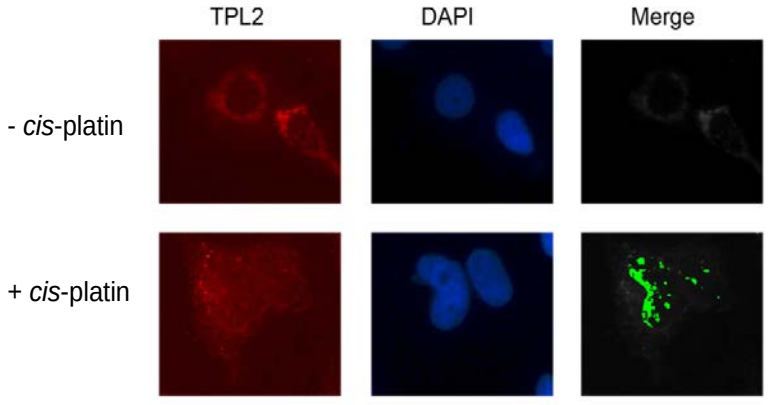

Figure 2. TPL2 subcellular localization. **A**. HEK 293T cells were transfected with MT-TPL2 and subsequently lysed in nuclear or cytoplasmic fractions. TPL2 is found in both the nucleus and the cytoplasm. Sp1 was used as a

nuclear marker. **B.** Immunofluorescence (IF) of endogenous (upper panel) or over-expressed (MT-TPL2, lower panel) TPL2 in MEFs. DAPI was used as nuclear marker. **C.** Endogenous TPL2 localizes both in the cytoplasm and in the nucleus of irradiated or not A549 cells. PARP: nuclear marker, β-tubulin: cytoplasmic marker. **D**. Immortalized fibroblasts from *tpl2*$^{-/-}$ mice stably reconstituted *in vitro* with near-physiological levels of HA-tagged TPL2 were irradiated with 20 J/m^2 UVC for four hours. HA (TPL2) was detected with IF. Lamin A, a marker of the nuclear lamina, was used to define the nuclear perimeter. **E.** MCF7 breast ca cells were treated with *cis*-platin for eight hours. TPL2 localization was monitored with IF and DAPI was used as a nuclear marker. Analysis of the merged pictures was performed with Image J software. Green spots depict co-localization.

TPL2 colocalizes and interacts with NPM mainly in the nucleus.

Data presented thus far raise the question of whether TPL2 colocalizes with NPM and if so which is the sub-cellular compartment that supports this notion. To address this question we collaborated with Professor S. Volarevic (School of Medicine, University of Rijeka, Croatia) for further in depth cell fractionation assays. A549 cells treated or not with UVC for various time points were subjected to nucleolar, nucleoplasmic and cytoplasmic fractionation. As shown in Figure 3A, TPL2 was found both in the cytoplasm and the nucleoli of untreated cultures but it was absent in the nucleoplasm. Following UVC treatment, TPL2 levels decreased in both cytoplasm and nucleoli and increased in the nucleoplasm. At the same time NPM was found mainly in the nucleoli of untreated cells and irradiation led to the translocation of NPM from nucleoli to nucleoplasm, consistent with previous reports [177]. The data support that the two proteins colocalize mainly in the nucleus while shifting between all three subcellular compartments depending on the ongoing stress. Immunofluorescence analysis of TPL2 and NPM in irradiated versus untreated A549 cells (Fig. 3C) corroborates the observed nuclear colocalization of the two proteins.

3A.

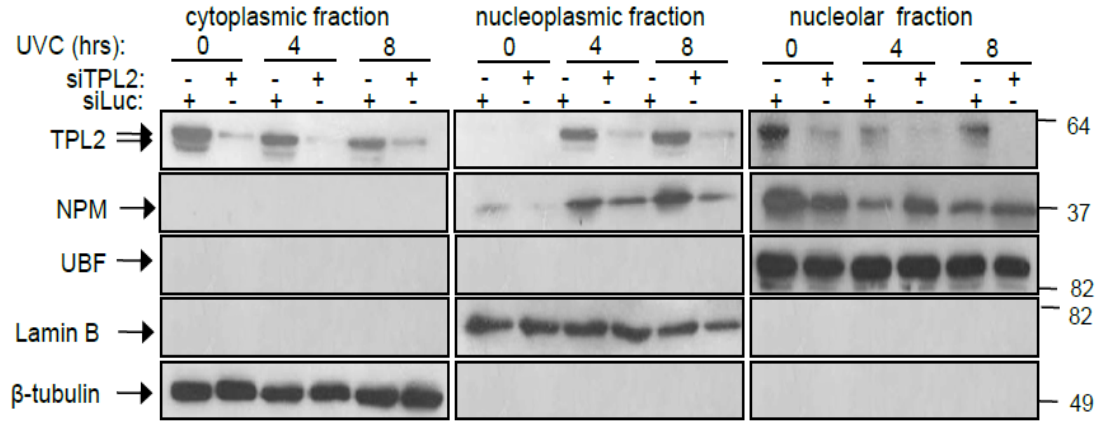

3B.

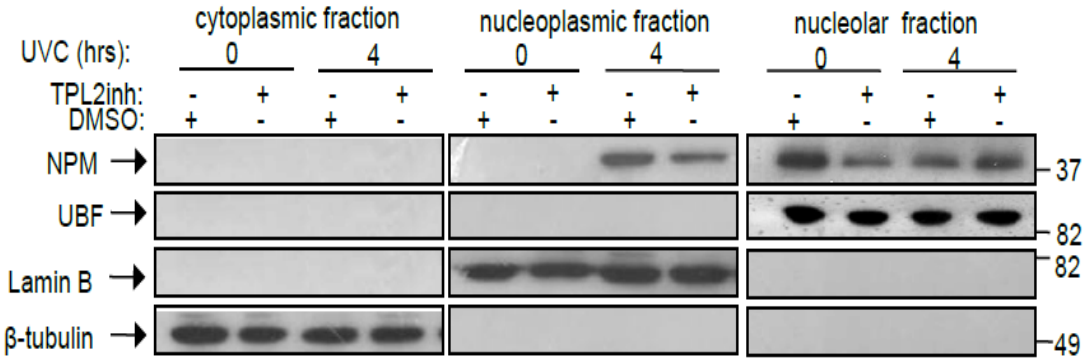

3C.

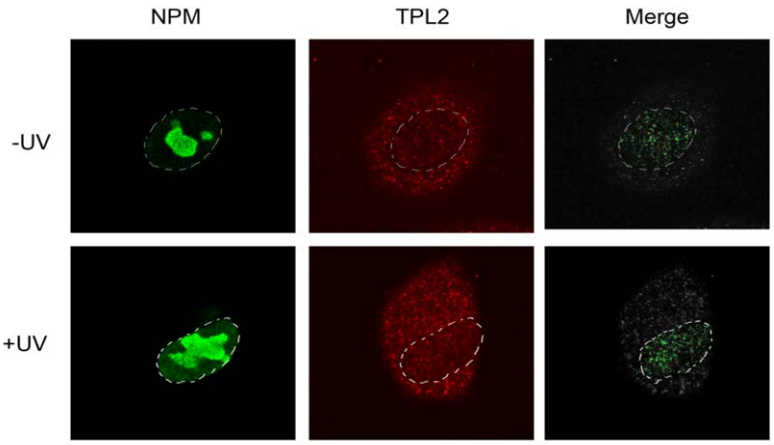

Figure 3. TPL2 co-localizes with NPM and regulates NPM endo-nuclear translocation following genotoxic stress. **A.** Western blot analysis of NPM and

TPL2 in fractionated A549 cells irradiated with UVC or left untreated. The figure shows also NPM localization in TPL2-depleted (siTPL2) or not (siLuc) A549 prior to irradiation. **B.** TPL2 kinase activity was blocked with a small chemical compound (TPL2inh) and TPL2-NPM localization was detected as in A. UBF: nucleolar marker, β-tubulin: cytoplasmic marker, Lamin B: nucleoplasmic marker. DMSO vehicle was used as control to TPL2inh. Data shown in figures **A** & **B** were kindly provided by S. Bursac (School of Medicine, University of Rijeka, Croatia). **C.** IF of TPL2 and NPM in A549 cells irradiated or not with UVC for 8 hours. Merged pictures were analyzed with Image J software. Spliced lines indicate the nuclear periphery and green spots co-localization regions.

These findings were followed by experiments aiming to ascertain whether the interaction between TPL2 and NPM actually occurs in the nucleus where colocalization was observed. Nuclear and cytoplasmic proteins were extracted from HEK 293T cells transiently transfected with MT-TPL2 (Fig. 4A) or a TPL2 kinase-dead mutant (Fig. 4B) and incubated with GST-NPM immobilized on glutathione sepharose beads. NPM interactions were analyzed by immunoblot using α-TPL2 Ab. The results showed a profound association of GST-NPM with nuclear but not cytoplasmic TPL2 (Fig. 4A). In contrast, kinase-inactive TPL2 failed to interact with NPM irrespective of localization (Fig. 4B). Nuclear interaction of TPL2 with NPM was further demonstrated in co-imnunoprecipitation assays of endogenous proteins in A549 lung cancer cells. NPM was found to co-precipitate with TPL2 in nuclear extracts from UVC-treated cells whereas little association was observed in untreated cultures (Fig. 4C). In contrast, no interaction between the two proteins was observed in cytoplasmic lysates.

4A.

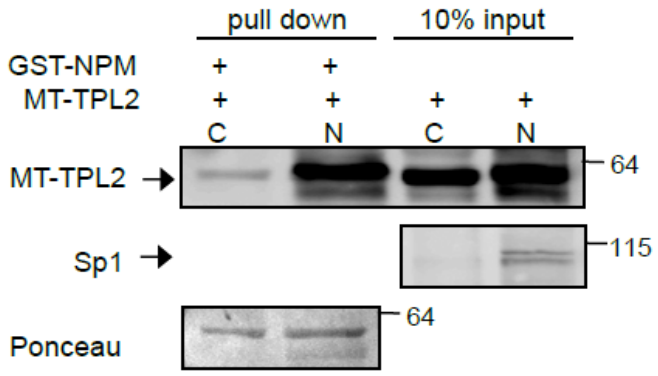
pull down
10% input
GST-NPM + +
MT-TPL2 + + + +
C N C N
MT-TPL2
64
Sp1
115
Ponceau
64

4B.

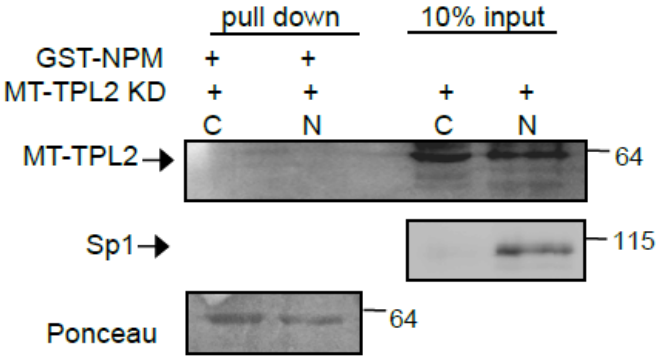
pull down
10% input
GST-NPM + +
MT-TPL2 KD + + + +
C N C N
MT-TPL2
64
Sp1
115
Ponceau
64

4C.

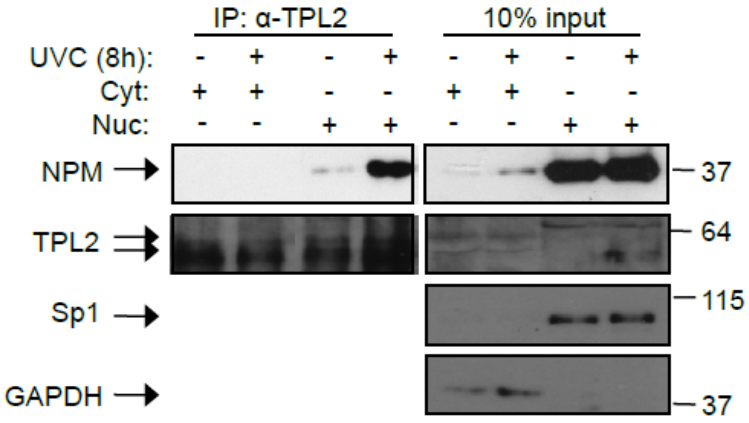
IP: α-TPL2
10% input
UVC (8h): - + - + - + - +
Cyt: + + - - + + - -
Nuc: - - + + - - + +
NPM
37
TPL2
64
Sp1
115
GAPDH
37

Figure 4. TPL2 binds NPM preferentially in the nucleus. **A.** GST-pull down of NPM with MT-TPL2 exogenously expressed in HEK 293T cells. The cells were separated in their cytoplasmic and nuclear sub-domains prior to the pull-down assay. Ponceau staining was used for the visualization of the GST-bound proteins. **B.** TPL2 kinase activity is essential for the interaction with NPM. Kinase inactive TPL2 (MT-TPL2-KD) does not bind NPM in GST pull down assays performed as in A. **C.** Nuclear-cytoplasmic fractionation of irradiated with UVC or not A549 cells followed by immunoprecipitation of endogenous TPL2 shows enhanced binding of NPM to TPL2 mainly in the nucleus. Sp1 serves as a nuclear marker and GAPDH as a cytoplasmic one.

TPL2 modulates both the localization and protein levels of NPM following DNA damage

NPM-TPL2 colocalization coupled to the fact that the two proteins interact with each other led to the examination of a possible functional relationship between them. To this end, NPM levels were analyzed by immunoblot in fractionated A549 cells depleted of TPL2 (siRNA) and treated with UVC. Interestingly, the RNAi-mediated reduction in TPL2 levels attenuated the translocation of NPM from the nucleoli to nucleoplasm (Fig. 3A). As purification and loading control in these experiments, lysates from each fraction were immunoblotted for tubulin, lamin B and UBF which are expressed in the cytoplasm, nucleoplasm and nucleoli respectively (Fig. 3A). Similar results were obtained when A549 cells were cultured in the presence of a small molecule TPL2 kinase inhibitor prior to exposure to UVC (Fig. 3B), suggesting that the catalytic activity of TPL2 contributes to the regulation of NPM re-localization.

NPM expression increases in response to DNA damage [175], hypoxia [349] and treatment with hormones [98] . In line with these reports, A549 cells exposed to UVC (Fig. 5A, B), *cis*-platin (Fig. 5C) or actinomycin D (Fig. 5D) displayed elevated NPM levels compared to untreated controls. Intriguingly, the knock-down of TPL2 led to higher NPM levels in untreated cultures which did not increase further following treatment of the cells under the stimuli mentioned (Fig. 5A-D). This phenomenon is not particular to transformed cells as TPL2 ablation (Fig. 5E) in immortalized fibroblasts (*TPL2*$^{-/-}$ mice) also displayed abnormal NPM kinetics following either UVC irradiation in a dose- (Fig. 5F) and time-dependent (Fig. 5G) manner or treatment with the anti-cancer agent *cis*-platin (Fig. 5H).

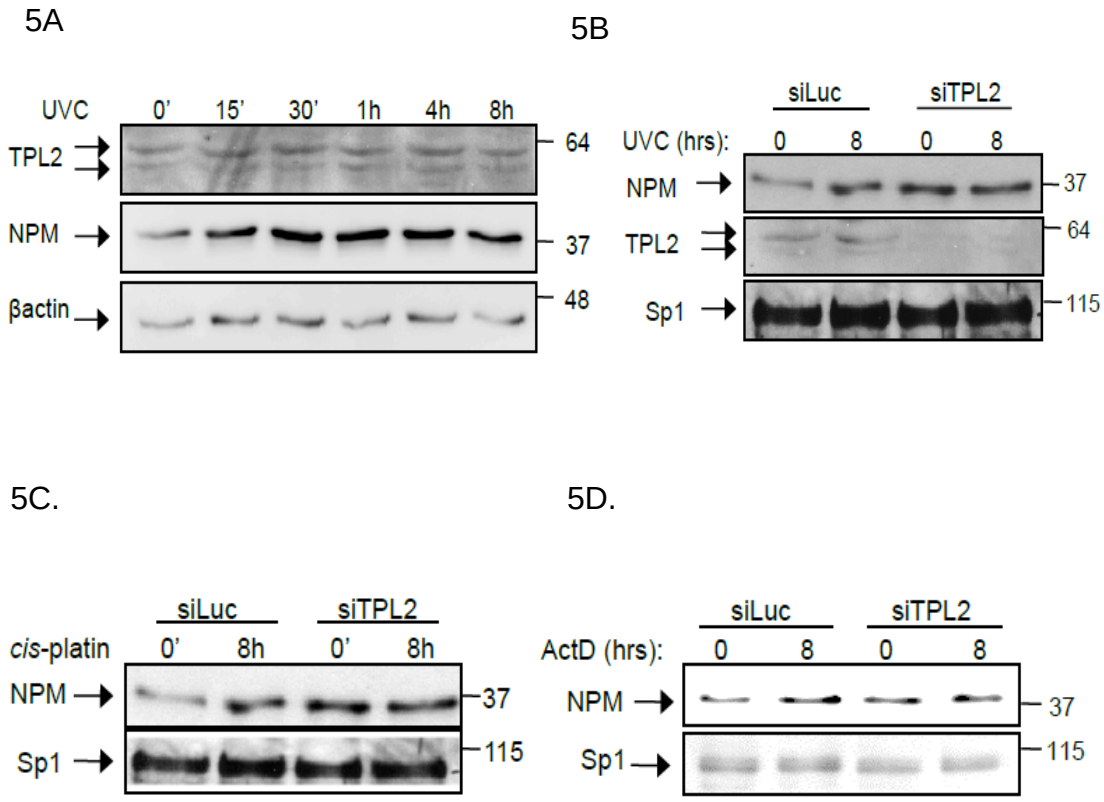

Figure 5 continues overleaf

5E.

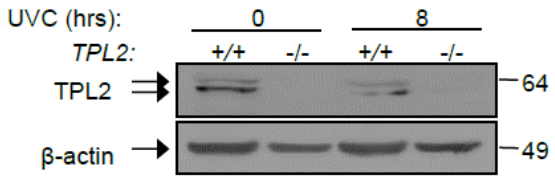

5F.

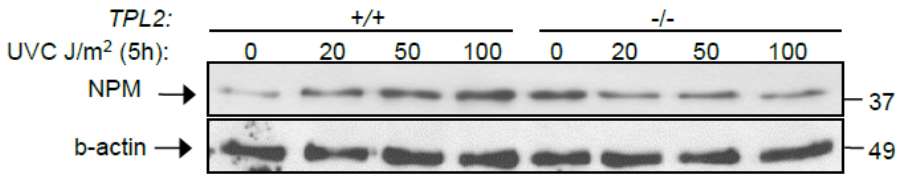

5G.

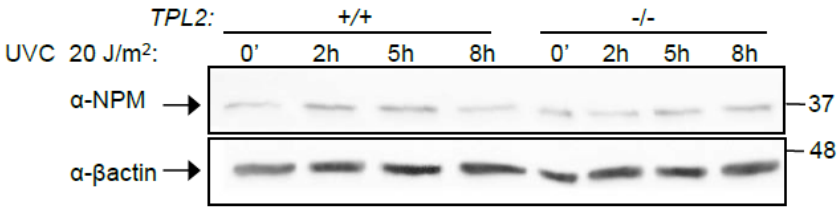

5H.

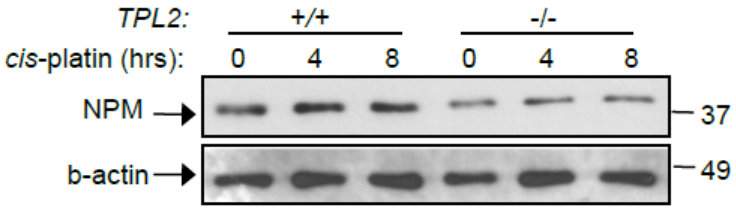

Figure 5. TPL2 is pivotal for normal NPM induction after genotoxic or ribosomal stress. **A.** Immonoblotting of NPM and TPL2 in irradiated A549 cells for various time points. TPL2 depletion in A549 cells (siTPL2) blocks NPM upregulation following either genotoxic stress induced by UVC **(B)** and cis-platin **(C)** or ribosomal stress caused by ActD **(D)**. Control siRNA was used against Luciferase. **E.** WT or TPL2 knock out (KO) immortalized MEFs were radiated as in A. Total TPL2 protein levels are shown with immunoblotting. Dose- **(F)** and time-dependent **(G)** effect of TPL2 absence on NPM accumulation following UVC irirradiation of immortalized MEFs. **(H)**. TPL2 ablation hinders NPM accumulation in *cis*-platin-treated MEFs. β-actin or Sp1 were used as loading controls in all cases.

TPL2 regulates the phosphorylation of NPM at threonine 199.

NPM is subject to various post-translational modifications which affect its localization and function, including phosphorylation [350]. This fact coupled to the findings that TPL2 kinase activity affects NPM translocation from the nucleus to the nucleoplasm following UVC irradiation (Fig. 3B) and that kinase dead TPL2 does not associate with NPM (Fig. 4B) prompted us to investigate a possible kinase-substrate relationship between NPM and TPL2. Due to the structural and functional complexity of NPM [80] the need to focus on a specific NPM region, important for its interaction with TPL2, was requisite. To this end we constructed a number of GST-bound plasmid vectors carrying a serial of NPM deletions (ΔNPM) based on the most profound activities of the protein (Fig. 6A). The plasmid DNAs were subsequently expressed in BL21 *E.Coli* bacteria, purified by immobilization on Glutathione Sepharose beads and subjected to GST-pull down assays with TPL2 ectopically expressed in HEK 293T cells. Efficient binding of ΔNPM 1-244 (aa) but not ΔNPM 1-120 or ΔNPM 1-188 to MT-TPL2, shown in Figure 6B, designates that the region between amino acids 188-244 is pivotal for NPM's interaction with TPL2.

6A.

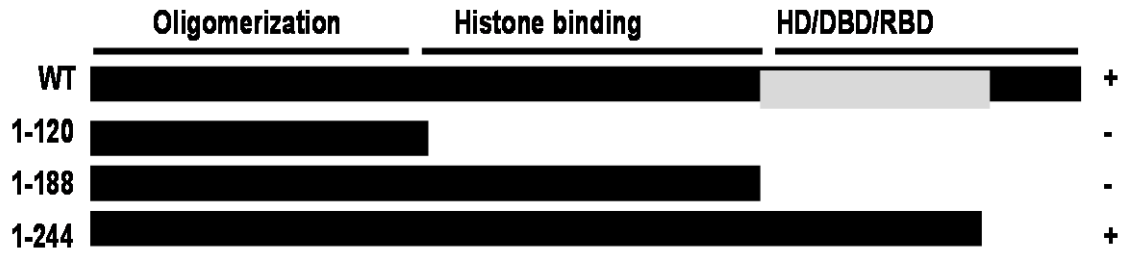

Figure 6 continues overleaf

6B.

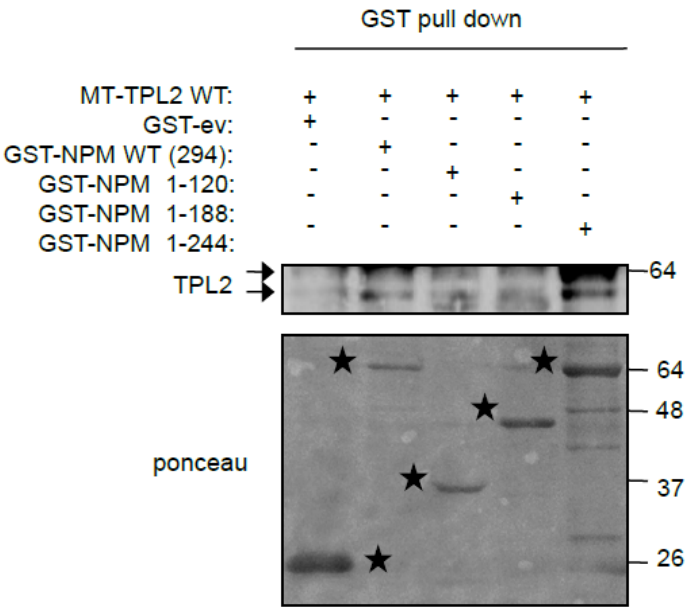

Figure 6. NPM C terminus is essential for the interaction with TPL2. **A**. Schematic representation of serial deletions in NPM gene. The major domains of NPM are high-lightened depending on their activities. **B**. GST-pull down of MT-TPL2 over-expressed in HEK293T cells with GST-bound WT NPM or various NPM serial deletions. The numbers on the right side of NPM refer to amino acid sequences. Asterisks indicate the size of the various GST-bound proteins labeled here with ponceau stain.

As TPL2 is a *de novo* Ser/Thr kinase and partial phosphorylation of NPM at Thr[199] was shown to be required for its dissociation from nucleolar components [351], it was surmised that TPL2 may regulate NPM localization through phosphorylation. In line with this prediction, it was found that Thr[199] NPM phosphorylation is severely affected by the knock-down of TPL2 with siRNA in both untreated A549 cells and in cultures exposed to UVC (Fig. 7A). To determine if this effect requires the catalytic activity of TPL2, A549 cells were treated with a TPL2 kinase inhibitor (prior to UVC exposure) in concentrations which impair TNF-mediated ERK phosphorylation (Fig. 7C), in line with the established role of TPL2 in the TNFR1 - MAPK signaling axis [12].

The results showed that treatment with the TPL2 kinase inhibitor reduced basal Thr^{199} phosphorylation levels and accelerated their decline following exposure to UVC (Fig. 7B). The ability of over-expressed TPL2 to phosphorylate NPM directly at Thr^{199} was then examined in an *in vitro* kinase reaction using recombinant GST-NPM as substrate. MEK1 which directly interacts with and is phosphorylated by TPL2 at Ser$^{217/221}$ [4] was used as a positive control. Immunoprecipitated TPL2 from MT-TPL2 transfected HEK 293T cells was found to phosphorylate both GST-MEK1 (Fig. 7E) and GST-NPM *in vitro* whereas a Thr^{199}→Ala mutated NPM fused to GST remained unresponsive (Fig. 7D). Collectively, these findings underscore an important role for TPL2 in the regulation of NPM phosphorylation at Thr^{199}.

7A.

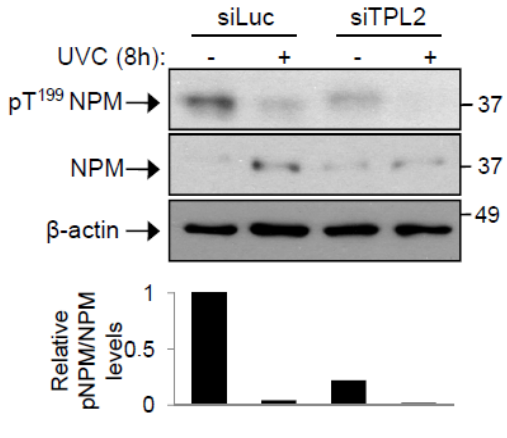

7B.

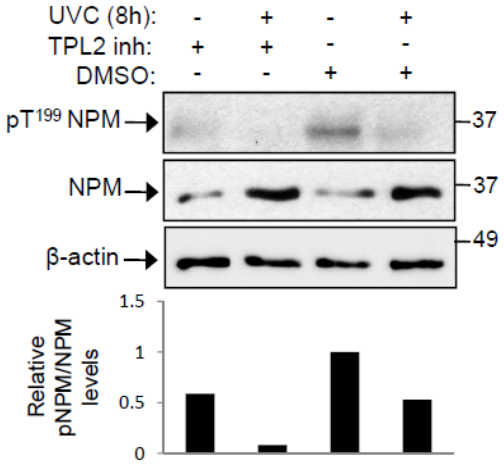

7C.

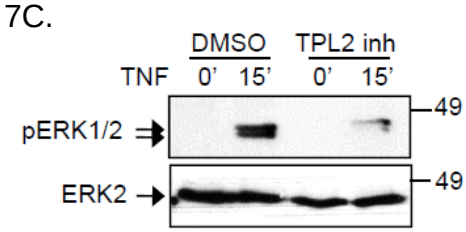

Figure 7 continues overleaf

7D. 7E.

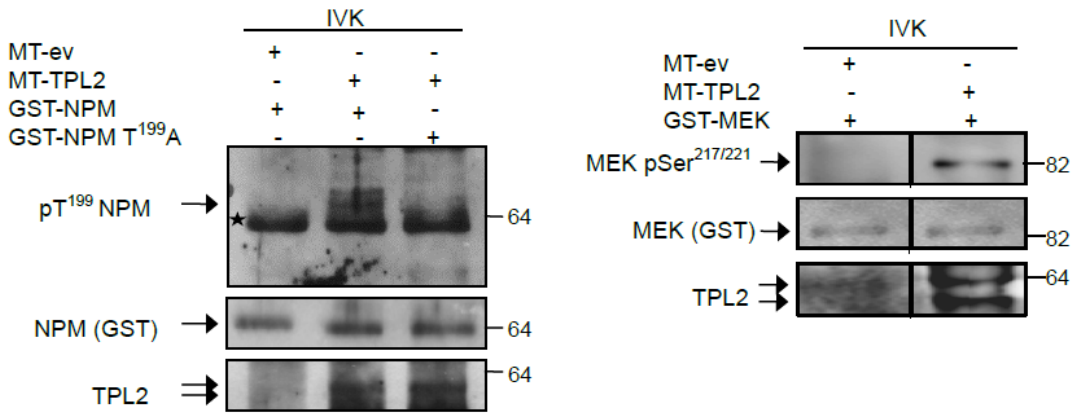

Figure 7. TPL2 phosphorylates NPM directly at threonine 199. **A.** Knocking down TPL2 (siTPL2) or blocking its kinase activity **(B)** with a chemical inhibitor (TPL2inh) accelerates dephosphorylation of NPM at T199 both at steady state and after UVC irradiation of A549 ca cells. The expression levels ratio of pNPM T199/total NPM was calculated with Image J software and is shown as a graph of bars. **C.** TPL2 inhibitor efficiently blocks TPL2-mediated ERK phosphorylation in A549 ca cells treated with 20ng/ml TNFα for the indicated time points. **D.** HEK 293T cells were transfected with MT-ev- or MT-TPL2 and immunoprecipitated TPL2 was readily used for *in vitro* phosphorylation assay of bacterially expressed and purified (glutathione beads resin) GST-NPM or -NPMT^{199}A (substitution of threonine 199 to alanine). Phosphorylation was detected with a phospho-specific antibody. Equal loading of GST-NPM substrate and TPL2 expression was detected with immunoblotting. **E.** Efficient *in vitro* phosphorylation of kinase inactive MEK1 (K207A) by TPL2. MEK phosphorylation was detected with specific antibody.

TPL2 regulates phosphorylation-mediated NPM ubiquitination.

The next question to be addressed was how TPL2 affected NPM kinetics following genotoxic or ribosomal stress as evidenced in Figure 5. To test whether the observed data relate to differences in K48-linked ubiquitination, TPL2 was knocked-down by siRNA in A549 cells followed by UVC treatment

in the presence or absence of the proteasome inhibitor MG132. NPM was immunoprecipitated from whole cell lysates and ubiquitin-bound NPM was detected with α-Ubiquitin (FK2H) Ab. UVC radiation led to reduction of NPM ubiquitination in control siRNA-transfected cells compared to untreated cells. Interestingly, TPL2 depletion significantly reduced NPM ubiquitination in untreated cultures which was marginally affected by UVC (Fig. 8A). To examine whether TPL2 may influence NPM ubiquitination via Thr^{199} phosphorylation, HEK293 cells were co-transfected with TPL2, HA-tagged Ub expression vectors and either MT-NPM or a MT-NPM construct in which Thr^{199} has been mutated to Ala ($T^{199}A$). Lysates were immunoprecipitated with anti-HA and immunoblotted using α-NPM Ab. The results (Fig. 8B) demonstrated robust ubiquitination of WT NPM by TPL2 whereas NPM ($T^{199}A$) remained unaffected.

In search of a possible NPM ubiquitination site affected by NPM phosphorylation, NPM lysine K299 was mutated to arginine ($K^{299}R$), cloned into the pRK5-MT vector and used in ubiquitination assays. More specifically, Ubiquitin was immunoprecipitated from extracts of HEK 293T cell transfected with HA-Ub and a combination of WT or KD MT-TPL2 and WT, $T^{199}A$ or $K^{229}R$ MT-NPM plasmid DNA and Ub-bound NPM was detected with immunoblotting (Fig. 8C). Inactivation of TPL2 (kinase dead) or substitutions of NPM T199 to A and K229 to R abate NPM ubiquitination compared to the effect of the WT TPL2/WT NPM combination. Nevertheless, the presence of both NPM mutants (lane 9) rescues the phenotype of NPM ubiquitination showing that TPL2 may regulate NPM turn-over through an interplay between Lys^{299} ubiquitination and phosphorylation at Thr^{199}.

The link between ubiquitination and Thr^{199} phosphorylation of NPM and the influence of TPL2 on these effects was further explored in A549 cells transfected with siRNAs targeting TPL2 or the unrelated Luciferase gene and exposed to UVC irradiation in the presence or absence of the proteasome inhibitor MG132. Following lysis of the cells, phosphorylation of NPM at Thr^{199} and NPM total protein levels were detected by immunoblotting. Interestingly, inhibition of the proteasome activity led to significant increase in the levels of

phosphorylated NPM in both untreated cultures and cells exposed to UVC (Fig. 8D). The possibility that MG132 does not directly exert its effects on pNPM turn-over but leads to increased NPM phosphorylation through TPL2 stabilization was subsequently explored. To this end, A549 cells were treated with MG132 prior to UVC irradiation and TPL2 levels were examined by western blot. As control, lysates from the same cultures were immunoblotted for p53. As shown in Figure 8E, MG132 showed no profound effect on TPL2 expression levels whereas p53 was stabilized both in untreated and UVC-treated cells. On the basis of the aforementioned findings it was concluded that TPL2 regulates threonine 199 phosphorylation of a fraction of NPM prone to ubiquitination and degradation. NPM stability is also affected by its SUMOylation status [96] and thus a possible role of TPL2 in this context was examined. NPM was immunoprecipitated with α-NPM Ab from lysates of A549 cells treated with TPL2 or control Luciferase siRNA followed by UVC irradiation and SUMO-conjugated NPM was immunodetected with α-SUMO I, II antibodies (Fig. 8F). Depletion of TPL2 did not alter NPM SUMOylation status neither in UVC treated nor in unstimulated cells and TPL2 was thus excluded from such a hypothesis.

8A.

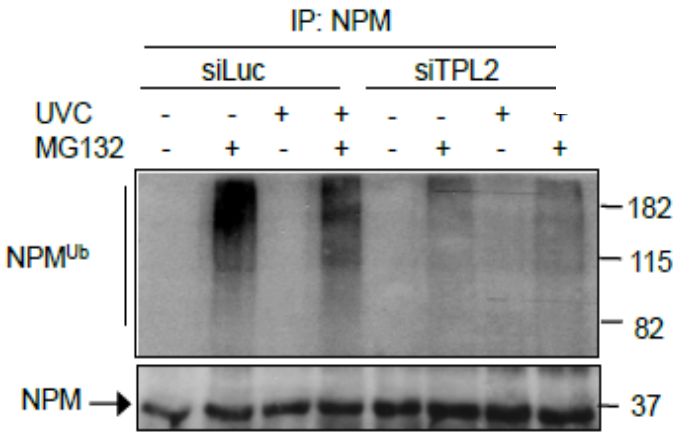

Figure 8 continues overleaf

8B.

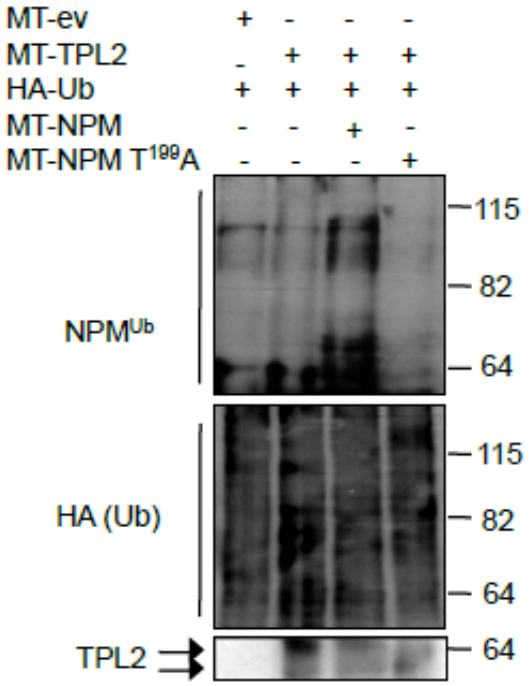

8C.

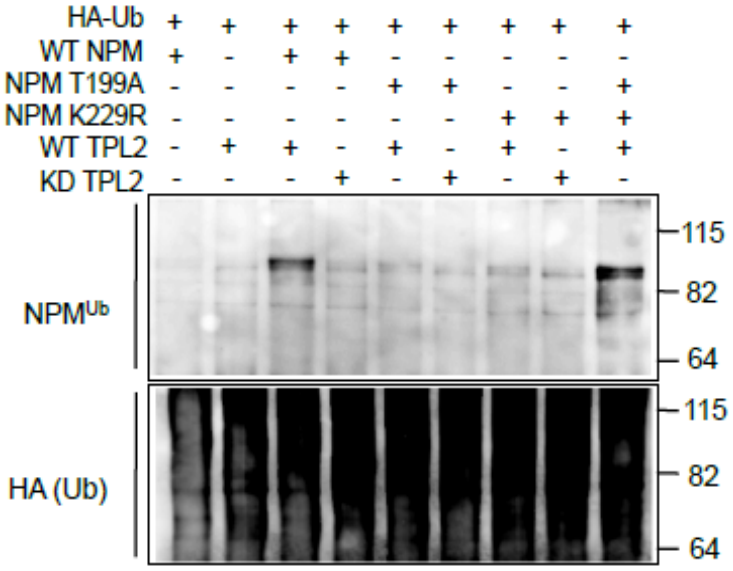

Figure 8 continues overleaf

8D.

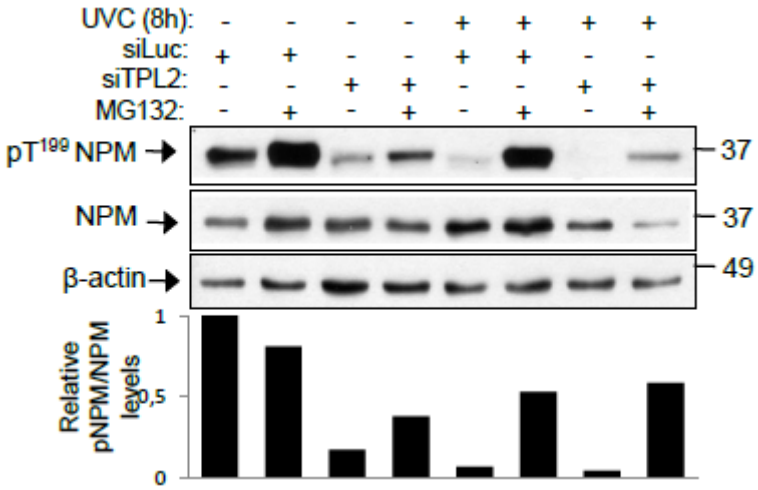
UVC (8h): - - - - + + + +
siLuc: + + - - + + - -
siTPL2: - - + + - - + +
MG132: - + - + - + - +
pT199 NPM
NPM
β-actin
37
37
49
Relative pNPM/NPM levels
1
0,5
0

8E.

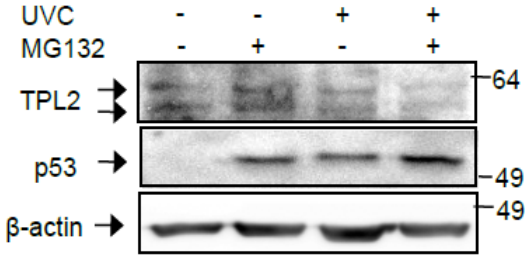
UVC - - + +
MG132 - + - +
TPL2
p53
β-actin
64
49
49

8F.

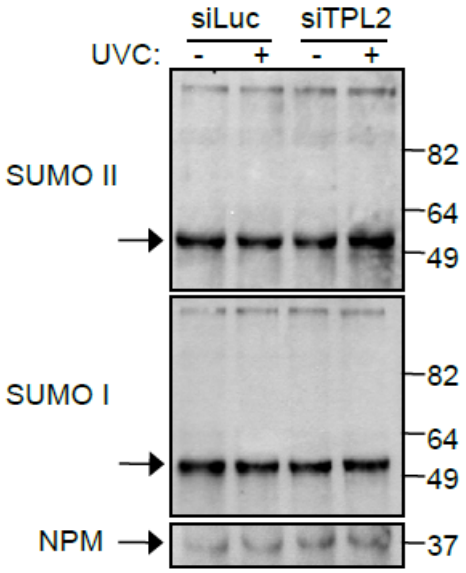
siLuc
siTPL2
UVC: - + - +
SUMO II
SUMO I
NPM
82
64
49
82
64
49
37

Figure 8. TPL2 regulates phosphorylation-mediated NPM ubiquitination and pT^{199}NPM turnover. **A.** TPL2 depletion (siTPL2) suppresses MG132-induced NPM ubiquitination. *In vivo* ubiquitination assay of immunoprecipitated endogenous NPM in A549 cells treated with UVC +/- siTPL2 +/- proteasome inhibitor MG132. **B.** NPM T^{199}A mutation blocks TPL2-mediated NPM ubiquitination. HEK293T cells were transfected with the indicated plasmid DNA combinations. Ub-bound NPM was immunodetected following immunoprecipitation of HA-Ub. **C.** NPM K^{229}R mutation rescues the effect of NPM T^{199}A on TPL2-mediated NPM ubiquitination. HA-Ub was immunoprecipitated from HEK293T cells transfected with the indicated plasmid DNA combinations and Ub-bound NPM was detected with western blotting. **D.** MG132 rescues the effect of TPL2 knock down on pT^{199}NPM both in unstimulated and UVC-treated A549 ca cells. The expression levels ratio of pT^{199}NPM/total NPM was calculated with Image J software and is shown as a graph of bars. **E.** MG132 does not rescue TPL2 protein levels following UVC irradiation. P53 was used here as a positive control for the activity of the proteasome inhibitor MG132. **F.** TPL2 downregulation with siRNA does not affect NPM SUMOylation after UVC-induced genotoxic stress.

TPL2 regulates p53 accumulation in response to DNA damage and ribosomal stress by modulating the interaction of NPM with HDM2.

Following UVC-induced DNA damage, the release of NPM from the nucleolus to the nucleoplasm contributes to increased p53 stability by counteracting p53 binding to HDM2 [160]. In line with the reported findings, p53 failed to accumulate after *cis*-platin (Fig. 9A) or UVC (Fig. 9B) treatment of A549 cells depleted of NPM by RNAi. Given the fact that TPL2 affects both the localization and expression levels of NPM following DNA damage-induced stress (Fig. 3 & Fig. 5) it was assumed that TPL2 might also regulate p53 accumulation under these circumstances. To support this hypothesis, A549 cells depleted of TPL2 by RNAi were subjected to genotoxic stress induced by *cis*-platin and UVC or ribosomal stress evoked by low concentrations of actinomycin D [344]. Respectively to the effect of NPM knock down in A549 cells (Fig. 9A & 9B), p53 induction was attenuated by the knock-down of TPL2 in

response to these agents (Fig. 9C – 9E). This observation was not restricted to tumor cells as immortalized fibroblasts from *TPL2*$^{-/-}$ mice also responded to UVC with reduced accumulation of p53 compared to *TPL2*$^{+/+}$ cells (Fig. 9G). The effect of TPL2 on p53 at least partially relates to TPL2 kinase activity since pre-treatment of A549 cells with TPL2 kinase inhibitor mimicked the effects of TPL2 knock-down and attenuated the p53 response to UVC (Fig. 9F).

9A.

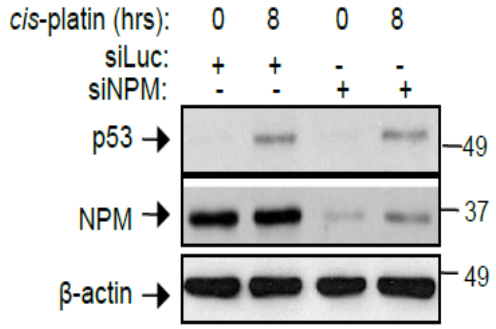

9B.

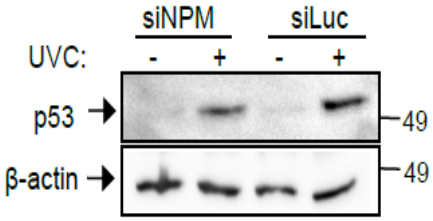

9C.

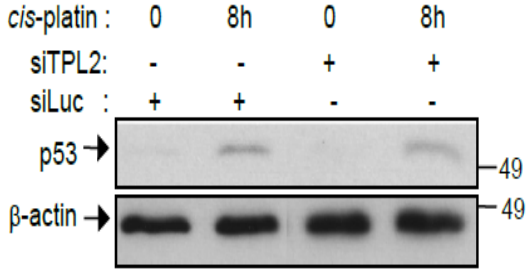

9D.

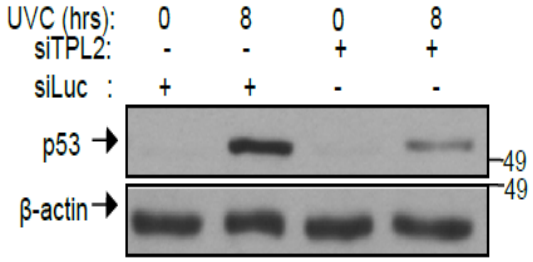

9E.

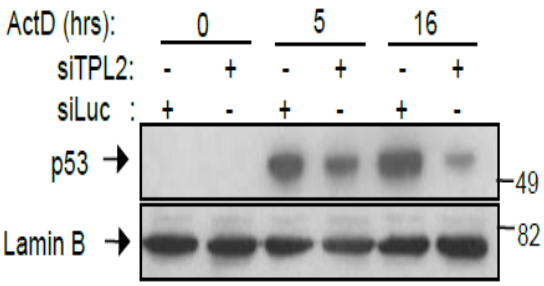

9F.

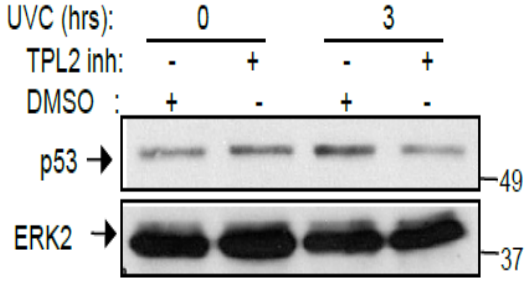

Figure 9 continues overleaf

9G.

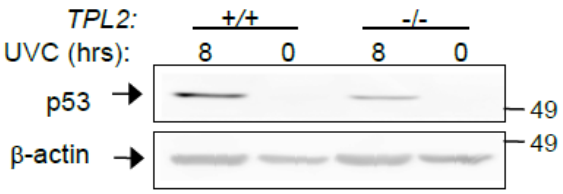

Figure 9. TPL2 regulates p53 levels following genotoxic or ribosomal stress. NPM downregulation (siNPM) hinders p53 accumulation after genotoxic stress of A549 cells induced either by *cis*-platin **(A)** or UVC radiation **(B)**. TPL2 ablation (siRNA) blocks p53 induction in A549 cells following genotoxic stress caused by *cis*-platin **(C)** or UVC radiation **(D)** or ribosomal stress caused by ActD **(E)**. **F**. P53 response to UVC radiation is ameliorated in A549 cells treated with a chemical inhibitor of TPL2 (TPL2inh). DMSO vehicle was used as control. **G**. TPl2 Knock-out (KO) MEFs show reduced p53 accumulation compared to their WT counterparts following UVC treatment. β-actin, Lamin-B and ERK2 were used as loading controls.

In quest of a possible mechanism underlying the observed p53 phenotype in siTPL2 treated cells, HDM2 was immunoprecipitated from A549 cells depleted of TPL2 with siRNA prior to UVC irradiation and HDM2-bound NPM was detected by western blot. As demonstrated in Figure 10A, exposure to UVC led to reduction in total HDM2 levels but increased interaction of HDM2 with NPM, in agreement with a previous report [160]. However, less NPM co-precipitated with HDM2 following TPL2 knock-down. More interestingly, UVC enhanced TPL2 co-immunoprecipitation with NPM and HDM2 simultaneously (Fig. 10B), supporting a docking role of TPL2 in a multi-protein complex necessary for the proper binding of HDM2 with NPM. Based on these data, it was presumed that TPL2 silencing can swift the binding capacity of free HDM2 from NPM towards p53, leading to higher HDM2-mediated p53 ubiquitination and proteasomal degradation. In line with this prediction, treatment with MG132 restored p53 levels in TPL2-depleted cells exposed to UVC (Fig. 10C). The impact of TPL2-mediated p53 accumulation was further investigated on the basis of cell survival. MMT analysis performed on UVC

irradiated A549 cells treated with TPL2 or Luciferase control siRNA (Fig. 10D) shows that whereas UVC normally induces cell death probably through p53-regulated DNA damage mechanisms, the absence of TPL2 rescues partially the phenotype rendering the cells less susceptible to death. Even more interestingly A549 cells transfected with TPL2 siRNA show reduced apoptosis following UVC treatment shown either through caspase 8 (Fig. 10E) or PARP (Fig. 10F) cleavage. Conclusively, it could be speculated that TPL2 is pivotal for normal p53-mediated DNA damage responses that detect cell fate through senescence induction or apoptosis.

10A.

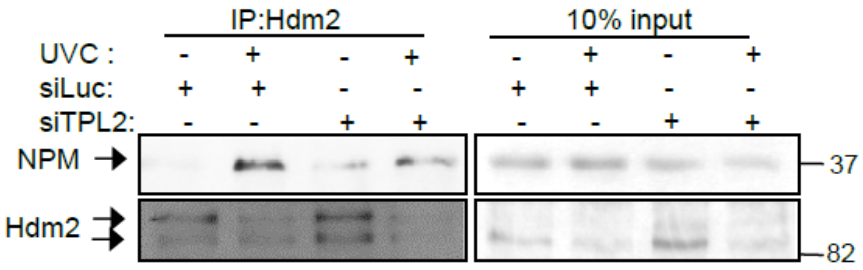

10B.

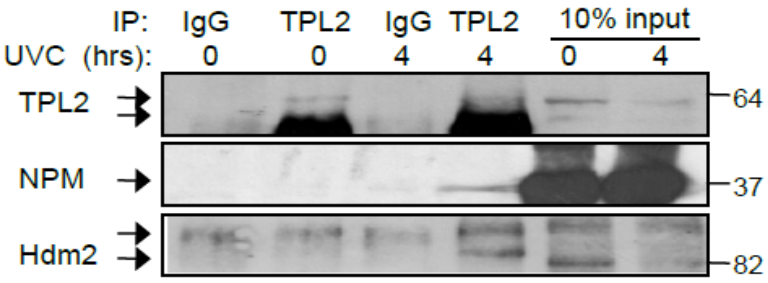

10C.

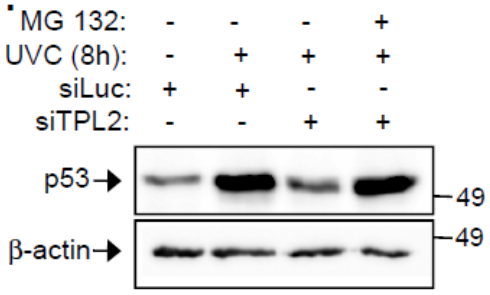

Figure 10 continues overleaf

10D.

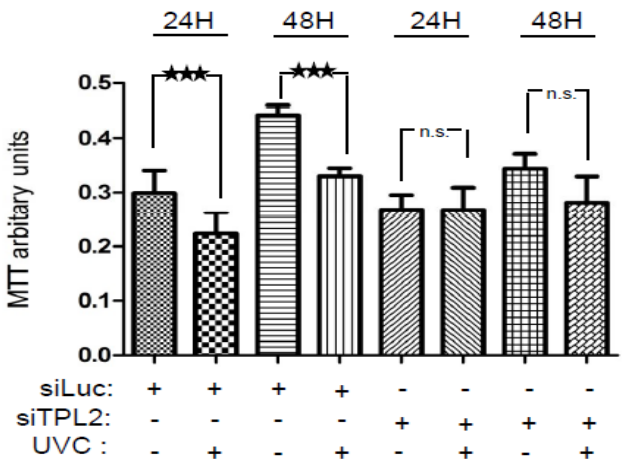

10E.

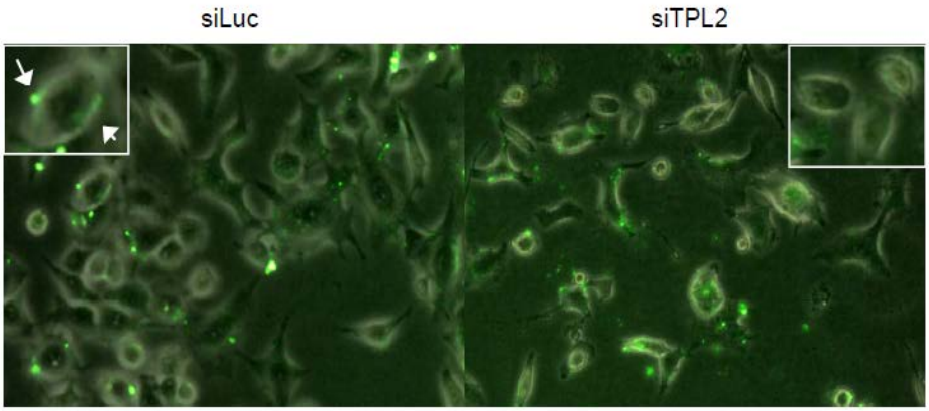

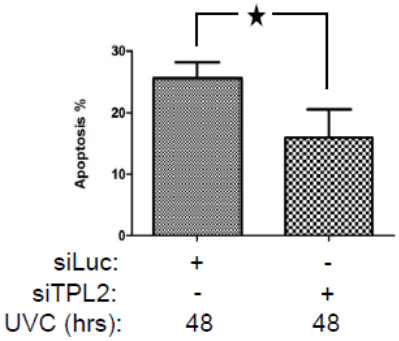

Figure 10 continues overleaf

10F.

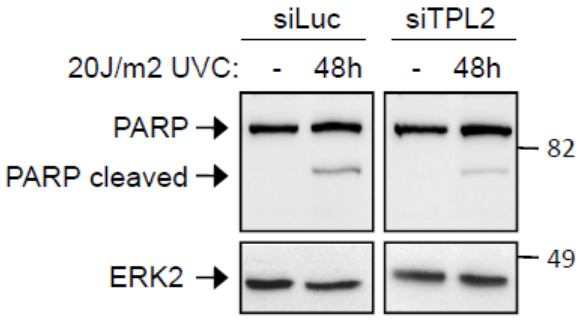

Figure 10. TPL2 regulates the HDM2-NPM-p53 interplay and affects cell survival upon DNA stress. **A.** TPL2 ablation (siTPL2) reduces HDM2-NPM binding after UVC irradiation of A549 cells. **B.** UVC irradiation of A549 cells enhances the interaction between TPL2, NPM and HDM2. **C.** Proteasome inhibitor MG132 rescues the effect of siTPL2 on p53 accumulation following UVC irradiation of A549 cells. **D.** Downregulation of TPL2 with siRNA enhances the survival threshold of UVC-treated A549 cells. Statistical analysis was performed with unpaired t-test (*** $p<0.001$). The figure shows the median of three experiments +/- st.dev. **E, F**. Reduced expression of TPL2 rescues partially the apoptotic effect of UVC on A549 ca cells evidenced here by reduced caspase 8 (E) or PARP cleavage (F). Apoptosis was monitored with the Green FLICA™ Caspase 8 Assay Kit (Immunochemistry Technologies, MN, USA) according to the manufacturer's guidelines. Images were collected with a Leica DM1000 fluorescence microscopy and processed with Image J. 100 cells from three different regions were counted and presented in the graph are the average values (+/- standard deviation) of cells (%) positive for green staining. Unpaired t-test was used for statistical analysis. *: $p< 0.05$.

NPM blocks the transcription of exogenously expressed TPL2.

Following the data presented thus far it was speculated that constant high levels of NPM observed in various human cancer types [80] could be correlated to reduced TPL2 protein levels and activity. To validate this hypothesis, HEK

293T cells were transfected with a combination of MT-TPL2 and increasing concentration of MT-NPM plasmid DNA and total NPM and TPL2 protein levels were detected by immunoblotting. Figure 11A shows a dose-dependent net effect of NPM over-expression on protein levels of exogenously expressed TPL2.

The observed effect was not solely exerted on TPL2 but was further conveyed to its collateral signaling effector molecules ERK and NF-κB1[1]. NPM over-expression ameliorated activation of both proteins, shown either by immunoblotting of pERK (Fig. 11A) or luciferase assays performed with an ERK (Fig. 11B) or an NF-κB1 responsive element (Fig. 11C). The effect of NPM on TPL2 is accomplished (post-) transcriptionally since exogenously expressed NPM had no effect on endogenous TPL2 protein levels detected here by western blot (Fig. 11D). In line with this, NPM over-expression led to reduced TPL2 mRNA levels only in total RNA samples from HEK 293T cells carrying ectopically expressed TPL2 as demonstrated in Figure 11E by qRT-PCR.

11A.

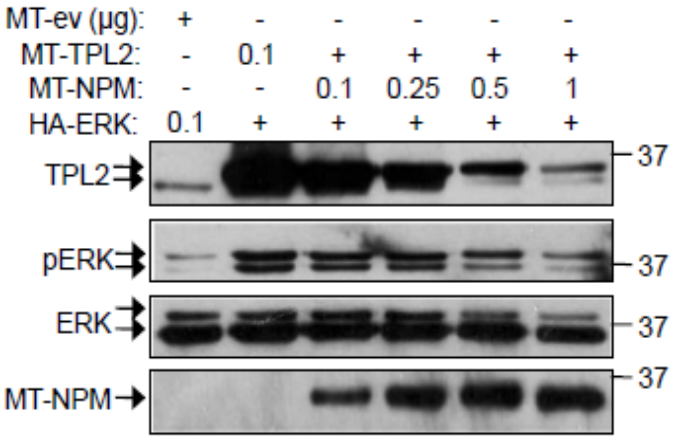

Figure 11 continues overleaf

11B.

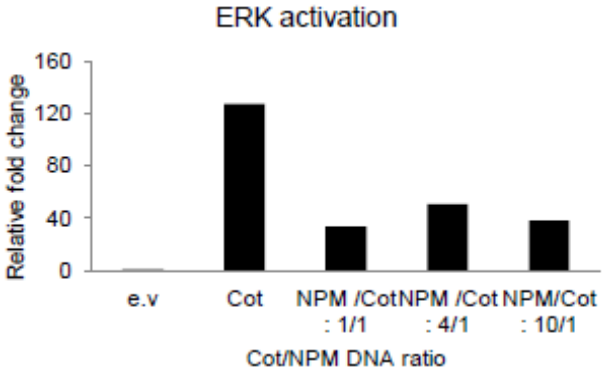

11C.

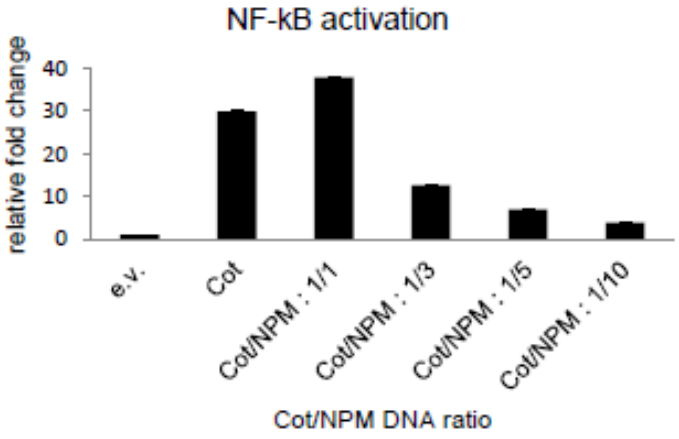

11D.

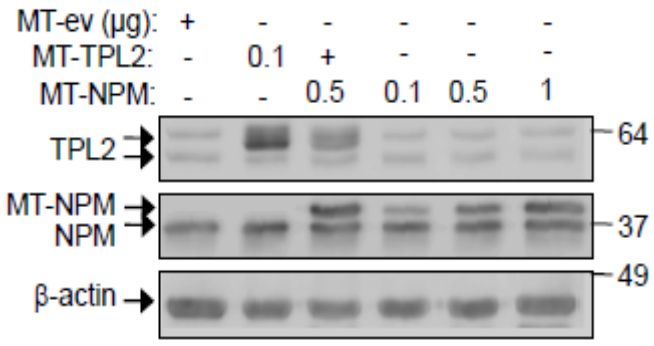

Figure 11 continues overleaf

11E.

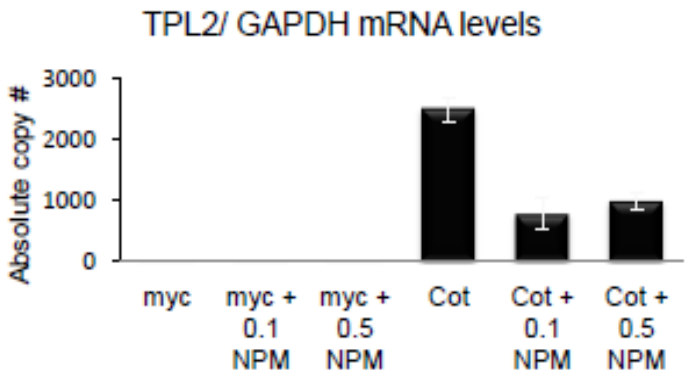

Figure 11. NPM regulates TPL2 transcriptionally. **A.** NPM overexpression reduces TPL2 levels and TPL2-mediated ERK phosphorylation. HEK293T cells were transfected with the indicated plasmid DNA combinations and total protein levels of TPL2, NPM, pERK and ERK (loading control) were detected with western blot. **B.** Overexpression of the proteins indicated in the legend was followed by luciferase assays that show an effect of NPM on TPL2-associated ERK activation. **C**. Exogenously expressed NPM blocks TPL2-mediated NF-κB1 activation shown here by utilization of an NF-κB activation luciferase reporter. **D**. Overexpressed NPM does not affect endogenous TPL2 levels. **E**. The effect of induced NPM expression on TPL2 levels is concluded in the transcriptional level. qRT-PCR of TPL2 mRNA levels (median of three experiments +/- st.dev.) in HEK293T cells transfected with the indicated DNA plasmid combinations.

To investigate the role of NPM on TPL2 regulation under more cancer-related conditions we utilized a plasmid vector bearing the lymphoma-associated fusion product of NPM with ALK [352]. Immunoblotting of TPL2 in lysates from HEK 293T cells transfected with MT-TPL2 in combination with MT-NPM or MT-NPM-ALK (Fig. 12A) showed that over-expression of NPM-ALK led to a more profound reduction of MT-TPL2 levels compared to NPM alone. Even more surprisingly ectopic expression of NPM-ALK reduces the levels of endogenous TPL2 as well, undermining a more complicated mechanism of

TPL2 regulation from the fusion NPM-ALK protein compared to sole NPM. Blocking TPL2 kinase activity with a chemical inhibitor or a plasmid vector containing kinase dead TPL2 did not affect NPM-ALK-mediated constitutive ERK phosphorylation, a hallmark of NPM-ALK-driven cancer pathophysiology [353] as detected by immunoblotting of pERK (Fig. 12B). Combined the data presented here support loss of TPL2 and TPL2-mediated signaling in NPM-ALK positive cells.

12A.

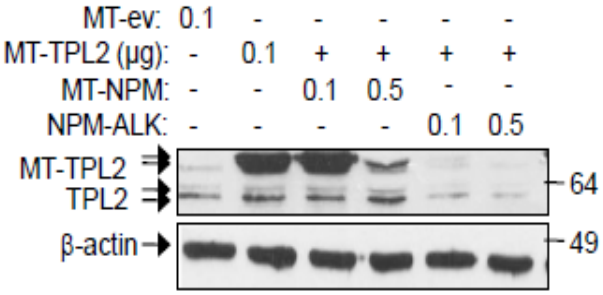

12B.

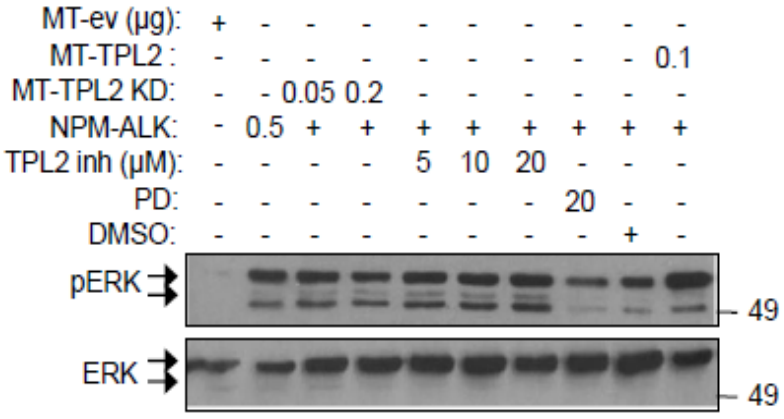

Figure 12. ALCL-related fusion mutant NPM-ALK regulates ERK phosphorylation irrespectively of TPL2. **A.** NPM-ALK overexpression causes reduction of both exogenously expressed and endogenous TPL2. **B.** MEK1 (PD) but not TPL2 inhibition (MT-TPL2-KD, TPL2inh) blocks NPM-ALK-mediated constitutive ERK phosphorylation.

TNF promotes TPL2-IKKα interaction and nuclear colocalization.

Interaction of TPL2 with IKKα was initially shown by co-immnunoprecipitation assays in Jurkat T cells stably expressing MT-TPL2 [11]. In an attempt to validate this interaction under a more physiological-relevant context, immortalized MEFs were treated with TNF, known to affect both IKKα and TPL2-mediated signaling in inflammatory responses [1,188]. Immunoprecipitation of IKKα followed by western blotting of IKKα-bound TPL2 (Fig. 13A) pinpointed the capacity of the two proteins to interact both in unstimulated and TNF-treated cells.

To examine the sub-cellular localization of the two proteins, MEFs (Fig. 13B) or HeLa cells (Fig. 13C) treated or not with TNF were subjected to nuclear versus cytoplasmic fractionation and both TPL2 and IKKα were detected by immunoblotting in both fractions. In line with previous published data [224], TNF treatment of both cell types caused IKKα nuclear translocation. Surprisingly, TPL2 followed similar kinetics implicating that the interaction of the two proteins may take place either in the cytoplasmic or the nuclear compartment. To further evaluate the competence of TPL2 to enter the nucleus we performed immunofluorescence assays either in TNF-treated TPL2 knock out MEFs reconstituted with HA-TPL2 (Fig. 13D) or in HeLa cells (Fig. 13E). Whereas TPL2 showed a profound cytoplasmic localization in unstimulated cultures, it would partially translocate to the nucleus (DAPI) following TNF treatment in a short time frame.

13A.

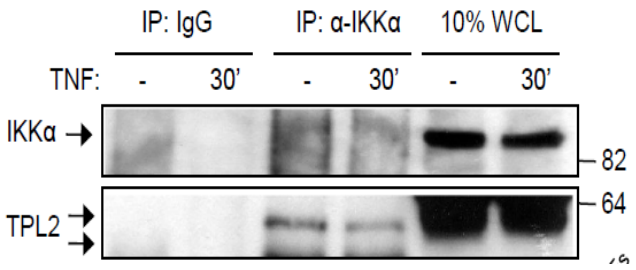

Figure 13 continues overleaf

13B.

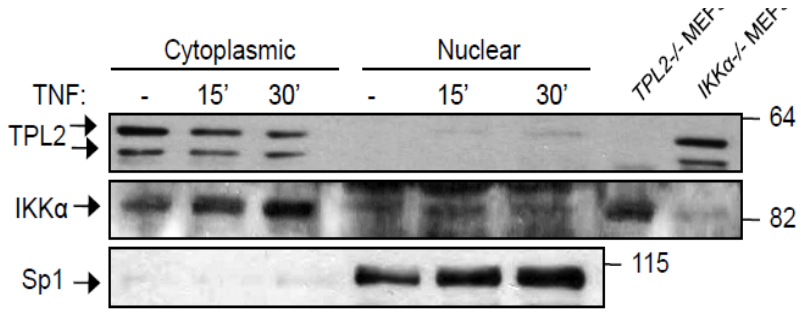

13C.

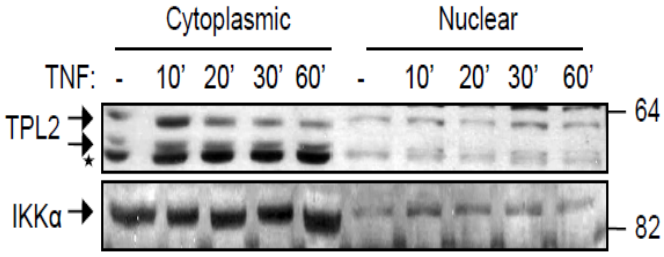

13D.

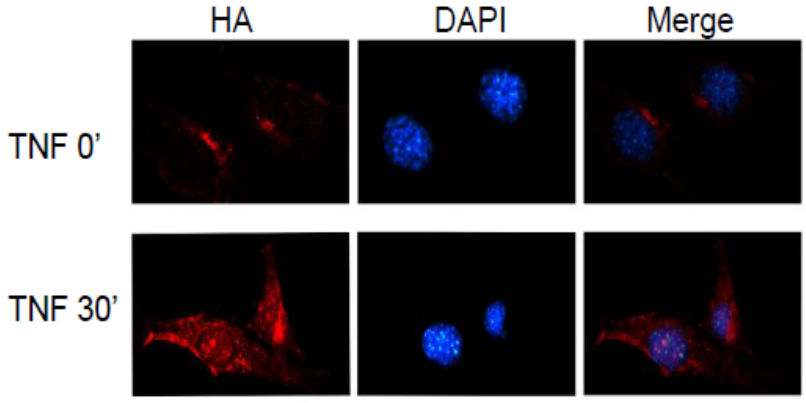

Figure 13 continues overleaf

13E.

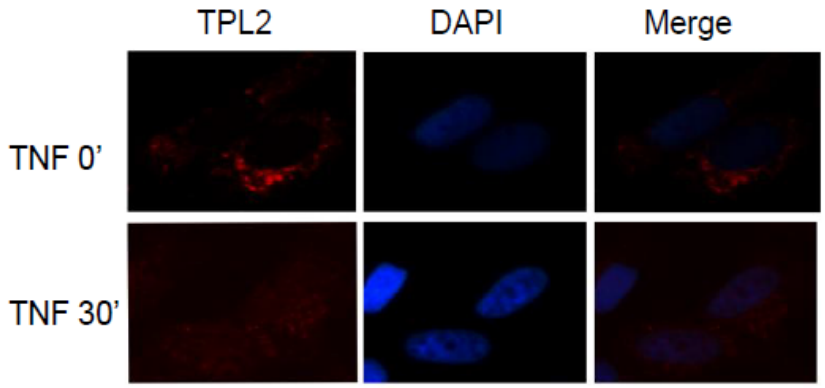

Figure 13. TNF promotes TPL2-IKKα interaction and nuclear co-localization. **A.** TPL2 and IKKα interact *in vivo*. IKKα was immunoprecipitated from WT MEFs treated or not with TNF for the indicated time point and the IKKα-bound TPL2 was detected with Western blotting. **B, C.** TPL2 colocalizes with IKKα both in the cytoplasm and in the nucleus. Immunodetection of TPL2, IKKα and Sp1 (nuclear marker) in WT MEFs (B) or HeLa (C) cervical cancer cells, treated with TNF and fractionated in cytoplasmic/nuclear compartments. Asterisk indicates non-specific band. **D, E**. TNF promotes TPL2 translocation from the cytoplasm to the nucleus. Immunofluoresence (IF) of TPL2 in TPL2 KO MEFs reconstituted with HA-TPL2 expressed in physiological levels (D) or in HeLa cells (E) treated or not with TNF.

TPL2 regulates TNF-induced IL-6 production through IKKα

TNF is known to induce the transcriptional activity of IKKα on IL-6 promoter [224] but no evidence exists up to date that support an implication of TPL2 in this pathway. To address this point we firstly searched whether TPL2 affects IKKα nuclear translocation following TNF stimulation. IKKα localization was detected by immunoblotting in cytoplasmic versus nuclear extracts of WT or TPL2 knock out MEFs treated with TNF. Figure 14A shows that a small fraction of IKKα resides in the nucleus of unstimulated WT MEFs and is slightly enhanced following TNF treatment. TPL2 ablation however, abolishes IKKα nuclear residence not only in TNF stimulated cells but also in untreated

cultures. In line with this, chromatin immunoprecipitation analysis of IL-6 promoter in WT versus TPL2 knock out MEFs treated with TNF revealed a disability of IKKα to bind the promoter of IL-6 in the absence of TPL2 (Fig. 14B). The overall impact of TPL2 on IL-6 production is further demonstrated in Figure 14C. WT or TPL2 knock out MEFs were treated with TNF and the secreted IL-6 was measured with ELISA. TPL2 ablation causes a dramatic reduction on IL-6 in accordance with previously shown data [354]. The same effect is evidenced when TPL2 kinase activity is blocked with a chemical inhibitor.

14A.

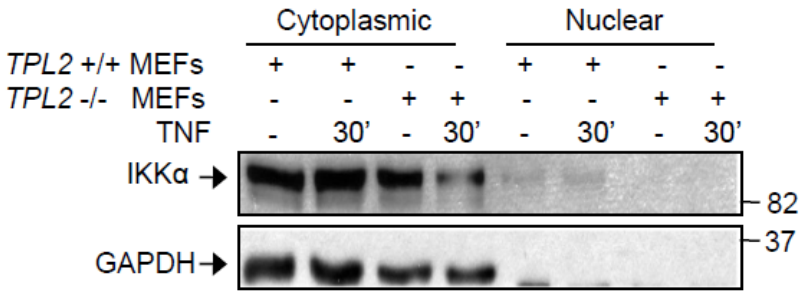

14B.

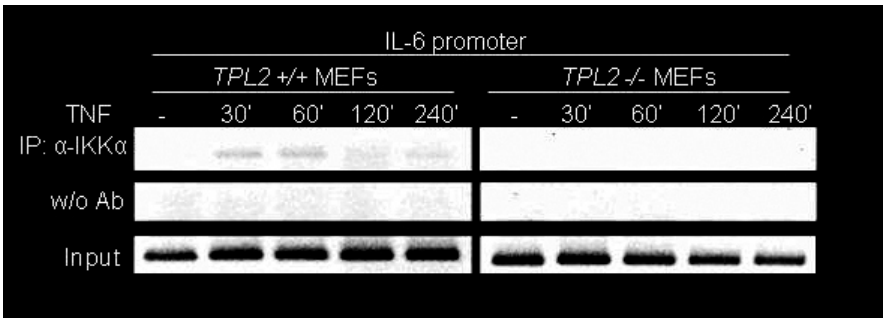

Figure 14 continues overleaf

14C.

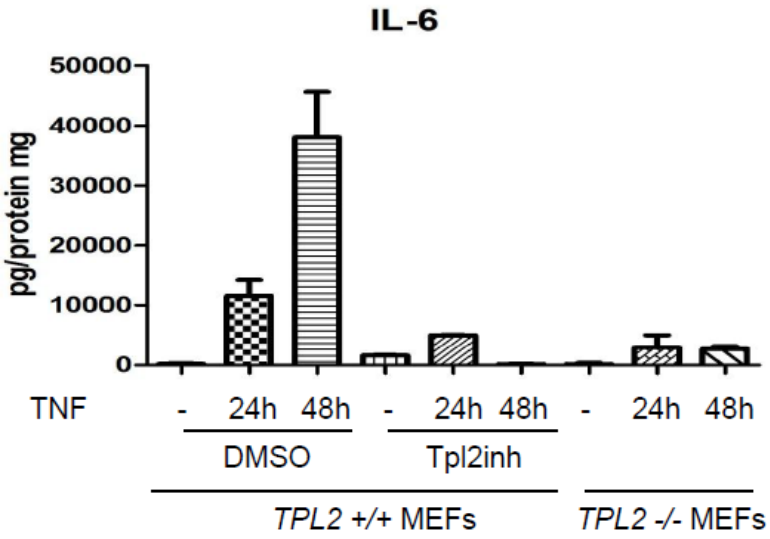

Figure 14. TPL2 regulates TNF-induced and IKKα-mediated IL-6 production. **A.** TPl2 is essential for IKKα nuclear translocation following TNF stimulation. WT- or TPL2 KO MEFs treated with TNF were fractionated in cytoplasmic and nuclear compartments. IKKα and GAPDH (cytoplasmic marker) were detected by immunoblotting. **B.** TPL2 promotes IKKα binding on IL-6 promoter. Ch-IP assay of IKKα on IL-6 promoter in WT- or TPL2 KO MEFs treated or not with TNF for the indicated time course. **C.** TPL2 ablation diminishes the production of secretable IL-6. WT- or TPL2 KO MEFs were treated with TNF and the production of IL-6 was calculated with ELISA in the supernatant. TPL2inh used in parallel in WT MEFs, shows that TPL2 kinase activity is prerequisite for its effect on IL-6 production. Shown here is the median of three experiments +/- st.dev.

TPL2 is not essential for activation of the alternative NF-κB pathway

In quest of a functional relationship between TPL2 and IKKα, we primarily asked whether TPL2 participates in the activation of the alternative NF-κB pathway, known to be regulated by IKKα [214]. To this end, HEK 293T cells were transfected with plasmid DNA carrying MT-TPL2 in combination or not with MT-NF-κB2 and the processing of NF-κB2 was detected by

immunoblotting (Fig. 15A). TPL2 over-expression led to a slight enhanced processing of ectopically expressed NF-κB2 but showed no profound effect in the endogenous p100 to p52 processing. Under the same conditions HA-NIK showed robust NF-κB2 activation in line with previous reported data [355]. Implication of TPL2 in the alternative NF-κB pathway was further quested in a more physiological relevant context. Primary B cells were extracted from WT or TPL2 knock out mice and stimulated with CD40L, one of the most effective inducers of the alternative NF-κB pathway [355]. TPL2 ablation did not alter NF-κB2 processing showed in Figure 15B by immunoblotting.

The incompetence of TPL2 to activate the alternative NF-κB pathway was also evidenced in primary bone marrow derived macrophages (BMDM) extracted from WT or TPL2 knock out mice. As expected, treatment of the cells with CD40L for various time points led to TRAF3 degradation (Fig. 15C) a hallmark of the alternative NF-κB pathway activation. The absence of TPL2, however failed to affect TRAF3 kinetics.

15A.

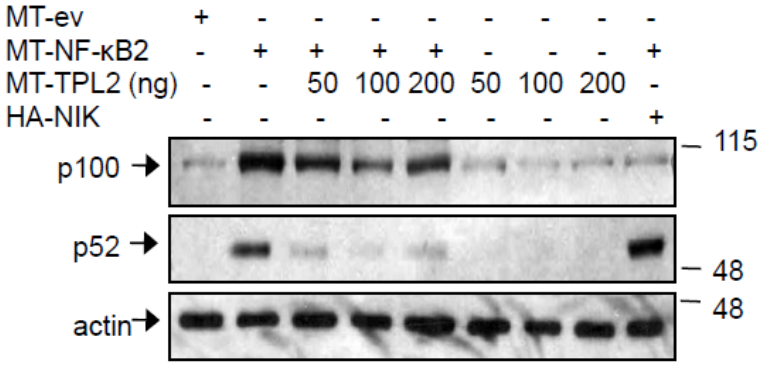

Figure 15 continues overleaf

15B.

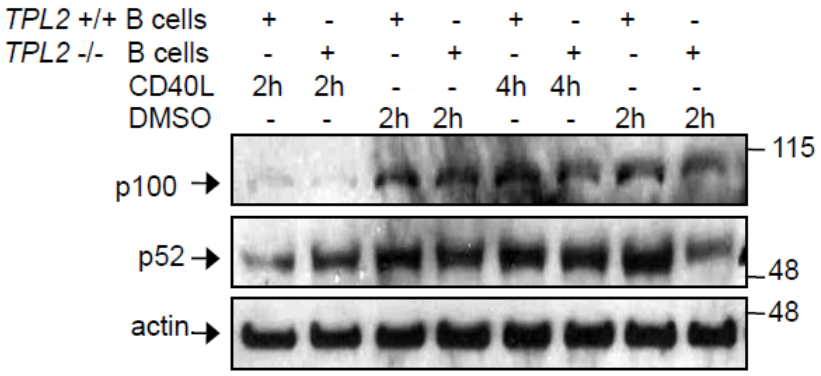

15C.

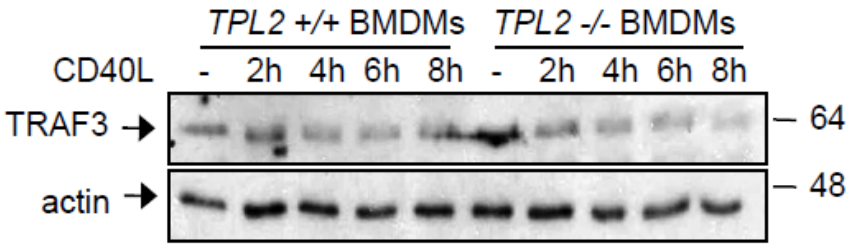

Figure 15. TPL2 is not implicated in the activation of the alternative NF-κB pathway. **A**. Overexpressed TPL2 does not affect basal NF-κB2 processing. HEK293T cells were transfected with the indicated plasmid DNA mixture and NF-kB2 processing was detected with western blot. HA-NIK was used as a positive control. **B.** Activation of the alternative NF-κB pathway shows no significant difference in WT- or TPL2 KO primary B cells stimulated with CD40L for the indicated time points. **C, D.** CD40L does not promote TPL2-mediated activation of the alternative NF-κB pathway shown here through TRAF3 degradation in WT versus TPL2 KO primary BMDMs stimulated for the indicated time points.

TPL2 and IKKα synergize in MAPK but not NF-κB activation downstream of TNF.

Being unable to implicate TPL2 in the activation of the alternative NF-κB pathway, we then asked whether IKKα could affect signaling cascades orchestrated by TPL2. To this end, immortalized WT or IKKα MEFs were treated with TNF in the presence or absence of a TPL2 kinase chemical inhibitor for various time points (Fig. 16A). Activation of the ERK and JNK MAP kinases as well as canonical and non-canonical NF-κB pathway processing, detected with immunoblotting, showed that simultaneous ablation of IKKα and TPL2 kinase activity ameliorated ERK and JNK phosphorylation following TNF treatment of MEFs. On the contrary, IKKα had no impact on NF-κB activation irrespective of TPL2 ability to act as a kinase. More specifically, IKKα ablation did not affect either IκBα degradation, serving here as an activation marker for the canonical pathway, or NF-κB2 processing. The inability of IKKα to promote the activation of the canonical NF-κB pathway was further demonstrated with p65 nuclear translocation by immunofluorescence in WT versus IKKα knock out MEFs treated with TNF or left unstimulated (Fig. 16B). Proper use of TNF in these experiments was ensured by western blot analysis of ERK phosphorylation and IκBα degradation (Fig. 16C) in WT or TPL2 knock out MEFs treated with TNF as previously described [354].

16A.

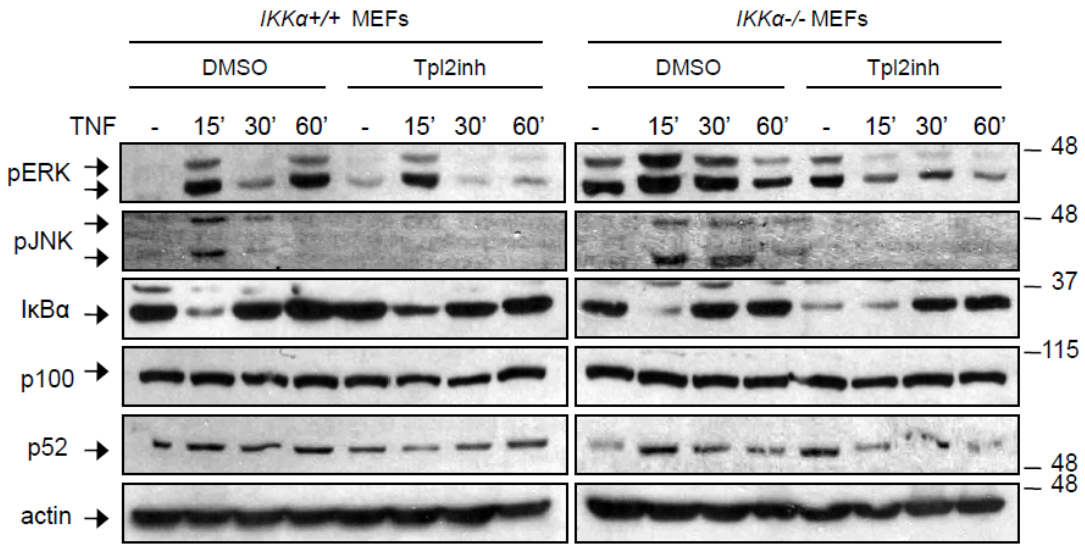

Figure 16 continues overleaf

16B.

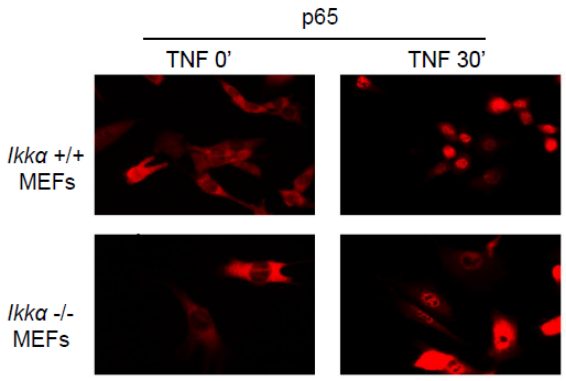

16C.

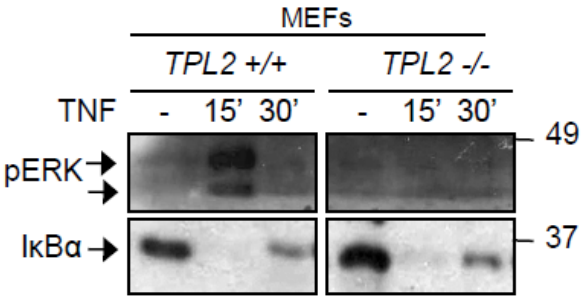

Figure 16. TPL2-IKKα functional interaction in the activation of MAPK and NF-κB pathways. **A.** Western blot analysis of various MAPK and NF-κB pathway mediators in WT- or IKKα KO MEFs treated or not with TNF +/- TPL2inh for the indicated time points. **B.** Immunofluoresence showing nuclear translocation of cytoplasmic p65 in WT versus IKKα MEFs stimulated or not with TNF for 30 min. **C.** Immunoblotting of pERK and IκBα degradation following TNF stimulation of WT or TPL2 KO immortalized MEFs.

TPL2 modulates the expression of microRNAs mmu-let-7a, mmu-let-7i and mmu-miR-223 downstream of TNF.

Having shown that TPL2 is able to regulate both DNA damage and inflammatory responses, it was surmised that it could orchestrate the cross-talk of the related signaling pathways. To address this issue, primary bone

marrow cells (converted to BMDMs in the presence of GM-CSF) were extracted from WT or TPL2 knock out mice and cultured as monolayers until reaching 80% confluency. Following treatment with TNF for various time points, the cells were lysed and the RNA was extracted and used as raw material for a microRNA (miRNA) microarray analysis performed in the laboratory of Dr. D. Iliopoulos (Harvard Medical School). Differential expression of miRNAs affected either solely by TNF (Fig. 17A) or by the combination of TNF and TPL2 ablation (Fig. 17B) supported a significant diversity of miRNAs implicated in TNF-mediated inflammatory signaling pathways. Proper maturation of bone marrow cells towards the macrophage lineage (BMDMs) was detected by FACS analysis of CD11b/F480 double positive cells (Fig. 17C).

17A.

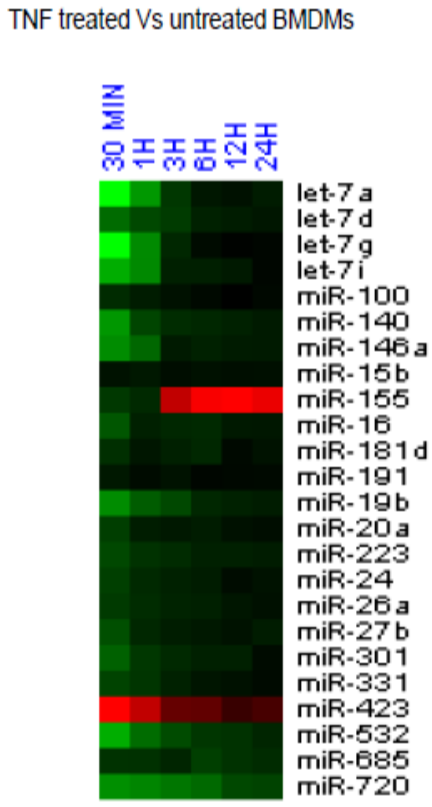

17B.

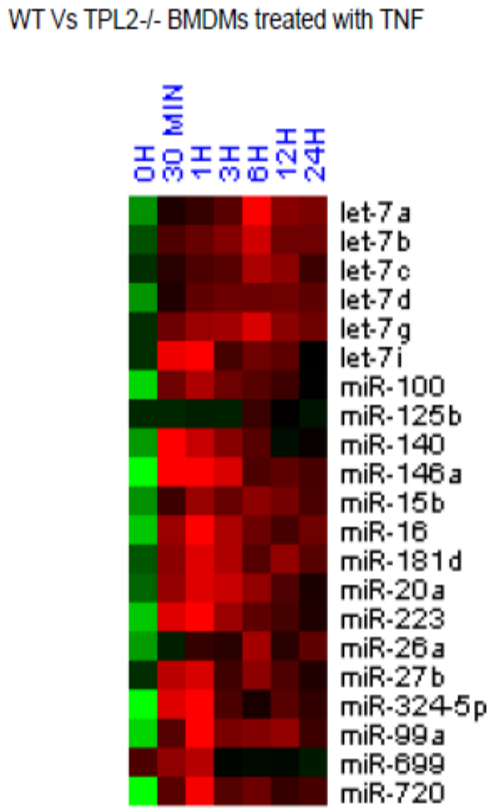

Figure 17 continues overleaf

17C.

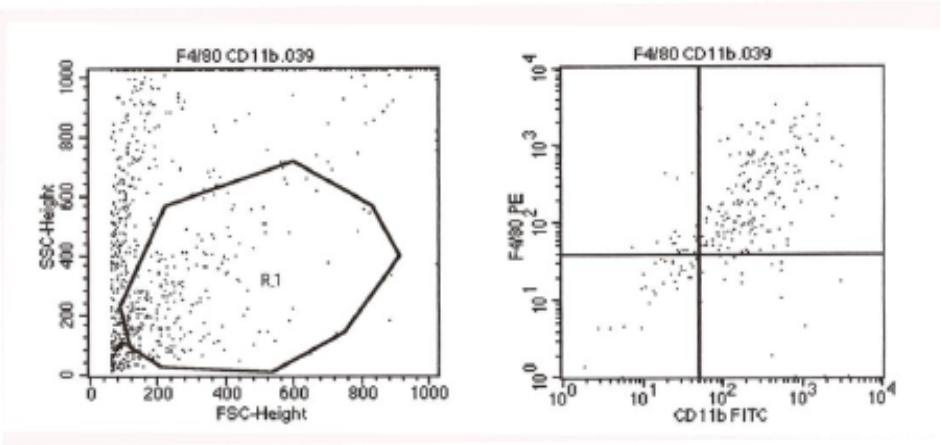

Figure 17. TNF and TPL2 regulate synergistically the expression of various miRNAs. **A, B**. MiRNA microarray expression profile analysis in RNA samples from primary BMDMs treated or not with TNF for the indicated time points (A) or in WT- versus TPL2 KO BMDMs treated with TNF (B) for the time course depicted. RNA was extracted from cells collected and pooled from at least 3 mice (of matched age and sex) per condition. Green colour density in (A) represents suppression, while red shows expression enhancement. In (B) red colour density is proportionate to the difference in expression values detected in WT versus KO cells. **C.** Differentiation of bone marrow cells to macrophages was calculated as the percentage of CD11b/F480 double positive cells detected with FACS (representative figure).

Following thorough interpretation of the microarray data, it was decided to focus on miRNAs targeting IL-6 as this cytokine was already shown to be regulated by TPL2 (Fig. 16). The pool of miRNAs showing a differential expression pattern after TNF stimulation of WT or TPL2 knock out BMDMs (Fig. 17B) was filtered *in silico* based on the miRanda algorithm (http://www.microrna.org/microrna/home.do). Three miRNAs were found (Fig. 18A) to bind efficiently the 3' UTR of IL-6 mRNA and their expression was further validated with qRT-PCR (Fig. 18B-D). In all cases TNF caused a

gradual reduction in miRNA expression levels which was either accelerated (mmu-let-7a, mmu-let-7i) or even changed to increase (mmu-miR-223) in the absence of TPL2.

18A.

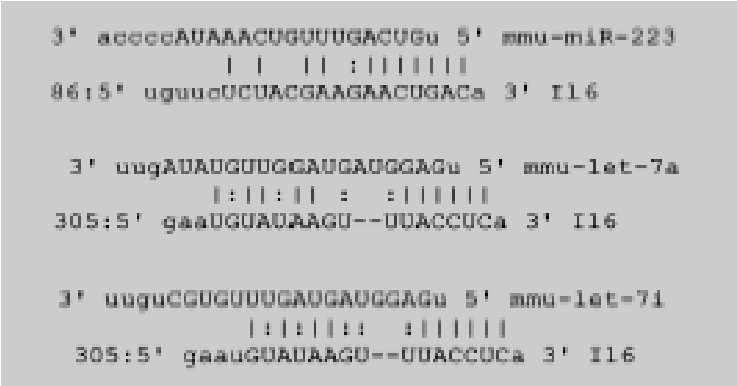

18B.

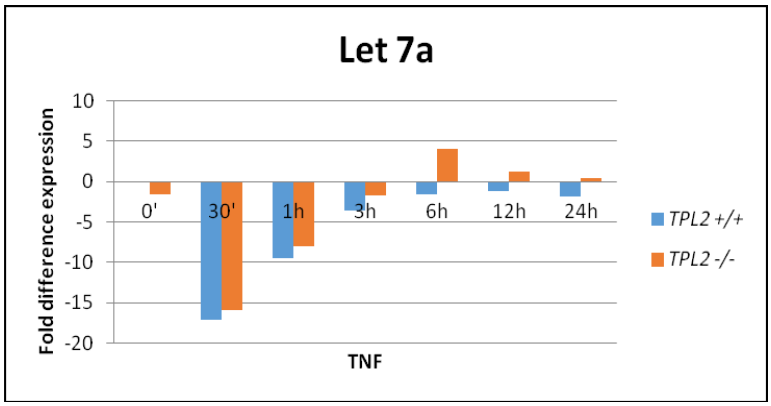

18C.

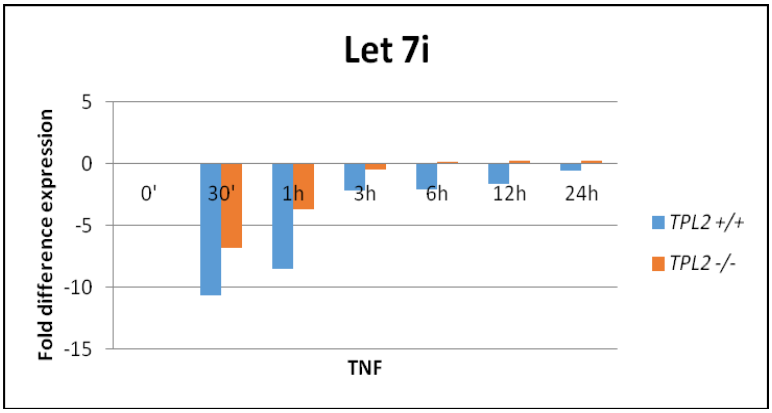

Figure 18 continues overleaf

18D.

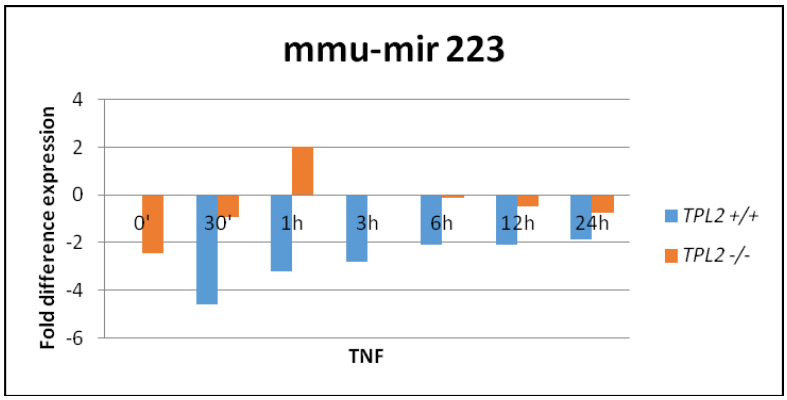

Figure 18. TPL2 is essential for the proper induction of various IL-6-related miRNAs following TNF treatment. **A.** *In silico* prediction of miRNAs targeting IL-6 mRNA using the miRanda database (http://www.microrna.org /microRNA/ home.do). qRT-PCR analysis of miRNAs let-7a **(B)**, Let-7i **(C)** and mmu-mir-223 **(D)** in total RNA of WT versus TPL2 knock out BMDMs treated with TNF for the indicated time points.

The impact of miRNA activity on IL-6 production was thence investigated in a two-fold manner. RNA was extracted from WT or TPL2 knock out BMDMs treated with TNF or left unstimulated and the IL-6 mRNA levels were measured with qRT-PCR. Following TNF treatment of WT TPL2 BMDMs, IL-6 mRNA levels oscillate through an immediate increase one hour post-treatment followed by a gradual decrease. However, this effect of TNF on IL-6 mRNA was ameliorated in the absence of TPL2 (Fig. 19A). Furthermore, ELISA-based detection of secreted IL-6 in the cell medium of WT versus TPL2 knock out BMDMs treated or not with TNF showed a robust upregulation of IL-6 levels upon TNF treatment in WT TPL2 BMDMs which was blocked in the absence of TPL2 or when its kinase activity was ameliorated with a chemical inhibitor (Fig. 19B) in line with previously shown data on MEFs (Fig. 16C).

19A.

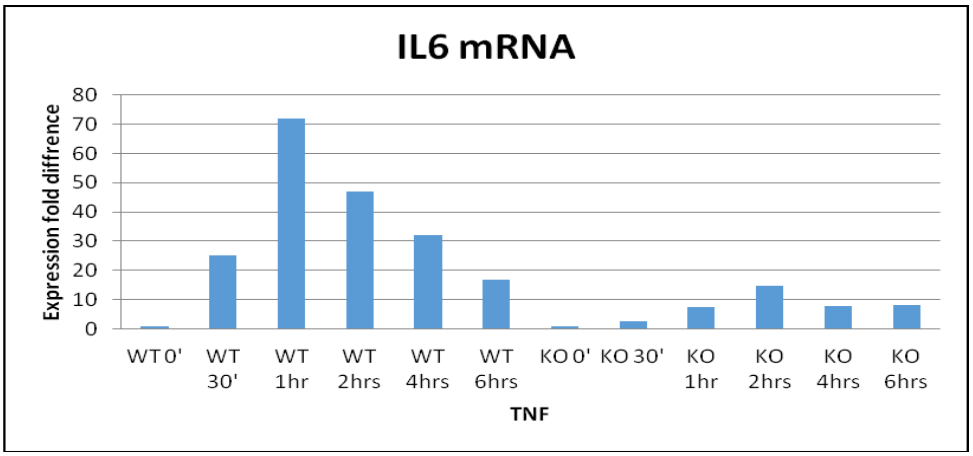

19B.

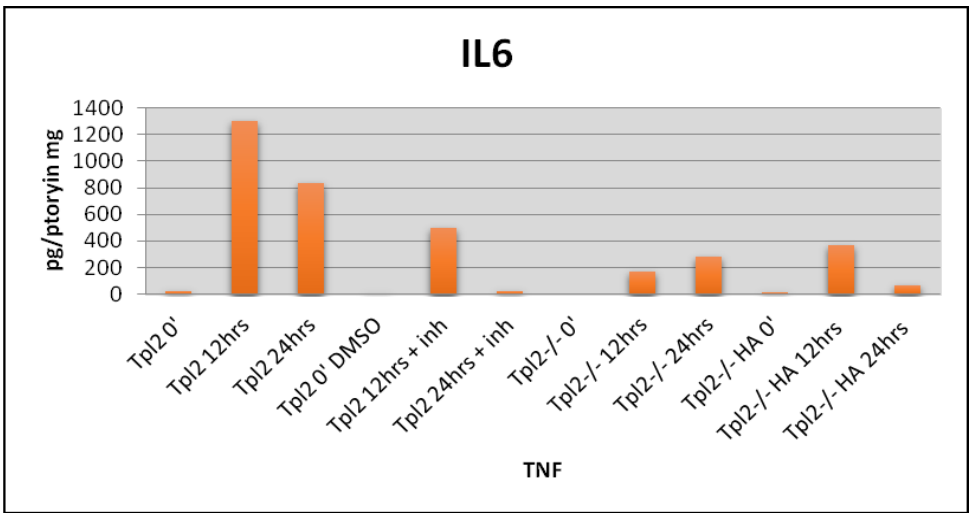

Figure 19. TPL2 regulates the physiological levels of IL-6. **A.** qRT-PCR analysis of IL-6 mRNA levels in WT versus TPL2 KO BMDMs treated or not with TNF for the time course indicated. **B.** IL-6 secretion measured with ELISA in WT or TPL2 KO BMDMs treated or not with TNF. Blocking the kinase activity of TPL2 with a chemical inhibitor (TPL2inh) resumes the effect of TPL2 ablation on IL-6 secretion.

DISCUSSION

NPM-TPL2

Nucleophosmin (NPM, B23) is a multitasking nucleolar phosphoprotein, vital for cell survival as evidenced from the fact that *npm-/-* mice die *in utero* and show high susceptibility in developmental defects linked to p53-associated tumorigenesis [78]. As such, its tight regulation is of paramount importance for cell physiology supported by the fact that loss of proper NPM function associated with point mutations or fusion-protein chimeras directly relate to a wide range of blood or solid cancers [80]. Appealing data underlie a cascade of serial NPM phosphorylation events during the cell cycle that altogether secure a proper cell division [80]. Little is known however, of MAP kinases being directly involved in NPM post-translational regulation. The present thesis presents novel data regarding NPM interaction with the MAP3 kinase TPL2/Cot. Originally identified as a proto-oncogene, TPL2 was mainly associated with inflammatory and immune responses [20,36]. During the last years however, accumulative data connected TPL2 to cancer either as pro- or anti-tumorigenic molecule [56,70]. A recent publication from our lab pinpointed the protective role TPL2 plays in the establishment of lung cancer in human specimens and a chemically-induced lung cancer mouse model [71]. A possible molecular mechanism underlying this effect of TPL2 is presented herein in an effort to resolve TPL2 role in tumor biology.

In agreement with unpublished data rising from a high-throughput proteomics MS/MS analysis described elsewhere [346], ectopically expressed TPL2 in HEK 293T cells was found to interact *in vitro* (GST pull down assays) and *in vivo* (co-immunoprecipitation assays) with NPM (Fig. 1). The observed interaction could not be attributed to aberrant TPL2 levels achieved through transfection of the cells, since endogenous proteins could also interact sufficiently and their association was enhanced upon UVC irradiation, a stimulus known to cause a p53-dependent DNA damage response regulated by NPM [161].

Being able to bind NPM *in vivo*, TPL2 was suspected to regulate the function of its partner. The pleiotropic character of NPM activities is close related to its sub-cellular localization and thus it comes as no surprise that it bears NoLS, NLS and NES signal peptides rendering the protein capable of constantly

translocating between subnuclear compartments and the cytoplasm [83]. Surprisingly enough, we show that a portion of TPL2 localizes in the nucleus as well, either at steady state, when the protein is ectopically expressed or under genotoxic stress initiated by UVC radiation or treatment with the anti-cancer agent *cis*-platin (Fig. 2, 3). This finding is in line with an article supporting TPL2 nuclear translocation under UVB irradiation [51], but since TPL2 lacks a “canonical” nuclear localization signal it was speculated that it’s nuclear translocation could be supported by a chaperone, reminiscent of the cytoplasmic kinases Raf-1 and Akt2, which have also been described to partly localize to the nucleus and confer nuclear functions [96,356].

Even though both TPL2 and NPM could be found in the nucleus, the specific sub-cellular compartment where their association takes places was still under question. This issue was addressed with immunofluorescence experiments supporting NPM-TPL2 nuclear co-localization following UVC radiation, while in depth analysis of fractionated cells under the same conditions (Fig. 3) high-lightened the nucleoplasm as the sub-nuclear domain where both proteins concentrate following genotoxic stress. These observations led to the conclusion that UVC irradiation primes TPL2 translocation to the nucleoplasm, where it could bind the portion of NPM leaving simultaneously the nucleoli towards the nucleoplasm in line with previous reported data [177]. As proof of evidence, TPL2 could preferentially bind to NPM inside the nucleus rather in the cytoplasm, evidenced by GST pull-down and co-IP assays in fractionated cells (Fig. 4) and this interaction was enhanced following UVC radiation.

In order to set the NPM-TPL2 interaction under a functional perspective, TPL2 was either silenced with RNAi (A549 cells) or ablated (MEFs) and focus was driven towards two major hallmarks of NPM response to genotoxic or ribosomal stress. TPL2 amelioration was shown to affect both NPM nucleoplasmic translocation (Fig. 3) and upregulation (Fig. 5) normally evidenced under these circumstances [161,177]. The dual effect of TPL2 on NPM was shown under various stimuli (UVC, *cis*-platin, ActD) and in more than one cell lines excluding thus the possibility of random observed data and underlining a robust, universal role of TPL2 in NPM physiology.

NPM is subject to various post-translational modifications that define its sub-cellular localization and stability. NPM phosphorylation by CDK/cyclin complexes orchestrate its proper binding to the centrosomes and subsequent formation of the mitotic spindle [146]. Being a bona-fide kinase, TPL2 was suspected to phosphorylate NPM supported by the fact that kinase dead TPL2 was incompetent to bind NPM neither in the cytoplasm nor in the nucleus (Fig. 4). In line with this, utilization of a TPL2 chemical kinase inhibitor recapitulated the effect of TPL2 silencing on NPM nucleoplasmic translocation following UVC radiation (Fig. 3). The precise residue of NPM however, affected by TPL2 was unknown. To address this, NPM was subjected to serial truncation events and used in GST-pull down assays with TPL2 (Fig. 6). The data high-lightened the NPM region between aa 188-244 as pivotal for the interaction with TPL2. Even though there are numerous phosphorylation competent NPM residues within this region [83], we decided to focus on Thr^{199}, since it has been reported that it affects the dissociation of NPM from nucleolar components [351], NPM recruitment to DNA damage foci and its participation in DNA repair mechanisms [181,357]. Although previous studies have shown that NPM is phosphorylated at Thr^{199} by the cyclin E/cdk2 complex [146] and becomes de-phosphorylated by the phosphatase PP1β following cell exposure to UV [357], it has been proposed that additional kinases must be utilized to phosphorylate Thr^{199} as this NPM modification is detected throughout the cell cycle and inhibition of cdk2 does not impair Thr^{199} phosphorylation [159]. Our data show that knocking down TPL2 with RNAi alleviates NPM phosphorylation at Thr^{199} (Fig. 7) at steady state and accelerates dephosphorylation following UVC treatment. In line with this, blocking TPL2 kinase activity with a commercial available inhibitor in concentrations similar to those used to deactivate TPL2 in the TNFRI-MEK-ERK axis [12] has the same impact on NPM phosphorylation while *in vitro* kinase assays support that the effect of TPL2 on NPM phosphorylation at Thr^{199} is direct (Fig. 7).

Even though TPL2-mediated NPM phosphorylation could explain the impact of TPL2 on NPM localization under genotoxic stress, no former data could relate this event to the regulation of its stability. Whilst *de novo* transcription

may also associate with the protein levels under these conditions [175], the physical association of TPL2 with NPM oriented our research to previously reported stability-related post-translational modifications such as NPM SUMOylation mediated by Akt [96] or K48-linked ubiquitination by EDAG and ER [97,98]. Having excluded the possibility that Tpl2 could affect NPM SUMOylation status either at steady state or in UVC-induced stress (Fig. 8) we focused on ubiquitination events. To our surprise RNAi-mediated TPL2 silencing ameliorated MG132-associated NPM ubiquitination (Fig. 8) and this posed an interesting finding since TPL2 is not known to date to possess E3 ubiquitin ligase properties, nor to affect the only known NPM E3 ubiquitin ligase BRCA1/BRDA1 [92]. We speculated, thus, that NPM ubiquitination might associate with a phosphorylation event mediated by the kinase TPL2 and this was proven by the fact that a phosphorylation incompetent mutant of NPM at Thr^{199} (Thr^{199}→Ala substitution) impeded TPL2-mediated NPM ubiquitination. In search of a possible NPM ubiquitination site affected by its phosphorylation at Thr^{199} we focused on Lys^{229} and Lys^{230} within the 188-244 aa NPM region shown to be essential for the interaction with TPL2 (Fig. 6). Since Lys^{230} substitution to arginine (Lys^{230}→Arg) did not affect NPM sub-cellular localization [95], we decided to focus on Lys^{229}. Substitution of this lysine to arginine (Lys^{299}→Arg) rescued the phenotype of T199A on NPM ubiquitination status showing thus for the first time that NPM Lys^{299} was a ubiquitination site specifically associated with NPM phosphorylation at Thr^{199}. Although proteasomal inhibition with MG132 did not rescue total NPM levels following UVC irradiation of siTPL2 treated cells it could however, compensate the UVC-triggered reduction in Thr^{199} phosphorylation levels irrespectively of TPL2 total protein levels (Fig. 8). This fact indicates that the phosphorylated form represents a pool of NPM which is preferentially targeted for degradation.

Together these data support the hypothesis that Tpl2 phosphorylates NPM at steady state, a fact that is closely linked to constant pNPM ubiquitination-degradation and maintenance of normal NPM levels. Following genotoxic or ribosomal stress NPM gets partially dephosphorylated a signal that triggers NPM stabilization and nucleoplasmic exodus (Fig. 3, 8). Dephosphorylated or

unphosphorylated NPM dimerized with pNPM prior to genotoxic stress travels to the nucleoplasm and competes with HDM2 for p53 binding thereby protecting the latter from HDM2-mediated degradation [160] and allowing the cell to engage p53-mediated cell cycle arrest and/or senescence mechanisms in DNA damaged cells [93,161].

Ablation of TPL2 or reduction of its levels, a feature of some common forms of human cancer[1], leads to significant inhibition of p53 activation following genotoxic or ribosomal stress (Fig. 9), similar to NPM knock-down as previously described [164]. The effect of TPL2 on p53 stabilization is mediated through NPM inasmuch as TPL2 participates in a UVC-induced multi-protein complex with HDM2 and NPM and the knock down of TPL2 results in decreased interaction of NPM with HDM2 in DNA damaged cells (Fig. 10). In agreement with this finding, blocking proteasomal function with MG132 to prevent HDM2-mediated p53 ubiquitination restores p53 levels in TPL2-ablated cells exposed to UVC. The overall outcome of the mechanism presented here is the enhanced survival of A549 cells following UVC irradiation when TPL2 is knocked down with RNAi compared to control siRNA treated cells (Fig. 10).

The gradual reduction of TPL2 following UVC radiation (Fig. 5) that cannot be reversed by blocking the proteasome with a chemical inhibitor (Fig. 8) and the simultaneous NPM upregulation under the circumstances prompted our investigation towards the existence of a regulatory feedback loop between the two proteins. Quite interestingly, NPM overexpression that could resemble the physiological upregulation of the protein in DNA damage responses [160] caused a reduction in TPL2 protein levels and TPL2-associated signaling cascades. NPM-mediated TPL2 regulation takes place probably in a transcriptional or a post-transcriptional level since the effect could not be observed in endogenous, rather in exogenously expressed TPL2 (Fig. 11). Cancer-related NPM aberrant expression [80] could thus block a simultaneous raise in TPL2 levels, depriving the cell of a proper response to genotoxic stimuli through the TPL2-NPM-p53 axis as shown in the present thesis. Even more interestingly, ALCL-associated NPM fusion chimera with ALK [353] seems

to avoid TPL2-mediated surveillance in a two-fold manner. First, NPM-ALK lacks the region of NPM [358] that interacts with TPL2 according to the data presented here, meaning that TPL2 cannot regulate post-translationally NPM-ALK. Secondly, the residual NPM molecules rising from the heterozygotic character of NPM-ALK production [359] , cannot be regulated by TPL2 since NPM-ALK downregulates not only ectopically expressed but also endogenous TPL2 (Fig. 12) and renders the kinase incapable of exerting its effects on established downstream effectors such as ERK [20]. This observation could possibly explain the tumorigenic role of NPM-ALK-mediated constitutive ERK phosphorylation [360].

TPL2-IKKα

The concept of inflammation-associated carcinogenesis has lately started to attract attention due to epidemiological and genetic-linkage data, that connect chronic inflammation cases to tumor initiation and progression [361]. Of paramount importance in the interplay of these pathological conditions are the cytokines secreted by immunoregulatory cells that can either promote or suppress an arising tumor, depending on the extent of their induction or their effect on regulation of other proteins and genes [362]. The attraction of tumor-associated macrophages (TAMs) in the inflammatory milieu is linked to the secretion of multiple cytokines such as TNF and IL-6 that exert their functions on by-standing fibroblasts and epithelial cells promoting their epithelia to mesenchymal transition, a hallmark of carcinogenesis [363]. IL-6 production downstream of TNF stimulation was shown to be TPL2- and IKKα-mediated [224,354], both of which have been implicated in carcinogenic mechanisms [71,239]. Although TPL2 and IKKα associate when over-expressed in T cells [364], no evidence up to date supports a functional association downstream of TNFRI signaling. We show here for the first time a novel interaction of endogenous TPL2 with IKKα at steady state, which is gradually reduced upon TNF treatment, following probably the kinetics of TPL2 under the circumstances (Fig. 13).

TNF promotes IKKα [224] and TPL2 nuclear translocation (Fig. 13) but TPL2 ablation blocks IKKα nuclear residence not only in TNF-stimulated cells but also in untreated cultures supporting a cytoplasmic rather than a nuclear effect of TPL2 on IKKα (Fig. 14). The incompetence of IKKα to enter the nucleus in the absence of TPL2 is followed by its inability to bind IL-6 promoter and upregulate its gene expression downstream of TNF as previously shown [224]. This could explain the defect in IL-6 secretion in mouse fibroblasts lacking TPL2 (Fig. 14) in line with data shown in the past [354]. Reduced IL-6 production is also observed when TPL2 kinase activity is blocked with a chemical inhibitor raising thus the suspicion that upon TNF stimulation, TPL2 may directly phosphorylate IKKα to render it capable of nuclear translocation and IL-6 promoter engagement. A direct effect is further supported by the fact that TPL2 is not interfered in the regulation of the alternative NF-κB pathway (Fig. 15), in the process of which IKKα is pivotal [355]. Even more interestingly, TNF-induced processing of the canonical NF-κB pathway is not affected by the ablation of IKKα irrespective of TPL2 kinase activity (Fig. 16). Nevertheless, IKKα absence is associated with aberrant activation of ERK and JNK upon TNF stimulation, a phenotype that is reversed by simultaneous blocking of TPL2 kinase activity with a chemical inhibitor. Since both MAP kinases are activated through TPL2 downstream of TNFRI signaling [354] and affect IL-6 production in this context, we can conclude that TPL2 mediates TNF-induced and IKKα-mediated IL-6 production in two ways. TPL2-IKKα association is essential for proper induction of ERK and JNK following TNF stimulation and at the same time TPL2 mediates IKKα nuclear translocation. The net effect is the induction of the pro-inflammatory and carcinogenesis-related IL-6. Anti-TNF molecules are already the pipeline drugs against various autoimmune diseases [365] while their role against cancer is also under investigation [366]. The presence of side-effects however drives research to the discovery of new, more specific targets and the present study supports a promising solution through a simultaneous block of both TPL2 and IKKα activity that could eliminate the production of pro-inflammatory cytokines.

TPL2-miRNAs

The idea that small chemical protein inhibitors can substitute traditional therapies for cancer due to their effectiveness and easy administration has enjoyed mounting support in recent years [367]. Apparently, targeting small RNA molecules (miRNAs) serves as a promising therapeutic alternative, since they were, shortly after discovery, acknowledged as master regulators of gene expression in a post-transcriptional level [274]. In line with this, we explored the potential of TPL2 to affect the expression of miRNAs as the cross-talk point of inflammatory and carcinogenic responses [368]. To this end, we performed a high-throughput microarray miRNA expression analysis following TNF treatment of primary BMDMs in the presence or absence of TPL2 (Fig.17) and searched for miRNAs regulating cancer-associated genes. The results support a gradual effect of TNF on suppression of multiple miRNAs and underline a microRNA expression signature following TNF-induced inflammation. This effect is hindered in the absence of TPL2 suggesting that Tpl2 inhibition results in decreased inflammatory response through microRNA up-regulation.

Validation of the results was evaluated in three miRNAs (mmu-let-7a, mmu-let-7i and mmu-miR-223) predicted through the miRanda algorithm to bind IL-6 3' UTR and in all cases TPL2 was found to either reduce or block the effect of TNF on microRNA suppression (Fig. 18). This fact could explain the lower secreted IL-6 levels seen in *TPL2-/-* BMDMs compared to their WT counterparts following TNF treatment (Fig. 19). Even more interestingly, the effect was detected not only in the secreted but also in the mRNA levels of IL-6 posing the suspicion that these miRNAs could mediate not only translational inhibition but also degradation of IL-6 mRNA, an alternative action of miRNAs [369]. The fact that at least one of these miRNAs (let-7a) is implicated in inflammation-associated carcinogenesis signaling circuits [370] renders the findings of this thesis promising towards unraveling similar networks. Future experiments will focus on discovering the exact binding sites of miRNAs on IL-6 3' UTR and other targets with the ultimate goal to reverse malignant phenotypes through blocking miRNAs with antagomiRs [295].

In conclusion, the data presented here support an overall pro-inflammatory but anti-carcinogenic role of TPL2. Apparently, blocking TPL2 with commercial available chemical inhibitors may suppress an aberrant inflammatory response in line with previously published data [29]. This could provide a barrier towards induction of inflammation-associated cancer. Nevertheless, once cancer has been established following chronic persistence of an inflammatory microenvironment, TPL2 activity becomes beneficial in terms of cancer cell elimination through the proper p53 response. It is thus important to estimate the specific origin and the progression status of a tumor in order to use successfully a therapeutic scheme based on TPL2 inhibition. The complexity further escalates given the fact that cancer cells may adopt resistance to specific MAP kinase inhibitors used as therapy targets, through activation of redundant signaling pathways [64], a case where a combination of agents is needed in order to achieve successful treatment.

Concluding remarks and future prospects

The present thesis provides novel and enthusiastic data regarding TPL2 biology. In summary, it is shown for the first time that i) TPL2 may reside not only in the cytoplasm as it was traditionally believed but also in the nucleus (and nuclei) of various cell lines tested, ii) TPL2 colocalizes and interacts directly with NPM in the nucleus, iii) TPL2 participates in pathways triggered by genotoxic stress, iv) TPL2 regulates NPM phosphorylation at Thr^{199} and phosphorylation-mediated Ubiquitination at Lys^{229} two modifications crucial for the proper participation of NPM in DNA damage responses and v) TPL2 affects the p53-driven apoptotic program of the cells under genotoxic stress through the axis NPM-HDM2-p53. In another experimental context it is evidenced that under the treatment of cells with the pro-apoptotic cytokine TNF vi) TPL2 interacts with IKKα and regulates its subcellular localization and its binding to the promoter of IL-6 gene, vii) TPL2 synergizes with IKKα in the regulation of MAPKs p38 and JNK and finally viii) TPL2 regulates the expression of various miRNAs that target a diverse set of genes implicated in carcinogenesis and may thus offer a molecular signature linking an inflammatory milieu with tumor microenvironment. Following the data presented here it will be interesting to study other nuclear functions of TPL2

that may help us understand its overall impact in DNA damage responses. Moreover, implication of TPL2 in inflammation-associated pathways renders it an attractive target for therapies in the future. More robust evidence on the regulation and act of TPL2 under these circumstances will emerge from large cohort studies of patients, high-throughput screenings of TPL2 expression in normal versus pathological specimens and studies in mouse models of disease. Finally, it is of paramount importance to discover new chemical compounds that block TPL2 kinase activity with high specificity and may be eligible to enter clinical trials for the treatment of numerous pathological states.

.

REFERENCES

1. Vougioukalaki, M., Kanellis, D. C., Gkouskou, K. & Eliopoulos, A. G. Tpl2 kinase signal transduction in inflammation and cancer. *Cancer Lett.* **304,** 80–9 (2011).

2. Patriotis, C., Makris, a, Chernoff, J. & Tsichlis, P. N. Tpl-2 acts in concert with Ras and Raf-1 to activate mitogen-activated protein kinase. *Proc. Natl. Acad. Sci. U. S. A.* **91,** 9755–9 (1994).

3. Troppmair, J. *et al.* Mitogen-activated protein kinase/extracellular signal-regulated protein kinase activation by oncogenes, serum, and 12-O-tetradecanoylphorbol-13-acetate requires Raf and is necessary for transformation. *J. Biol. Chem.* **269,** 7030–5 (1994).

4. Salmeron, A. *et al.* Activation of MEK-1 and SEK-1 by Tpl-2 proto-oncoprotein, a novel MAP kinase kinase kinase. *EMBO J.* **15,** 817–26 (1996).

5. Hagemann, D., Troppmair, J. & Rapp, U. R. Cot protooncoprotein activates the dual specificity kinases MEK-1 and SEK-1 and induces differentiation of PC12 cells. *Oncogene* **18,** 1391–400 (1999).

6. Ballester, A., Tobeña, R., Lisbona, C., Calvo, V. & Alemany, S. Cot kinase regulation of IL-2 production in Jurkat T cells. *J. Immunol.* **159,** 1613–8 (1997).

7. Ballester, A., Velasco, A., Tobeña, R. & Alemany, S. Cot kinase activates tumor necrosis factor-alpha gene expression in a cyclosporin A-resistant manner. *J. Biol. Chem.* **273,** 14099–106 (1998).

8. Tsatsanis, C., Patriotis, C., Bear, S. E. & Tsichlis, P. N. The Tpl-2 protooncoprotein activates the nuclear factor of activated T cells and induces interleukin 2 expression in T cell lines. *Proc. Natl. Acad. Sci. U. S. A.* **95,** 3827–32 (1998).

9. Tsatsanis, C., Patriotis, C. & Tsichlis, P. N. Tpl-2 induces IL-2 expression in T-cell lines by triggering multiple signaling pathways that activate NFAT and NF-kappaB. *Oncogene* **17,** 2609–18 (1998).

10. O'Mahony, A., Lin, X., Geleziunas, R. & Greene, W. C. Activation of the heterodimeric IkappaB kinase alpha (IKKalpha)-IKKbeta complex is directional: IKKalpha regulates IKKbeta under both basal and stimulated conditions. *Mol. Cell. Biol.* **20,** 1170–8 (2000).

11. Lin, X., Cunningham, E. T., Mu, Y., Geleziunas, R. & Greene, W. C. The proto-oncogene Cot kinase participates in CD3/CD28 induction of NF-kappaB acting through the NF-kappaB-inducing kinase and IkappaB kinases. *Immunity* **10,** 271–80 (1999).

12. Eliopoulos, A. G., Wang, C.-C., Dumitru, C. D. & Tsichlis, P. N. Tpl2 transduces CD40 and TNF signals that activate ERK and regulates IgE induction by CD40. *EMBO J.* **22,** 3855–64 (2003).

13. Belich, M. P., Salmerón, A., Johnston, L. H. & Ley, S. C. TPL-2 kinase regulates the proteolysis of the NF-kappaB-inhibitory protein NF-kappaB1 p105. *Nature* **397,** 363–8 (1999).

14. Cho, J. & Tsichlis, P. N. Phosphorylation at Thr-290 regulates Tpl2 binding to NF-kappaB1/p105 and Tpl2 activation and degradation by lipopolysaccharide. *Proc. Natl. Acad. Sci. U. S. A.* **102,** 2350–5 (2005).

15. Lang, V. *et al.* ABIN-2 forms a ternary complex with TPL-2 and NF-kappa B1 p105 and is essential for TPL-2 protein stability. *Mol. Cell. Biol.* **24,** 5235–48 (2004).

16. Waterfield, M. R., Zhang, M., Norman, L. P. & Sun, S. C. NF-kappaB1/p105 regulates lipopolysaccharide-stimulated MAP kinase signaling by governing the stability and function of the Tpl2 kinase. *Mol. Cell* **11,** 685–94 (2003).

17. Beinke, S., Robinson, M. J., Hugunin, M. & Ley, S. C. Lipopolysaccharide activation of the TPL-2/MEK/extracellular signal-regulated kinase mitogen-activated protein kinase cascade is regulated by IkappaB kinase-induced proteolysis of NF-kappaB1 p105. *Mol. Cell. Biol.* **24,** 9658–67 (2004).

18. Beinke, S. *et al.* NF-kappaB1 p105 negatively regulates TPL-2 MEK kinase activity. *Mol. Cell. Biol.* **23,** 4739–52 (2003).

19. Jia, Y. *et al.* Purification and kinetic characterization of recombinant human mitogen-activated protein kinase kinase kinase COT and the complexes with its cellular partner NF-kappa B1 p105. *Arch. Biochem. Biophys.* **441,** 64–74 (2005).

20. Dumitru, C. D. *et al.* TNF-alpha induction by LPS is regulated posttranscriptionally via a Tpl2/ERK-dependent pathway. *Cell* **103,** 1071–83 (2000).

21. Eliopoulos, A. G., Dumitru, C. D., Wang, C.-C., Cho, J. & Tsichlis, P. N. Induction of COX-2 by LPS in macrophages is regulated by Tpl2-dependent CREB activation signals. *EMBO J.* **21,** 4831–40 (2002).

22. De Gregorio, R., Iñiguez, M. A., Fresno, M. & Alemany, S. Cot kinase induces cyclooxygenase-2 expression in T cells through activation of the nuclear factor of activated T cells. *J. Biol. Chem.* **276,** 27003–9 (2001).

23. Tomczak, M. F. *et al.* Defective activation of ERK in macrophages lacking the p50/p105 subunit of NF-kappaB is responsible for elevated

expression of IL-12 p40 observed after challenge with Helicobacter hepaticus. *J. Immunol.* **176,** 1244–51 (2006).

24. Kontoyiannis, D. *et al.* Genetic dissection of the cellular pathways and signaling mechanisms in modeled tumor necrosis factor-induced Crohn's-like inflammatory bowel disease. *J. Exp. Med.* **196,** 1563–74 (2002).

25. Zacharioudaki, V. *et al.* Adiponectin promotes endotoxin tolerance in macrophages by inducing IRAK-M expression. *J. Immunol.* **182,** 6444–51 (2009).

26. Sugimoto, K. *et al.* A serine/threonine kinase, Cot/Tpl2, modulates bacterial DNA-induced IL-12 production and Th cell differentiation. *J. Clin. Invest.* **114,** 857–66 (2004).

27. Serebrennikova, O. B. *et al.* Tpl2 ablation promotes intestinal inflammation and tumorigenesis in Apcmin mice by inhibiting IL-10 secretion and regulatory T-cell generation. *Proc. Natl. Acad. Sci. U. S. A.* **109,** E1082–91 (2012).

28. Gavrin, L. K. *et al.* Inhibition of Tpl2 kinase and TNF-alpha production with 1,7-naphthyridine-3-carbonitriles: synthesis and structure-activity relationships. *Bioorg. Med. Chem. Lett.* **15,** 5288–92 (2005).

29. Hall, J. P. *et al.* Pharmacologic inhibition of tpl2 blocks inflammatory responses in primary human monocytes, synoviocytes, and blood. *J. Biol. Chem.* **282,** 33295–304 (2007).

30. Cusack, K. *et al.* Identification of a selective thieno[2,3-c]pyridine inhibitor of COT kinase and TNF-alpha production. *Bioorg. Med. Chem. Lett.* **19,** 1722–5 (2009).

31. Kim, J.-E. *et al.* Luteolin, a novel natural inhibitor of tumor progression locus 2 serine/threonine kinase, inhibits tumor necrosis factor-alpha-induced cyclooxygenase-2 expression in JB6 mouse epidermis cells. *J. Pharmacol. Exp. Ther.* **338,** 1013–22 (2011).

32. Aoki, M., Akiyama, T., Miyoshi, J. & Toyoshima, K. Identification and characterization of protein products of the cot oncogene with serine kinase activity. *Oncogene* **6,** 1515–9 (1991).

33. Aoki, M. *et al.* The human cot proto-oncogene encodes two protein serine/threonine kinases with different transforming activities by alternative initiation of translation. *J. Biol. Chem.* **268,** 22723–32 (1993).

34. Ohara, R., Miyoshi, J., Aoki, M. & Toyoshima, K. The murine cot proto-oncogene: genome structure and tissue-specific expression. *Jpn. J. Cancer Res.* **84,** 518–25 (1993).

35. Miyoshi, J., Higashi, T., Mukai, H., Ohuchi, T. & Kakunaga, T. Structure and transforming potential of the human cot oncogene encoding a putative protein kinase. *Mol. Cell. Biol.* **11,** 4088–96 (1991).

36. Patriotis, C., Makris, a, Bear, S. E. & Tsichlis, P. N. Tumor progression locus 2 (Tpl-2) encodes a protein kinase involved in the progression of rodent T-cell lymphomas and in T-cell activation. *Proc. Natl. Acad. Sci. U. S. A.* **90,** 2251–5 (1993).

37. Makris, a, Patriotis, C., Bear, S. E. & Tsichlis, P. N. Genomic organization and expression of Tpl-2 in normal cells and Moloney murine leukemia virus-induced rat T-cell lymphomas: activation by provirus insertion. *J. Virol.* **67,** 4283–9 (1993).

38. Erny, K. M., Peli, J., Lambert, J. F., Muller, V. & Diggelmann, H. Involvement of the Tpl-2/cot oncogene in MMTV tumorigenesis. *Oncogene* **13,** 2015–20 (1996).

39. Gándara, M. L., López, P., Hernando, R., Castaño, J. G. & Alemany, S. The COOH-terminal domain of wild-type Cot regulates its stability and kinase specific activity. *Mol. Cell. Biol.* **23,** 7377–90 (2003).

40. Ceci, J. D. *et al.* Tpl-2 is an oncogenic kinase that is activated by carboxy-terminal truncation. *Genes Dev.* **11,** 688–700 (1997).

41. Ohara, R. *et al.* Identification of the cells expressing cot proto-oncogene mRNA. *J. Cell Sci.* **108 (Pt 1,** 97–103 (1995).

42. Sourvinos, G., Tsatsanis, C. & Spandidos, D. a. Overexpression of the Tpl-2/Cot oncogene in human breast cancer. *Oncogene* **18,** 4968–73 (1999).

43. Krcova, Z., Ehrmann, J., Krejci, V., Eliopoulos, A. & Kolar, Z. Tpl-2/Cot and COX-2 in breast cancer. *Biomed. Pap. Med. Fac. Univ. Palacky. Olomouc. Czech. Repub.* **152,** 21–5 (2008).

44. Eliopoulos, A. G. *et al.* The Oncogenic Protein Kinase Tpl-2 / Cot Contributes to Epstein-Barr Virus-Encoded Latent Infection Membrane Protein 1-Induced NF-κB Signaling Downstream of TRAF2. *J. Virol.* **76,** 4567–4579 (2002).

45. Christoforidou, A. V, Papadaki, H. a, Margioris, A. N., Eliopoulos, G. D. & Tsatsanis, C. Expression of the Tpl2/Cot oncogene in human T-cell neoplasias. *Mol. Cancer* **3,** 34 (2004).

46. Clark, A. M., Reynolds, S. H., Anderson, M. & Wiest, J. S. Mutational activation of the MAP3K8 protooncogene in lung cancer. *Genes. Chromosomes Cancer* **41,** 99–108 (2004).

47. Shirali, S. *et al.* TPL-2 MEK kinase is not targeted by mutation in diffuse large B cell lymphoma and myeloid leukemia. *Leuk. Res.* **31,** 1604–7 (2007).

48. Chiariello, M., Marinissen, M. J. & Gutkind, J. S. Multiple mitogen-activated protein kinase signaling pathways connect the cot oncoprotein to the c-jun promoter and to cellular transformation. *Mol. Cell. Biol.* **20,** 1747–58 (2000).

49. Babu, G., Waterfield, M., Chang, M., Wu, X. & Sun, S.-C. Deregulated activation of oncoprotein kinase Tpl2/Cot in HTLV-I-transformed T cells. *J. Biol. Chem.* **281,** 14041–7 (2006).

50. Khanal, P., Lee, K.-Y., Kang, K.-W., Kang, B. S. & Choi, H. S. Tpl-2 kinase downregulates the activity of p53 and enhances signaling pathways leading to activation of activator protein 1 induced by EGF. *Carcinogenesis* **30,** 682–9 (2009).

51. Choi, H. S. *et al.* Cot, a novel kinase of histone H3, induces cellular transformation through up-regulation of c-fos transcriptional activity. *FASEB J.* **22,** 113–26 (2008).

52. Meng, F., Wehbe-Janek, H., Henson, R., Smith, H. & Patel, T. Epigenetic regulation of microRNA-370 by interleukin-6 in malignant human cholangiocytes. *Oncogene* **27,** 378–86 (2008).

53. Lee, D. E. *et al.* 7,3',4'-Trihydroxyisoflavone, a metabolite of the soy isoflavone daidzein, suppresses ultraviolet B-induced skin cancer by targeting Cot and MKK4. *J. Biol. Chem.* **286,** 14246–56 (2011).

54. Lee, K. M., Lee, K. W., Bode, A. M., Lee, H. J. & Dong, Z. Tpl2 is a key mediator of arsenite-induced signal transduction. *Cancer Res.* **69,** 8043–9 (2009).

55. Park, H. D. *et al.* Pancreatic adenocarcinoma upregulated factor promotes metastasis by regulating TLR/CXCR4 activation. *Oncogene* **30,** 201–11 (2011).

56. Fernández, M. *et al.* Involvement of Cot activity in the proliferation of ALCL lymphoma cells. *Biochem. Biophys. Res. Commun.* **411,** 655–60 (2011).

57. Hebron, E. *et al.* MAP3K8 kinase regulates myeloma growth by cell-autonomous and non-autonomous mechanisms involving myeloma-associated monocytes/macrophages. *Br. J. Haematol.* **160,** 779–84 (2013).

58. Kim, G. *et al.* Interleukin-17 induces AP-1 activity and cellular transformation via upregulation of tumor progression locus 2 activity. *Carcinogenesis* **34,** 341–50 (2013).

59. Rodríguez, C. *et al.* COX2 expression and Erk1/Erk2 activity mediate Cot-induced cell migration. *Cell. Signal.* **20,** 1625–31 (2008).

60. Hatziapostolou, M. *et al.* Tumor progression locus 2 mediates signal-induced increases in cytoplasmic calcium and cell migration. *Sci. Signal.* **4,** ra55 (2011).

61. Hatziapostolou, M., Polytarchou, C., Panutsopulos, D., Covic, L. & Tsichlis, P. N. Proteinase-activated receptor-1-triggered activation of tumor progression locus-2 promotes actin cytoskeleton reorganization and cell migration. *Cancer Res.* **68,** 1851–61 (2008).

62. Hamamoto, T. *et al.* Differences in effects of oncogenes on sensitivity to anticancer drugs. *J. Radiat. Res.* **46,** 197–203 (2005).

63. Barbie, D. a *et al.* Systematic RNA interference reveals that oncogenic KRAS-driven cancers require TBK1. *Nature* **462,** 108–12 (2009).

64. Johannessen, C. M. *et al.* COT drives resistance to RAF inhibition through MAP kinase pathway reactivation. *Nature* **468,** 968–72 (2010).

65. Paraiso, K. H. T. *et al.* The HSP90 inhibitor XL888 overcomes BRAF inhibitor resistance mediated through diverse mechanisms. *Clin. Cancer Res.* **18,** 2502–14 (2012).

66. Tsatsanis, C. *et al.* Tpl2 and ERK transduce antiproliferative T cell receptor signals and inhibit transformation of chronically stimulated T cells. *Proc. Natl. Acad. Sci. U. S. A.* **105,** 2987–92 (2008).

67. Velasco-Sampayo, A. & Alemany, S. p27kip protein levels and E2F activity are targets of Cot kinase during G1 phase progression in T cells. *J. Immunol.* **166,** 6084–90 (2001).

68. Decicco-Skinner, K. L., Trovato, E. L., Simmons, J. K., Lepage, P. K. & Wiest, J. S. Loss of tumor progression locus 2 (tpl2) enhances tumorigenesis and inflammation in two-stage skin carcinogenesis. *Oncogene* **30,** 389–97 (2011).

69. DeCicco-Skinner, K. L. *et al.* Altered prostanoid signaling contributes to increased skin tumorigenesis in Tpl2 knockout mice. *PLoS One* **8,** e56212 (2013).

70. Koliaraki, V., Roulis, M. & Kollias, G. Tpl2 regulates intestinal myofibroblast HGF release to suppress colitis-associated tumorigenesis. *J. Clin. Invest.* **122,** 4231–4242 (2012).

71. Gkirtzimanaki, K. *et al.* TPL2 kinase is a suppressor of lung carcinogenesis. *Proc. Natl. Acad. Sci. U. S. A.* **110,** E1470–9 (2013).

72. Kang, Y. J., Olson, M. O., Jones, C. & Busch, H. Nucleolar phosphoproteins of normal rat liver and Novikoff hepatoma ascites cells. *Cancer Res.* **35,** 1470–5 (1975).

73. Chang, J. H., Dumbar, T. S. & Olson, M. O. cDNA and deduced primary structure of rat protein B23, a nucleolar protein containing highly conserved sequences. *J. Biol. Chem.* **263,** 12824–7 (1988).

74. Li, S., Wang, L. & Dorf, M. E. PKC phosphorylation of TRAF2 mediates IKKalpha/beta recruitment and K63-linked polyubiquitination. *Mol. Cell* **33,** 30–42 (2009).

75. Li, X. Z., McNeilage, L. J. & Whittingham, S. The nucleotide sequence of a human cDNA encoding the highly conserved nucleolar phosphoprotein B23. *Biochem. Biophys. Res. Commun.* **163,** 72–8 (1989).

76. Chan, P. K. & Chan, F. Y. Nucleophosmin/B23 (NPM) oligomer is a major and stable entity in HeLa cells. *Biochim. Biophys. Acta* **1262,** 37–42 (1995).

77. Hingorani, K., Szebeni, a & Olson, M. O. Mapping the functional domains of nucleolar protein B23. *J. Biol. Chem.* **275,** 24451–7 (2000).

78. Grisendi, S. *et al.* Role of nucleophosmin in embryonic development and tumorigenesis. *Nature* **437,** 147–53 (2005).

79. Colombo, E. & Bonetti, P. Nucleophosmin is required for DNA integrity and p19Arf protein stability. *Mol. Cell. Biol.* **25,** 8874–8886 (2005).

80. Grisendi, S., Mecucci, C., Falini, B. & Pandolfi, P. P. Nucleophosmin and cancer. *Nat. Rev. Cancer* **6,** 493–505 (2006).

81. Chang, J. H. & Olson, M. O. Structure of the gene for rat nucleolar protein B23. *J. Biol. Chem.* **265,** 18227–33 (1990).

82. MacArthur, C. a & Shackleford, G. M. Npm3: a novel, widely expressed gene encoding a protein related to the molecular chaperones nucleoplasmin and nucleophosmin. *Genomics* **42,** 137–40 (1997).

83. Okuwaki, M. The structure and functions of NPM1/Nucleophsmin/B23, a multifunctional nucleolar acidic protein. *J. Biochem.* **143,** 441–8 (2008).

84. Chan, P. K., Chan, F. Y., Morris, S. W. & Xie, Z. Isolation and characterization of the human nucleophosmin/B23 (NPM) gene: identification of the YY1 binding site at the 5' enhancer region. *Nucleic Acids Res.* **25,** 1225–32 (1997).

85. Liu, H. *et al.* Nucleophosmin acts as a novel AP2alpha-binding transcriptional corepressor during cell differentiation. *EMBO Rep.* **8,** 394–400 (2007).

86. Zeller, K. I. *et al.* Characterization of nucleophosmin (B23) as a Myc target by scanning chromatin immunoprecipitation. *J. Biol. Chem.* **276,** 48285–91 (2001).

87. Yeh, C., Huang, S., Lee, R. & Yung, B. Y. Ras-Dependent Recruitment of c-Myc for Transcriptional Activation of Nucleophosmin / B23 in Highly Malignant U1 Bladder Cancer Cells. *Mol. Pharmacol.* **70,** 1443–1453 (2006).

88. Jones, C. E., Busch, H. & Olson, M. O. J. Sequence of a phosphorylation site in nucleolar protein B23. *Biochim. Biophys. Acta* **667,** 209–212 (1981).

89. Jiang, P. S., Chang, J. H. & Yung, B. Y. Different kinases phosphorylate nucleophosmin/B23 at different sites during G(2) and M phases of the cell cycle. *Cancer Lett.* **153,** 151–60 (2000).

90. Tawfic, S., Olson, M. O. & Ahmed, K. Role of protein phosphorylation in post-translational regulation of protein B23 during programmed cell death in the prostate gland. *J. Biol. Chem.* **270,** 21009–15 (1995).

91. Hayami, R. *et al.* Down-regulation of BRCA1-BARD1 ubiquitin ligase by CDK2. *Cancer Res.* **65,** 6–10 (2005).

92. Sato, K. *et al.* Nucleophosmin/B23 is a candidate substrate for the BRCA1-BARD1 ubiquitin ligase. *J. Biol. Chem.* **279,** 30919–22 (2004).

93. Itahana, K. *et al.* Tumor suppressor ARF degrades B23, a nucleolar protein involved in ribosome biogenesis and cell proliferation. *Mol. Cell* **12,** 1151–64 (2003).

94. Tago, K., Chiocca, S. & Sherr, C. J. Sumoylation induced by the Arf tumor suppressor: a p53-independent function. *Proc. Natl. Acad. Sci. U. S. A.* **102,** 7689–94 (2005).

95. Liu, X. *et al.* Sumoylation of nucleophosmin/B23 regulates its subcellular localization, mediating cell proliferation and survival. *Proc. Natl. Acad. Sci. U. S. A.* **104,** 9679–84 (2007).

96. Lee, S. B. *et al.* Nuclear Akt interacts with B23/NPM and protects it from proteolytic cleavage, enhancing cell survival. *Proc. Natl. Acad. Sci. U. S. A.* **105,** 16584–9 (2008).

97. Zhang, M.-J. *et al.* Erythroid differentiation-associated gene interacts with NPM1 (nucleophosmin/B23) and increases its protein stability, resisting cell apoptosis. *FEBS J.* **279,** 2848–62 (2012).

98. Chao, A. *et al.* Estrogen stimulates the proliferation of human endometrial cancer cells by stabilizing nucleophosmin/B23 (NPM/B23). *J. Mol. Med. (Berl).* **91,** 249–59 (2013).

99. Cullen, S. P. *et al.* Nucleophosmin is cleaved and inactivated by the cytotoxic granule protease granzyme M during natural killer cell-mediated killing. *J. Biol. Chem.* **284,** 5137–47 (2009).

100. Drygin, D. *et al.* Targeting RNA polymerase I with an oral small molecule CX-5461 inhibits ribosomal RNA synthesis and solid tumor growth. *Cancer Res.* **71,** 1418–30 (2011).

101. Olanich, M. E., Moss, B. L., Piwnica-Worms, D., Townsend, R. R. & Weber, J. D. Identification of FUSE-binding protein 1 as a regulatory mRNA-binding protein that represses nucleophosmin translation. *Oncogene* **30,** 77–86 (2011).

102. Herrera, J. E., Correia, J. J., Jones, a E. & Olson, M. O. Sedimentation analyses of the salt- and divalent metal ion-induced oligomerization of nucleolar protein B23. *Biochemistry* **35,** 2668–73 (1996).

103. Jian, Y. *et al.* RNA aptamers interfering with nucleophosmin oligomerization induce apoptosis of cancer cells. *Oncogene* **28,** 4201–11 (2009).

104. Prinos, P., Lacoste, M.-C., Wong, J., Bonneau, A.-M. & Georges, E. Mutation of cysteine 21 inhibits nucleophosmin/B23 oligomerization and chaperone activity. *Int. J. Biochem. Mol. Biol.* **2,** 24–30 (2011).

105. Finch, R. a, Revankar, G. R. & Chan, P. K. Nucleolar localization of nucleophosmin/B23 requires GTP. *J. Biol. Chem.* **268,** 5823–7 (1993).

106. Choi, J. W., Lee, S. B., Ahn, J.-Y. & Lee, K.-H. Disruption of ATP binding destabilizes NPM/B23 and inhibits anti-apoptotic function. *BMB Rep.* **41,** 840–5 (2008).

107. Choi, J. W. *et al.* Lysine 263 residue of NPM/B23 is essential for regulating ATP binding and B23 stability. *FEBS Lett.* **582,** 1073–80 (2008).

108. Yung, B. Y. M., Busch, R. K., Busch, H., Mauger, A. B. & Chan, P. K. EFFECTS OF ACTINOMYCIN D ANALOGS ON NUCLEOLAR PHOSPHOPROTEIN. *Biochem. Pharmacol.* **34,** 4059–4063 (1985).

109. Yung, B. Y., Busch, H. & Chan, P. Effects of Luzopeptins on Protein B23 Translocation and Ribosomal RNA Synthesis in HeLa Cells. *Cancer Res.* **46,** 922–925 (1986).

110. Olson, M. O., Wallace, M. O., Herrera, a H., Marshall-Carlson, L. & Hunt, R. C. Preribosomal ribonucleoprotein particles are a major

component of a nucleolar matrix fraction. *Biochemistry* **25,** 484–91 (1986).

111. Dumbar, T. S., Gentry, G. a & Olson, M. O. Interaction of nucleolar phosphoprotein B23 with nucleic acids. *Biochemistry* **28,** 9495–501 (1989).

112. Herrera, J. E., Savkur, R. & Olson, M. O. The ribonuclease activity of nucleolar protein B23. *Nucleic Acids Res.* **23,** 3974–9 (1995).

113. Yu, Y. *et al.* Nucleophosmin Is Essential for Ribosomal Protein L5 Nuclear Export. *Mol. Cell. Biol.* **26,** 3798–3809 (2006).

114. Maggi, L. B. *et al.* Nucleophosmin serves as a rate-limiting nuclear export chaperone for the Mammalian ribosome. *Mol. Cell. Biol.* **28,** 7050–65 (2008).

115. Savkur, R. S. & Olson, M. O. J. Preferential cleavage in pre-ribosomal RNA by protein B23 endoribonuclease. *Nucleic Acids Res.* **26,** 4508–4515 (1998).

116. Okuwaki, M., Tsujimoto, M. & Nagata, K. The RNA Binding Activity of a Ribosome Biogenesis Factor , Nucleophosmin / B23 , Is Modulated by Phosphorylation with a Cell Cycle-dependent Kinase and by Association with Its Subtype. *Mol. Biol. Cell* **13,** 2016–2030 (2002).

117. Tarapore, P. *et al.* Thr199 phosphorylation targets nucleophosmin to nuclear speckles and represses pre-mRNA processing. *FEBS Lett.* **580,** 399–409 (2006).

118. Murano, K., Okuwaki, M., Hisaoka, M. & Nagata, K. Transcription regulation of the rRNA gene by a multifunctional nucleolar protein, B23/nucleophosmin, through its histone chaperone activity. *Mol. Cell. Biol.* **28,** 3114–26 (2008).

119. Hisaoka, M., Ueshima, S., Murano, K., Nagata, K. & Okuwaki, M. Regulation of nucleolar chromatin by B23/nucleophosmin jointly depends upon its RNA binding activity and transcription factor UBF. *Mol. Cell. Biol.* **30,** 4952–64 (2010).

120. Vascotto, C. *et al.* APE1/Ref-1 interacts with NPM1 within nucleoli and plays a role in the rRNA quality control process. *Mol. Cell. Biol.* **29,** 1834–54 (2009).

121. Inouye, C. J. & Seto, E. Relief of YY1-induced Transcriptional Repression by Protein-Protein Interaction with the Nucleolar Phosphoprotein B23. *J. Biol. Chem.* **269,** 6506–6510 (1994).

122. Kondo, T. *et al.* Identification and characterization of nucleophosmin/B23/numatrin which binds the anti-oncogenic

transcription factor IRF-1 and manifests oncogenic activity. *Oncogene* **15,** 1275–1281 (1997).

123. Takemura, M. *et al.* Nucleolar protein B23.1 binds to retinoblastoma protein and synergistically stimulates DNA polymerase alpha activity. *J. Biochem.* **125,** 904–9 (1999).

124. Okuwaki, M., Iwamatsu, a, Tsujimoto, M. & Nagata, K. Identification of nucleophosmin/B23, an acidic nucleolar protein, as a stimulatory factor for in vitro replication of adenovirus DNA complexed with viral basic core proteins. *J. Mol. Biol.* **311,** 41–55 (2001).

125. Léotoing, L. *et al.* Influence of nucleophosmin/B23 on DNA binding and transcriptional activity of the androgen receptor in prostate cancer cell. *Oncogene* **27,** 2858–67 (2008).

126. Dhar, S. K., Lynn, B. C., Daosukho, C. & St Clair, D. K. Identification of nucleophosmin as an NF-kappaB co-activator for the induction of the human SOD2 gene. *J. Biol. Chem.* **279,** 28209–19 (2004).

127. Zou, Y. *et al.* Nucleophosmin/B23 negatively regulates GCN5-dependent histone acetylation and transactivation. *J. Biol. Chem.* **283,** 5728–37 (2008).

128. Szebeni, a & Olson, M. O. Nucleolar protein B23 has molecular chaperone activities. *Protein Sci.* **8,** 905–12 (1999).

129. Lindström, M. S. & Zhang, Y. Ribosomal protein S9 is a novel B23/NPM-binding protein required for normal cell proliferation. *J. Biol. Chem.* **283,** 15568–76 (2008).

130. Fankhauser, C., Izaurralde, E., Adachi, Y., Wingfield, P. & Laemmli, U. K. Specific complex of human immunodeficiency virus type 1 rev and nucleolar B23 proteins: dissociation by the Rev response element. *Mol. Cell. Biol.* **11,** 2567–75 (1991).

131. Li, Y. P. Protein B23 is an important human factor for the nucleolar localization of the human immunodeficiency virus protein Tat . Protein B23 Is an Important Human Factor for the Nucleolar Localization of the Human Immunodeficiency Virus Protein Tat. *J. Virol.* **71,** 4098–4102 (1997).

132. Szebeni, A., Hingorani, K., Negi, S. & Olson, M. O. J. Role of protein kinase CK2 phosphorylation in the molecular chaperone activity of nucleolar protein b23. *J. Biol. Chem.* **278,** 9107–15 (2003).

133. Endo, A., Kitamura, N. & Komada, M. Nucleophosmin/B23 regulates ubiquitin dynamics in nucleoli by recruiting deubiquitylating enzyme USP36. *J. Biol. Chem.* **284,** 27918–23 (2009).

134. Yun, C. *et al.* Nucleolar protein B23/nucleophosmin regulates the vertebrate SUMO pathway through SENP3 and SENP5 proteases. *J. Cell Biol.* **183,** 589–95 (2008).

135. Michalik, J., Yeoman, L. C. & Busch, H. Nucleolar localization of protein B23 (37/5.1) by immunocytochemical techniques. *Life Sci.* **28,** 1371–1379 (1981).

136. Nishimura, Y., Ohkubo, T., Furuichi, Y. & Umekawa, H. Tryptophans 286 and 288 in the C-terminal region of protein B23.1 are important for its nucleolar localization. *Biosci. Biotechnol. Biochem.* **66,** 2239–42 (2002).

137. Falini, B., Nicoletti, I., Martelli, M. F. & Mecucci, C. Acute myeloid leukemia carrying cytoplasmic / mutated nucleophosmin (NPMc+ AML): biologic and clinical features. *Blood* **109,** 874–885 (2007).

138. Chan, P., Aldrich, M. B., Yung, B. Y. & Cells, T. Nucleolar Protein B23 Translocation after Doxorubicin Treatment in Murine Tumor Cells. *Cancer Res.* **47,** 3798–3801 (1987).

139. Busch, H., Chan, P. K. & Aldrich, M. Alterations in Immunolocalization of the Phosphoprotein B23 in HeLa Cells during Serum Starvation. *Exp. Cell Res.* **161,** 101–110 (1985).

140. Borer, R. a, Lehner, C. F., Eppenberger, H. M. & Nigg, E. a. Major nucleolar proteins shuttle between nucleus and cytoplasm. *Cell* **56,** 379–90 (1989).

141. Yogev, O., Saadon, K., Anzi, S., Inoue, K. & Shaulian, E. DNA damage-dependent translocation of B23 and p19 ARF is regulated by the Jun N-terminal kinase pathway. *Cancer Res.* **68,** 1398–406 (2008).

142. Khandelwal, N. *et al.* Nucleolar NF-κB/RelA mediates apoptosis by causing cytoplasmic relocalization of nucleophosmin. *Cell Death Differ.* **18,** 1889–903 (2011).

143. Nawa, Y. *et al.* Nucleophosmin may act as an alarmin: implications for severe sepsis. *J. Leukoc. Biol.* **86,** 645–53 (2009).

144. Chou, Y.-H. & Yung, B. Y. Cell cycle phase-dependent changes of localization and oligomerization stats of nucleophosmin/B23. *Biochem. Biophys. Res. Commun.* **217,** 313–325 (1995).

145. Yun, J.-P. *et al.* Nuclear matrix protein expressions in hepatocytes of normal and cirrhotic rat livers under normal and regenerating conditions. *J. Cell. Biochem.* **91,** 1269–79 (2004).

146. Okuda, M. *et al.* Nucleophosmin/B23 is a target of CDK2/cyclin E in centrosome duplication. *Cell* **103,** 127–40 (2000).

147. Peter, M., Nakagawa, J., Dorée, M., Labbé, J. C. & Nigg, E. a. Identification of major nucleolar proteins as candidate mitotic substrates of cdc2 kinase. *Cell* **60,** 791–801 (1990).

148. Tokuyama, Y., Horn, H. F., Kawamura, K., Tarapore, P. & Fukasawa, K. Specific phosphorylation of nucleophosmin on Thr(199) by cyclin-dependent kinase 2-cyclin E and its role in centrosome duplication. *J. Biol. Chem.* **276,** 21529–37 (2001).

149. Krause, A. & Hoffmann, I. Polo-like kinase 2-dependent phosphorylation of NPM/B23 on serine 4 triggers centriole duplication. *PLoS One* **5,** e9849 (2010).

150. Zhang, H. *et al.* B23/nucleophosmin serine 4 phosphorylation mediates mitotic functions of polo-like kinase 1. *J. Biol. Chem.* **279,** 35726–34 (2004).

151. Yao, J. *et al.* Nek2A kinase regulates the localization of numatrin to centrosome in mitosis. *FEBS Lett.* **575,** 112–8 (2004).

152. Wang, W., Budhu, A., Forgues, M. & Wang, X. W. Temporal and spatial control of nucleophosmin by the Ran-Crm1 complex in centrosome duplication. *Nat. Cell Biol.* **7,** 823–30 (2005).

153. Cuomo, M. E. *et al.* p53-Driven apoptosis limits centrosome amplification and genomic instability downstream of NPM1 phosphorylation. *Nat. Cell Biol.* **10,** 723–30 (2008).

154. Sarek, G. *et al.* Nucleophosmin phosphorylation by v-cyclin-CDK6 controls KSHV latency. *PLoS Pathog.* **6,** e1000818 (2010).

155. Bertwistle, D., Sugimoto, M. & Sherr, C. J. Physical and Functional Interactions of the Arf Tumor Suppressor Protein with Nucleophosmin / B23. *Mol. Cell. Biol.* **24,** 985–996 (2004).

156. Kuo, M.-L., den Besten, W., Bertwistle, D., Roussel, M. F. & Sherr, C. J. N-terminal polyubiquitination and degradation of the Arf tumor suppressor. *Genes Dev.* **18,** 1862–74 (2004).

157. Chen, D., Shan, J., Zhu, W.-G., Qin, J. & Gu, W. Transcription-independent ARF regulation in oncogenic stress-mediated p53 responses. *Nature* **464,** 624–7 (2010).

158. Korgaonkar, C. *et al.* Nucleophosmin (B23) Targets ARF to Nucleoli and Inhibits Its Function. *Mol. Cell. Biol.* **25,** 1258–1271 (2005).

159. Brady, S. N., Yu, Y., Maggi, L. B. & Weber, J. D. ARF Impedes NPM / B23 Shuttling in an Mdm2-Sensitive Tumor Suppressor Pathway. *Mol. Cell. Biol.* **24,** 9327–9338 (2004).

160. Kurki, S. *et al.* Nucleolar protein NPM interacts with HDM2 and protects tumor suppressor protein p53 from HDM2-mediated degradation. *Cancer Cell* **5,** 465–75 (2004).

161. Colombo, E., Marine, J.-C., Danovi, D., Falini, B. & Pelicci, P. G. Nucleophosmin regulates the stability and transcriptional activity of p53. *Nat. Cell Biol.* **4,** 529–33 (2002).

162. Li, J., Zhang, X., Sejas, D. P. & Pang, Q. Negative regulation of p53 by nucleophosmin antagonizes stress-induced apoptosis in human normal and malignant hematopoietic cells. *Leuk. Res.* **29,** 1415–23 (2005).

163. Lambert, B. & Buckle, M. Characterisation of the interface between nucleophosmin (NPM) and p53: potential role in p53 stabilisation. *FEBS Lett.* **580,** 345–50 (2006).

164. Maiguel, D. A., Jones, L., Chakravarty, D., Yang, C. & Carrier, F. Nucleophosmin Sets a Threshold for p53 Response to UV Radiation. *Mol. Cell. Biol.* **24,** 3703–3711 (2004).

165. Xiao, J. *et al.* Nucleophosmin / B23 interacts with p21 WAF1 / CIP1 and contributes to its stability. *Cell cycle* **6,** 889–895 (2009).

166. Li, Z., Boone, D. & Hann, S. R. Nucleophosmin interacts directly with c-Myc and controls c-Myc-induced hyperproliferation and transformation. *Proc. Natl. Acad. Sci. U. S. A.* **105,** 18794–9 (2008).

167. Li, Z. & Hann, S. R. Nucleophosmin is essential for c-Myc nucleolar localization and c-Myc-mediated rDNA transcription. *Oncogene* **32,** 1988–94 (2013).

168. Inder, K. L. *et al.* Nucleophosmin and nucleolin regulate K-Ras plasma membrane interactions and MAPK signal transduction. *J. Biol. Chem.* **284,** 28410–9 (2009).

169. Chan, P. K. Characterization and cellular localization of nucleophosmin/B23 in HeLa cells treated with selected cytotoxic agents (studies of B23-translocation mechanism). *Exp. Cell Res.* **203,** 174–81 (1992).

170. Yao, Z. *et al.* B23 acts as a nucleolar stress sensor and promotes cell survival through its dynamic interaction with hnRNPU and hnRNPA1. *Oncogene* **29,** 1821–34 (2010).

171. Bergstralh, D. T. *et al.* Global functional analysis of nucleophosmin in Taxol response, cancer, chromatin regulation, and ribosomal DNA transcription. *Exp. Cell Res.* **313,** 65–76 (2007).

172. Sautkina, E. N., Potapenko, N. a. & Vladimirova, N. M. State of nucleolar proteins B23/nucleophosmin and UBF in HeLa cells during

apoptosis induced by tumor necrosis factor. *Biochem.* **71,** 634–643 (2006).

173. Hsu, C. Y. & Yung, B. Y. Down-regulation of nucleophosmin/B23 during retinoic acid-induced differentiation of human promyelocytic leukemia HL-60 cells. *Oncogene* **16,** 915–23 (1998).

174. Chou, C. C. & Yung, B. Y. Increased stability of nucleophosmin/B23 in anti-apoptotic effect of ras during serum deprivation. *Mol. Pharmacol.* **59,** 38–45 (2001).

175. Wu, M. H. & Yung, B. Y. M. UV stimulation of nucleophosmin/B23 expression is an immediate-early gene response induced by damaged DNA. *J. Biol. Chem.* **277,** 48234–40 (2002).

176. Wu, M. H., Chang, J. H. & Yung, B. Y. M. Resistance to UV-induced cell-killing in nucleophosmin/B23 over-expressed NIH 3T3 fibroblasts: enhancement of DNA repair and up-regulation of PCNA in association with nucleophosmin/B23 over-expression. *Carcinogenesis* **23,** 93–100 (2002).

177. Moore, H. M. *et al.* Quantitative proteomics and dynamic imaging of the nucleolus reveal distinct responses to UV and ionizing radiation. *Mol. Cell. Proteomics* **10,** M111.009241–1–15 (2011).

178. Moore, H. M. *et al.* Proteasome activity influences UV-mediated subnuclear localization changes of NPM. *PLoS One* **8,** e59096 (2013).

179. Chen, S. *et al.* Interaction with Checkpoint Kinase 1 Modulates the Recruitment of Nucleophosmin to Chromatin. *J. Proteome Res.* **8,** 4693–4704 (2009).

180. Dalenc, F. *et al.* Increased expression of a COOH-truncated nucleophosmin resulting from alternative splicing is associated with cellular resistance to ionizing radiation in HeLa cells. *Int. J. Cancer* **100,** 662–8 (2002).

181. Koike, A. *et al.* Recruitment of phosphorylated NPM1 to sites of DNA damage through RNF8-dependent ubiquitin conjugates. *Cancer Res.* **70,** 6746–56 (2010).

182. Hsieh, S. *et al.* Identifying Apoptosis-Evasion Proteins / Pathways in Human Hepatoma Cells via Induction of Cellular Hormesis by UV Irradiation. *J. prote* **8,** 3977–3986 (2009).

183. Yee, H. *et al.* Molecular characterization of the t(2;5) (p23; q35) translocation in anaplastic large cell lymphoma (Ki-1) and Hodgkin's disease. *Blood* **87,** 1081–1088 (1996).

184. Redner, B. R. L., Rush, E. A., Faas, S., Rudert, W. A. & Corey, S. J. The t(5; 17) Variant of Acute Promyelocytic Leukemia Expresses a Nucleophosmin-Retinoic Acid Receptor Fusion. *Blood* **87,** 882–886 (1996).

185. Hitzler, J. K. *et al.* cDNA Cloning, Expression Pattern, and Chromosomal Localization of Mlf1, Murine Homologue of a Gene Involved in Myelodysplasia and Acute Myeloid Leukemia. *Am. J. Pathol.* **155,** 53–59 (1999).

186. Falini, B. *et al.* Cytoplasmic nucleophosmin in acute myelogenous leukemia with a normal karyotype. *N. Engl. J. Med.* **352,** 254–66 (2005).

187. Falini, B. *et al.* Acute myeloid leukemia with mutated nucleophosmin (NPM1): is it a distinct entity? *Blood* **117,** 1109–20 (2011).

188. Hayden, M. S. & Ghosh, S. Signaling to NF-kappaB. *Genes Dev.* **18,** 2195–224 (2004).

189. Shih, V. F.-S., Tsui, R., Caldwell, A. & Hoffmann, A. A single NFκB system for both canonical and non-canonical signaling. *Cell Res.* **21,** 86–102 (2011).

190. DiDonato, J. *et al.* Mapping of the inducible IkappaB phosphorylation sites that signal its ubiquitination and degradation . *Mol. Cell. Biol.* **16,** 1295–1304 (1996).

191. Mock, B. A., Connelly, M. A., Wesley, M., Kozak, christine A. & Marcu, K. B. CHUK, a Conserved Helix-Loop-Helix Ubiquitous Kinase, Maps to Human Chromosome 10 and Mouse Chromosome 19. *Genomics* **27,** 348–351 (1995).

192. DiDonato, J. a, Hayakawa, M., Rothwarf, D. M., Zandi, E. & Karin, M. A cytokine-responsive IkappaB kinase that activates the transcription factor NF-kappaB. *Nature* **388,** 548–54 (1997).

193. Zandi, E., Rothwarf, D. M., Delhase, M., Hayakawa, M. & Karin, M. The IkappaB Kinase Complex (IKK) Contains Two Kinase Subunits , IKKalpha and IKKbeta , Necessary for IkappaB Phosphorylation and NF-kappaB Activation. *Cell* **91,** 243–252 (1997).

194. Mercurio, F. IKK-1 and IKK-2: Cytokine-Activated IB Kinases Essential for NF-B Activation. *Science (80-.).* **278,** 860–866 (1997).

195. Regnier, C. H. *et al.* Identification and Characterization of an IκB Kinase. *Cell* **90,** 373–383 (1997).

196. Ling, L., Cao, Z. & Goeddel, D. V. NF-kappaB-inducing kinase activates IKK-alpha by phosphorylation of Ser-176. *Proc. Natl. Acad. Sci. U. S. A.* **95,** 3792–7 (1998).

197. Nemoto, S., DiDonato, J. a & Lin, a. Coordinate regulation of IkappaB kinases by mitogen-activated protein kinase kinase kinase 1 and NF-kappaB-inducing kinase. *Mol. Cell. Biol.* **18,** 7336–43 (1998).

198. Geleziunas, R. *et al.* Human T-Cell Leukemia Virus Type 1 Tax Induction of NF-kappaB Involves Activation of the IkappaB Kinase alpha (IKKalpha) and IKKbeta Cellular Kinases. *Mol. Cell. Biol.* **18,** 5157–5165 (1998).

199. Gregory, D., Hargett, D., Holmes, D., Money, E. & Bachenheimer, S. L. Efficient Replication by Herpes Simplex Virus Type 1 Involves Activation of the IkappaB Kinase-IkappaB-p65 Pathway. *J. Virol.* **78,** 13582–13590 (2004).

200. Huang, N.-L. *et al.* Metformin inhibits TNF-alpha-induced IkappaB kinase phosphorylation, IkappaB-alpha degradation and IL-6 production in endothelial cells through PI3K-dependent AMPK phosphorylation. *Int. J. Cardiol.* **134,** 169–75 (2009).

201. Merkhofer, E. C., Cogswell, P. & Baldwin, a S. Her2 activates NF-kappaB and induces invasion through the canonical pathway involving IKKalpha. *Oncogene* **29,** 1238–48 (2010).

202. Srivastava, R., Burbach, B. J. & Shimizu, Y. NF-kappaB activation in T cells requires discrete control of IkappaB kinase alpha/beta (IKKalpha/beta) phosphorylation and IKKgamma ubiquitination by the ADAP adapter protein. *J. Biol. Chem.* **285,** 11100–5 (2010).

203. Delhase, M., Hayakawa, M., Chen, Y. & Karin, M. Positive and negative regulation of IkappaB kinase activity through IKKbeta subunit phosphorylation. *Science* **284,** 309–13 (1999).

204. Takeda, K. Limb and Skin Abnormalities in Mice Lacking IKK. *Science (80-.).* **284,** 313–316 (1999).

205. Hu, Y. Abnormal Morphogenesis But Intact IKK Activation in Mice Lacking the IKK Subunit of IB Kinase. *Science (80-.).* **284,** 316–320 (1999).

206. Kwak, Y. T. Analysis of Domains in the IKKalpha and IKKbeta Proteins That Regulate Their Kinase Activity. *J. Biol. Chem.* **275,** 14752–14759 (2000).

207. Yamamoto, Y., Yin, M. & Gaynor, R. B. IkappaB Kinase alpha (IKKalpha) Regulation of IKKbeta Kinase Activity. *Mol. Cell. Biol.* **20,** 3655–3666 (2000).

208. Lam, L. T. *et al.* Compensatory IKKalpha activation of classical NF-kappaB signaling during IKKbeta inhibition identified by an RNA

interference sensitization screen. *Proc. Natl. Acad. Sci. U. S. A.* **105,** 20798–803 (2008).

209. Leotoing, L. *et al.* A20-binding inhibitor of nuclear factor-kappaB (NF-kappaB)-2 (ABIN-2) is an activator of inhibitor of NF-kappaB (IkappaB) kinase alpha (IKKalpha)-mediated NF-kappaB transcriptional activity. *J. Biol. Chem.* **286,** 32277–88 (2011).

210. Shembade, N., Pujari, R., Harhaj, N. S., Abbott, D. W. & Harhaj, E. W. The kinase IKKα inhibits activation of the transcription factor NF-κB by phosphorylating the regulatory molecule TAX1BP1. *Nat. Immunol.* **12,** 834–43 (2011).

211. Zhi, H. *et al.* NF-κB hyper-activation by HTLV-1 tax induces cellular senescence, but can be alleviated by the viral anti-sense protein HBZ. *PLoS Pathog.* **7,** e1002025 (2011).

212. Ho, Y.-K. *et al.* HTLV-1 tax-induced rapid senescence is driven by the transcriptional activity of NF-κB and depends on chronically activated IKKα and p65/RelA. *J. Virol.* **86,** 9474–83 (2012).

213. Li, Q. *et al.* IKK1-deficient mice exhibit abnormal development of skin and skeleton. *Genes Dev.* **13,** 1322–8 (1999).

214. Senftleben, U. *et al.* Activation by IKKalpha of a second, evolutionary conserved, NF-kappa B signaling pathway. *Science* **293,** 1495–9 (2001).

215. Balkhi, M. Y. *et al.* IKKα-mediated signaling circuitry regulates early B lymphopoiesis during hematopoiesis. *Blood* **119,** 5467–77 (2012).

216. Razani, B. *et al.* Negative Feedback in Noncanonical NFkappaB Signaling Modulates NIK Stability Through IKKalpha-Mediated Phosphorylation. *Sci. Signal.* **3,** ra41 (2011).

217. Bonizzi, G. *et al.* Activation of IKKalpha target genes depends on recognition of specific kappaB binding sites by RelB:p52 dimers. *EMBO J.* **23,** 4202–10 (2004).

218. Xiao, G., Fong, A. & Sun, S.-C. Induction of p100 processing by NF-kappaB-inducing kinase involves docking IkappaB kinase alpha (IKKalpha) to p100 and IKKalpha-mediated phosphorylation. *J. Biol. Chem.* **279,** 30099–105 (2004).

219. Gustin, J. a, Korgaonkar, C. K., Pincheira, R., Li, Q. & Donner, D. B. Akt regulates basal and induced processing of NF-kappaB2 (p100) to p52. *J. Biol. Chem.* **281,** 16473–81 (2006).

220. Olivotto, E. *et al.* Differential requirements for IKKalpha and IKKbeta in the differentiation of primary human osteoarthritic chondrocytes. *Arthritis Rheum.* **58,** 227–39 (2008).

221. Li, T. *et al.* MicroRNAs modulate the noncanonical transcription factor NF-kappaB pathway by regulating expression of the kinase IKKalpha during macrophage differentiation. *Nat. Immunol.* **11,** 799–805 (2010).

222. Birbach, A. *et al.* Signaling molecules of the NF-kappa B pathway shuttle constitutively between cytoplasm and nucleus. *J. Biol. Chem.* **277,** 10842–51 (2002).

223. Yamamoto, Y., Verma, U. N., Prajapati, S., Kwak, Y.-T. & Gaynor, R. B. Histone H3 phosphorylation by IKK-alpha is critical for cytokine-induced gene expression. *Nature* **423,** 655–9 (2003).

224. Anest, V. *et al.* A nucleosomal function for IkappaB kinase-alpha in NF-kappaB-dependent gene expression. *Nature* **423,** 659–663 (2003).

225. Park, G. Y. *et al.* NIK is involved in nucleosomal regulation by enhancing histone H3 phosphorylation by IKKalpha. *J. Biol. Chem.* **281,** 18684–90 (2006).

226. Wang, R.-P. *et al.* Differential regulation of IKK alpha-mediated activation of IRF3/7 by NIK. *Mol. Immunol.* **45,** 1926–34 (2008).

227. Rattan, R., Giri, S., Singh, A. K. & Singh, I. Rho a negatively regulates cytokine-mediated inducible nitric oxide synthase expression in brain-derived transformed cell lines: negative regulation of IKKα. *Free Radic. Biol. Med.* **35,** 1037–1050 (2003).

228. Aguilera, C., Hoya-Arias, R., Haegeman, G., Espinosa, L. & Bigas, A. Recruitment of IkappaBalpha to the hes1 promoter is associated with transcriptional repression. *Proc. Natl. Acad. Sci. U. S. A.* **101,** 16537–42 (2004).

229. Lu, Y. & Wahl, L. M. Production of matrix metalloproteinase-9 by activated human monocytes involves a phosphatidylinositol-3 kinase/Akt/IKKalpha/NF-kappaB pathway. *J. Leukoc. Biol.* **78,** 259–65 (2005).

230. Hirata, Y. *et al.* Helicobacter pylori Induces IkappaB Kinase alpha Nuclear Translocation and Chemokine Production in Gastric Epithelial Cells. *Infect. Immun.* **74,** 1452–1461 (2006).

231. Malinge, S., Monni, R., Bernard, O. & Penard-Lacronique, V. Activation of the NF-kappaB pathway by the leukemogenic TEL-Jak2 and TEL-Abl fusion proteins leads to the accumulation of antiapoptotic IAP proteins and involves IKKalpha. *Oncogene* **25,** 3589–97 (2006).

232. Albanese, C. *et al.* IKKalpha Regulates Mitogenic Signaling through Transcriptional Induction of Cyclin D1 via Tcf. *Mol. Biol. Cell* **14,** 585–599 (2003).

233. Kwak, Y.-T. *et al.* IkappaB kinase alpha regulates subcellular distribution and turnover of cyclin D1 by phosphorylation. *J. Biol. Chem.* **280,** 33945–52 (2005).

234. Park, K.-J., Krishnan, V., O'Malley, B. W., Yamamoto, Y. & Gaynor, R. B. Formation of an IKKalpha-dependent transcription complex is required for estrogen receptor-mediated gene activation. *Mol. Cell* **18,** 71–82 (2005).

235. Schneider, G. *et al.* IKKalpha controls p52/RelB at the skp2 gene promoter to regulate G1- to S-phase progression. *EMBO J.* **25,** 3801–12 (2006).

236. Prajapati, S., Tu, Z., Yamamoto, Y. & Gaynor, R. B. IKKαlpha Regulates the Mitotic Phase of the Cell Cycle by Modulating Aurora A phosphorylation. *Cell cycle* **5,** 2371–2380 (2006).

237. Zhu, F. *et al.* IKKalpha shields 14-3-3sigma, a G(2)/M cell cycle checkpoint gene, from hypermethylation, preventing its silencing. *Mol. Cell* **27,** 214–27 (2007).

238. Liu, B. *et al.* A critical role for I kappaB kinase alpha in the development of human and mouse squamous cell carcinomas. *Proc. Natl. Acad. Sci. U. S. A.* **103,** 17202–7 (2006).

239. Marinari, B. *et al.* The tumor suppressor activity of IKKalpha in stratified epithelia is exerted in part via the TGF-beta antiproliferative pathway. *Proc. Natl. Acad. Sci. U. S. A.* **105,** 17091–6 (2008).

240. Moreno-Maldonado, R. *et al.* IKKalpha enhances human keratinocyte differentiation and determines the histological variant of epidermal squamous cell carcinomas. *Cell Cycle* **7,** 2021–9 (2008).

241. Marinari, B. *et al.* IKKalpha is a p63 transcriptional target involved in the pathogenesis of ectodermal dysplasias. *J. Invest. Dermatol.* **129,** 60–9 (2009).

242. Temmerman, S. T. *et al.* Defective nuclear IKKα function in patients with ectodermal dysplasia with immune deficiency. *J. Clin. Invest.* **122,** 315–326 (2012).

243. Yamaguchi, T., Kimura, J., Miki, Y. & Yoshida, K. The deubiquitinating enzyme USP11 controls an IkappaB kinase alpha (IKKalpha)-p53 signaling pathway in response to tumor necrosis factor alpha (TNFalpha). *J. Biol. Chem.* **282,** 33943–8 (2007).

244. Liu, B. *et al.* Proinflammatory stimuli induce IKKalpha-mediated phosphorylation of PIAS1 to restrict inflammation and immunity. *Cell* **129,** 903–14 (2007).

245. Huang, W.-C., Ju, T.-K., Hung, M.-C. & Chen, C.-C. Phosphorylation of CBP by IKKalpha promotes cell growth by switching the binding preference of CBP from p53 to NF-kappaB. *Mol. Cell* **26,** 75–87 (2007).

246. Luo, J.-L. *et al.* Nuclear cytokine-activated IKKalpha controls prostate cancer metastasis by repressing Maspin. *Nature* **446,** 690–4 (2007).

247. Song, L. L. *et al.* Notch-1 associates with IKKalpha and regulates IKK activity in cervical cancer cells. *Oncogene* **27,** 5833–44 (2008).

248. Hao, L. *et al.* Notch-1 activates estrogen receptor-alpha-dependent transcription via IKKalpha in breast cancer cells. *Oncogene* **29,** 201–13 (2010).

249. Liu, M. *et al.* IKKα activation of NOTCH links tumorigenesis via FOXA2 suppression. *Mol. Cell* **45,** 171–84 (2012).

250. Charalambous, M. P., Lightfoot, T., Speirs, V., Horgan, K. & Gooderham, N. J. Expression of COX-2, NF-kappaB-p65, NF-kappaB-p50 and IKKalpha in malignant and adjacent normal human colorectal tissue. *Br. J. Cancer* **101,** 106–15 (2009).

251. Jiang, R. *et al.* High expression levels of IKKalpha and IKKbeta are necessary for the malignant properties of liver cancer. *Int. J. Cancer* **126,** 1263–74 (2010).

252. Mahato, R., Qin, B. & Cheng, K. Blocking IKKα expression inhibits prostate cancer invasiveness. *Pharm. Res.* **28,** 1357–69 (2011).

253. Xia, X. *et al.* Reduction of IKKalpha expression promotes chronic ultraviolet B exposure-induced skin inflammation and carcinogenesis. *Am. J. Pathol.* **176,** 2500–8 (2010).

254. Song, L. *et al.* A novel role of IKKalpha in the mediation of UVB-induced G0/G1 cell cycle arrest response by suppressing Cyclin D1 expression. *Biochim. Biophys. Acta* **1803,** 323–32 (2010).

255. Li, N. *et al.* Loss of acinar cell IKKα triggers spontaneous pancreatitis in mice. *J. Clin. Invest.* **123,** 2231–2243 (2013).

256. Liu, B. *et al.* IKKα represses a network of inflammation and proliferation pathways and elevates c-Myc antagonists and differentiation in a dose-dependent manner in the skin. *Cell Death Differ.* **18,** 1854–64 (2011).

257. Descargues, P. *et al.* IKKalpha is a critical coregulator of a Smad4-independent TGFbeta-Smad2/3 signaling pathway that controls

keratinocyte differentiation. *Proc. Natl. Acad. Sci. U. S. A.* **105,** 2487–92 (2008).

258. Li, Q., Pène, V., Krishnamurthy, S., Cha, H. & Liang, T. J. Hepatitis C virus infection activates an innate pathway involving IKK-α in lipogenesis and viral assembly. *Nat. Med.* **19,** 722–9 (2013).

259. Xiao, Z. *et al.* The pivotal role of IKKα in the development of spontaneous lung squamous cell carcinomas. *Cancer Cell* **23,** 527–40 (2013).

260. Lee, R. C., Feinbaum, R. L. & Ambros, V. The C. elegans heterochronic gene lin-4 encodes small RNAs with antisense complementarity to lin-14. *Cell* **75,** 843–54 (1993).

261. Pasquinelli, a E. *et al.* Conservation of the sequence and temporal expression of let-7 heterochronic regulatory RNA. *Nature* **408,** 86–9 (2000).

262. Reinhart, B. J. *et al.* The 21-nucleotide let-7 RNA regulates developmental timing in Caenorhabditis elegans. *Nature* **403,** 901–6 (2000).

263. Cai, X., Hagedorn, C. H. & Cullen, B. R. Human microRNAs are processed from capped , polyadenylated transcripts that can also function as mRNAs. *RNA* **10,** 1957–1966 (2004).

264. Lee, Y. *et al.* MicroRNA genes are transcribed by RNA polymerase II. *EMBO journalo* **23,** 4051–4060 (2004).

265. Han, J. *et al.* The Drosha-DGCR8 complex in primary microRNA processing. *Genes Dev.* **18,** 3016–27 (2004).

266. Lee, Y. *et al.* The nuclear RNase III Drosha initiates microRNA processing. *Nature* **425,** 415–419 (2003).

267. Lund, E., Güttinger, S., Calado, A., Dahlberg, J. E. & Kutay, U. Nuclear export of microRNA precursors. *Science* **303,** 95–8 (2004).

268. Bernstein, E. *et al.* Dicer is essential for mouse development. *Nat. Genet.* **35,** 215–7 (2003).

269. Meister, G. Argonaute proteins: functional insights and emerging roles. *Nat. Rev. Genet.* **14,** 447–59 (2013).

270. Schwarz, D. S. *et al.* Asymmetry in the assembly of the RNAi enzyme complex. *Cell* **115,** 199–208 (2003).

271. Khvorova, A., Reynolds, A. & Jayasena, S. D. Functional siRNAs and miRNAs exhibit strand bias. *Cell* **115,** 209–16 (2003).

272. Krol, J. *et al.* Structural features of microRNA (miRNA) precursors and their relevance to miRNA biogenesis and small interfering RNA/short hairpin RNA design. *J. Biol. Chem.* **279,** 42230–9 (2004).

273. Du, T. & Zamore, P. D. Beginning to understand microRNA function. *Cell Res.* **17,** 661–3 (2007).

274. Rana, T. M. Illuminating the silence: understanding the structure and function of small RNAs. *Nat. Rev. Mol. Cell Biol.* **8,** 23–36 (2007).

275. Berezikov, E., Chung, W.-J., Willis, J., Cuppen, E. & Lai, E. C. Mammalian mirtron genes. *Mol. Cell* **28,** 328–36 (2007).

276. Yang, J.-S. & Lai, E. C. Alternative miRNA biogenesis pathways and the interpretation of core miRNA pathway mutants. *Mol. Cell* **43,** 892–903 (2011).

277. Blow, M. J. *et al.* RNA editing of human microRNAs. *Genome Biol.* **7,** R27 (2006).

278. Baskerville, S. & Bartel, D. P. Microarray profiling of microRNAs reveals frequent coexpression with neighboring miRNAs and host genes. *RNA* **11,** 241–247 (2005).

279. Altuvia, Y. *et al.* Clustering and conservation patterns of human microRNAs. *Nucleic Acids Res.* **33,** 2697–706 (2005).

280. Houbaviy, H. B., Dennis, L., Jaenisch, R. & Sharp, P. a. Characterization of a highly variable eutherian microRNA gene. *RNA* **11,** 1245–57 (2005).

281. Weber, M. J. New human and mouse microRNA genes found by homology search. *FEBS J.* **272,** 59–73 (2005).

282. Rodriguez, A., Griffiths-jones, S., Ashurst, J. L. & Bradley, A. Identification of Mammalian microRNA Host Genes and Transcription Units. *Genome Res.* **14,** 1902–1910 (2004).

283. Lagos-Quintana, M. *et al.* Identification of tissue-specific microRNAs from mouse. *Curr. Biol.* **12,** 735–9 (2002).

284. Sun, Y. *et al.* Development of a micro-array to detect human and mouse microRNAs and characterization of expression in human organs. **32,** (2004).

285. Babak, T., Zhang, W., Morris, Q., Blencowe, B. J. & Hughes, T. R. Probing microRNAs with microarrays: tissue specificity and functional inference. *RNA* **10,** 1813–9 (2004).

286. Lim, L. P. *et al.* Microarray analysis shows that some microRNAs downregulate large numbers of target mRNAs. *Nature* **433,** 769–73 (2005).

287. Calin, G. A. *et al.* Human microRNA genes are frequently located at fragile sites and genomic regions involved in cancers. *Proc. Natl. Acad. Sci. U. S. A.* **101,** 2999–3004 (2004).

288. Lewis, B. P., Shih, I., Jones-Rhoades, M. W., Bartel, D. P. & Burge, C. B. Prediction of mammalian microRNA targets. *Cell* **115,** 787–98 (2003).

289. Lewis, B. P., Burge, C. B. & Bartel, D. P. Conserved seed pairing, often flanked by adenosines, indicates that thousands of human genes are microRNA targets. *Cell* **120,** 15–20 (2005).

290. Ye, W. *et al.* The Effect of Central Loops in miRNA : MRE Duplexes on the Efficiency of miRNA-Mediated Gene Regulation. *PLoS One* **3,** e1719 (2008).

291. Pillai, R. S. MicroRNA function : Multiple mechanisms for a tiny RNA ? *RNA* **11,** 1753–1761 (2005).

292. Giraldez, A. J. *et al.* Zebrafish MiR-430 Promotes Deadenylation and Clearance of Maternal mRNAs. *Science (80-.).* **312,** 75–79 (2008).

293. Nottrott, S., Simard, M. J. & Richter, J. D. Human let-7a miRNA blocks protein production on actively translating polyribosomes. *Nat. Struct. Mol. Biol.* **13,** 1108–14 (2006).

294. Meister, G., Landthaler, M., Dorsett, Y. & Tuschl, T. Sequence-specific inhibition of microRNA- and siRNA-induced RNA silencing. *RNA* **10,** 544–550 (2004).

295. Krützfeldt, J. *et al.* Silencing of microRNAs in vivo with “antagomirs”. *Nature* **438,** 685–9 (2005).

296. Bartel, D. P. MicroRNAs: target recognition and regulatory functions. *Cell* **136,** 215–33 (2009).

297. Kuhn, D. E. *et al.* Experimental validation of miRNA targets. *Methods* **44,** 47–54 (2008).

298. Hanahan, D. & Weinberg, R. A. The hallmarks of cancer. *Cell* **100,** 57–70 (2000).

299. Kefas, B. *et al.* microRNA-7 inhibits the epidermal growth factor receptor and the Akt pathway and is down-regulated in glioblastoma. *Cancer Res.* **68,** 3566–72 (2008).

300. Tsang, W. P. & Kwok, T. T. The miR-18a* microRNA functions as a potential tumor suppressor by targeting on K-Ras. *Carcinogenesis* **30,** 953–9 (2009).

301. Johnson, S. M. *et al.* RAS is regulated by the let-7 microRNA family. *Cell* **120,** 635–47 (2005).

302. Couts, K. L., Anderson, E. M., Gross, M. M., Sullivan, K. & Ahn, N. G. Oncogenic B-Raf signaling in melanoma cells controls a network of microRNAs with combinatorial functions. *Oncogene* **32,** 1959–70 (2013).

303. Geraldo, M. V, Yamashita, a S. & Kimura, E. T. MicroRNA miR-146b-5p regulates signal transduction of TGF-β by repressing SMAD4 in thyroid cancer. *Oncogene* **31,** 1910–22 (2012).

304. Deng, Y. *et al.* MiR-215 modulates gastric cancer cell proliferation by targeting RB1. *Cancer Lett.* 1–9 (2013). doi:10.1016/j.canlet.2013.08.033

305. Willimott, S. & Wagner, S. D. miR-125b and miR-155 contribute to BCL2 repression and proliferation in response to CD40 ligand (CD154) in human leukemic B-cells. *J. Biol. Chem.* **287,** 2608–17 (2012).

306. Cimmino, A. *et al.* miR-15 and miR-16 induce apoptosis by targeting BCL2. *Proc. Natl. Acad. Sci. U. S. A.* **102,** 13944–9 (2005).

307. Suffert, G. *et al.* Kaposi's sarcoma herpesvirus microRNAs target caspase 3 and regulate apoptosis. *PLoS Pathog.* **7,** e1002405 (2011).

308. Mitomo, S. *et al.* Downregulation of miR-138 is associated with overexpression of human telomerase reverse transcriptase protein in human anaplastic thyroid carcinoma cell lines. *Cancer Sci.* **99,** 280–6 (2008).

309. Chakrabarti, M., Banik, N. L. & Ray, S. K. miR-138 overexpression is more powerful than hTERT knockdown to potentiate apigenin for apoptosis in neuroblastoma in vitro and in vivo. *Exp. Cell Res.* **319,** 1575–85 (2013).

310. Wang, Y.-Y. *et al.* MiR-21 modulates hTERT through a STAT3-dependent manner on glioblastoma cell growth. *CNS Neurosci. Ther.* **18,** 722–8 (2012).

311. Zhou, B. *et al.* MicroRNA-503 targets FGF2 and VEGFA and inhibits tumor angiogenesis and growth. *Cancer Lett.* **333,** 159–69 (2013).

312. Vecchione, A. *et al.* A microRNA signature defines chemoresistance in ovarian cancer through modulation of angiogenesis. *Proc. Natl. Acad. Sci. U. S. A.* **110,** 9845–50 (2013).

313. Zhang, J.-P. *et al.* MicroRNA-148a suppresses the epithelial-mesenchymal transition and metastasis of hepatoma cells by targeting Met/Snail signaling. *Oncogene* 1–8 (2013). doi:10.1038/onc.2013.369

314. Ahn, S.-M. *et al.* Smad3 regulates E-cadherin via miRNA-200 pathway. *Oncogene* **31,** 3051–9 (2012).

315. Harazono, Y. *et al.* miR-655 Is an EMT-suppressive MicroRNA targeting ZEB1 and TGFBR2. *PLoS One* **8,** e62757 (2013).

316. Yu, Z., Pestell, T. G., Lisanti, M. P. & Pestell, R. G. Cancer stem cells. *Int. J. Biochem. Cell Biol.* **44,** 2144–51 (2012).

317. Tu, Y. *et al.* MicroRNA-218 Inhibits Glioma Invasion, Migration, Proliferation and Cancer Stem-like Cell Self-renewal by Targeting the Polycomb Group Gene Bmi1. *Cancer Res.* (2013). doi:10.1158/0008-5472.CAN-13-0358

318. Bu, P. *et al.* A microRNA miR-34a-regulated bimodal switch targets notch in colon cancer stem cells. *Cell Stem Cell* **12,** 602–15 (2013).

319. Hanahan, D. & Weinberg, R. a. Hallmarks of cancer: the next generation. *Cell* **144,** 646–74 (2011).

320. Kefas, B. *et al.* Pyruvate kinase M2 is a target of the tumor-suppressive microRNA-326 and regulates the survival of glioma cells. *Neuro. Oncol.* **12,** 1102–12 (2010).

321. Yamasaki, T. *et al.* Tumor-suppressive microRNA-1291 directly regulates glucose transporter 1 (GLUT1) in renal cell carcinoma. *Cancer Sci.* 1–9 (2013). doi:10.1111/cas.12240

322. Valeri, N. *et al.* Modulation of mismatch repair and genomic stability by miR-155. *Proc. Natl. Acad. Sci. U. S. A.* **107,** 6982–7 (2010).

323. Le, M. T. N. *et al.* MicroRNA-125b is a novel negative regulator of p53. *Genes Dev.* **23,** 862–76 (2009).

324. O'Connell, R. M., Rao, D. S. & Baltimore, D. microRNA regulation of inflammatory responses. *Annu. Rev. Immunol.* **30,** 295–312 (2012).

325. Neill, L. A. O., Sheedy, F. J. & Mccoy, C. E. MicroRNAs: the fine-tuners of Toll-like receptor signalling. *Nat. Rev. Immunol.* **11,** 163–175 (2011).

326. Bhaumik, D. *et al.* Expression of microRNA-146 suppresses NF-kappaB activity with reduction of metastatic potential in breast cancer cells. *Oncogene* **27,** 5643–7 (2008).

327. Iliopoulos, D., Hirsch, H. a & Struhl, K. An epigenetic switch involving NF-kappaB, Lin28, Let-7 MicroRNA, and IL6 links inflammation to cell transformation. *Cell* **139,** 693–706 (2009).

328. Iliopoulos, D., Jaeger, S. a, Hirsch, H. a, Bulyk, M. L. & Struhl, K. STAT3 activation of miR-21 and miR-181b-1 via PTEN and CYLD are part of the epigenetic switch linking inflammation to cancer. *Mol. Cell* **39,** 493–506 (2010).

329. Löffler, D. *et al.* Interleukin-6 dependent survival of multiple myeloma cells involves the Stat3-mediated induction of microRNA-21 through a highly conserved enhancer. *Blood* **110,** 1330–3 (2007).

330. Meng, F. *et al.* The MicroRNA let-7a modulates interleukin-6-dependent STAT-3 survival signaling in malignant human cholangiocytes. *J. Biol. Chem.* **282,** 8256–64 (2007).

331. Zhang, J. *et al.* MiR-124 Suppresses Growth of Human Colorectal Cancer by Inhibiting STAT3. *PLoS One* **8,** e70300 (2013).

332. Zhang, X. *et al.* MicroRNA-21 modulates the levels of reactive oxygen species by targeting SOD3 and TNFα. *Cancer Res.* **72,** 4707–13 (2012).

333. Venkataraman, S. *et al.* MicroRNA 128a increases intracellular ROS level by targeting Bmi-1 and inhibits medulloblastoma cancer cell growth by promoting senescence. *PLoS One* **5,** e10748 (2010).

334. Mateescu, B. *et al.* miR-141 and miR-200a act on ovarian tumorigenesis by controlling oxidative stress response. *Nat. Med.* **17,** 1627–35 (2011).

335. Hu, S. *et al.* The microbe-derived short chain fatty acid butyrate targets miRNA-dependent p21 gene expression in human colon cancer. *PLoS One* **6,** e16221 (2011).

336. Hayashi, Y. *et al.* CagA mediates epigenetic regulation to attenuate let-7 expression in Helicobacter pylori-related carcinogenesis. *Gut* **62,** 1536–1546 (2013).

337. Sohn, J. J. *et al.* Macrophages, nitric oxide and microRNAs are associated with DNA damage response pathway and senescence in inflammatory bowel disease. *PLoS One* **7,** e44156 (2012).

338. Olaru, A. V *et al.* Dynamic changes in the expression of MicroRNA-31 during inflammatory bowel disease-associated neoplastic transformation. *Inflamm. Bowel Dis.* **17,** 221–31 (2011).

339. Fabbri, M. *et al.* MicroRNAs bind to Toll-like receptors to induce prometastatic inflammatory response. *Proc. Natl. Acad. Sci. U. S. A.* **109,** E2110–6 (2012).

340. Ruan, W., Xu, J., Li, S., Yuan, L. & Dai, R. Effects of down-regulation of microRNA-23a on TNF-α-induced endothelial cell apoptosis through caspase-dependent pathways. *Cardiovasc. Res.* **93,** 623–32 (2012).

341. Eliopoulos, A. G., Das, S. & Tsichlis, P. N. The tyrosine kinase Syk regulates TPL2 activation signals. *J. Biol. Chem.* **281,** 1371–80 (2006).

342. Eliopoulos, A. G. *et al.* Epstein-Barr virus-encoded latent infection membrane protein 1 regulates the processing of p100 NF-kappaB2 to p52 via an IKKgamma/NEMO-independent signalling pathway. *Oncogene* **22,** 7557–69 (2003).

343. Heffernan, T. P. *et al.* An ATR- and Chk1-Dependent S Checkpoint Inhibits Replicon Initiation following UVC-Induced DNA Damage. *Mol. Cell. Biol.* **22,** 8552–8561 (2002).

344. Bursać, S. *et al.* Mutual protection of ribosomal proteins L5 and L11 from degradation is essential for p53 activation upon ribosomal biogenesis stress. *Proc. Natl. Acad. Sci. U. S. A.* **109,** 20467–72 (2012).

345. Hatzis, P. & Talianidis, I. Dynamics of enhancer-promoter communication during differentiation-induced gene activation. *Mol. Cell* **10,** 1467–77 (2002).

346. Black, T. M. *et al.* Characterization of Phosphorylation Sites on Tpl2 Using IMAC Enrichment and a Linear Ion Trap Mass Spectrometer. *J. Proteome Res.* **6,** 2269–2276 (2007).

347. Latonen, L. & Laiho, M. Cellular UV damage responses--functions of tumor suppressor p53. *Biochim. Biophys. Acta* **1755,** 71–89 (2005).

348. Gantke, T., Sriskantharajah, S. & Ley, S. C. Regulation and function of TPL-2, an IκB kinase-regulated MAP kinase kinase kinase. *Cell Res.* **21,** 131–45 (2011).

349. Li, J., Zhang, X., Sejas, D. P., Bagby, G. C. & Pang, Q. Hypoxia-induced nucleophosmin protects cell death through inhibition of p53. *J. Biol. Chem.* **279,** 41275–9 (2004).

350. Lindström, M. S. NPM1/B23: A Multifunctional Chaperone in Ribosome Biogenesis and Chromatin Remodeling. *Biochem. Res. Int.* **2011,** 195209 (2011).

351. Negi, S. S. & Olson, M. O. J. Effects of interphase and mitotic phosphorylation on the mobility and location of nucleolar protein B23. *J. Cell Sci.* **119,** 3676–85 (2006).

352. Falini, B. *et al.* Translocations and mutations involving the nucleophosmin (NPM1) gene in lymphomas and leukemias. *Haematologica* **92,** 519–532 (2007).

353. Pearson, J. D., Lee, J. K. H., Bacani, J. T. C., Lai, R. & Ingham, R. J. NPM-ALK: The Prototypic Member of a Family of Oncogenic Fusion Tyrosine Kinases. *J. Signal Transduct.* **ID 123253,** 1–14 (2012).

354. Das, S. *et al.* Tpl2/cot signals activate ERK, JNK, and NF-kappaB in a cell-type and stimulus-specific manner. *J. Biol. Chem.* **280,** 23748–57 (2005).

355. Sun, S.-C. Non-canonical NF-κB signaling pathway. *Cell Res.* **21,** 71–85 (2011).

356. Wang, S., Ghosh, R. N. & Chellappan, S. P. Raf-1 physically interacts with Rb and regulates its function: a link between mitogenic signaling and cell cycle regulation. *Mol. Cell. Biol.* **18,** 7487–98 (1998).

357. Lin, C. Y. *et al.* Dephosphorylation of Nucleophosmin by PP1β Facilitates pRB Binding and Consequent E2F1-dependent DNA Repair. *Mol. Biol. Cell* **21,** 4409–4417 (2010).

358. Cordell, J. L. *et al.* Detection of normal and chimeric nucleophosmin in human cells. *Blood* **93,** 632–42 (1999).

359. Mduff, F. K. E. *et al.* Determining the contribution of NPM1 heterozygosity to NPM-ALK-induced lymphomagenesis. *Lab. Invest.* **91,** 1298–303 (2011).

360. Watanabe, M. *et al.* JunB induced by constitutive CD30-extracellular signal-regulated kinase 1/2 mitogen-activated protein kinase signaling activates the CD30 promoter in anaplastic large cell lymphoma and reed-sternberg cells of Hodgkin lymphoma. *Cancer Res.* **65,** 7628–34 (2005).

361. Karin, M. & Greten, F. R. NF-kappaB: linking inflammation and immunity to cancer development and progression. *Nat. Rev. Immunol.* **5,** 749–59 (2005).

362. Elinav, E. *et al.* Inflammation-induced cancer: crosstalk between tumours, immune cells and microorganisms. *Nat. Rev. Cancer* **13,** 759–71 (2013).

363. Yuan, T., Wu, Y. & Zhou, B. P. in *Tumor Microenviron. Myelomonocytic Cells* ISBN: 978–953–51– 0439–1 (2008).

364. Lin, X., Cunningham, E. T., Mu, Y., Geleziunas, R. & Greene, W. C. The Proto-Oncogene Cot Kinase Participates in CD3/CD28 Induction of NF-

κB Acting through the NF-κB-Inducing Kinase and IκB Kinases. *Immunity* **10,** 271–280 (1999).

365. Feldmann, M. Development of anti-TNF therapy for rheumatoid arthritis. *Nat. Rev. Immunol.* **2,** 364–71 (2002).

366. Scott, K. A. *et al.* An Anti-Tumor Necrosis Factor- α Antibody Inhibits the Development of Experimental Skin Tumors. *Cancer Res.* **2,** 445–451 (2003).

367. Zhang, J., Yang, P. L. & Gray, N. S. Targeting cancer with small molecule kinase inhibitors. *Nat. Rev. Cancer* **9,** 28–39 (2009).

368. Tili, E., Michaille, J.-J. & Croce, C. M. MicroRNAs play a central role in molecular dysfunctions linking inflammation with cancer. *Immunol. Rev.* **253,** 167–84 (2013).

369. Ameres, S. L. & Zamore, P. D. Diversifying microRNA sequence and function. *Nat. Rev. Mol. Cell Biol.* **14,** 475–88 (2013).

370. Iliopoulos, D., Hirsch, H. a & Struhl, K. An epigenetic switch involving NF-kappaB, Lin28, Let-7 MicroRNA, and IL6 links inflammation to cell transformation. *Cell* **139,** 693–706 (2009).

Oncogene (2014), 1–11

www.nature.com/onc

ORIGINAL ARTICLE

Physical and functional interaction of the TPL2 kinase with nucleophosmin

DC Kanellis[1,2,5], S Bursac[3], PN Tsichlis[4], S Volarevic[3] and AG Eliopoulos[1,2]

Tumor Progression Locus 2 (TPL2) is widely recognized as a cytoplasmic mitogen-activated protein 3 kinase with a prominent role in the regulation of inflammatory and oncogenic signal transduction. Herein we report that TPL2 may also operate in the nucleus as a physical and functional partner of nucleophosmin (NPM/B23), a major nucleolar phosphoprotein with diverse cellular activities linked to malignancy. We demonstrate that TPL2 mediates the phosphorylation of a fraction of NPM at threonine 199, an event required for its proteasomal degradation and maintenance of steady-state NPM levels. Upon exposure to ultraviolet C, Tpl2 is required for the translocation of de-phosphorylated NPM from the nucleolus to the nucleoplasm. NPM is an endogenous inhibitor of HDM2:p53 interaction and knockdown of TPL2 was found to result in reduced binding of NPM to HDM2, with concomitant defects in p53 accumulation following genotoxic or ribosomal stress. These findings expand our understanding of the function of TPL2 as a negative regulator of carcinogenesis by defining a nuclear role for this kinase in the topological sequestration of NPM, linking p53 signaling to the generation of threonine 199-phosphorylated NPM.

Oncogene advance online publication, 7 July 2014; doi:10.1038/onc.2014.183

INTRODUCTION

The p53 pathway is a key monitor of several cellular stress signals preventing the survival of cells with irreparable genetic damage, thus limiting tumor development.[1,2] The significance of p53 in tumor suppression is highlighted by the fact that more than half of all human cancers are characterized by loss of p53 function through mutations within the p53 gene or other genetic and epigenetic changes affecting their ability to activate or respond to p53 (Freed-Pastor and Prives[3]).

The biochemical regulation of p53 function is complex and involves posttranslational modifications and interactions with other proteins. The E3 ubiquitin ligase murine double-minute 2 (MDM2 or HDM2 in human) directly associates with p53 and targets it for Lys[48]-linked ubiquitination and degradation. Accordingly, stress-induced p53 accumulation depends on the inactivation of HDM2, which is achieved through several mechanisms, including association with proteins that disrupt its interaction with p53. Interestingly, a number of these HDM2-regulatory proteins are related to the nucleolus, a non-membrane sub-nuclear structure which functions as a hub for ribosome biosynthesis. Specifically, ribosomal proteins L5, L11, L23 and S7 and nucleophosmin (NPM, also designated B23 or numatrin) serve as stress signal transmitters; following growth factor deprivation or exposure to ribosome biosynthesis inhibitors and DNA-damaging agents, they accumulate in the nucleoplasm[4,5] where they bind HDM2 releasing its inhibitory activity over p53 (Zhang and Lu[6] and Bursac *et al.*[7]).

Among these nucleolar proteins, NPM has attracted particular attention because of its diverse cellular activities related to proliferation, apoptosis, regulation of ribosome biogenesis, chromatin remodeling and centrosome duplication and its impact on disease pathogenesis.[8,9] Thus, NPM overexpression is observed in various solid tumors and is correlated with uncontrolled proliferation and cellular transformation, whereas low NPM expression levels or mutations which cause its localization to the cytoplasm, are associated with genomic instability, centrosome amplification and the development of myeloid disorders and hematopoietic malignancies. These reported findings suggest that fine-tuning of NPM expression and/or localization is required to control tumorigenesis. In line with this model, the levels of NPM set a threshold for p53 phosphorylation and activation by competing with ATR for Ser[15] phosphorylation[10] and with HDM2 for p53 binding.[11] NPM has also been shown to control the association of HDM2 with tumor-suppressor ARF upon oncogene-induced replication stress.[12]

Nevertheless, the molecular and biochemical features of NPM that enable it to modulate its pleiotropic biological activities remain largely unexplored. Posttranslational modifications and interactions with other proteins have been described and are likely to regulate at least some of the functional outputs of NPM. Herein we describe Tumor Progression Locus 2 (TPL2), also known as Cancer Osaka Thyroid), as a novel NPM-interacting protein that influences the stress-induced phosphorylation and translocation of NPM to the nucleoplasm.

TPL2 is a serine-threonine mitogen-activated protein 3 (MAP3) kinase with important roles in the immune system where it regulates signaling from Toll-like receptors,[13,14] the tumor necrosis factor (TNF) family of receptors[15,16] and G protein-coupled receptors[17] and the expression of various inflammation-related genes at transcriptional or posttranscriptional level.[18–22] Early studies indicated that TPL2 is a putative proto-oncogene

[1]Molecular and Cellular Biology Laboratory, Division of Basic Sciences, University of Crete Medical School, Heraklion, Greece; [2]Laboratory of Cancer Biology, Institute of Molecular Biology and Biotechnology, Foundation for Research and Technology Hellas (FORTH), Heraklion, Greece; [3]Department of Molecular Medicine and Biotechnology, School of Medicine, University of Rijeka, Rijeka, Croatia and [4]Molecular Oncology Research Institute, Tufts Medical Center, Boston, MA, USA. Correspondence: Professor AG Eliopoulos, Molecular and Cellular Biology Laboratory, Division of Basic Sciences, University of Crete Medical School, Voutes, Heraklion, Crete 71003, Greece.
E-mail: eliopag@imbb.forth.gr
[5]Graduate program: 'The molecular Basis of Human Diseases', University of Crete Medical School, Crete, Greece.
Received 26 November 2013; revised 1 May 2014; accepted 21 May 2014

inasmuch as C-terminal truncations caused by retrovirus insertion in the TPL2 gene locus are associated with enhanced transforming capacity in mice and rats.[23,24] Nevertheless, activating mutations in TPL2 have not been described in humans,[21] and recent data from our laboratory and others have demonstrated that endogenous TPL2 may physiologically function as suppressor of tumorigenesis in the lung,[25] colon[26,27] and skin.[28] Data presented in this study provide biochemical insight into the anti-cancer properties of TPL2 by uncovering a functional relationship between TPL2 and NPM that impacts on p53 response to DNA damage and nucleolar stress.

RESULTS

TPL2 interacts with nucleophosmin

A proteomic screen using overexpressed TPL2 as bait identified NPM as a putative TPL2-interacting protein. These data will be presented in detail elsewhere. Herein we have explored the TPL2:NPM association by glutathione *S* transferase (GST) pull-down and immunoprecipitation assays. Bacterially produced GST–NPM fusion protein immobilized on glutathione sepharose beads was incubated with lysates from human embryonic kidney (HEK) 293 cells transfected with a myc-tagged TPL2 (MT-TPL2) expression vector. As shown in Figure 1a, overexpressed MT-TPL2 was found to interact with GST-NPM. Further control experiments showed that MT-TPL2 did not associate with GST-IκBα (Figure 1b). To determine whether the interaction of TPL2 with NPM also occurs *in vivo*, myc-tagged NPM (MT-NPM) and untagged TPL2 were co-expressed in HEK293 cells, lysates were immunoprecipitated using anti-TPL2 antibody and immunoblotted with anti-NPM. The results showed that when overexpressed, MT-NPM and TPL2 co-precipitate (Figure 1c).

NPM predominantly resides in the nucleolus and undergoes translocation to the nucleoplasm upon cell exposure to DNA-damaging agents.[29] In contrast, TPL2 has mostly been studied as a cytoplasmic kinase in the context of cytokine and Toll-like receptor signal transduction.[30] However, recent studies have indicated that TPL2 may also have nuclear functions.[31] We have thus examined the presence of TPL2 in cytoplasmic and nuclear fractions of HEK293 cells transiently transfected with MT-TPL2. The results of the fractionation experiments showed that overexpressed TPL2 is present both in the cytoplasmic and nuclear extracts from these cells (Figure 2a).

We have also assessed the subcellular localization of TPL2 in immortalized fibroblasts from *tpl2*$^{-/-}$ mice stably reconstituted *in vitro* with near-physiological levels of hemagglutinin (HA)-tagged TPL2 (Cho and Tsichlis[32]). Cells were either exposed to ultraviolet C (UVC) or left untreated, and TPL2 localization was monitored by immunofluorescence using anti-HA antibody.

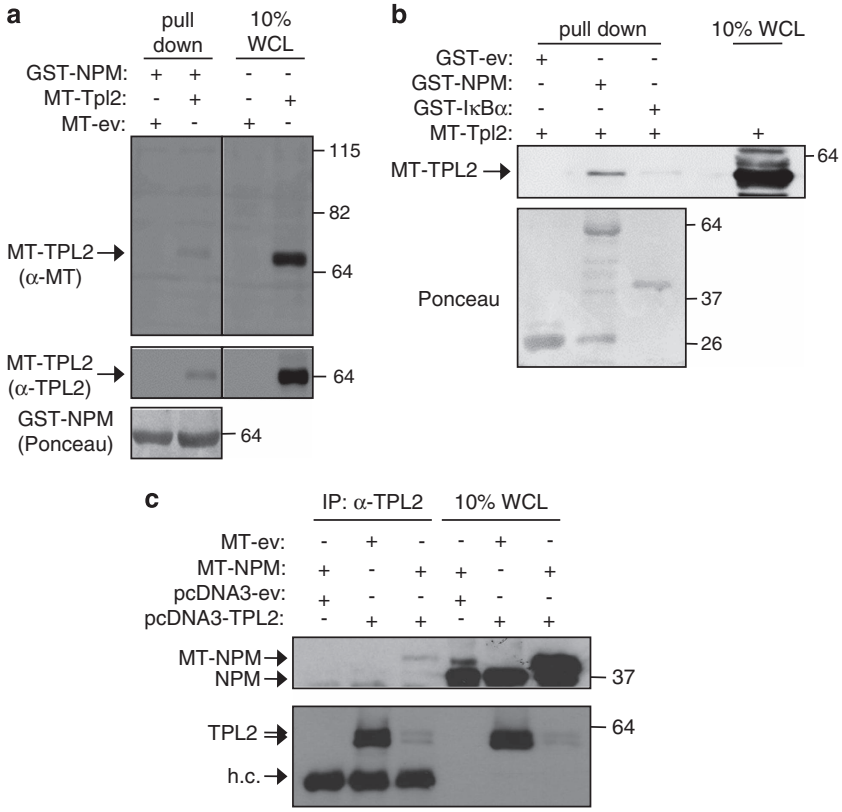

Figure 1. TPL2 interacts with NPM *in vitro* and *in vivo*. (**a**) Pull-down assay showing interaction of overexpressed TPL2 with bacterially produced NPM. GST-NPM was immobilized on glutathione sepharose beads and incubated with 0.3 mg lysates from HEK293 cells transfected with a myc-tagged (MT) TPL2 expression vector (lanes 2 and 4) or control empty vector (ev) plasmid (lanes 1 and 3). TPL2 associating with GST-NPM was detected by immunoblot using anti-MT 9E10 mAb (upper panel) or anti-TPL2 Ab (middle panel). GST proteins were detected by Ponceau staining (lower panel). The sizes of the molecular weight markers (kDa) are given on the right hand side of the gel. Data are representative of at least four independent experiments. (**b**) Pull-down assay showing interaction of exogenously expressed MT-TPL2 with bacterially produced GST-NPM but not GST-IκBα (aa 1–62) or GST alone. (**c**) NPM and TPL2 interact *in vivo* when co-expressed. HEK293 cells were transfected with a combination of myc-tagged (MT) NPM and untagged TPL2 or empty vectors (ev) as indicated. TPL2 was immunoprecipitated (IP) from 0.5 mg cell lysates and TPL2-bound NPM was detected by immunoblotting with anti-NPM. Ten percent of whole-cell lysates (WCL) were also immunoblotted; both the endogenous NPM and the transfected MT-NPM are shown. Note that despite the immunoprecipitation of lower amounts of overexpressed TPL2 shown in lane 3 compared with lane 2, significant interaction of MT-NPM with TPL2 is detected. h.c., Ig heavy chain.

Staining with anti-lamin Ab was used to mark the nuclear envelope. As shown in Supplementary Figure S1, TPL2 predominantly localized in the cytoplasm and plasma membrane in untreated cells, but some punctuated staining was also observed in the nucleus. However, significant mobilization of HA-TPL2 to the nucleus was detected following UVC irradiation. This observation is in agreement with a previous study demonstrating nuclear localization of TPL2 following exposure of cells to UVB.[31]

On the basis of these findings, we asked whether the interaction between TPL2 and NPM occurs in the nucleus where NPM mainly resides. Nuclear and cytoplasmic proteins were extracted from HEK293 cells transiently transfected with MT-TPL2 (Figure 2a) or a kinase-dead mutant (Figure 2b) and incubated with GST-NPM immobilized on glutathione sepharose beads. NPM interactions were analyzed by immunoblot using anti-TPL2 Ab. The results showed a profound association of GST-NPM with nuclear but not cytoplasmic TPL2 (Figure 2a). In contrast, kinase-inactive TPL2 failed to interact with NPM irrespective of localization (Figure 2b).

We next analyzed associations between the endogenous proteins in A549 lung cancer cells. Nuclear and cytoplasmic protein extracts were prepared from cultures exposed to 20 J/m^2 UVC and untreated cultures before evaluation of NPM:TPL2 interactions by co-immunoprecipitation. Endogenous NPM was found to co-precipitate with TPL2 in nuclear extracts from UVC-treated cells, whereas little association was observed in untreated cultures (Figure 2c). In contrast, no interaction between the two proteins was observed in cytoplasmic lysates.

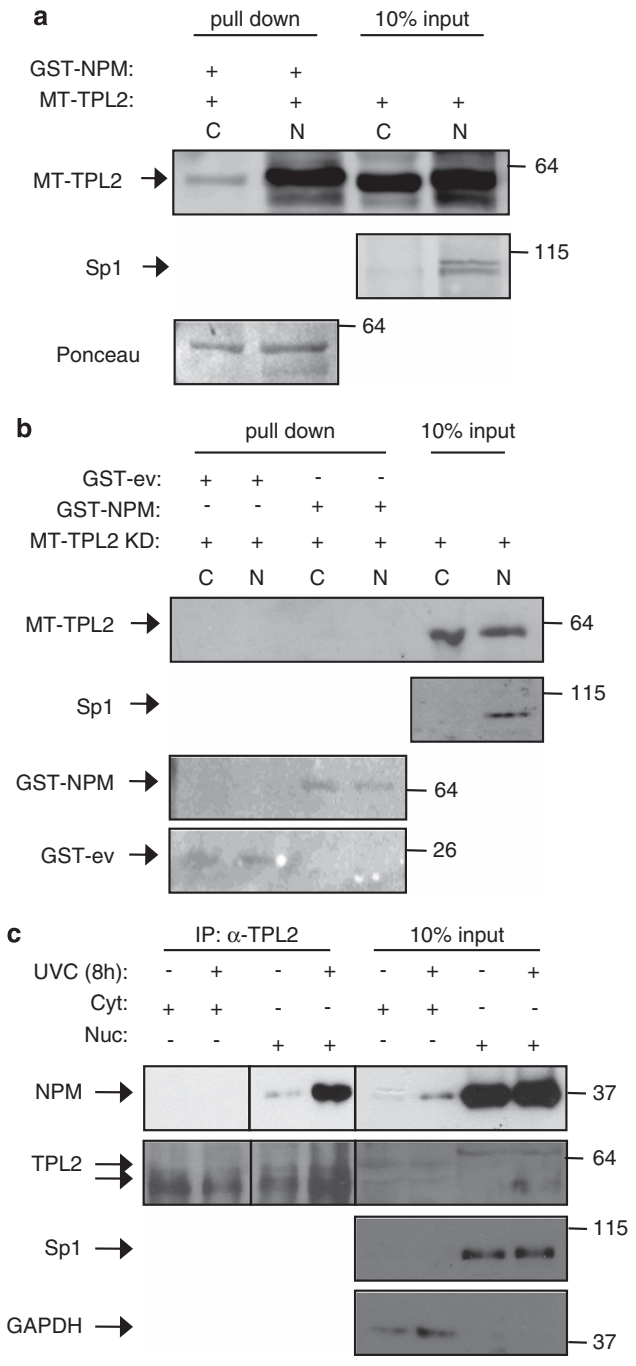

TPL2 modulates both the localization and levels of NPM following DNA damage

On the basis of the aforementioned findings, we proceeded to assess more specifically the localization of TPL2 and NPM before and after DNA damage. Nucleolar, nucleoplasmic and cytoplasmic fractions were obtained from A549 cells exposed to UVC for various time intervals and from untreated cultures and analyzed for TPL2 and NPM levels by immunoblot. As shown in Figure 3a, TPL2 was predominantly found in the cytoplasm of untreated cultures, was absent in the nucleoplasm but was detected in the nucleolar fraction. Following UVC treatment, TPL2 levels decreased in both cytoplasm and nucleoli and increased in the nucleoplasm. Irradiation also led to the translocation of NPM from nucleoli to nucleoplasm, consistent with previous reports.[33] Similar results were obtained when A549 cells were exposed to low concentrations of actinomycin D, which perturbs ribosome biogenesis triggering a p53-activating signaling pathway independently of DNA damage (data not shown).

The aforementioned findings, coupled with the fact that TPL2 and NPM interact (Figure 1), prompted us to examine whether a functional relationship between the two proteins exists. To this end, TPL2 was knocked down in A549 cells followed by cell exposure to UVC. Lysates from cytoplasmic, nucleolar and nucleoplasmic fractions were analyzed for NPM levels by immunoblot. Interestingly, the RNAi-mediated reduction in TPL2 levels attenuated the translocation of NPM from the nucleoli to nucleoplasm (Figure 3a). As purification and loading control in these analyses, lysates from each fraction were immunoblotted for tubulin, lamin B and UBF, which are expressed in the cytoplasm,

Figure 2. TPL2 predominantly associates with NPM in the nucleus and requires intact kinase activity. (**a**) Nuclear and cytoplasmic protein extracts of HEK293 cells transiently transfected with a MT-TPL2 expression vector were prepared and incubated with purified GST-NPM. TPL2 pulled down with GST-NPM was detected by immunoblot. The transcription factor Sp1 was used as a marker for the purity of the nuclear cell extract preparation, and Ponceau staining of the gel confirmed equal loading of recombinant GST-NPM. (**b**) Nuclear and cytoplasmic protein extracts of HEK293 cells transiently transfected with myc-tagged kinase-dead TPL2 (MT-TPL2 KD) were prepared and incubated with either purified GST-NPM or GST-ev (control GST). TPL2 that was pulled down with GST-NPM was detected by immunoblot. The transcription factor Sp1 was used as a marker for the purity of the nuclear cell extract preparation, and Ponceau staining of the gel confirmed equal loading of recombinant GSTs. (**c**) Endogenous nuclear TPL2 interacts with NPM. A549 cells were irradiated with UVC or left untreated for the indicated time period. TPL2 was immunoprecipitated (IP) from 0.5 mg cytoplasmic or nuclear lysates and TPL2-associating NPM was detected by western blotting (lower panel). Ten percent of the respective lysate was analyzed by immunoblotting for TPL2 and NPM levels as input control. SP1 and GAPDH were used as markers for the efficacy of nuclear and cytoplasmic fractionation, respectively.

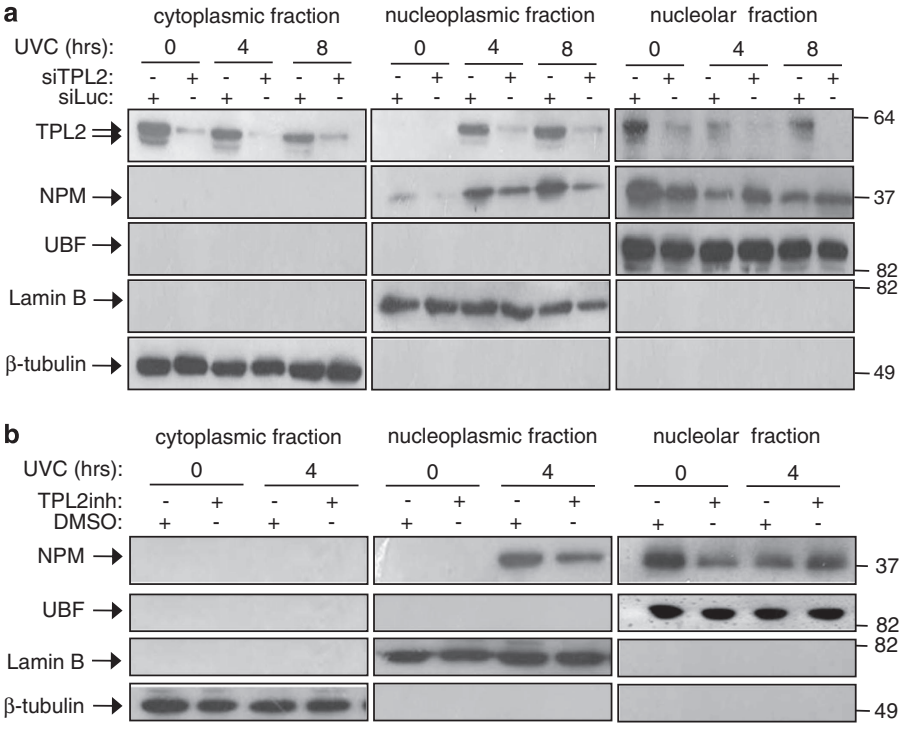

Figure 3. TPL2 affects the translocation of NPM from the nucleolus to the nucleoplasm following UVC treatment. (**a**) A549 cells were transfected with siRNA targeting TPL2 or control siRNA against Luciferase (siLuc) and were exposed to 20 J/m^2 UVC for various time intervals as indicated. Cytoplasmic, nucleoplasmic and nucleolar lysates were prepared and analyzed for TPL2 and NPM levels by immunoblot, using tubulin, lamin B and UBF as loading controls, respectively. (**b**) A549 cells were treated with a kinase inhibitor of TPL2 or vehicle DMSO as control for 1 h before UVC irradiation. Subsequent fractionation and immunodetection of TPL2 and NPM was performed as in panel (**a**).

nucleoplasm and nucleoli, respectively (Figure 3a). Similar results were obtained when A549 cells were cultured in the presence of a small molecule TPL2 kinase inhibitor before exposure to UVC (Figure 3b), suggesting that the catalytic activity of TPL2 contributes to the regulation of NPM re-localization.

NPM expression increases in response to DNA damage,[34] hypoxia[35] and treatment with hormones.[36] In line with these reports, A549 cells exposed to UVC displayed elevated NPM levels compared with untreated controls (Figure 4a). Intriguingly, the knockdown of TPL2 led to higher NPM levels in untreated cultures that did not increase further following UVC treatment (Figure 4a). This phenomenon is not particular to transformed cells as immortalized fibroblasts from *tpl2*$^{-/-}$ mice (Figure 4b) also displayed slightly elevated NPM levels and failed to upregulate NPM in response to different doses of UVC compared with wild-type fibroblasts (Figure 4c).

To test whether the aforementioned protein expression profile relates to differences in ubiquitination, TPL2 was knocked down in A549 cells followed by UVC treatment in the presence or absence of the proteasome inhibitor MG132. Total cell lysates were immunoprecipitated with anti-NPM and immunoblotted with anti-Ubiquitin Ab. Exposure of control siRNA-transfected cultures to UVC led to reduction in the levels of ubiquitinated NPM compared with untreated controls. Interestingly, the knockdown of TPL2 significantly reduced NPM ubiquitination in untreated cultures that was marginally affected by UVC (Figure 4d). These data demonstrate a correlation between NPM expression and ubiquitination and highlight a role for TPL2 in modulating both localization and expression of NPM.

TPL2 regulates the phosphorylation of NPM at threonine 199

NPM is subject to various posttranslational modifications, which affect its localization and function, including phosphorylation.[37] Previous studies have shown that phosphorylation of a fraction of NPM at Thr^{199} is required for its dissociation from nucleolar components.[38] As TPL2 functions as a Ser/Thr kinase, interacts with NPM (Figures 1 and 2) and regulates its localization (Figure 3), we surmised that TPL2 may phosphorylate NPM. In line with this prediction, we have found that Thr^{199} NPM phosphorylation is severely affected by the knockdown of TPL2 in both untreated A549 cells and in cultures exposed to UVC (Figure 5a). To determine whether this effect requires the catalytic activity of TPL2, A549 cells were treated with a TPL2 kinase inhibitor before UVC exposure. We used inhibitor concentrations that impair TNF-mediated extracellular signal-regulated kinase (ERK) phosphorylation (Supplementary Figure S2), in line with the established role of TPL2 in the TNFR1-MAPK signaling axis.[15] The results showed that treatment with the TPL2 kinase inhibitor reduced basal Thr^{199} phosphorylation levels and accelerated their decline following exposure to UVC (Figure 5b).

To provide further evidence linking TPL2 to NPM phosphorylation, we assessed the ability of overexpressed TPL2 to phosphorylate NPM at Thr^{199} in an *in vitro* kinase reaction using recombinant GST-NPM as substrate. As positive control in these assays, we used MEK1 which directly interacts with and is phosphorylated by TPL2 at Ser$^{217/221}$ (Salmeron *et al*.[39]). Immunoprecipitated TPL2 from MT-TPL2 transfected HEK293 cells was found to phosphorylate both GST-MEK1 (Supplementary Figure S3) and GST-NPM *in vitro*, whereas a Thr^{199} → Ala mutated NPM fused to GST remained unresponsive (Figure 5c). Collectively, these findings underscore an important role for TPL2 in the regulation of NPM phosphorylation at Thr^{199}.

To examine whether TPL2 may influence NPM ubiquitination via Thr^{199} phosphorylation, HEK293 cells were co-transfected with TPL2 and HA-tagged Ub expression vectors and either MT-NPM or a MT-NPM construct in which Thr^{199} has been mutated to Ala (T^{199}A). Lysates were immunoprecipitated with anti-HA and

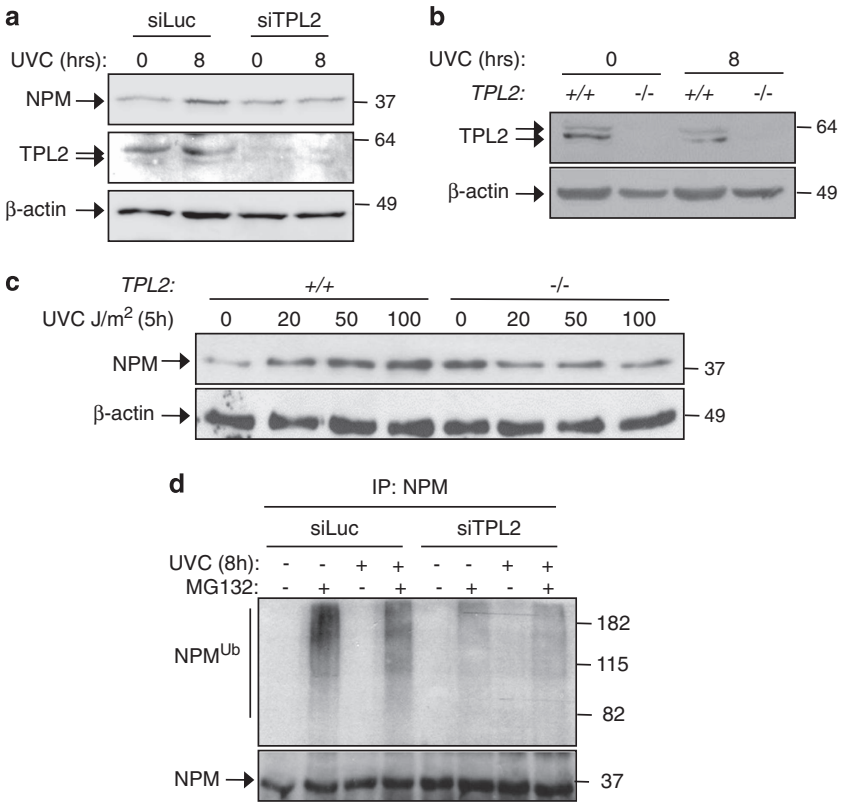

Figure 4. TPL2 regulates the expression levels of NPM following DNA damage. (**a**) A549 cells were transfected with TPL2 siRNA (siTPL2) or control siRNA targeting Luciferase and exposed to 20 J/m^2 UVC for 8 h or left untreated. Total NPM protein levels were detected by immunoblot using β-actin as a loading control. (**b**) Immunoblot showing expression levels of TPL2 in control *tpl2*$^{+/+}$ and *tpl2*$^{-/-}$ MEFs and MEFs exposed to UVC. (**c**) Dose-depended effect of UVC on NPM levels following exposure of *tpl2*$^{+/+}$ and *tpl2*$^{-/-}$ MEFs to UVC. (**d**) TPL2 regulates the ubiquitination status of NPM. A549 cells were transfected with TPL2 siRNA (siTPL2) or control siRNA (siLuc) and irradiated with 20 J/m^2 UVC for 8 h or left untreated. Proteasome inhibitor MG132 was added to the culture medium before irradiation. Cells were lysed in RIPA lysis buffer, and ubiquitination of immunoprecipitated endogenous NPM was detected with western blotting by probing with anti-Ub (FK2H). Results shown are representative of at least three independent experiments.

immunoblotted using anti-NPM Ab. The results (Figure 5d) demonstrated that TPL2 expression led to enhanced ubiquitination of wild-type NPM, whereas NPM(T^{199}A) remained unaffected.

To further explore the link between ubiquitination and Thr^{199} phosphorylation of NPM and the influence of TPL2 on these effects, A549 cells were transfected with siRNAs targeting TPL2 or the unrelated Luciferase gene and exposed to UVC treatment in the presence or absence of the proteasome inhibitor MG132. Lysates were immunoblotted with antibodies detecting NPM phosphorylated at threonine 199 or NPM, irrespective of phosphorylation status. Interestingly, MG132-mediated inhibition of proteasome activity led to significant increase in the levels of phosphorylated NPM in both untreated cultures and cells exposed to UVC (Figure 5e). The levels of total (phosphorylated and non-phosphorylated) NPM also partly increased following MG132 treatment.

We evaluated the possibility that MG132 does not directly exert its effects on NPM but leads to increased NPM phosphorylation through TPL2 stabilization. To this end, A549 cells were treated with MG132 and TPL2 levels were examined before and 8 h after exposure to 20 J/m^2 UVC. As control, lysates from the same cultures were immunoblotted for p53. As shown in Supplementary Figure S4, TPL2 expression levels remained unaffected by MG132 treatment, whereas p53 was stabilized both in untreated and UVC-treated cells. On the basis of the aforementioned findings, we conclude that TPL2 regulates threonine 199 phosphorylation of a fraction of NPM that undergoes ubiquitination and degradation.

TPL2 regulates p53 accumulation in response to DNA damage and ribosomal stress by modulating the interaction of NPM with HDM2

Following DNA damage, the release of NPM to the nucleoplasm contributes to increased p53 stability by binding to and inhibiting HDM2.[11] In line with the reported findings, the RNAi-mediated depletion of NPM in A549 cells resulted in reduced accumulation of p53 upon *cis*-platin (Figure 6a) or UVC (Figure 6b) treatment.

As TPL2 affects both the stress-induced localization and expression levels of NPM (Figures 3 and 4), we asked whether it also impacts on the activation of the p53 pathway. To this end, TPL2 was knocked down in A549 cells before stimulation of genotoxic stress by *cis*-platin or UVC or induction of ribosomal stress by low concentrations of actinomycin D.[4] In analogy to cells bearing reduced NPM levels (Figures 6a and b), p53 accumulation was attenuated by the knockdown of TPL2 in response to these agents (Figures 6c–e). This observation was not restricted to tumor cells as primary embryo fibroblasts from *tpl2*$^{-/-}$ mice also responded to UVC with reduced accumulation of p53 compared with *tpl2*$^{+/+}$ cells (Supplementary Figure S5). Moreover, pretreatment of A549 cells with TPL2 kinase inhibitor mimicked the effects of TPL2 knockdown and attenuated the p53 response to UVC (Figure 6f). In line with these observations, A549 cells transfected with TPL2 siRNA displayed reduced levels of apoptosis compared with controls upon exposure to UVC (Supplementary Figure S6).

These observations prompted us to determine whether TPL2 exerts its effect on p53 by influencing the interaction of NPM with HDM2. As demonstrated by co-immunoprecipitation analysis,

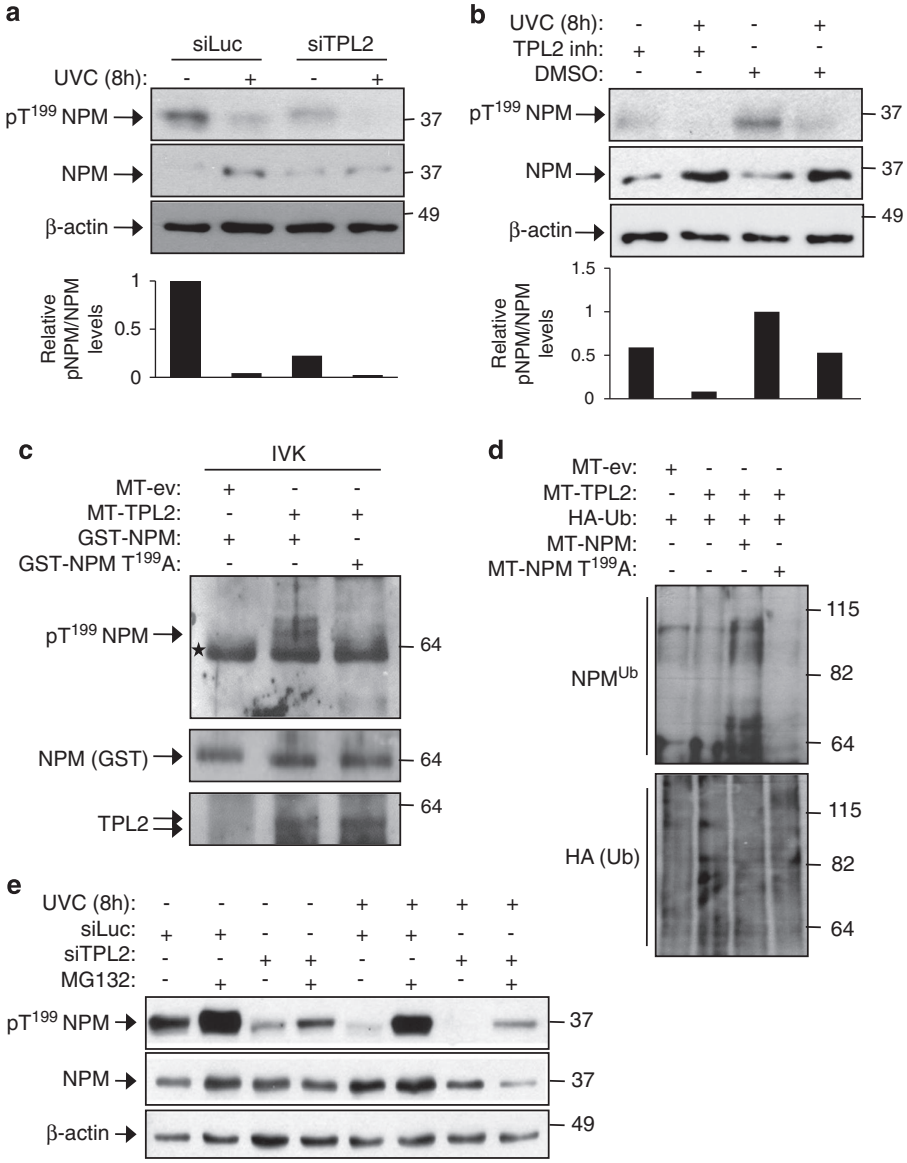

Figure 5. TPL2 phosphorylates NPM at Thr^{199} affecting NPM ubiquitination. (**a**) A549 cells were transfected with TPL2 siRNA (siTPL2) or control siRNA (siLuc) and irradiated. Total NPM protein levels and NPM phosphorylated at Thr^{199} (T^{199}) were detected using western blotting. Semi-quantitation of the levels of T^{199}-phosphorylated vs total (phosphorylated and non-phosphorylated) NPM was performed using the Image J software (http://rsbweb.nih.gov/ij/) and is shown in the lower panel relative to control cultures, which were given the arbitrary value of '1'. Results shown are representative of at least three independent experiments. (**b**) TPL2 kinase activity is required for Thr^{199} phosphorylation *in vivo*. A549 cells were pretreated for 1 h with TPL2 kinase inhibitor (TPL2 inh, lanes 1 and 2) and then exposed to UVC. DMSO was used as a vehicle control (lanes 3 and 4). Lysates were analyzed for pT^{199} NPM and 'total' NPM protein by immunoblot. Semi-quantitation of the levels of T^{199}-phosphorylated vs total NPM is also shown. Results shown are representative of at least three independent experiments. (**c**) Overexpressed TPL2 induces the phosphorylation of NPM *in vitro*. HEK293 cells were transfected with a MT-TPL2 expression vector or empty control plasmid (MT-ev). Tpl2 was immunoprecipitated from cell lysates and used in an *in vitro* kinase (IVK) reaction with GST-NPM or GST-NPM (T^{199}A) as substrate immobilized on gluatathione sepharose beads. GST fusion proteins were then immunoblotted and probed with antibodies specific for Thr^{199}-phosphorylated NPM (upper panel) or total NPM (middle panel). Anti-TPL2 immunoprecipitates were also immunoblotted for TPL2 to confirm that similar amounts of TPL2 were assayed in each reaction (lower panel). The star represents Ig heavy chain. (**d**) TPL2 regulates NPM ubiquitination through T^{199} phosphorylation. HEK293 cells were transfected with HA-tagged Ub, MT-TPL2 or empty vector (ev) and either MT-NPM or the NPM(T^{199}A) mutant. Lysates were immunoprecipitated with anti-HA and immunoblotted for NPM and HA-Ub. (**e**) Proteasome inhibition partly restores Thr^{199} NPM phosphorylation and total NPM levels upon TPL2 knock-down or following UVC irradiation. TPL2-depleted A549 cells were treated with UVC in the presence of MG132 or DMSO vehicle control. Detection of NPM pThr^{199}, total NPM and β-actin as loading control was performed by immunoblotting.

NPM and HDM2 were found to form complexes (Figure 6g). Exposure to UVC led to reduction in total HDM2 levels but increased interaction of HDM2 with NPM, in agreement with a previous report.[11] Interestingly, however, less NPM co-precipitated with HDM2 following depletion of TPL2 (Figure 6g), suggesting that the lower levels of p53 accumulation in these cells result from HDM2-mediated ubiquitination and proteosomal degradation of p53. In line with this prediction, treatment with MG132 restored p53 levels in TPL2-depleted cells exposed to UVC (Figure 6h). Together, these results suggest that TPL2 regulates p53 accumulation by interfering with the ability of NPM to interact with HDM2.

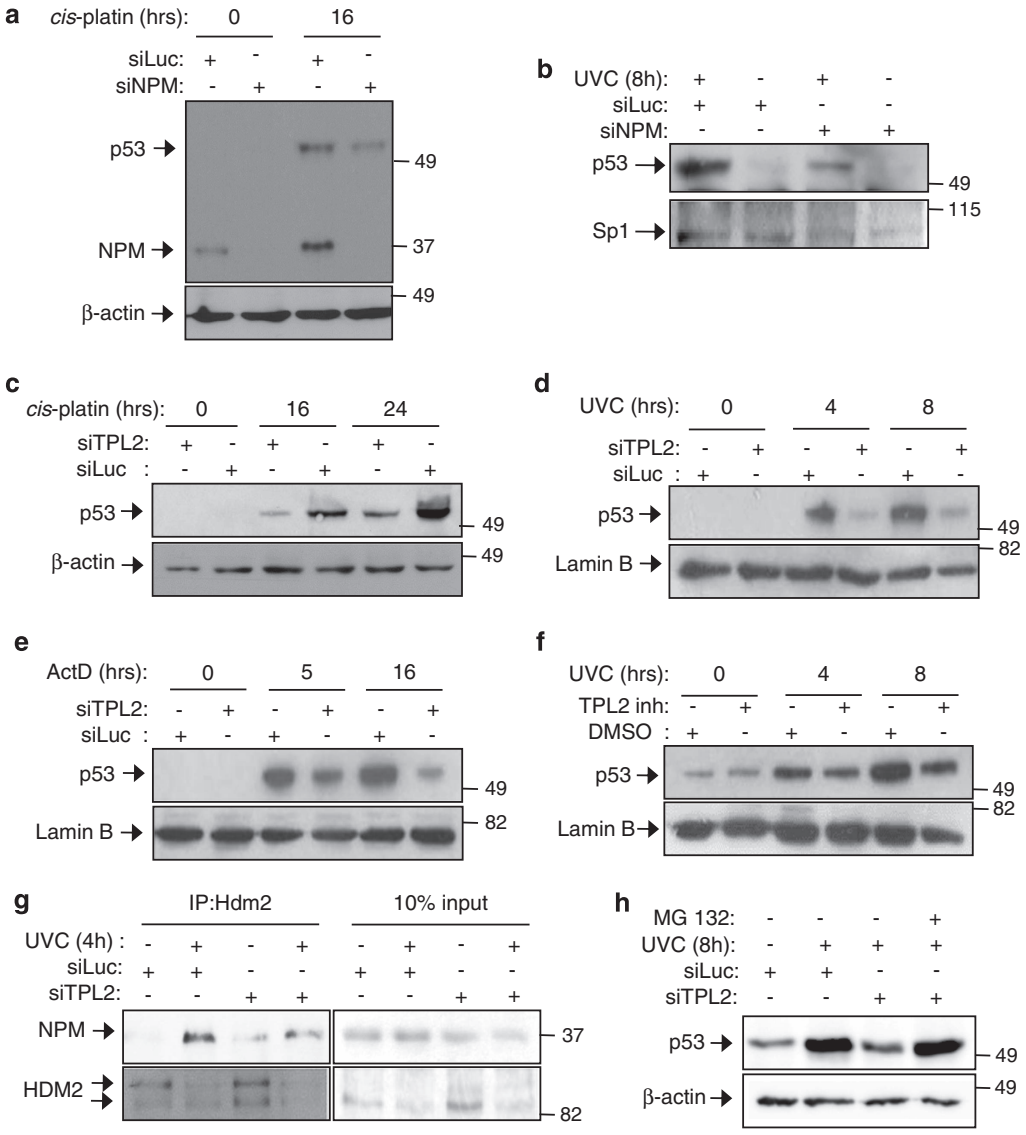

Figure 6. TPL2 regulates p53 accumulation in response to DNA damage. (**a**, **b**) Knockdown of NPM reduces the accumulation of p53 in response to DNA damage. A549 cells were transfected with siRNA targeting NPM or the unrelated Luciferase gene and exposed to *cis*-platin for 16 h (**a**) or to UVC for 8 h (**b**). Lysates from treated and untreated cultures were immunoblotted for NPM, p53, SP1 and actin levels as indicated. Note also the increase in NPM levels following treatment with *cis*-platin, in line with the UVC data presented in Figure 4a. (**c**–**e**) TPL2 regulates p53 accumulation in response to DNA-damaging agents and ribosomal stressors. Following RNAi-mediated TPL2 silencing, A549 cells were exposed to *cis*-platin, UVC or actinomycin D (ActD) for various time intervals as indicated. Lysates were analyzed for expression of p53 or β-actin/Lamin B as loading controls. Results shown are representative of at least three independent experiments. (**f**) Treatment of A549 cells with TPL2 kinase inhibitor reduces the UVC-induced accumulation of p53. Results shown are representative of at least three independent experiments. (**g**) Knockdown of TPL2 reduces the interaction of HDM2 with NPM. A549 cells were transfected with siRNA targeting TPL2 or with control Luciferase siRNA and then exposed to UVC or left untreated. Lysates were immunoprecipitated with anti-HDM2 and immunoblotted with anti-NPM. Note that the efficiency of immunoprecipitation differs between untreated and UVC-treated cells because of the UVC-mediated degradation of HDM2 pool. (**h**) The proteasome inhibitor MG132 stabilizes p53 levels in TPL2 knocked down cells irradiated with UVC. A549 cultures were transfected with siRNAs as in panel (**g**) and treated with MG132 before exposure to UVC for 8 h as indicated. The levels of p53 were assessed by immunoblotting.

DISCUSSION

TPL2 has largely been appreciated as a MAP3 kinase operating in the cytoplasm to control inflammatory and oncogenic signal transduction.[21,22,30] Data presented in this study show that a fraction of TPL2 resides in the nucleus (Figure 2a and Supplementary Figure S1) and identify the nucleolus as the main subnuclear structure of TPL2 localization (Figure 3). This finding indicates that TPL2 may affect targets outside the MAP kinase cascade. Indeed, we describe herein a novel nuclear role for TPL2 as a physical and functional interactor of NPM, a major nucleolar component. Interestingly, cytoplasmic TPL2 largely fails to bind NPM in pull-down and co-immunoprecipitation assays (Figure 2), raising the possibility that TPL2 undergoes posttranslational modifications and/or interaction with other protein(s) which enable its localization to the nucleus and association with NPM. As TPL2 lacks canonical nuclear localization signal, we postulate that it is chaperoned by another protein to enter the nucleus, reminiscent of the cytoplasmic kinases Raf-1 and Akt2 which have

also been described to partly translocate to the nucleus and confer nuclear functions.[40,41]

NPM is subject to various posttranslational modifications, including phosphorylation, SUMOylation and ubiquitination which are likely to dictate many of the pleiotropic biochemical and biological properties of this protein.[42] Thus phosphorylation of NPM at Thr^{199} has been reported to affect the dissociation of NPM from nucleolar components,[38] recruitment to DNA-damage foci and participation in DNA-repair mechanisms.[43,44] Previous studies have shown that NPM is phosphorylated at Thr^{199} by the cyclin E/cyclin-dependent kinase 2 (cdk2) complex[45,46] and becomes de-phosphorylated by the phosphatase PP1β following cell exposure to UV.[44] However, it has been proposed that additional kinases must be utilized to phosphorylate Thr^{199}, as this NPM modification is detected throughout the cell cycle and inhibition of cdk2 does not impair Thr^{199} phosphorylation.[47] In this study, we have described TPL2 as a novel Thr^{199} NPM kinase.

A functional link between TPL2 and phosphorylation of NPM at Thr^{199} was inferred by the observation that the catalytic activity of TPL2 is required for physical interaction with NPM (Figure 2b) and that TPL2 knockdown results in attenuated translocation of NPM from the nucleolus to nucleoplasm (Figure 3a), a process influenced by Thr^{199} phosphorylation.[38] In line with this prediction, we have demonstrated that TPL2 phosphorylates NPM at Thr^{199} *in vitro* (Figure 5c) and that the kinase activity of TPL2 is required for this modification *in vivo* (Figure 5b). Intriguingly, whereas the interaction between TPL2 and NPM increases upon exposure to UVC (Figure 2c), phosphorylation at Thr^{199} decreases (Figures 5a and b). This finding may relate to the degradation of the phosphorylated form of NPM (Figure 5e), or it may reflect the balance between the opposing effects of TPL2 on phosphorylation and of PP1β on Thr^{199} NPM de-phosphorylation in irradiated cells,[44] a possibility that merits further investigation.

NPM participates in signaling networks that govern DNA-damage responses and operates as a regulator of major tumor suppressors, such as p53 and Arf.[48,49] Upon exposure to stress stimuli, NPM interacts with HDM2 and sequesters it from interaction with p53, thereby protecting p53 from HDM2-mediated degradation.[11] The ensuing accumulation of p53 is required for cell cycle arrest and/or senescence in DNA-damaged cells.[48,50] Our findings demonstrate that, similar to NPM knockdown[11,48] (see also Figures 6a and b), the ablation (Supplementary Figure S5) or reduction (Figure 6) in TPL2 levels, a feature of some common forms of human cancer,[25] leads to significant inhibition of p53 activation following genotoxic or ribosomal stress. Importantly, we show that the effects of TPL2 on p53 stabilization are mediated through NPM inasmuch as the knockdown of TPL2 results in decreased interaction of NPM with HDM2 in DNA-damaged cells (Figure 6g). In line with this finding and the function of HDM2 as p53 ubiquitin ligase, treatment with a proteasome inhibitor restores p53 levels in TPL2-ablated cells exposed to UVC (Figure 6h).

A functional link between NPM phosphorylation and p53 activation was inferred by studies showing that Thr^{199} NPM phosphorylation by cyclin–CDK complexes is involved in centrosome duplication, which triggers CDKN1A-mediated cell cycle arrest or apoptosis in p53-positive backgrounds.[51] Loss of p53 eliminates this checkpoint, culminating in centrosome over-duplication, mitotic inaccuracy and genomic instability.[51] However, the molecular events linking NPM phosphorylation to p53 activation remain elusive. Previous reports have shown that NPM undergoes ubiquitination mediated by the E3 ubiquitin ligase BRCA1/BRDA1[52] and have implicated the ubiquitin–proteasome system in the stability of NPM.[53,54]

In this study, we confirm these findings and show a correlation between reduced ubiquitination and elevated NPM expression levels in UVC-treated cells (Figure 4d). Although *de novo* transcription may also contribute to this effect,[55] we have found that knockdown of TPL2 results in reduced ubiquitination of NPM in both untreated and UVC-treated cells (Figure 4d). Importantly, we report that TPL2 promotes NPM ubiquitination in a Thr^{199}-dependent manner (Figure 5d) and that the UVC-triggered reduction in Thr^{199}-phosphorylation levels is restored upon inhibition of proteasome activity in both control and TPL2-depleted cells (Figure 5e).

Collectively, our data uncover a novel role for TPL2 in the regulation of NPM phosphorylation and localization. On the basis of the presented findings, we propose that in untreated cells TPL2 phosphorylates a fraction of NPM at Thr^{199} (pNPM; Figure 7),

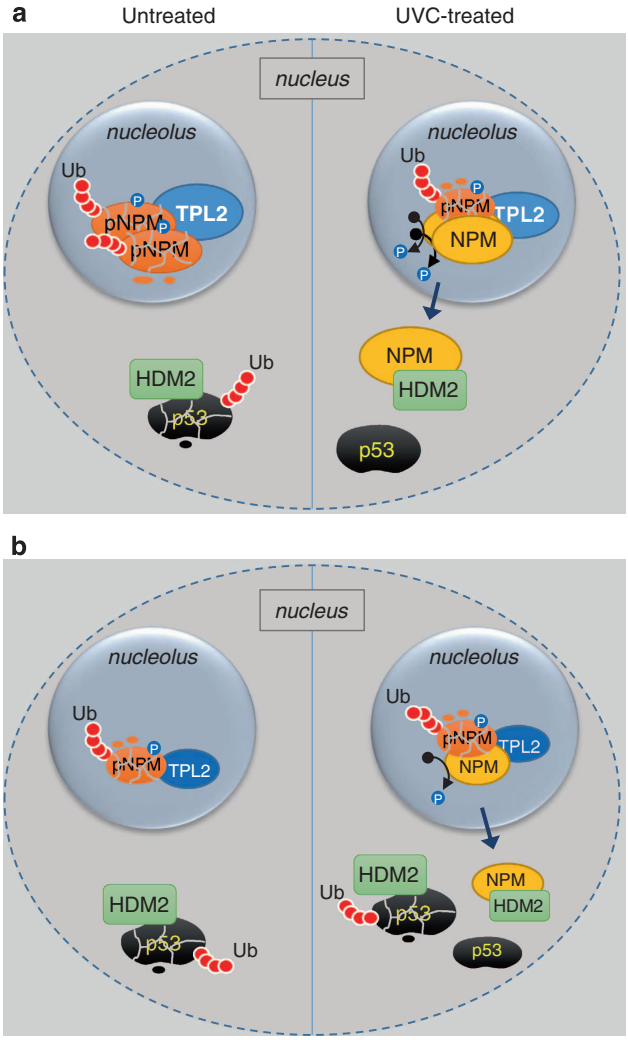

Figure 7. Proposed model of the impact of TPL2 on NPM phosphorylation, localization and function. In steady-state conditions (untreated cells; (**a**), left panel), a fraction of TPL2 resides in the nucleolus where it associates with and phosphorylates NPM molecules at Thr^{199} (pNPM), targeting them for ubiquitination and degradation. In the nucleoplasm of untreated cells, HDM2 ubiquitinates p53 which undergoes proteasomal degradation. Following exposure to UVC (**a**, right panel), pNPM is de-phosphorylated by PP1β,[44] stabilized (orange-colored oval) and translocates to the nucleoplasm where it associates with HDM2 alleviating its effect on p53 degradation. When TPL2 expression levels are reduced (**b**), a feature of certain forms of human cancer, the fraction of NPM which becomes phosphorylated diminishes. The pool of pNPM available for UV-induced, PP1β-mediated de-phosphorylation is thus reduced, resulting in impaired mobilization of NPM to the nucleoplasm (**b**, right panel). As a result, HDM2 maintains extensive control over p53, and p53 accumulation is impaired.

which is targeted for ubiquitination and degradation thereby contributing to the maintenance of steady-state NPM levels. Upon genotoxic damage ensued by UVC, pNPM becomes de-phosphorylated presumably by the PP1β phosphatase, which has been reported to convey this UV-mediated effect.[44] The de-phosphorylation of pNPM leads to reduced ubiquitination, NPM stabilization and translocation to the nucleoplasm where it regulates HDM2:p53 interactions. This model is supported by biochemical evidence demonstrating that Thr^{199}-phosphorylated NPM is detected in the nucleolus but not the nucleoplasm (Supplementary Figure S7) and by published data suggesting that, once de-phosphorylated, NPM functions outside the nucleolus to regulate E2F1 transcription and DNA repair of UVC-induced genotoxic damage.[44] In cells bearing reduced TPL2 expression levels, NPM phosphorylation at Thr^{199} is diminished and the pool of pNPM available for PP1β-mediated de-phosphorylation is decreased. As a result, the UV-induced mobilization of NPM to the nucleoplasm is reduced, leading to poor p53 response (Figure 7).

The findings reported herein thus expand our understanding of the function of TPL2 as negative regulator of carcinogenesis[25–28] by defining a nuclear role for this kinase in the topological sequestration of NPM and in coupling p53 signaling to the generation of Thr^{199}-phosphorylated NPM. The physical and functional relationship between TPL2 and NPM may thus influence the outcome of genotoxic and ribosomal stress, thereby achieving control of processes relevant to carcinogenesis. In light of a recent study implicating TPL2 re-activation in therapeutic resistance to MEK and ERK inhibitors in melanoma,[56] it would be of interest to examine the interplay between TPL2 and NPM in this response.

MATERIALS AND METHODS

Expression constructs and mutagenesis

Full-length NPM cDNA (NM_002520.6) designated as wild-type NPM was PCR-amplified from human cDNA using primers: 5′-GATTCGATGGACA TGGAC-3′ (sense) and 5′-TTAAAGAGACTTCCTCCACTG-3′ (antisense). The amplicon was inserted into pCR2.1 TOPO vector (Invitrogen, Life Technologies, Carlsbad, CA, USA) and then sub-cloned into myc-tagged (MT) pRK5 mammalian expression vector (pRK5-MT-NPM) or pGEX-2TK-GST (C terminal) bacterial expression vector (GE Healthcare, Little Chalfont, UK) as BamHI-EcoRI fragment. GST-IκBα (aa1-62) has previously been described.[57] Myc-tagged wild-type (MT-TPL2) and kinase-dead (K167M) TPL2 (MT-TPL2 KD) constructs were a kind gift from A Weiss (Rosalind Russell Medical Research Center for Arthritis, UCSF, CA, USA).[58] A threonine 199 to alanine (T199A) NPM mutation was generated as previously described[59] using MT-NPM or GST-NPM as template. All constructs were sequenced (Macrogen Co., Amsterdam, The Netherlands) to ensure error-proof cloning and/or mutagenesis.

Cell culture, transfections and gene silencing

Maintenance of A549, HEK293 cells and MEFs was performed as previously described.[17,25] Gene silencing was performed using Lipofectamine RNAiMax Reagent (Invitrogen) according to the manufacturer's instructions. TPL2 knockdown was achieved following one or two rounds of siRNA transfection using Dharmacon SMARTpool ON-TARGETplus MAP3K8 siRNA (no. L003511, Thermo Fisher Scientific, Leicestershire, UK) or a combination of three Stealth siRNAs (no. HSS102181-182-038; Invitrogen). The siRNA duplex sequences used for NPM depletion were designed according to previous published data[48] and were purchased from Dharmacon. Working concentration of each siRNA was 10–20 nM.

Cell treatment, lysis and fractionation

Cells were irradiated with 20 J/m^2 UVC (Vilber Lourmat, Eberhardzell, Germany),[60] treated with *cis*-platin (Sigma-Aldrich GmbH, Munich, Germany) at a final concentration of 25 μM or Actinomycin D (Sigma-Aldrich) at 0.05 μg/ml. Recombinant human TNFα (R&D systems, Abingdon, UK) was used at a final concentration of 20 ng/ml. MG132 (ENZO Life Sciences, Farmingdale, NY, USA) was used at a final concentration of 20 μM and was added to the medium 1 h before stimulation. TPL2 kinase inhibitor (Calbiochem, Merck-Millipore, Billerica, MA, USA) was added at the culture medium 1 h before stimulation at a final concentration of 20 μM. Following treatment, cells were lysed using a Triton X-100-based lysis buffer as previously described.[18,25] Alternatively RIPA lysis buffer was used to ensure efficient lysis of nuclei. Fractionation of cytoplasmic and nuclear proteins and isolation of highly pure nucleoli was performed as previously described.[4,15]

Immunoblotting and antibodies

Immunoblotting was performed as previously described.[18,25] The following antibodies were used: α-TPL2 (M-20), α-NPM (FC82291), α-myc (A-14), α-Sp1 (PEP-2), α-HA (Y-11),α-Lamin-B (C-20), α-UBF (F-9), α/β-tubulin (TU-02) and α-ERK2 (C-14) purchased from Santa Cruz (Dallas, TX, USA); α/β-actin (clone C4) purchased from Merck-Millipore; α-pERK (M8159) and α-GAPDH from Sigma-Aldrich; α-Ubiquitin (FK2H) from ENZO Life Sciences; and α-MEK1/2 pSer217/Ser22 and α-MEK1/2 from Cell Signaling (Danvers, MA, USA). Detection of NPM pThr199 was achieved with a cocktail of antibodies purchased from Cell Signaling (no. 3541) and Abcam (Cambridge, MA, USA) (EP1857Y). Anti-p53 (DO-1, pAb1801) and anti-HDM2 (4B2, 4B11, 2A9) hybridoma supernatants were kindly provided by Professor M Oren and Professor Varda Rotter (Weizmann Institute of Science, Israel).

Immunoprecipitation and GST pull-down assays

Cells were lysed in a buffer containing 0.5% Triton X-100, 150 mM NaCl, 50 mM Tris pH 7.6, 1% EDTA, 1 mM Na_3VO_4 and protease inhibitor cocktail (Sigma-Aldrich) at 48 h posttransfection or immediately after cell stimulation. Equal protein amounts (0.5–1 mg) were mixed with the appropriate antibody for 1 h at room temperature or overnight at 4 °C. The complexes were then bound to protein G sepharose beads (BD Biosciences, Oxford, UK) for 60 min at 4 °C. After excess washing with lysis buffer, bead-bound protein complexes were dissociated from the beads in Laemmli buffer (containing β-mercaptoethanol) and boiled for 5 min at 100 °C. Samples were then loaded on polyacrylamide gels for sodium dodecyl sulfate–polyacrylamide gel electrophoresis analysis. For the detection of immunoprecipitated (IP) TPL2, a light chain-specific secondary α-rabbit antibody was used to avoid heavy chain background (Jackson Immunoresearch Laboratories, Suffolk, UK). For Ubiquitin IP assays 20 μM MG132 (ENZO Life Sciences) was added to the cell culture medium for 4–5 h before cell lysis. Cells were then washed in 1× PBS pH 7.4 supplemented with 10 μM MG132 and 10 mM NEM (Sigma-Aldrich) and lysed in RIPA buffer containing MG132 and NEM. NPM was immunoprecipitated and analyzed for ubiquitination status by probing with anti-Ub Ab (FK2H). The GST pull-down assays were performed as previously described.[15]

In vitro kinase assay

HEK-293T cells transfected with MT-ev or MT-TPL2 were lysed in kinase lysis buffer,[57] and 0.5 mg protein lysate was used to immunoprecipitate TPL2 using 2 μg α-TPL2 (M-20) Ab and G-sepharose beads. The beads were washed twice in kinase lysis buffer and three times in kinase reaction buffer.[57] The supernatant was removed, and the beads were resuspended in kinase reaction buffer supplemented with 10 mM $MgCl_2$ and 2 mM freshly made ATP and 1–2 μg purified (with glutathione beads column) GST-NPM, GST-NPM(T199A) or kinase inactive GST-MEK1 (K207A)[39] as substrate. *In vitro* kinase reaction was performed for 30 min at 30 °C. Beads were separated from the supernatant, resuspended in 2× Laemmli buffer and boiled for 5 min at 100 °C. Supernatants were mixed with equal volumes of 2× Laemmli buffer and boiled. Phosphorylation was determined by western blotting of bead eluates and probing with α-pT199 NPM or α-pS217/S222 MEK1/2. Equal loading of GST-NPM and GST-MEK1 (K207A) protein was confirmed by blotting supernatants with α-NPM or α-MEK1/2 antibody.

CONFLICT OF INTEREST

The authors declare no conflict of interest.

ACKNOWLEDGEMENTS

We thank Moshe Oren and Varda Rotter (Weizmann Institute, Israel), Josef Papamatheakis (FORTH/IMBB, Greece), Angeliki Malliri (Patterson Institute for Cancer Research, UK), Vassilis Gorgoulis (University of Athens Medical School, Greece) and Charalambos Spilianakis (FORTH/IMBB, Greece) for their kind gift of reagents and

Marina Ioannou for excellent technical assistance. This work was supported by the European Commission (EC) research program 'Inflammation & Cancer Research in Europe' (INFLA-CARE; EC Contract 223151) to AGE and SV, the EC support program 'Translational Potential' (TransPOT; EC Contract 285948) to AGE and a University of Crete Maria Manassaki scholarship to DK.

REFERENCES

1 Levine AJ, Oren M. The first 30 years of p53: growing ever more complex. *Nat Rev Cancer* 2009; **9**: 749–758.
2 Zilfou JT, Lowe SW. Tumor suppressive functions of p53. *Cold Spring Harb Perspect Biol* 2009; **1**: a001883.
3 Freed-Pastor WA, Prives C. Mutant p53: one name, many proteins. *Genes Dev* 2012; **26**: 1268–1286.
4 Bursać S, Brdovčak MC, Pfannkuchen M, Orsolić I, Golomb L, Zhu Y *et al.* Mutual protection of ribosomal proteins L5 and L11 from degradation is essential for p53 activation upon ribosomal biogenesis stress. *Proc Natl Acad Sci USA* 2012; **109**: 20467–20472.
5 Donati G, Peddigari S, Mercer C a, Thomas G. 5S ribosomal RNA is an essential component of a nascent ribosomal precursor complex that regulates the Hdm2-p53 checkpoint. *Cell Rep* 2013; **4**: 87–98.
6 Zhang Y, Lu H. Signaling to p53: ribosomal proteins find their way. *Cancer Cell* 2009; **16**: 369–377.
7 Bursac S, Brdovcak MC, Donati G, Volarevic S. Activation of the tumor suppressor p53 upon impairment of ribosome biogenesis. *Biochim Biophys Acta Mol Basis Dis* 2013; **1842**: 817–830.
8 Grisendi S, Mecucci C, Falini B, Pandolfi PP. Nucleophosmin and cancer. *Nat Rev Cancer* 2006; **6**: 493–505.
9 Colombo E, Alcalay M, Pelicci PG. Nucleophosmin and its complex network: a possible therapeutic target in hematological diseases. *Oncogene* 2011; **30**: 2595–2609.
10 Maiguel DA, Jones L, Chakravarty D, Yang C, Carrier F. Nucleophosmin sets a threshold for p53 response to UV radiation. *Mol Cell Biol* 2004; **24**: 3703–3711.
11 Kurki S, Peltonen K, Latonen L, Kiviharju TM, Ojala PM, Meek D *et al.* Nucleolar protein NPM interacts with HDM2 and protects tumor suppressor protein p53 from HDM2-mediated degradation. *Cancer Cell* 2004; **5**: 465–475.
12 Korgaonkar C, Hagen J, Tompkins V, Frazier AA, Allamargot C, Quelle FW *et al.* Nucleophosmin (B23) targets ARF to nucleoli and inhibits its function. *Mol Cell Biol* 2005; **25**: 1258–1271.
13 Banerjee A, Gugasyan R, McMahon M, Gerondakis S. Diverse Toll-like receptors utilize Tpl2 to activate extracellular signal-regulated kinase (ERK) in hemopoietic cells. *Proc Natl Acad Sci USA* 2006; **103**: 3274–3279.
14 Beinke S, Robinson MJ, Hugunin M, Ley SC. Lipopolysaccharide activation of the TPL-2/MEK/extracellular signal-regulated kinase mitogen-activated protein kinase cascade is regulated by IkappaB kinase-induced proteolysis of NF-kappaB1 p105. *Mol Cell Biol* 2004; **24**: 9658–9667.
15 Eliopoulos AG, Wang C-C, Dumitru CD, Tsichlis PN. Tpl2 transduces CD40 and TNF signals that activate ERK and regulates IgE induction by CD40. *EMBO J* 2003; **22**: 3855–3864.
16 Das S, Cho J, Lambertz I, Kelliher M, Eliopoulos AG, Du K *et al.* Tpl2/cot signals activate ERK, JNK, and NF-kappaB in a cell-type and stimulus-specific manner. *J Biol Chem* 2005; **280**: 23748–23757.
17 Hatziapostolou M, Polytarchou C, Panutsopulos D, Covic L, Tsichlis PN. Proteinase-activated receptor-1-triggered activation of tumor progression locus-2 promotes actin cytoskeleton reorganization and cell migration. *Cancer Res* 2008; **68**: 1851–1861.
18 Eliopoulos AG, Dumitru CD, Wang C-C, Cho J, Tsichlis PN. Induction of COX-2 by LPS in macrophages is regulated by Tpl2-dependent CREB activation signals. *EMBO J* 2002; **21**: 4831–4840.
19 Rousseau S, Papoutsopoulou M, Symons A, Cook D, Lucocq JM, Prescott AR *et al.* TPL2-mediated activation of ERK1 and ERK2 regulates the processing of pre-TNF alpha in LPS-stimulated macrophages. *J Cell Sci* 2008; **121**: 149–154.
20 López-Pelaéz M, Fumagalli S, Sanz C, Herrero C, Guerra S, Fernandez M *et al.* Cot/tpl2-MKK1/2-Erk1/2 controls mTORC1-mediated mRNA translation in Toll-like receptor-activated macrophages. *Mol Biol Cell* 2012; **23**: 2982–2992.
21 Vougioukalaki M, Kanellis DC, Gkouskou K, Eliopoulos AG. Tpl2 kinase signal transduction in inflammation and cancer. *Cancer Lett* 2011; **304**: 80–89.
22 Arthur JSC, Ley SC. Mitogen-activated protein kinases in innate immunity. *Nat Rev Immunol* 2013; **13**: 679–692.
23 Patriotis C, Makris A, Bear SE, Tsichlis PN. Tumor progression locus 2 (Tpl-2) encodes a protein kinase involved in the progression of rodent T-cell lymphomas and in T-cell activation. *Proc Natl Acad Sci USA* 1993; **90**: 2251–2255.
24 Erny KM, Peli J, Lambert JF, Muller V, Diggelmann H. Involvement of the Tpl-2/cot oncogene in MMTV tumorigenesis. *Oncogene* 1996; **13**: 2015–2020.
25 Gkirtzimanaki K, Gkouskou KK, Oleksiewicz U, Nikolaidis G, Vyrla D, Liontos M *et al.* TPL2 kinase is a suppressor of lung carcinogenesis. *Proc Natl Acad Sci USA* 2013; **110**: E1470–E1479.
26 Serebrennikova OB, Tsatsanis C, Mao C, Gounaris E, Ren W, Siracusa LD *et al.* Tpl2 ablation promotes intestinal inflammation and tumorigenesis in Apcmin mice by inhibiting IL-10 secretion and regulatory T-cell generation. *Proc Natl Acad Sci USA* 2012; **109**: E1082–E1091.
27 Koliaraki V, Roulis M, Kollias G. Tpl2 regulates intestinal myofibroblast HGF release to suppress colitis-associated tumorigenesis. *J Clin Invest* 2012; **122**: 4231–4242.
28 Decicco-Skinner KL, Trovato EL, Simmons JK, Lepage PK, Wiest JS. Loss of tumor progression locus 2 (tpl2) enhances tumorigenesis and inflammation in two-stage skin carcinogenesis. *Oncogene* 2011; **30**: 389–397.
29 Latonen L, Laiho M. Cellular UV damage responses--functions of tumor suppressor p53. *Biochim Biophys Acta* 2005; **1755**: 71–89.
30 Gantke T, Sriskantharajah S, Ley SC. Regulation and function of TPL-2, an IκB kinase-regulated MAP kinase kinase kinase. *Cell Res* 2011; **21**: 131–145.
31 Choi HS, Kang BS, Shim J-H, Cho Y-Y, Choi BY, Bode AM *et al.* Cot, a novel kinase of histone H3, induces cellular transformation through up-regulation of c-fos transcriptional activity. *FASEB J* 2008; **22**: 113–126.
32 Cho J, Tsichlis PN. Phosphorylation at Thr-290 regulates Tpl2 binding to NF-kappaB1/p105 and Tpl2 activation and degradation by lipopolysaccharide. *Proc Natl Acad Sci USA* 2005; **102**: 2350–2355.
33 Moore HM, Bai B, Boisvert F-M, Latonen L, Rantanen V, Simpson JC *et al.* Quantitative proteomics and dynamic imaging of the nucleolus reveal distinct responses to UV and ionizing radiation. *Mol Cell Proteomics* 2011; **10**: 009241–001.
34 Wu MH, Chang JH, Yung BYM. Resistance to UV-induced cell-killing in nucleophosmin/B23 over-expressed NIH 3T3 fibroblasts: enhancement of DNA repair and up-regulation of PCNA in association with nucleophosmin/B23 over-expression. *Carcinogenesis* 2002; **23**: 93–100.
35 Li J, Zhang X, Sejas DP, Bagby GC, Pang Q. Hypoxia-induced nucleophosmin protects cell death through inhibition of p53. *J Biol Chem* 2004; **279**: 41275–41279.
36 Chao A, Lin C-Y, Tsai C-L, Hsueh S, Lin Y-Y, Lin C-T *et al.* Estrogen stimulates the proliferation of human endometrial cancer cells by stabilizing nucleophosmin/B23 (NPM/B23). *J Mol Med (Berl)* 2013; **91**: 249–259.
37 Lindström MS. NPM1/B23: a multifunctional chaperone in ribosome biogenesis and chromatin remodeling. *Biochem Res Int* 2011; **2011**: 195209.
38 Negi SS, Olson MOJ. Effects of interphase and mitotic phosphorylation on the mobility and location of nucleolar protein B23. *J Cell Sci* 2006; **119**: 3676–3685.
39 Salmeron A, Ahmad TB, Carlile GW, Pappin D, Narsimhan RP, Ley SC. Activation of MEK-1 and SEK-1 by Tpl-2 proto-oncoprotein, a novel MAP kinase kinase kinase. *EMBO J* 1996; **15**: 817–826.
40 Wang S, Ghosh RN, Chellappan SP. Raf-1 physically interacts with Rb and regulates its function: a link between mitogenic signaling and cell cycle regulation. *Mol Cell Biol* 1998; **18**: 7487–7498.
41 Lee SB, Xuan Nguyen TL, Choi JW, Lee K-H, Cho S-W, Liu Z *et al.* Nuclear Akt interacts with B23/NPM and protects it from proteolytic cleavage, enhancing cell survival. *Proc Natl Acad Sci USA* 2008; **105**: 16584–16589.
42 Okuwaki M. The structure and functions of NPM1/Nucleophsmin/B23, a multifunctional nucleolar acidic protein. *J Biochem* 2008; **143**: 441–448.
43 Koike A, Nishikawa H, Wu W, Okada Y, Venkitaraman AR, Ohta T. Recruitment of phosphorylated NPM1 to sites of DNA damage through RNF8-dependent ubiquitin conjugates. *Cancer Res* 2010; **70**: 6746–6756.
44 Lin CY, Tan BC, Liu H, Shih C, Chien K, Lin C *et al.* Dephosphorylation of nucleophosmin by PP1β facilitates pRB binding and consequent E2F1-dependent DNA repair. *Mol Biol Cell* 2010; **21**: 4409–4417.
45 Okuda M, Horn HF, Tarapore P, Tokuyama Y, Smulian a G, Chan PK *et al.* Nucleophosmin/B23 is a target of CDK2/cyclin E in centrosome duplication. *Cell* 2000; **103**: 127–140.
46 Tokuyama Y, Horn HF, Kawamura K, Tarapore P, Fukasawa K. Specific phosphorylation of nucleophosmin on Thr(199) by cyclin-dependent kinase 2-cyclin E and its role in centrosome duplication. *J Biol Chem* 2001; **276**: 21529–21537.
47 Brady SN, Maggi LB, Winkeler CL, Ea Toso, Gwinn a S, Pelletier CL *et al.* Nucleophosmin protein expression level, but not threonine 198 phosphorylation, is essential in growth and proliferation. *Oncogene* 2009; **28**: 3209–3220.
48 Colombo E, Marine J-C, Danovi D, Falini B, Pelicci PG. Nucleophosmin regulates the stability and transcriptional activity of p53. *Nat Cell Biol* 2002; **4**: 529–533.
49 Chen D, Shan J, Zhu W-G, Qin J, Gu W. Transcription-independent ARF regulation in oncogenic stress-mediated p53 responses. *Nature* 2010; **464**: 624–627.
50 Itahana K, Bhat KP, Jin A, Itahana Y, Hawke D, Kobayashi R *et al.* Tumor suppressor ARF degrades B23, a nucleolar protein involved in ribosome biogenesis and cell proliferation. *Mol Cell* 2003; **12**: 1151–1164.

51 Cuomo ME, Knebel A, Morrice N, Paterson H, Cohen P, Mittnacht S. p53-Driven apoptosis limits centrosome amplification and genomic instability downstream of NPM1 phosphorylation. *Nat Cell Biol* 2008; **10**: 723–730.
52 Sato K, Hayami R, Wu W, Nishikawa T, Nishikawa H, Okuda Y *et al*. Nucleophosmin/B23 is a candidate substrate for the BRCA1-BARD1 ubiquitin ligase. *J Biol Chem* 2004; **279**: 30919–30922.
53 Endo A, Matsumoto M, Inada T, Yamamoto A, Nakayama KI, Kitamura N *et al*. Nucleolar structure and function are regulated by the deubiquitylating enzyme USP36. *J Cell Sci* 2009; **122**: 678–686.
54 Zhang M-J, Ding Y-L, Xu C-W, Yang Y, Lian W-X, Zhan Y-Q *et al*. Erythroid differentiation-associated gene interacts with NPM1 (nucleophosmin/B23) and increases its protein stability, resisting cell apoptosis. *FEBS J* 2012; **279**: 2848–2862.
55 Wu MH, Yung BYM. UV stimulation of nucleophosmin/B23 expression is an immediate-early gene response induced by damaged DNA. *J Biol Chem* 2002; **277**: 48234–48240.
56 Johannessen CM, Boehm JS, Kim SY, Thomas SR, Wardwell L, Johnson LA *et al*. COT drives resistance to RAF inhibition through MAP kinase pathway reactivation. *Nature* 2010; **468**: 968–972.
57 Eliopoulos AG, Davies C, Blake SSM, Murray P, Najafipour S, Tsichlis PN *et al*. The oncogenic protein kinase Tpl-2/Cot contributes to Epstein-Barr virus-encoded latent infection membrane protein 1-induced NF-κB signaling downstream of TRAF2. *J Virol* 2002; **76**: 4567–4579.
58 Kane LP, Mollenauer MN, Xu Z, Turck CW, Weiss A. Akt-dependent phosphorylation specifically regulates Cot induction of NF-kappaB-dependent transcription. *Mol Cell Biol* 2002; **22**: 5962–5974.
59 Louvet E, Junéra RH, Berthuy I, Hernandez-Verdum D. Compartmentation of the nucleolar processing proteins in the granular component is a CK2-driven process. *Mol Biol Cell* 2006; **17**: 2537–2546
60 Heffernan TP, Simpson DA, Frank AR, Heinloth AN, Paules RS, Cordeiro-stone M *et al*. An ATR- and Chk1-dependent S checkpoint inhibits replicon initiation following UVC-induced DNA damage. *Mol Cell Biol* 2002; **22**: 8552–8561.

Supplementary Information accompanies this paper on the Oncogene website (http://www.nature.com/onc)

TPL2 kinase is a suppressor of lung carcinogenesis

Katerina Gkirtzimanaki[a,b,1], Kalliopi K. Gkouskou[b,1], Urszula Oleksiewicz[c], Georgios Nikolaidis[c], Dimitra Vyrla[a,b], Michalis Liontos[d], Vassiliki Pelekanou[e], Dimitris C. Kanellis[a,b], Kostantinos Evangelou[d], Efstathios N. Stathopoulos[e], John K. Field[c], Philip N. Tsichlis[f], Vassilis Gorgoulis[d], Triantafillos Liloglou[c,2], and Aristides G. Eliopoulos[a,b,2]

[a]Molecular and Cellular Biology Laboratory, Division of Basic Sciences and [e]Department of Pathology, University of Crete Medical School, 710 03 Heraklion, Greece; [b]Laboratory of Cancer Biology, Institute of Molecular Biology and Biotechnology, Foundation for Research and Technology Hellas (FORTH), 700 13 Heraklion, Crete, Greece; [c]Department of Molecular and Clinical Cancer Medicine, University of Liverpool, Liverpool L3 9TA, United Kingdom; [d]Molecular Carcinogenesis Group, Department of Histology and Embryology, Medical School of Athens, 115 27 Athens, Greece; and [f]Molecular Oncology Research Institute, Tufts Medical Center, Boston, MA 02111

Edited by Elliott Kieff, Harvard Medical School and Brigham and Women's Hospital, Boston, MA, and approved February 26, 2013 (received for review September 14, 2012)

Lung cancer is a heterogeneous disease at both clinical and molecular levels, posing conceptual and practical bottlenecks in defining key pathways affecting its initiation and progression. Molecules with a central role in lung carcinogenesis are likely to be targeted by multiple deregulated pathways and may have prognostic, predictive, and/or therapeutic value. Here, we report that Tumor Progression Locus 2 (TPL2), a kinase implicated in the regulation of innate and adaptive immune responses, fulfils a role as a suppressor of lung carcinogenesis and is subject to diverse genetic and epigenetic aberrations in lung cancer patients. We show that allelic imbalance at the TPL2 locus, up-regulation of microRNA-370, which targets TPL2 transcripts, and activated RAS (rat sarcoma) signaling may result in down-regulation of TPL2 expression. Low TPL2 levels correlate with reduced lung cancer patient survival and accelerated onset and multiplicity of urethane-induced lung tumors in mice. Mechanistically, TPL2 was found to antagonize oncogene-induced cell transformation and survival through a pathway involving p53 downstream of cJun N-terminal kinase (JNK) and be required for optimal p53 response to genotoxic stress. These results identify multiple oncogenic pathways leading to TPL2 deregulation and highlight its major tumor-suppressing function in the lung.

Tumor Progression Locus 2 (TPL2), also known as Cancer Osaka Thyroid (COT) and MAP3K8, is a serine-threonine kinase with essential functions in innate immune cells, where it transmits signals through Toll-like receptors (1–3), the TNF family of receptors (4), and G protein-coupled receptors (5). As a result, TPL2 ablation in mice ameliorates the severity of a variety of inflammatory pathologies (1, 6), suggesting that it could be explored as a therapeutic target. In contrast, however, TPL2-deficient mice show increased susceptibility to infection with the T helper 1 (Th1)-inducing parasite *T. gondii* (7) and ovalbumin-induced bronchoalveolar inflammation (8) because of a T-cell intrinsic defect rather than an altered innate immune response, highlighting cell type- and stimulus-dependent roles for TPL2 in the immune system.

Early studies identified the TPL2 gene as a target of provirus insertion in Moloney Murine Leukemia Virus-induced T-cell lymphomas and Mouse Mammary Tumor Virus-induced mammary adenocarcinomas, yielding a truncated, C terminus-deleted product with transforming capacity (9, 10). Because the overexpression of WT TPL2 did not exert similar oncogenic effects in vivo, it has been proposed that TPL2 is a proto-oncogene activated by C-terminal truncation (10). Nevertheless, activating mutations in TPL2 have not been described in humans (11). Although elevated levels of TPL2 have been reported in certain tumor types, a detailed comparative evaluation of TPL2 expression in human malignancy and normal tissue is missing, and its physiological role in carcinogenesis remains enigmatic. Interestingly, the overexpression of TPL2 in melanoma cells carrying oncogenic B-RAF (Rapidly Accelerated Fibrosarcoma) has recently been associated with resistance to the RAF kinase inhibitor PLX4720 because of TPL2-mediated ERK pathway reactivation (12). In contrast, a genome-wide RNAi screen has shown that TPL2 is required for TRAIL (TNF-related apoptosis-inducing ligand)-induced apoptosis in human breast cancer cells (13). Additionally, mice lacking TPL2 rapidly develop T-cell lymphomas under conditions of chronic T-cell stimulation (14). Therefore, TPL2 may impact oncogenic events, including the cellular response to therapy in a tissue type- and stimulus-dependent manner.

Lung cancer is a leading cause of cancer-related deaths, reflecting the need for a better understanding of the mechanisms that underlie the development of pulmonary carcinomas (15). In this paper, we show that TPL2 fulfills a role as negative regulator of lung carcinogenesis and describe genetic and epigenetic aberrations that lead to loss of TPL2 in a human malignancy. An important functional interaction between TPL2, cJun N-terminal kinase (JNK), and p53 affecting apoptosis is revealed, providing a telling example of how tumor cells exploit alternative pathways that lower intrinsic barriers to malignant transformation and tumor growth.

Results

TPL2 Levels Are Reduced in Human Lung Tumors and Associate with Poor Patient Survival. The expression of TPL2 in human lung cancer and its relevance to this type of malignancy remain unexplored. We determined *TPL2* mRNA levels by quantitative PCR (qPCR) in 100 nonsmall cell lung carcinomas (NSCLCs) and adjacent nontumoral tissue (Table S1) and observed down-regulation of *TPL2* expression in the tumor (Fig. 1*A*). When this analysis was repeated separately for the two major lung cancer histologies, squamous cell carcinoma (SqCCL; $n = 63$) and adenocarcinoma (AdenoCa; $n = 37$), we found that the down-regulation of *TPL2* did not significantly differ between these groups (Fig. S1*A*) (χ^2 test, $P = 0.556$).

Investigating the clinical relevance of *TPL2* mRNA levels in human lung carcinomas, we found no association with TNM (Tumor, lymph Nodes, Metastasis) or differentiation status, age, sex, and smoking history (Table S1). However, low *TPL2* expression correlated with reduced patient survival both in the overall NSCLC cohort (log rank test; $P = 0.009$) (Fig. 1*B*) and after adjustment for histology (Fig. S1*B*). In line with this prediction was the inverse correlation between *TPL2* mRNA levels and Ki67 proliferation index (Fig. 1*C*), indicating that

Author contributions: A.G.E. and T.L. conceived the project; K.G., T.L., and A.G.E. designed experiments; K.G., K.K.G., U.O., G.N., D.V., M.L., V.P., D.C.K., and K.E. performed research; J.K.F. and P.N.T. contributed new reagents/analytic tools; K.G., K.K.G., G.N., D.V., M.L., V.P., E.N.S., J.K.F., P.N.T., V.G., T.L., and A.G.E. analyzed data; and T.L. and A.G.E. wrote the paper.

The authors declare no conflict of interest.

This article is a PNAS Direct Submission.

[1]K.G. and K.K.G. contributed equally to this work.

[2]To whom correspondence may be addressed. E-mail: eliopag@imbb.forth.gr or T.Liloglou@liverpool.ac.uk.

See Author Summary on page 6260 (volume 110, number 16).

This article contains supporting information online at www.pnas.org/lookup/suppl/doi:10.1073/pnas.1215938110/-/DCSupplemental.

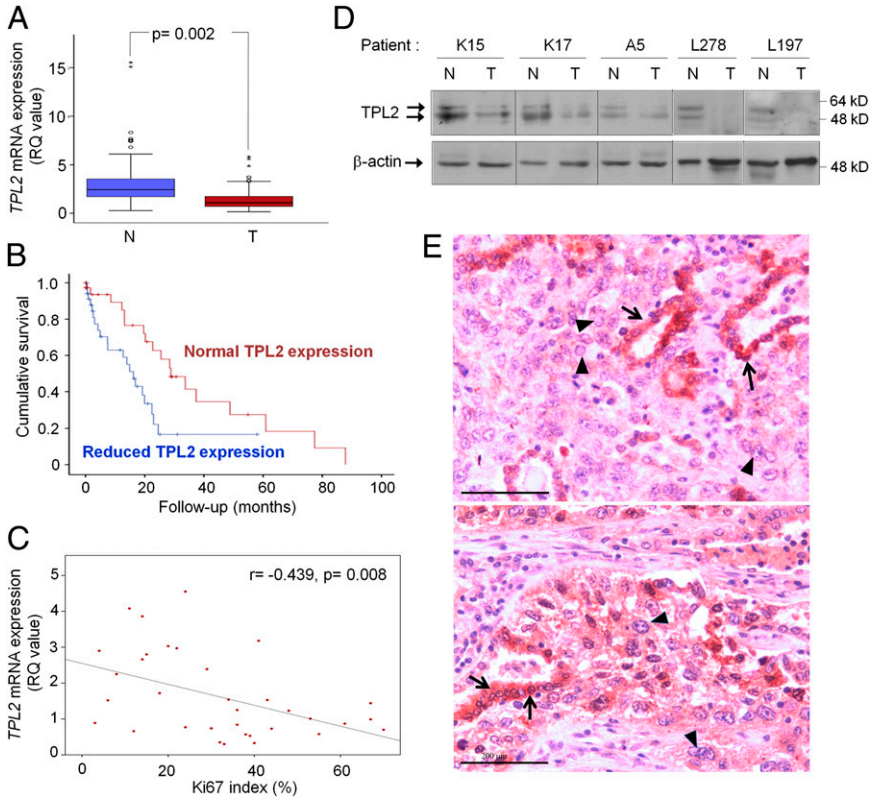

Fig. 1. TPL2 levels are reduced in primary human lung carcinomas and correlate with poor patient survival. (*A*) Comparison of TPL2 mRNA expression in the 100 available pairs of NSCLCs (T) and adjacent nonmalignant (N) lung tissues by qPCR. Results were normalized to the housekeeping β-actin gene and are expressed as RQ values using the IMR-90 human fibroblast cell line as calibrator. Stars and circles in the box plot indicate outliers. (*B*) Kaplan–Meier survival plot showing the cumulative survival of lung cancer patients who displayed more than twofold reduction in *TPL2* mRNA levels in T compared with N and patients with less than twofold reduction in expression levels. Patients with low *TPL2* expression have median survival of 16.2 mo (95% confidence interval = 11.8–20.6) compared with patients with less than twofold reduction, who have median survival of 28.8 mo (95% confidence interval = 18.4–39.2, $P = 0.009$; log rank test). (*C*) Inverse correlation between *TPL2* mRNA levels and Ki67 expression in cancer subset of NSCLC samples within this study ($n = 35$) for which Ki67 data were available (r coefficient and P values obtained from Spearman correlation). (*D*) TPL2 protein levels are reduced in T compared with N. TPL2 is expressed as two isoforms (noted with arrows) generated by the use of alternative translation start sites at methionines 1 and 30. (*E*) Representative immunohistochemical analysis showing a marked down-regulation of TPL2 expression in malignant cells (arrowheads) compared with nonmalignant epithelium (arrows). (Final magnification: 400×; objective lens: 40×/0.65; scale bars: 200 μm.)

reduced levels of *TPL2* expression are associated with a more aggressive tumor phenotype.

Lower expression of TPL2 was confirmed in protein lysates from representative primary lung tumor specimens vs. nonmalignant tissue from the same patients (Fig. 1*D*). To verify that this reduction reflects changes in the tumor cells, we analyzed TPL2 by immunohistochemistry in 20 representative NSCLC specimens containing malignant and nonmalignant epithelium in the same section. The results showed that nontumoral lung epithelial cells display maximal immunostaining compared with adjacent malignant cells (Fig. 1*E*), thus confirming our RT-qPCR data. Collectively, these observations suggest that the down-regulation of TPL2 may represent a broader phenomenon in NSCLC, which impacts on patient survival and merits additional investigation and validation in larger clinical studies.

TPL2 Deficiency Enhances Susceptibility to Experimental Lung Carcinogenesis. The aforementioned findings prompted us to experimentally evaluate the functional significance of TPL2 down-regulation in lung cancer. Chemical carcinogens have been extensively used to model multistage human lung carcinogenesis in the mouse (reviewed in refs. 16 and 17). Among them, urethane is a commonly used carcinogen, which reproducibly causes lung tumors in mice with histological and molecular features similar to human lung AdenoCa (18–21). These aberrations include mutational activation of K-*ras* (Kirsten rat sarcoma viral oncogene homolog) in a proportion of carcinogen-induced tumors and inactivation of tumor suppressor genes such as *p53*, reminiscent of the partial (approximately 20%) incidence of K-*ras* mutations and frequent (>75%) loss of *p53* function in human lung cancer (17). Currently, there are no mouse models for SqCCL (16, 17), precluding experimental analysis of the role of TPL2 in this lung tumor type.

We, thus, examined the relative susceptibility of $TPL2^{-/-}$ vs. $TPL2^{+/+}$ mice to develop lung AdenoCas after exposure to urethane. At 4 mo posttreatment, all $TPL2^{-/-}$ mice were found to already harbor multiple lung adenomas, whereas only hyperplasia, without atypia, had developed in WT animals (Fig. 2 *A* and *B*). Ki67 staining was increased in hyperplastic lesions from $TPL2^{-/-}$ compared with $TPL2^{+/+}$ mice (Fig. 2 *E* and *F*). At 6 mo after urethane administration, lungs from $TPL2^{-/-}$ animals (or heterozygous $TPL2^{+/-}$ mice) contained significantly higher numbers of AdenoCas compared with $TPL2^{+/+}$ mice (Fig. 2 *A*, *B*, and *D*). The tumors developed in $TPL2^{-/-}$ mice showed loss of normal alveolar architecture, increased nuclear/cytoplasmic ratio, cytologic atypia, and invasion into adjacent bronchioles. At 12 mo, the effect of *TPL2* deficiency was macroscopically evident by the dramatic difference in both the number and size of lung tumors developed in these animals (Fig. 2*C*), indicating that TPL2 not only influences the carcinogenic process at an early stage but could also exert negative effects during tumor growth. In line with this observation and the findings in human tissue (Fig. 1*C*), lung tumor cells isolated from urethane-treated $TPL2^{+/+}$ mice express

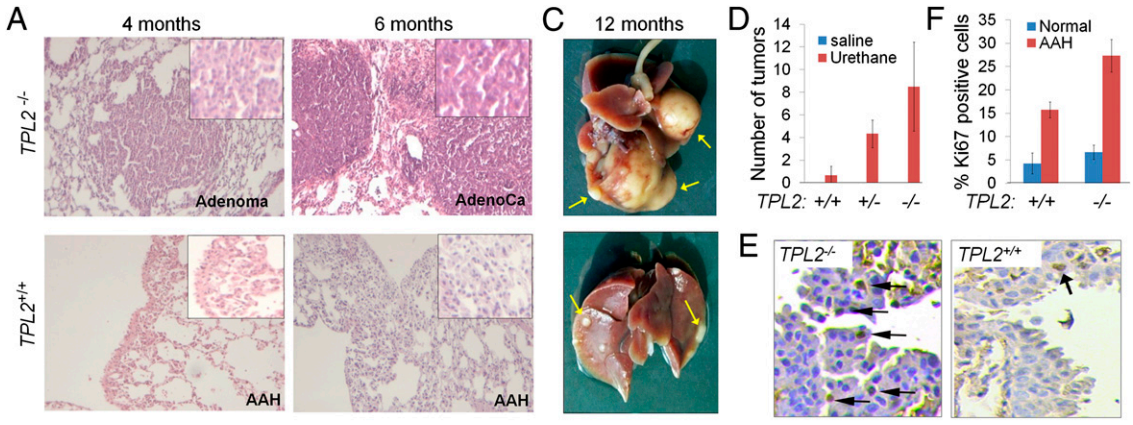

B

Time of analysis	*TPL2* status	Number and histopathology of lesions (n=5 animals per group)				
4 months	+/+	1 AAH	3 AAH	2 AAH	2 AAH	2 AAH
	-/-	6 Adenomas + Multiple foci of AAH	4 Adenomas + Multiple foci of AAH	2 Adenomas + Multiple foci of AAH	2 Adenomas + Multiple foci of AAH	6 Adenomas + Multiple foci of AAH
6 months	+/+	2 Adenomas + Multiple foci of AAH	Multiple foci of AAH	Multiple foci of AAH	1 AdenoCa + Multiple foci of AAH	1 AdenoCa + Multiple foci of AAH
	-/-	6 AdenoCa	5 AdenoCa	4 AdenoCa	> 10 AdenoCa	> 10 AdenoCa

Fig. 2. TPL2 suppresses lung cancer growth in vivo. (*A*) H&E staining of lung tissue isolated from $TPL2^{+/+}$ and $TPL2^{-/-}$ mice at 4 or 6 mo posttreatment with the chemical carcinogen urethane. AAH, atypical adenomatous hyperplasia. (*B*) Summary of histopathology data of $TPL2^{+/+}$ and $TPL2^{-/-}$ mouse lung sections analyzed at 4 or 6 mo posttreatment with the chemical carcinogen urethane. Each cell denotes an experimental animal. Three independent experiments using 15 $TPL2^{+/+}$ and 18 $TPL2^{-/-}$ mice have been performed with similar results. $TPL2^{-/-}$ or $TPL2^{+/+}$ mice administered saline (0.9% NaCl) did not develop tumors up to the age of 14 mo. (*C*) Lungs of $TPL2^{+/+}$ and $TPL2^{-/-}$ mice at 12 mo posttreatment with the chemical carcinogen urethane. Representative tumors are shown by arrows. (*D*) Collective data of tumor formation in different *TPL2* genotypes analyzed at 6 mo posttreatment with the chemical carcinogen urethane. (*E*) Representative immunohistochemical analysis of Ki67 status in hyperplastic lung tissue from urethane-treated $TPL2^{+/+}$ and $TPL2^{-/-}$ mice. The arrows show Ki67-positive cells. (*F*) Collective data of Ki67 staining in normal and AAH from urethane-treated $TPL2^{+/+}$ (n = 5) and $TPL2^{-/-}$ mice (n = 5).

reduced levels of TPL2 compared with normal bronchial epithelium (Fig. S2*A*), and the knockdown of TPL2 in H1299 human lung carcinoma cells (Fig. S2*B*) increased their anchorage-independent growth in vitro (Fig. S2*C*).

We have recently reported that TPL2 ablation enhances inflammation induced by the Apc^{min} mutation, resulting in dramatic increase in polyposis (22). Theoretically, an exaggerated inflammatory response caused by urethane administration in $TPL2^{-/-}$ mice could be responsible for their increased susceptibility to lung tumorigenesis. We, thus, analyzed immune cell content in lungs and spleens from $TPL2^{-/-}$ and $TPL2^{+/+}$ mice at 2 and 10 wk after urethane treatment (that is, during the early stages of adenoma development). By using flow cytometric analysis of $CD3^+$, $CD4^+$, and $CD8^+$ T cells and their activation status ($CD69^+$), macrophages, $Gr1^+/CD11b^+$ myeloid-derived suppressor cells, natural killer, and natural killer T cells in the spleens of $TPL2^{-/-}$ and $TPL2^{+/+}$ mice exposed to urethane or histological assessment of H&E-stained lung tissue sections, we did not detect statistically significant differences between strains (Fig. S3). Additionally, urethane did not elevate the expression of soluble mediators of inflammation, such as TNF and IL-6, in blood serum (measured by ELISA) and lung tissue (measured by qPCR) above background levels during this time course. Collectively, although we cannot exclude the possibility that TPL2 may also function in the immune system to enhance chemical-induced carcinogenesis, our data do not indicate an association between TPL2 status and heightened systemic or local inflammation at early stages of urethane-induced lung carcinogenesis, thus suggesting that TPL2 functions predominantly in lung epithelial cells to negatively regulate malignant transformation.

Genetic and Epigenetically Controlled Mechanisms Account for TPL2 Down-Regulation in Human Lung Cancer. The aforementioned clinical (Fig. 1 and Fig. S1) and experimental (Fig. 2) data warranted additional investigations into the molecular mechanisms that account for the reduced TPL2 expression in human lung cancer.

We first examined the frequency of loss of heterozygosity (LOH) at the *TPL2* locus (chromosome 10p, nucleotides 30722866–30750761). We used fluorescent microsatellite analysis at four positions on the TPL2 gene (two internal and two flanking) (Fig. 3*A*) to assess LOH in the available set of human primary lung tumors. As shown in a representative analysis in Fig. 3*B* and collective data in Fig. S4*A*, allelic imbalance at the *TPL2* locus was observed in a significant 52% of NSCLC. The frequency of LOH at the TPL2 locus was similar between SqCCL and AdenoCa (Fig. S4 *A* and *B*) (P = 0.954). Cases with LOH displayed lower *TPL2* mRNA levels but at borderline significance (Mann–Whitney test, P = 0.051) (Fig. 3*C*), indicating the contribution of additional mechanisms affecting TPL2 expression in lung cancer.

We surmised that TPL2 could be subject to epigenetic silencing, which was observed in certain lung tumor suppressor genes (23–25). The presence of a putative CpG (CG dinucleotide) island located at positions −973 to +981 relative to the *TPL2* transcription start site (Fig. 3*A*), indicated by *in silico* analysis (http://cpgislands.usc.edu/), was in line with this notion. We performed pyrosequencing methylation analysis (PMA) in our panel of 100

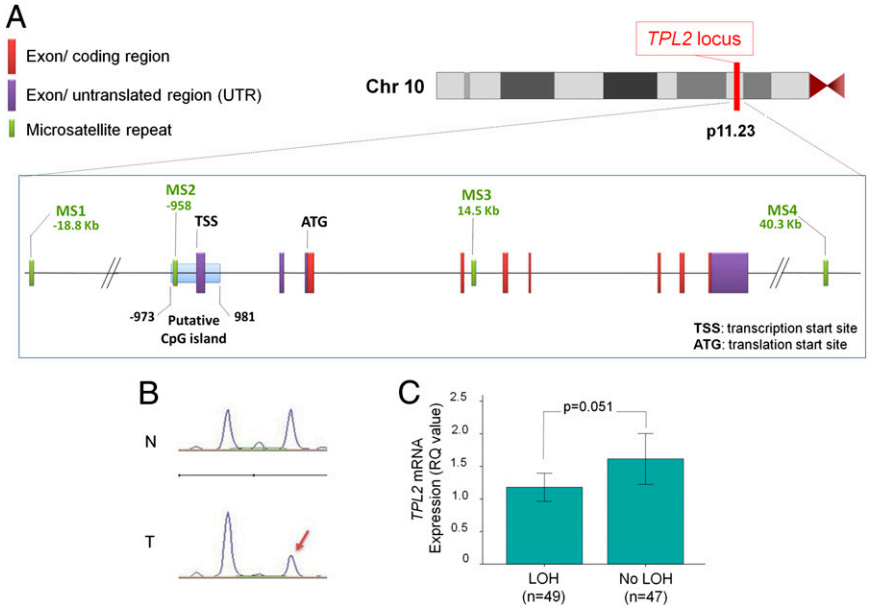

Fig. 3. Allelic imbalance partly accounts for the down-regulation of TPL2 in human lung cancer. (*A*) Schematic representation of the *TPL2* locus on human chromosome 10 and relative positions of microsatellite repeats MS1, MS2, MS3, and MS4 used as markers for detection of LOH. Numbering refers to the TSS. The position of a putative CpG island in the *TPL2* promoter is also indicated. (*B*) Example of allelic imbalance/LOH in the TPL2 locus in a pair of tumor and adjacent nonmalignant samples from a lung cancer patient. Electropherogram traces for the normal (N) and tumor (T) genotypes are shown, with the two peaks representing the two alleles. The arrow depicts loss of allele. An allelic ratio cutoff level of 0.75 (25% reduction of one allele intensity) was used to score LOH (52). (*C*) Expression of *TPL2* mRNA, measured by qPCR, in relation to allelic imbalance (LOH) in the TPL2 locus.

primary lung tumors and paired nontumoral tissue (Fig. S5). Collectively, the results showed absence of *TPL2* promoter methylation in both malignant and nonmalignant lung tissue.

Previous work has shown that microRNA-370 (miR-370) negatively regulates the expression of TPL2 in malignant cholangiocytes in vitro (26). In agreement with this report, we have found that transfection of miR-370 in A549 lung cancer cells results in a time-dependent reduction in TPL2 protein (Fig. 4*A*) and mRNA levels, whereas an unrelated miR-328 had no effect. To determine if this pathway could operate in vivo, we assessed miR-370 expression by qPCR in the lung cancer set under evaluation. This analysis showed that miR-370 levels are significantly elevated in the malignant vs. nonmalignant lung tissue (Fig. 4*B*) and that miR-370 up-regulation was independent of histology (Fig. S4*C*).

Because miR-370 is embedded in a CpG island and subject to epigenetic control (26), we evaluated by PMA the methylation status of this region in lung cancer (Fig. 4*C*). The results showed a statistically significant reduction of miR-370 methylation levels in the tumor tissue (Fig. 4*D*). Moreover, this reduction closely correlated with the methylation status of the retrotransposable long interspersed nuclear element-1 (LINE-1), a surrogate marker of global methylation (27, 28), suggesting that miR-370 hypomethylation in NSCLC is most likely the result of global genome hypomethylation (Fig. 4*E*).

Oncogenic RAS Mediates Down-Regulation of TPL2. Activating mutations in *ras* genes have been recorded in 10–25% of lung tumors. A recent study has shown that oncogenic RAS stimulates a TANK-binding kinase 1 (TBK1)-dependent signaling pathway in vitro, which leads to reduction in p105 NF-κB1 protein levels (29). NF-κB1 physically interacts with and regulates the stability of TPL2, which was highlighted by the fact that TPL2 is absent in macrophages (30, 31) and lung tissue (Fig. S2*A*) from *NFKB1*$^{-/-}$ mice. We, therefore, reasoned that, by modulating NF-κB1 levels, activated RAS may impact on TPL2 expression.

We have explored this association in A549 and H1299 human lung carcinoma cells stably transfected with HA-tagged H-RAS^{G12V} expression vector or infected with K-RAS^{G12V}–expressing retrovirus, respectively. Interestingly, the expression of either form of oncogenic RAS mediated dramatic down-regulation of TPL2 concomitant to reduction in p105 NF-κB1 expression (Fig. 5 *A* and *B*).

Evaluation of the mutational status of K-*ras* codons 12 and 13 by direct sequencing in the lung cancer set used in our study identified only 5 of 37 (13.5%) AdenoCas and 4 of 63 (6.3%) squamous carcinomas to carry K-*ras* mutations (Fig. S6). Because the incidence of LOH in the TPL2 locus (Fig. 3) supersedes the frequency of *ras* mutations, we could not establish a direct correlation between mutated RAS and expression of TPL2 in vivo. However, as shown in Fig. 5*C*, reduced levels of TPL2 were observed in lysates from mouse lungs expressing K-RAS^{G12D} (32), suggesting that oncogenic RAS may contribute to the down-regulation of TPL2 expression in vivo.

Down-Regulation of TPL2 Levels Impacts on Cell Survival and Oncogenic Transformation Through Regulation of p53. The operation of multiple mechanisms (LOH, miR-370, and mutated RAS) leading to down-regulation of TPL2 expression in vivo prompted us to explore pathways that may link TPL2 to oncogenic transformation. To this end, we transiently introduced a *TPL2*-expressing vector in A549/H-RAS^{G12V} cell clones, which display strong suppression of endogenous TPL2 (Fig. 5*A*), and observed decreased cell proliferation and elevated levels of apoptosis (Fig. 6*A*). TPL2-mediated cytotoxicity required caspase activation, because it was abolished by treatment with the pan-caspase inhibitor zVAD-fmk. Moreover, the proapoptotic effect of TPL2 on RAS^{G12V}-transfected cells correlated with increased p53 accumulation (Fig. 6*B*) and was alleviated by the RNAi-mediated knockdown of p53 (Fig. 6*A*). These data suggest that TPL2 antagonizes oncogenic RAS in transformed cells, at least partly, by modulating p53 activity and apoptosis induction.

TPL2 also counteracted the oncogenic effects of K-RAS^{G12V} in nontransformed cells. Immortalized 208F fibroblasts were transfected with K-RAS^{G12V} in the presence or absence of a *TPL2* expression vector, and cell transformation was quantified by

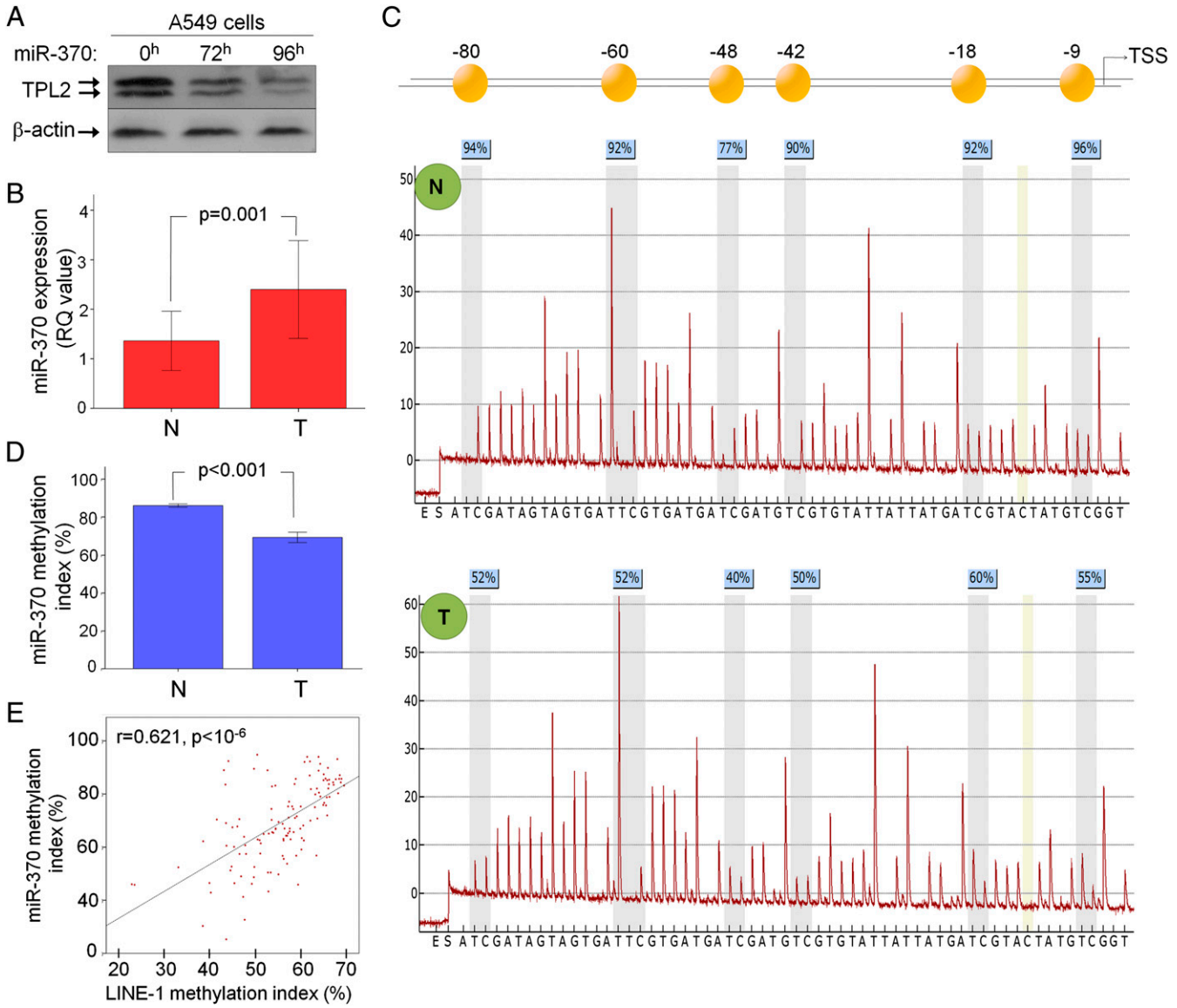

Fig. 4. An epigenetic mechanism of regulation of TPL2 expression involving miR-370. (*A*) TPL2 protein levels are reduced in A549 lung cancer cells transfected with miR-370. Results are representative of three independent experiments. (*B*) Expression of miR-370 (RQ value) was measured in 96 carcinoma specimens and paired nonmalignant lung tissue by qPCR and showed significantly higher miR-370 levels in the tumor tissues (Wilcoxon test, $P = 0.001$). (*C*) Representative pyrograms from PMA of the miR-370 locus in a lung tumor (T) and corresponding nonmalignant (N) adjacent tissue. Gray areas indicate the CpG sites that were analyzed at positions −9, −18, −42, −48, −60, and −80 relative to the TSS of the premicroRNA sequence, which are schematically represented by orange circles in *Upper*. The letters below each graph represent the dispensation order (E, enzyme mix; S, substrate; A, G, C, and T, nucleotides). Gray lanes indicate the CpG sites that were analyzed, and the *y* axis depicts the light levels produced after the incorporation of each nucleotide. Percentages indicate the extent of bisulfate conversion of C to T; unmethylated C should be fully converted to T. (*D*) The miR-370 locus is significantly (Wilcoxon test, $P < 0.001$) hypomethylated in lung tumors (T) compared with adjacent nonmalignant tissue (N). The methylation index of the miR-370 locus was calculated from PMA of 96 carcinoma specimens and paired normal lung tissue and is depicted in histogram form as methylation index. (*E*) Correlation between the methylation indexes of miR-370 and LINE-1 (r coefficient and *P* value obtained from Spearman correlation).

anchorage-independent growth in soft agar. As shown in Fig. 6*C*, expression of TPL2 reduced the number of foci formed by activated K-RAS by 60%, whereas a kinase-inactive TPL2 mutant had no effect.

Genotoxic agents typically found in tobacco smoke and chemicals used to model lung cancer in the mouse, such as urethane, damage the respiratory epithelium, eventually leading to malignant transformation. To determine if the observed link between TPL2 and p53 applies to genotoxic insults in addition to oncogenic stress, TPL2 was knocked down in A549 cells, and cells were exposed to the DNA damaging agent *cis*-platin. The knockdown of TPL2 attenuated p53 accumulation and increased the survival of drug-treated cells (Fig. 6 *D* and *E*). Importantly, the expression of two known p53-regulated genes, *cdkn1a*-encoding p21 and *bax*, were attenuated in lungs from *TPL2*$^{-/-}$ mice exposed to urethane, highlighting the in vivo relevance of the TPL2–p53 link (Fig. 6*F*). Next, we examined the mechanism by which TPL2 impacts on p53 levels.

TPL2 Regulates p53 Through a JNK–Nucleophosmin Signaling Pathway. Nucleophosmin (NPM/B23) is a DNA damage-response gene (33) that negatively regulates the interaction of p53 with HDM2 and thus, controls p53 stability (34, 35). Our *in silico* analysis of the NPM promoter (36) indicated the presence of multiple binding

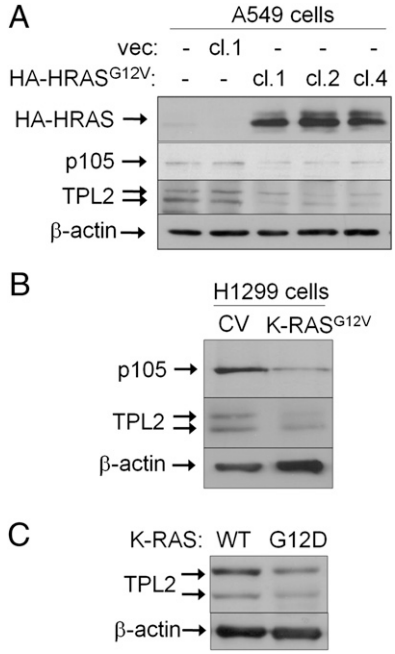

Fig. 5. Down-regulation of TPL2 levels by activated RAS associates with cell survival and oncogenic transformation. (*A*) Stable transfection of oncogenic *ras* leads to down-regulation of p105 NF-κB1 and TPL2 expression. Lysates from parental (lane 1), control vector (vec) -transfected (lane 2), or three HA-tagged H-RAS^{G12V}–transfected A549 (lanes 3–5) clones were immunoblotted with antibodies against HA, NF-κB1, TPL2, or β-actin as indicated. (*B*) Expression of K-RAS^{G12V} in retrovirus-transduced H1299 lung cancer cells results in reduced p105 NF-κB1 and TPL2 levels. CV, control virus. (*C*) TPL2 levels are reduced in mouse lungs expressing K-RAS^{G12D}.

sites of cJun/AP1, a transcription factor that is activated by the JNK signaling pathway. Because TPL2 directly phosphorylates MKK4/7 (the JNK kinases) (37, 38), we surmised that TPL2 may influence the p53 response through JNK-mediated NPM transactivation. Indeed, TPL2 knockdown attenuated both JNK phosphorylation and NPM up-regulation in *cis*-platin–treated cells (Fig. 6*E*). Conversely, the overexpression of TPL2 in A549/H-RAS^{G12V} clones stimulated JNK phosphorylation and led to increased NPM levels concomitant to p53 stabilization (Fig. 6*G*).

To provide additional evidence supporting the association between JNK signaling and NPM transactivation, A549 cells were exposed to the JNK inhibitor SP600125 before *cis*-platin treatment. As shown in Fig. 6 *H* and *I*, inhibition of JNK activity diminished the effect of *cis*-platin on NPM protein and mRNA expression levels. Collectively, these observations identify TPL2 as a physiological regulator of p53 that operates through a JNK–NPM signaling pathway.

Discussion

The substantial variability that typifies the genomes of malignant cells within a tumor (39) has generated conceptual and practical bottlenecks in defining key pathways affecting initiation and progression of malignancy. Molecules with a central role in carcinogenesis are likely to be targeted by multiple deregulated pathways and may have prognostic, predictive, and/or therapeutic value. We, thus, reason that the operation of multiple genetic (LOH and *ras* mutations) and epigenetic (miR-370) aberrations leading to loss of TPL2 in human lung cancer of both major histological types, SqCCL and AdenoCa, cannot be coincidental and points to a previously unappreciated significant role for the TPL2 pathway in this type of malignancy. This notion is corroborated by the poor prognosis of lung cancer patients carrying reduced TPL2 tumor levels and the reverse association of TPL2 expression with Ki67 index (Fig. 1 and Fig. S1). Additional evidence is provided by the demonstration that TPL2-deficient mice display increased susceptibility to chemically induced lung carcinogenesis (Fig. 2). This finding, coupled with our recently published work showing that *TPL2* ablation enhances the oncogenic potential of the *Apc*^{min} mutation in the gut (22), indicates that TPL2 may have a broader role as a negative regulator of carcinogenesis. However, whereas the enhancement of polyposis in *Apc*$^{min/+}$/*TPL2*$^{-/-}$ mice was found to be partially (but not exclusively) hematopoietic cell-driven, the in vitro and in vivo data presented in this paper suggest that TPL2 also confers powerful effects on epithelial cells in response to genotoxic and oncogenic insults. These observations are in agreement with the mechanism of action of urethane, which metabolizes to mutagenic mediators in Clara and type II alveolar epithelial cells (the progenitors of lung adenomas) (16, 17), and the finding that the accelerated early lesions observed in *TPL2*$^{-/-}$ mice occur in the absence of heightened systemic or local inflammatory response compared with WT animals (Fig. S3).

Human lung cancer is characterized by extensive alterations of microRNA expression and allelic imbalance, which may influence cancer-related genes and thus, impact on patient survival (23, 40). Known targets of LOH in lung cancer include tumor suppressor genes, such as *RASSF1A*, *p16*, and *p53* (15). Our data show that the *TPL2* gene locus is subject to LOH in a human malignancy, resulting in reduced TPL2 expression (Fig. 3).

The molecular mechanisms accounting for the altered expression of microRNAs in lung cancer are unclear (23, 40). Our finding that miR-370 is up-regulated in primary lung tumors and closely associated with reduced TPL2 levels (Fig. 4) expands our appreciation of the in vivo effects of microRNAs on gene expression. Moreover, our data reveal a mechanism of in vivo regulation of microRNA expression influenced by global DNA hypomethylation. Aberrant methylation of CpG dinucleotides is a commonly observed epigenetic modification in human malignancies and includes both global genomic hypomethylation and hypermethylation of gene promoter regions. The latter is often associated with transcriptional silencing of tumor suppressors, such as *p16*, *FHIT* (fragile histidine triad protein), *APC* (Adenomatous polyposis coli), and *DAPK* (death-associated protein kinase), in lung cancer (15). Despite the presence of a rich CpG island in the *TPL2* promoter, we found no evidence that it is differentially methylated in tumor vs. normal lung tissue. However, we report that *TPL2* gene expression may indirectly be affected by global genomic DNA hypomethylation through the epigenetic regulation of miR-370. Indeed, a close association between miR-370 and LINE-1 methylation indexes was noted in primary human lung tumors (Fig. 4*E*). Hypomethylation of LINE-1 serves as a surrogate marker of global methylation status (27), correlates with genomic instability (28), and has been identified as an independent marker of poor prognosis in early stage NSCLC (41). It is, thus, tempting to speculate that the down-regulation of TPL2 caused by miR-370 hypomethylation may impact on the early stages of the disease in humans, similar to the effects of TPL2 ablation on urethane-induced lung cancer initiation in the mouse.

Clinical studies have shown that 10–25% of human AdenoCas and ∼7% of SqCCLs of the lung carry activating mutations in K-*ras* (23, 42) and H-*ras* (43, 44) genes, which represent an early event in lung carcinogenesis and mark poor prognosis. Experimental evidence supporting the role of this gene in lung cancer comes from transgenic mice expressing mutated K-*ras*, in which atypical adenomatous hyperplasia and AdenoCa develop (16, 17). In these models, high expression of oncogenic RAS promotes carcinogenesis through a signaling pathway that critically depends on c-RAF (45) and NF-κB (21, 46). In vitro analyses based on RNAi screens also point to NF-κB and the atypical IκB kinase family member TBK1 as positive regulators of survival and tumorigenicity of human lung cancer cells bearing mutated K-*ras* (29).

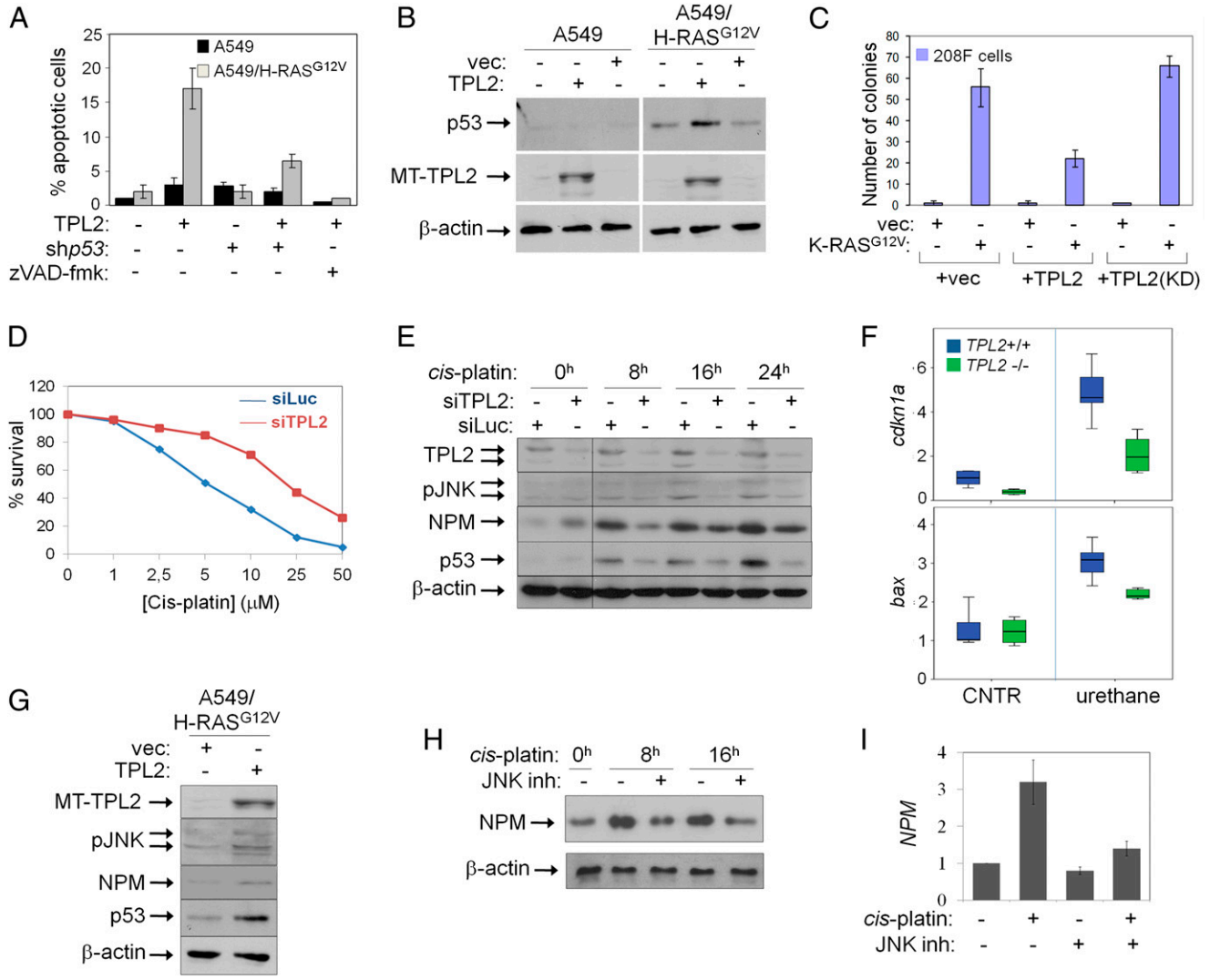

Fig. 6. TPL2 antagonizes oncogenic RAS in transformed cells by modulating apoptosis induction in a p53-dependent manner. (*A*) Quantitative determination of apoptosis in A549 and A549/H-RAS^{G12V} clone 2 cells was performed 24 h posttransfection with Myc epitope-tagged (MT) TPL2 in the presence or absence of shRNA targeting p53 or the pan-caspase inhibitor zVAD-fmk (15 μM). Mean values (± SD) from three independent experiments are shown. (*B*) TPL2 expression results in increased accumulation of p53 in A549/H-RAS^{G12V} cells. (*C*) TPL2 suppresses oncogenic RAS-mediated transformation. Immortalized 208F fibroblasts were transfected with K-RAS^{G12V} in the presence or absence of TPL2 or a kinase-inactive TPL2 mutant (KD) and plated in soft agar, and the number of foci formed 2 wk later was measured and presented in a histogram form. (*D*) Knockdown of TPL2 in A549 cells confers resistance to *cis*-platin–induced cytotoxicity. Cells were transfected with TPL2 or luciferase-targeting siRNA and then treated with various concentrations of *cis*-platin for 48 h. Viability was determined by using the MTT conversion assay. Data shown are the average of triplicates from a representative experiment. Three additional experiments were performed with similar results. (*E*) Knockdown of TPL2 reduces the NPM and p53 induction and the extent of JNK phosphorylation in A549 cells treated with 25 μM *cis*-platin. Results are representative of at least four independent experiments. (*F*) TPL2 impacts on p53 activity in vivo. To quantitatively assess p53 activation in vivo, RNA was isolated from *TPL2*$^{+/+}$ and *TPL2*$^{-/-}$ mouse lungs at 2 wk after urethane treatment and used to determine the levels of two established p53-regulated genes, *cdkn1a* encoding p21 and *bax* by qPCR. The *y* axis represents the RQ values determined as described in Fig. 1*A*. (*G*) TPL2 expression results in increased accumulation of p53 and NPM and elevated phosphorylation of JNK in A549/H-RAS^{G12V} cells. A549/H-RAS^{G12V} clone 2 cells transfected with MT-TPL2 or control vector (vec) were analyzed for the expression of TPL2, NPM, p53, phosphorylated JNK, and β-actin as indicated. (*H*) Treatment of A549 cells with the JNK inhibitor (inh) SP600125 reduces the *cis*-platin–induced NPM up-regulation. (*I*) SP600125 (20 μM) inhibits the *cis*-platin–induced up-regulation of NPM mRNA measured by qPCR.

In contrast, WT RAS functions as an endogenous suppressor of its mutated counterpart, and the oncogenic effects of activated K-RAS largely depend on loss of a WT *ras* allele (19). Expression of WT *ras* and low K-*ras* oncogene copy number have also been proposed to account for the observation that certain lung cancer cell lines carrying mutated K-*ras* allele, including A549, do not display dependency (addiction) on the endogenous K-*ras* oncogene, inasmuch as their proliferation, survival, ERK phosphorylation, or PI3K activation status remain unaffected on RAS knockdown (47). Data presented in this paper show that elevated levels of oncogenic RAS mediate the down-regulation of TPL2 in vitro (Fig. 5 *A* and *B*) and in vivo (Fig. 5*C*) and that coexpression of these genes is incompatible for optimal tumor cell survival and malignant transformation in vitro (Fig. 6 *A* and *C*). These findings, thus, identify TPL2 as a physiological antagonist of activated RAS in both transformed and nontransformed cells (Fig. 7).

Which is the molecular pathway that orchestrates the tumor-suppressive effects of TPL2? Our results show that, in response to oncogenic or genotoxic stress, TPL2 participates in JNK-

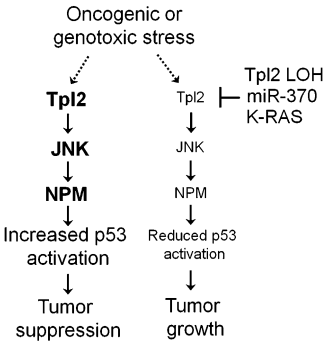

Fig. 7. Proposed model of the tumor-suppressive effects of TPL2 in the lung. On the basis of the data presented in this paper, we propose that TPL2 suppresses lung carcinogenesis by contributing to p53 response to DNA damage caused by genotoxic agents or oncogenic stress through JNK-dependent NPM up-regulation. Genetic or epigenetic aberrations (LOH, overexpression of miR-370, or oncogenic RAS signaling) may independently induce TPL2 down-regulation, leading to diminished JNK and p53 responses, reduced cell death, and accelerated cell transformation.

dependent up-regulation of NPM, thereby influencing p53 stabilization (Fig. 7); p53 is a major factor in preventing transformation and has a crucial role in tumor suppression, in part by regulating apoptosis, a barrier to cancer (48). Molecular aberration leading to loss of p53 function occurs in 50–70% of AdenoCas (23) and nearly all SqCCLs (44). We show that low TPL2 levels lead to diminished JNK and p53 responses, reduced cell death, and accelerated malignant transformation (Fig. 6 and Fig. S1). In line with these in vitro findings, the absence of *TPL2* in mouse lungs associates with diminished p53 responses to the mutagen urethane, which were determined by the impaired up-regulation of two p53 target genes, *bax* and *cdkn1a* (Fig. 6*F*). Collectively, these data define TPL2 as a regulator of the p53 pathway and provide a mechanistic explanation for the operation of multiple pathways leading to down-regulation of TPL2 in human lung cancer (Fig. 1). However, TPL2 may have a broader role in dictating the balance between cell survival and death, thereby influencing tumorigenicity and/or the response to therapy. Indeed, an RNAi screen performed in breast cancer cells has shown that reduced TPL2 expression associates with resistance to TRAIL-induced apoptosis (13), a p53-independent process (49).

Our findings, coupled with a recent study describing a lung tumor suppressor function for the JNK kinase MKK7 (mitogen-activated protein kinase kinase 7) (32), expand our appreciation of the impact of MAP3Ks in malignancy. Similar to TPL2, inhibition of MKK7 leads to reduced JNK activation and p53 response in lung cancer cells (32), providing a telling example of how tumor cells exploit MAPK pathways to lower intrinsic barriers to malignant transformation.

Materials and Methods

Human Tissue. Frozen tissues from 124 NSCLCs (46 AdenoCas and 78 SqCCLs) as well as 100 adjacent normal lung tissues were obtained from Liverpool Heart and Chest Hospital. In 100 NSCLCs, matched normal tissue was available; 82 patients were males, and 44 patients were females. Specimens comprised the following pathological stages: 8 T1, 103 T2, 9 T3, and 2 T4. Immunohistochemical detection of TPL2 was performed as previously described (50).

DNA and RNA Isolation and cDNA Synthesis. DNA and total RNA extraction from tissues was performed using the DNeasy and miRNeasy Kits (Qiagen), respectively, following the manufacturer's protocol; 20×40-μm frozen sections from each patient sample were used. The first and last sections underwent pathological review to ensure ≥80% tumor cell content, and 500 ng total RNA were reverse-transcribed in a 20-μL reaction using the Quantitect Kit (Qiagen) following the supplier's protocol.

qPCR Expression Assays. TaqMan gene expression assays for human COT [MAP3K8; ID Hs00178297_m1, FAM (6 - Carboxyfluorescein)-labeled] and β-actin (ACTB; 4326315E) as endogenous control (VIC-labeled), mouse *Cdkn1a*, (Mm04205640_g1), *bax* (Mm00432051_m1), and GAPD (glyceraldehyde-3-phosphate dehydrogenase) assays were obtained from Applied Biosystems and used on an Applied Biosystems 7500 FAST Real-Time PCR Instrument. For microRNA analysis, the hsa-miR-370 (assay ID 2275) and RNU48 (assay ID 1006) were used as target and endogenous control, respectively, following the manufacturer's protocol. All assays were run in triplicate, and the mean value was used for the analysis. mRNA and microRNA levels were expressed as relative quantification (RQ) values, which were calculated as $RQ = 2^{(-\Delta\Delta Ct)}$, where the expression of IMR-90 human lung fibroblasts was used as a calibrator in each run.

DNA Methylation Analysis. Pyrosequencing assays were developed using the Pyromark Assay Design 2.0 software (Qiagen) to measure the DNA methylation levels of MAP3K8 promoter and miR-370 region. One assay (TPLmeth1) covered the transcription start site (TSS) and proximal promoter (CpGs at positions −42, −40, −37, −16, −4, 1, and 5 relative to TSS). The second assay (TPLmeth2) covered CpGs within the 5′ UTR (positions 27, 30, 38, 53, 55, 68, and 70 relative to TSS). The miR-370 methylation assay covered CpGs at positions −9, −18, −42, −48, −60, and −80 relative to the TSS of the premicroRNA sequence. The primer sequences used are provided in *SI Materials and Methods* One microgram genomic DNA was treated with sodium bisulphite (EZ DNA Methylation Kit; ZymoResearch) following the manufacturer's protocol. PCR amplifications were performed in a final volume of 25 μL using Qiagen HotStarTaq Master Mix, 150 nM biotinylated primer, 300 nM nonbiotinylated primer, and ∼60 ng bisulphite treated genomic DNA. The thermal profile was 95 °C for 5 min followed by 40 cycles of 94 °C for 30 s, 52 °C for 30 s, and 72 °C for 30 s. For Pyrosequencing analysis, the PyroMark Gold Q96 SQA Reagents and the PyroMark Q96 ID Instrument (Qiagen) were used following the supplier's protocol. The methylation index for each promoter was calculated as the mean value of mC/(mC + C) for all examined CpGs in the target sequence (51).

Allelic Imbalance Analysis. Primers flanking the repeat regions MS1–4 were designed (Fig. 3*A*), and their sequences are provided in *SI Materials and Methods*. The thermal profile was 95 °C for 5 min followed by 25 cycles of 94 °C for 30 s, 52 °C for 30 s, and 72 °C for 30 s. Two microliters PCR reactions were mixed with 10 μL formamide, denatured at 95 °C for 2 min, chilled on ice, and analyzed on a 3130 capillary sequencer (Applied Biosystems). Genemapper software was used to analyze the signal and quantify allelic peak areas. Allelic imbalance was scored if the allelic ratio tumor/normal was outside the region of 0.75–1.25 (52).

Mutational Analysis of Human K-*ras*. K-*ras* mutational analysis for the hot-spot codons 12 and 13 was carried out by PCR and direct sequencing using primers described in *SI Materials and Methods*. Mutations were determined by comparing each tumor with the K-*ras* codon 12/13 WT sequence (GGTGGC).

Cell Culture, Transfections, RNAi, and Apoptosis Assays. Lung cancer cell lines (ATCC) were passaged for fewer than 6 mo after resuscitation and cultured according to the provider's instructions. Cells are authenticated by short tandem repeat profiling analysis. Liposome-mediated transfections were performed using lipofectamin (Invitrogen) in Optimem media (Invitrogen) according to the instructions of the manufacturer. RAS^{G12V} expression vectors were a gift from A. Malliri (Paterson Institute for Cancer Research, Manchester, United Kingdom). The p53 shRNA vector was provided by Reuven Agami (The Netherlands Cancer Institute, Amsterdam, The Netherlands). TPL2 expression vectors have been previously described (2). For the delivery of siRNAs and miR370, 5×10^4 A549 cells were plated into each well of a 24-well plate (Costar), and two rounds of transfection with siRNA duplexes were performed as previously described (4). The COT siRNA (AM16708) and miR-370 (hsa-miR-370) were from Ambion (Applied Biosystems). Cell survival was determined using fluorescence microscopy of propidium iodide-stained cells and MTT (Dimethyl thiazolyl diphenyl tetrazolium salt) conversion assays as previously described (4).

Soft Agar Assay. Tissue culture dishes (60 mL) were layered with 3 mL 0.7% (wt/vol) SeaPlaque Low Melting Point Agarose (FMC Bioproducts) dissolved in serum-containing medium. Cells were then mixed with 1.6 mL 0.35% (wt/vol) warm agar (42 °C) in serum-containing medium and plated on the solidified agarose layer in triplicates. Fresh agar was added weekly, and cellular foci were enumerated on day 17.

Antibodies and Immunoblotting. The following Abs were used for immunoblotting, which was performed as previously described (4): COT/TPL2 M20 (Santa Cruz), IκBα L35A5 (Cell Signaling Technology), phospho-ERK M8159 (Sigma), β-actin clone C4 (Millipore), NF-κB1 clone E381 (Novus Biologicals), and anti-p53 mAb 1801 (a gift from Moshe Oren; Weizmann Institute, Rehovot, Israel).

Mouse Maintenance, Carcinogenesis Protocol, and Histological Analyses. *TPL2*$^{+/+}$ and *TPL2*$^{-/-}$ mice (C57/BL6 background) (1) were housed in plastic cages containing hardwood bedding and dust covers in a High-Efficiency Particulate Air–filtered environmentally controlled room (24 °C, 12/12-h light/dark cycle) and given Rodent Lab Chow and water ad libitum. For the induction of lung tumors, a chemical carcinogenesis protocol based on urethane was applied as previously described for C57/BL6 mice (53). Briefly, 7-wk-old mice were injected i.p. with 1 mg freshly prepared urethane (Sigma-Aldrich) in 0.9% wt/vol NaCl per gram body weight one time per week for a total of 10 doses. Lungs were excised at various time points, fixed overnight in 10% buffered formalin, and paraffin-embedded. Sections cut into 4-μm size were prepared, placed on glass slides, stained with H&E, and reviewed by the study pathologists (V.P., E.N.S., and V.G.) blindly and in consensus in case of discrepancy more than 10%. The same procedure was followed for lung inflammation grade evaluation. The histopathological classification of the pulmonary lesions was performed in accordance with the recommendations of the mouse models of the human cancers consortium (National Institutes of Health/National Cancer Institute, 2004) (54). To estimate the growth rate of tumors, the percentage of tumor cells expressing the proliferation marker Ki67 was measured. A proliferation index was calculated for each tumor lesion by counting the total number of tumor cell nuclear profiles and the number of Ki67-positive nuclear profiles in randomly selected fields. Spleens from euthanized animals at 2 or 10 wk after urethane administration were processed for flow cytometry as previously described (4). Lysates from mouse lungs expressing K-RAS^{G12D} (32) were provided by Josef Penninger, Austrian Academy of Sciences, Vienna, Austria.

Mouse Splenocyte Isolation and FACS Analysis. Mouse splenic cells were isolated as previously described (4) and stained with fluorescently labeled antibodies (clones are indicated in parentheses) against CD3 (145-2C11), NK1.1 (PK136), CD4 (GK1.5), CD8α (53-6.7), CD69 (H1.2F3), F4/80 (BM8), CD11c (N418), Gr1 (RB6-8C5), and CD11b (M1/70; purchased from eBioscience).

Statistical Analyses. The one-sample Smirnov–Kolmogorov test was used to assess normal distribution in continuous variables (e.g., expression and methylation levels). In the absence of normal distribution, nonparametric tests were used. The Mann–Whitney (independent) and Wilcoxon ranking (paired comparisons) tests were used to determine significant differences in expression and methylation levels among groups. Pearson χ^2 test was performed to assess differences in categorical data groups, whereas Spearman correlation assessed the relationship between continuous variables. Survival analysis was undertaken by constructing Kaplan–Meier curves and using log-rank test.

Ethics Statement. Ethical approval has been obtained from the Liverpool Ethics Committee for this study involving human tissue, and informed consent was obtained from each individual. Animal experiments were approved by the local ethics committee of the University of Crete Medical School, Greece (license number 1406/14–03-2006) in line with the corresponding national and European Union legislation.

ACKNOWLEDGMENTS. We thank Moshe Oren, Josef Penninger, Angeliki Malliri, and Reuven Agami for their kind gifts of reagents; Chris Tsatsanis for critical reading of the manuscript; and Marina Ioannou and Eleftheria Anastasiou for technical assistance. This work was supported by the European Commission (EC) research program Inflammation & Cancer Research in Europe (INFLA-CARE; EC Contract 223151) to A.G.E. and V.G., the EC support program Translational Potential (TransPOT; EC Contract 285948), a General Secreteriat of Research & Technology of Greece grant to A.G.E., a grant from the Roy Castle Lung Cancer Research Foundation, United Kingdom to J.K.F. and T.L., and NIH Grant R01 CA124835 to P.N.T.

1. Dumitru CD, et al. (2000) TNF-alpha induction by LPS is regulated posttranscriptionally via a Tpl2/ERK-dependent pathway. *Cell* 103(7):1071–1083.
2. Eliopoulos AG, Dumitru CD, Wang C-C, Cho J, Tsichlis PN (2002) Induction of COX-2 by LPS in macrophages is regulated by Tpl2-dependent CREB activation signals. *EMBO J* 21(18):4831–4840.
3. Banerjee A, Gugasyan R, McMahon M, Gerondakis S (2006) Diverse Toll-like receptors utilize Tpl2 to activate extracellular signal-regulated kinase (ERK) in hemopoietic cells. *Proc Natl Acad Sci USA* 103(9):3274–3279.
4. Eliopoulos AG, Wang CC, Dumitru CD, Tsichlis PN (2003) Tpl2 transduces CD40 and TNF signals that activate ERK and regulates IgE induction by CD40. *EMBO J* 22(15): 3855–3864.
5. Hatziapostolou M, Polytarchou C, Panutsopulos D, Covic L, Tsichlis PN (2008) Proteinase-activated receptor-1-triggered activation of tumor progression locus-2 promotes actin cytoskeleton reorganization and cell migration. *Cancer Res* 68(6):1851–1861.
6. Kontoyiannis D, et al. (2002) Genetic dissection of the cellular pathways and signaling mechanisms in modeled tumor necrosis factor-induced Crohn's-like inflammatory bowel disease. *J Exp Med* 196(12):1563–1574.
7. Watford WT, et al. (2008) Tpl2 kinase regulates T cell interferon-gamma production and host resistance to Toxoplasma gondii. *J Exp Med* 205(12):2803–2812.
8. Watford WT, et al. (2010) Ablation of tumor progression locus 2 promotes a type 2 Th cell response in Ovalbumin-immunized mice. *J Immunol* 184(1):105–113.
9. Tsatsanis C, Patriotis C, Bear SE, Tsichlis PN (1998) The Tpl-2 protooncoprotein activates the nuclear factor of activated T cells and induces interleukin 2 expression in T cell lines. *Proc Natl Acad Sci USA* 95(7):3827–3832.
10. Ceci JD, et al. (1997) Tpl-2 is an oncogenic kinase that is activated by carboxy-terminal truncation. *Genes Dev* 11(6):688–700.
11. Vougioukalaki M, Kanellis DC, Gkouskou K, Eliopoulos AG (2011) Tpl2 kinase signal transduction in inflammation and cancer. *Cancer Lett* 304(2):80–89.
12. Johannessen CM, et al. (2010) COT drives resistance to RAF inhibition through MAP kinase pathway reactivation. *Nature* 468(7326):968–972.
13. Ovcharenko D, Kelnar K, Johnson C, Leng N, Brown D (2007) Genome-scale microRNA and small interfering RNA screens identify small RNA modulators of TRAIL-induced apoptosis pathway. *Cancer Res* 67(22):10782–10788.
14. Tsatsanis C, et al. (2008) Tpl2 and ERK transduce antiproliferative T cell receptor signals and inhibit transformation of chronically stimulated T cells. *Proc Natl Acad Sci USA* 105(8):2987–2992.
15. Larsen JE, Minna JD (2011) Molecular biology of lung cancer: Clinical implications. *Clin Chest Med* 32(4):703–740.
16. Tuveson DA, Jacks T (1999) Modeling human lung cancer in mice: Similarities and shortcomings. *Oncogene* 18(38):5318–5324.
17. Meuwissen R, Berns A (2005) Mouse models for human lung cancer. *Genes Dev* 19(6): 643–664.
18. Malkinson AM (1992) Primary lung tumors in mice: An experimentally manipulable model of human adenocarcinoma. *Cancer Res* 52(9, Suppl):(Suppl):2670s–2676s.
19. Zhang Z, et al. (2001) Wildtype Kras2 can inhibit lung carcinogenesis in mice. *Nat Genet* 29(1):25–33.
20. To MD, et al. (2008) Kras regulatory elements and exon 4A determine mutation specificity in lung cancer. *Nat Genet* 40(10):1240–1244.
21. Stathopoulos GT, et al. (2007) Epithelial NF-kappaB activation promotes urethane-induced lung carcinogenesis. *Proc Natl Acad Sci USA* 104(47):18514–18519.
22. Serebrennikova OB, et al. (2012) Tpl2 ablation promotes intestinal inflammation and tumorigenesis in Apcmin mice by inhibiting IL-10 secretion and regulatory T-cell generation. *Proc Natl Acad Sci USA* 109(18):E1082–E1091.
23. Herbst RS, Heymach JV, Lippman SM (2008) Lung cancer. *N Engl J Med* 359(13): 1367–1380.
24. Brock MV, et al. (2008) DNA methylation markers and early recurrence in stage I lung cancer. *N Engl J Med* 358(11):1118–1128.
25. Nikolaidis G, et al. (2012) DNA methylation biomarkers offer improved diagnostic efficiency in lung cancer. *Cancer Res* 72(22):5692–5701.
26. Meng F, Wehbe-Janek H, Henson R, Smith H, Patel T (2008) Epigenetic regulation of microRNA-370 by interleukin-6 in malignant human cholangiocytes. *Oncogene* 27(3): 378–386.
27. Chalitchagorn K, et al. (2004) Distinctive pattern of LINE-1 methylation level in normal tissues and the association with carcinogenesis. *Oncogene* 23(54):8841–8846.
28. Daskalos A, et al. (2009) Hypomethylation of retrotransposable elements correlates with genomic instability in non-small cell lung cancer. *Int J Cancer* 124(1):81–87.
29. Barbie DA, et al. (2009) Systematic RNA interference reveals that oncogenic KRAS-driven cancers require TBK1. *Nature* 462(7269):108–112.
30. Waterfield MR, Zhang M, Norman LP, Sun SC (2003) NF-kappaB1/p105 regulates lipopolysaccharide-stimulated MAP kinase signaling by governing the stability and function of the Tpl2 kinase. *Mol Cell* 11(3):685–694.
31. Beinke S, et al. (2003) NF-kappaB1 p105 negatively regulates TPL-2 MEK kinase activity. *Mol Cell Biol* 23(14):4739–4752.
32. Schramek D, et al. (2011) The stress kinase MKK7 couples oncogenic stress to p53 stability and tumor suppression. *Nat Genet* 43(3):212–219.
33. Grisendi S, Mecucci C, Falini B, Pandolfi PP (2006) Nucleophosmin and cancer. *Nat Rev Cancer* 6(7):493–505.
34. Colombo E, Marine JC, Danovi D, Falini B, Pelicci PG (2002) Nucleophosmin regulates the stability and transcriptional activity of p53. *Nat Cell Biol* 4(7):529–533.
35. Kurki S, et al. (2004) Nucleolar protein NPM interacts with HDM2 and protects tumor suppressor protein p53 from HDM2-mediated degradation. *Cancer Cell* 5(5):465–475.
36. Chan PK, Chan FY, Morris SW, Xie Z (1997) Isolation and characterization of the human nucleophosmin/B23 (NPM) gene: Identification of the YY1 binding site at the 5′ enhancer region. *Nucleic Acids Res* 25(6):1225–1232.
37. Salmeron A, et al. (1996) Activation of MEK-1 and SEK-1 by Tpl-2 proto-oncoprotein, a novel MAP kinase kinase. *EMBO J* 15(4):817–826.
38. Das S, et al. (2005) Tpl2/cot signals activate ERK, JNK, and NF-kappaB in a cell-type and stimulus-specific manner. *J Biol Chem* 280(25):23748–23757.
39. Folkman J, Hahnfeldt P, Hlatky L (2000) Cancer: Looking outside the genome. *Nat Rev Mol Cell Biol* 1(1):76–79.
40. Yanaihara N, et al. (2006) Unique microRNA molecular profiles in lung cancer diagnosis and prognosis. *Cancer Cell* 9(3):189–198.

41. Saito K, et al. (2010) Long interspersed nuclear element 1 hypomethylation is a marker of poor prognosis in stage IA non-small cell lung cancer. *Clin Cancer Res* 16(8): 2418–2426.
42. Slebos RJ, et al. (1990) K-ras oncogene activation as a prognostic marker in adenocarcinoma of the lung. *N Engl J Med* 323(9):561–565.
43. Sugio K, et al. (1992) ras gene mutations as a prognostic marker in adenocarcinoma of the human lung without lymph node metastasis. *Cancer Res* 52(10):2903–2906.
44. Hammerman PS, et al. (2012) Comprehensive genomic characterization of squamous cell lung cancers. *Nature* 489(7417):519–525.
45. Blasco RB, et al. (2011) c-Raf, but not B-Raf, is essential for development of K-Ras oncogene-driven non-small cell lung carcinoma. *Cancer Cell* 19(5):652–663.
46. Meylan E, et al. (2009) Requirement for NF-kappaB signalling in a mouse model of lung adenocarcinoma. *Nature* 462(7269):104–107.
47. Singh A, et al. (2009) A gene expression signature associated with "K-Ras addiction" reveals regulators of EMT and tumor cell survival. *Cancer Cell* 15(6):489–500.
48. Levine AJ, Oren M (2009) The first 30 years of p53: Growing ever more complex. *Nat Rev Cancer* 9(10):749–758.
49. Chinnaiyan AM, et al. (2000) Combined effect of tumor necrosis factor-related apoptosis-inducing ligand and ionizing radiation in breast cancer therapy. *Proc Natl Acad Sci USA* 97(4):1754–1759.
50. Eliopoulos AG, et al. (2002) The oncogenic protein kinase Tpl-2/Cot contributes to Epstein-Barr virus-encoded latent infection membrane protein 1-induced NF-kappaB signaling downstream of TRAF2. *J Virol* 76(9):4567–4579.
51. Daskalos A, et al. (2011) UHRF1-mediated tumor suppressor gene inactivation in nonsmall cell lung cancer. *Cancer* 117(5):1027–1037.
52. Liloglou T, et al. (2001) Cancer-specific genomic instability in bronchial lavage: A molecular tool for lung cancer detection. *Cancer Res* 61(4):1624–1628.
53. Miller YE, et al. (2003) Induction of a high incidence of lung tumors in C57BL/6 mice with multiple ethyl carbamate injections. *Cancer Lett* 198(2):139–144.
54. Nikitin AY, et al. (2004) Classification of proliferative pulmonary lesions of the mouse: recommendations of the mouse models of human cancers consortium. *Cancer Res* 64(7):2307–2316.

ARTICLE IN PRESS

Cancer Letters xxx (2011) xxx–xxx

Contents lists available at ScienceDirect

Cancer Letters

journal homepage: www.elsevier.com/locate/canlet

Mini-review

Tpl2 kinase signal transduction in inflammation and cancer

Maria Vougioukalaki [1], Dimitris C. Kanellis [1], Kalliopi Gkouskou, Aristides G. Eliopoulos *

Molecular and Cellular Biology Laboratory, Division of Basic Sciences, University of Crete Medical School and Institute for Molecular Biology and Biotechnology, Foundation of Research and Technology Hellas, Heraklion, Crete, Greece

ARTICLE INFO

Article history:
Received 11 January 2011
Received in revised form 3 February 2011
Accepted 3 February 2011
Available online xxxx

Keywords:
Tpl2
Cot kinase
MAP3K8
NF-κB1
tnip2
ABIN2
IKKβ
Inflammation
Cancer

ABSTRACT

The activation of mitogen-activated protein kinases (MAPKs) is critically involved in inflammatory and oncogenic events. Tumor progression locus 2 (Tpl2), also known as COT and MAP3 kinase 8 (MAP3K8), is a serine-threonine kinase with an important physiological role in tumor necrosis factor, interleukin-1, CD40, Toll-like receptor and G protein-coupled receptor-mediated ERK MAPK signaling. Whilst the full characterization of the biochemical events that lead to the activation of Tpl2 still represent a major challenge, genetic and molecular evidence has highlighted interesting interactions with the NF-κB network. Here, we provide an overview of the multifaceted functions of Tpl2 and the molecular mechanisms that govern its regulation.

1. Introduction

Mitogen-activated protein kinases (MAPKs) are critically involved in the pathogenesis of a plethora of inflammatory and malignant diseases. There are three main families of MAPKs in mammals, the extracellular signal regulated kinases (ERKs), cJun N-terminal kinases (JNKs) and p38 MAPKs which function upstream of numerous kinases, transcription factors and other effector proteins and are important regulators of immune, oncogenic and cell death pathways. The highly conserved cascade that leads to MAPK activation involves a dual specificity MAPK kinase (MAP2K) that phosphorylates MAPK on Serine/Tyrosine residues and a MAP3K that acts upstream of MAP2K and phosphorylates it on Serine/Threonine residues. Activation of the limited number of MAPKs is controlled by an abundance of MAP3Ks which provide the stimulus and cell context specificity of signaling responses.

Tpl2 is a MAP3K with a major role in the activation of the ERK MAPK through direct phosphorylation of MEK, the ERK kinase. The *Tpl2* gene locus encodes for two protein isoforms of 58 (Tpl2 long; $Tpl2_L$) and 52 kDa (Tpl2 short; $Tpl2_S$), generated by the utilization of alternative translation start sites at methionine 1 and methionine 30. The encoded proteins contain a serine/threonine kinase domain, an amino-terminal region with unknown function and a carboxy-terminal tail which carries sequences important for Tpl2 stability and regulation of catalytic activity (Fig. 1). There is 94% similarity in the amino-acid sequences of mouse and rat Tpl2 compared to human, allowing for the establishment of reliable models to dissect the impact of this kinase on immune and inflammatory responses and oncogenesis. Indeed, a plethora of recent studies reveal major roles for Tpl2 in inflammation and cancer. Here, we review the pleiotropic functions of Tpl2 and the molecular mechanisms involved in its regulation.

* Corresponding author. Tel./fax: +30 2810 394565.
E-mail address: eliopag@med.uoc.gr (A.G. Eliopoulos).
URL: http://mcb.med.uoc.gr (A.G. Eliopoulos).
[1] These authors contributed equally to the work.

0304-3835/$ - see front matter © 2011 Elsevier Ireland Ltd. All rights reserved.
doi:10.1016/j.canlet.2011.02.004

Please cite this article in press as: M. Vougioukalaki et al., Tpl2 kinase signal transduction in inflammation and cancer, Cancer Lett. (2011), doi:10.1016/j.canlet.2011.02.004

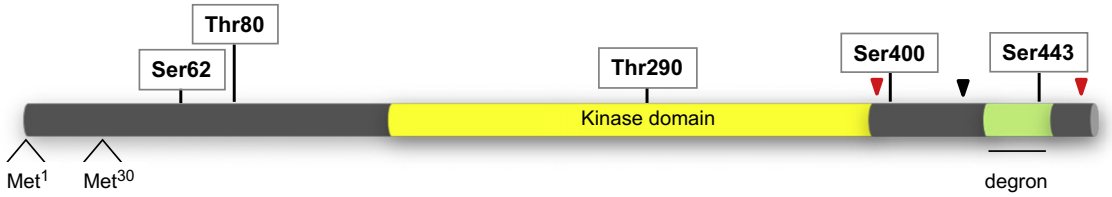

Fig. 1. Schematic representation of the Tpl2 primary structure. Tpl2 is expressed as 2 isoforms generated by the utilization of alternative translation start sites, methionine 1 and methionine 30. The C-terminus carries a reported 'degron' sequence (aa 435–457) that targets Tpl2 for proteasomal degradation. NF-κB1 binds to and masks 'degron' thus stabilizing Tpl2. C-terminal truncations that occur as a result of provirus insertion in MoMuLV – induced T-cell lymphomas and MMTV – induced mammary adenocarcinomas in rats (black arrowhead, aa 424) also remove the 'degron' sequence, increasing the stability of Tpl2. NF-κB1 also binds to the kinase domain of Tpl2 preventing access to MEK, the ERK kinase. The red arrowheads represent Tpl2 mutations that were identified through our data mining of the Sanger Institute Catalogue of Somatic Mutations in Cancer (COSMIC) database (http://www.sanger.ac.uk/genetics/CGP/cosmic/) and include an $Ala^{387} \rightarrow Thr$ mutation found in one case of 31 astrocytomas studied and a $Pro^{461} \rightarrow Leu$ mutation found in three cases of 30 breast tumors analysed. Phosphorylation sites identified through mass spectrometry [11,73] and molecular analyses [61,62] are also shown.

2. The function of Tpl2 in inflammation and cancer

2.1. Tpl2 in innate immune responses

Innate immune responses, orchestrated by macrophages, dendritic cells, natural killer cells and neutrophils, represent the first line of defense against infections. Crucial to this process is the detection of pathogen-associated molecules by Toll-like receptors (TLRs), such as the recognition of the bacterial cell wall component lipopolysaccharide (LPS) by TLR4. In a seminal paper published in Cell in 2000, the team of Philip Tsichlis at Thomas Jefferson University (Philadelphia, USA) provided the first genetic evidence linking Tpl2 to innate immunity. They showed that macrophage responses to LPS, such as production of the pro-inflammatory cytokine TNF, are largely attenuated in $Tpl2^{-/-}$ macrophages because of a defect in ERK activation. As a result, *Tpl2*-deficient mice are resistant to endotoxin shock caused by administration of LPS/D-galactosamine which is largely provoked by over-production of TNF [1]. These observations sparked a tremendous interest in the role of Tpl2 in inflammation with emphasis on the Tpl2 - macrophage link (Table 1).

Indeed, additional macrophage responses were soon found to be influenced by Tpl2. Thus, production of the pro-inflammatory mediator prostaglandin E2 (PGE2) and its regulatory enzyme COX-2 are attenuated in LPS-stimulated $Tpl2^{-/-}$ cells [2] and in human monocytes treated with Tpl2 kinase inhibitors [3]. The Tpl2-mediated COX-2 transactivation signals depend on ERK which stimulates the Msk1 kinase [2]. Msk1 in turn phosphorylates CREB, a key regulator of COX-2 transcription (Fig. 2). A transcriptional mechanism has also been inferred in a study showing that *Tpl2* deficiency results in reduced production of the pro-inflammatory Th17 promoting cytokine IL-23 in LPS-stimulated macrophages [4] and of IL-1β following stimulation of macrophages and DC with LPS or the TLR9 ligand CpG [5]. In contrast, Tpl2 regulates TNF synthesis by post-transcriptional mechanisms involving control of nucleo-cytoplasmic transport of the TNF mRNA [1] and processing of pre-TNF to the secreted form of the cytokine through the ERK-mediated phosphorylation of the TNF-converting enzyme TACE on Thr^{735} [6]. The importance of Tpl2 in the post-translational control of TNF synthesis is further highlighted by studies in a mutant mouse strain called *Sluggish* which carries a partially deleted Tpl2 kinase domain. Macrophages from these mice display defects in maturation of pre-TNF in response to LPS [7]. Therefore, Tpl2 may control macrophage gene expression to TLR ligands at transcriptional or post-transcriptional level.

Activation of the Tpl2/MEK/ERK pathway in macrophages not only regulates the production of cytokines but also the cellular response to TNF, IL-1β and CD154, the CD40 ligand [8–11], suggesting that Tpl2 may have a broader role in inflammatory signal transduction in innate immune cells and could be exploited as anti-inflammatory drug target. Along these lines, several pharmaceutical companies including Wyeth/Pfizer and Abbott are developing small-molecule Tpl2 inhibitors with some of them showing relative specificity *in vitro* and anti-inflammatory efficacy *in vivo* [3,12].

However, recent studies raise questions about the generality of this concept. Thus, infection of $Tpl2^{-/-}$ macrophages with *Listeria monocytogenes,* an intracellular Gram-positive bacterium, leads to weakened TNF and IL-1β production but greater sensitivity to the bacteria-provoked pathology [5]. TLRs also respond to pathogen-derived products by stimulating the production of the pro-inflammatory effector molecules IL-12 and interferon-β. Intriguingly, Tpl2 deficiency was found to result in over-production of both cytokines in response to TLR4 and TLR9 agonists in macrophages and myeloid dendritic cells. Several mechanisms have been proposed to explain this effect, including defective activation of the transcription factors cMAF, GAP12 and c-Fos which negatively regulate IL-12p40 expression [13,14]. Additionally, TLR4 or TLR9 activation in $Tpl2^{-/-}$ macrophages or myeloid dendritic cells leads to reduced synthesis of IL-10 which functions to suppress inflammation [14].

What is the molecular basis of the diverse and often contradictory effects of Tpl2 on innate immune cell function? Whilst the molecular pathways involved in Tpl2-dependent cytokine regulation remain to be fully delineated, ERK MAPK appears to be a major physiological target of Tpl2 signaling. Reduced ERK activation could positively or negatively impact on gene expression with the final outcome influenced by additional signals in a cell type-dependent manner. It is thus of interest that whereas

Please cite this article in press as: M. Vougioukalaki et al., Tpl2 kinase signal transduction in inflammation and cancer, Cancer Lett. (2011), doi:10.1016/j.canlet.2011.02.004

Table 1
Effects of Tpl2 ablation on experimentally-induced inflammation and cancer.

Disease	Mouse model	Phenotype	Reference
Septic Shock	LPS/D-gal induced septic shock	Resistance Reduced levels of serum TNFα and IL-1β	[1]
Pathogen infection	*Listeria monocytogenes* infection	Enhanced susceptibility	[5]
	Toxoplasma gondii infection	Enhanced susceptibility; Normal serum levels of TNFα; increased IL-12 serum levels	[17]
Asthma- like	OVA-induced brochoalveolar inflammation	More severe eosinophilic inflammation Higher levels of IgE production T-cell intrinsic Th2 polarization defect	[18]
Inflammatory bowel disease	TNF-driven Crohn's like IBD (*Tnf* $^{\Delta ARE/+}$)	Delayed IBD onset and attenuated progression Increased $CD4^{+}CD44^{lo}$, reduced $CD8^{+}CD44^{hi}$ T cells in the spleen.	[20]
Severe acute pancreatitis	Caerulein-induced pancreatitis;	Markedly reduced pancreatic and lung inflammation	[22]
	Bile salt-induced pancreatitis	Reduced expression of IL-6, MIP-2 and MCP-1 by non-myeloid cells; Reduced neutrophil sequestration in pancreas	
Periodontitis	Mechanically induced periodontal inflammation	Reduced inflammation Significant reduction in TNFα and RANKL expression in periodontal tissue	[21]
T- cell lymphoma	$TCR2C^{tg/tg}$ transgenic mouse	T-cell lymphomas in $TCR2C^{tg/tg} \times Tpl2^{-/-}$ mice Enhanced T cell proliferation; Decreased CTLA4 expression in $CD8^{+}$ T cells	[44]
Skin cancer	Two stage DMBA/TPA induced skin carcinogenesis	Increased incidence of skin tumor formation and progression; Increased keratinocyte proliferation and neutrophil infiltration	[45]

ablation of *Tpl2* has no apparent effect on LPS-triggered NF-κB signaling in bone marrow-derived macrophages [1,2], it associates with accelerated NF-κB activation in dendritic cells [5]. Moreover, *Tpl2*$^{-/-}$ fibroblasts do not only display defects in TNF-induced ERK signaling but also partial impairment in NF-κB transcriptional activity and JNK activation [9]. Furthermore, Tpl2 is required for the optimal induction of p38 MAPK in LPS or CpG-stimulated bone marrow-derived dendritic cells but not macrophages [9,14].

Other microenvironmental signals may also impinge on the Tpl2 response to pro-inflammatory factors. For example adiponectin, a product of adipose tissue and most abundant hormone in the plasma, requires Tpl2 to induce the expression of IRAK-M in macrophages. IRAK-M is an inactive isoform of the IL-1R-associated kinase (IRAK) family of kinases that competes with active IRAKs in TLR4 signaling. Thus, adiponectin may inhibit LPS-mediated macrophage activation and production of pro-inflammatory cytokines through the Tpl2-mediated expression of IRAK-M [15].

2.2. The role of Tpl2 in adaptive immunity

The role of Tpl2 in adaptive immune responses is only recently beginning to emerge. Tpl2 is expressed in B lymphocytes and various T cell subsets [1,8,16] with Th1 cells expressing higher levels than Th2 [17]. The latter observation may in part explain the stronger defect in ERK activation seen in *Tpl2*$^{-/-}$ Th1 compared to Th2 cells when challenged with anti-CD3, indicating that T cell receptor (TCR) signaling depends heavily on Tpl2 in Th1 but not in Th2 cells [18]. As a result, anti-CD3 stimulated *Tpl2*$^{-/-}$ T cell cultures produce lower levels of the Th1 cytokine IFNγ and higher levels of the Th2 cytokine IL-4 than *Tpl2*$^{+/+}$ controls, suggesting that Tpl2 may favor a Th1 immune response. Indeed, in a mouse model of ovalbumin-induced bronchoalveolar inflammation, *Tpl2* ablation leads to Th2 polarization of the T cell response with concomitant increase in IgE levels [18]. This is in agreement with recent data showing that the defense of *Tpl2* knockout mice to the intracellular pathogen *Toxoplama gondii* is impaired because of defective Th1 responses [17].

The function of Tpl2 in B lymphocytes is less well defined. The activation of the CD40 receptor on the surface of *Tpl2*$^{-/-}$ B cells results in defective ERK signaling which may partly influence immunoglobulin isotype switching [8]. Moreover, the ERK defect associates with failure to phosphorylate and inactivate the pro-apoptotic protein Bim, leading to enhanced sensitivity to LPS-mediated B cell apoptosis [19].

2.3. Tpl2 in acute and chronic inflammatory disorders

The role of Tpl2 in inflammatory disorders has been studied in mouse disease models (Table 1). The overall picture that emerges from these studies is that Tpl2 has predominantly a pro-inflammatory function. Thus, in a TNF-driven Crohn's-like inflammatory bowel disease (IBD) mouse model, the absence of Tpl2 ameliorates the onset and progression of the disease by maintaining low numbers of memory CD4+ and peripheral CD8 + lymphocytes [20]. *Tpl2*$^{-/-}$ mice produce reduced levels of TNF, COX-2 and IL-1 in a mechanically-induced model of murine periodontitis [21] and low amounts of neutrophil chemoattractant chemokines MIP-2, MCP-1 and IL-6 in an acute pancreatitis mouse model [22]. As a result, both pathologies are ameliorated in the absence of Tpl2. Interestingly, bone marrow chimeras revealed that pancreatic inflammation is controlled by Tpl2 expressed in non-myeloid cells,

Please cite this article in press as: M. Vougioukalaki et al., Tpl2 kinase signal transduction in inflammation and cancer, Cancer Lett. (2011), doi:10.1016/j.canlet.2011.02.004

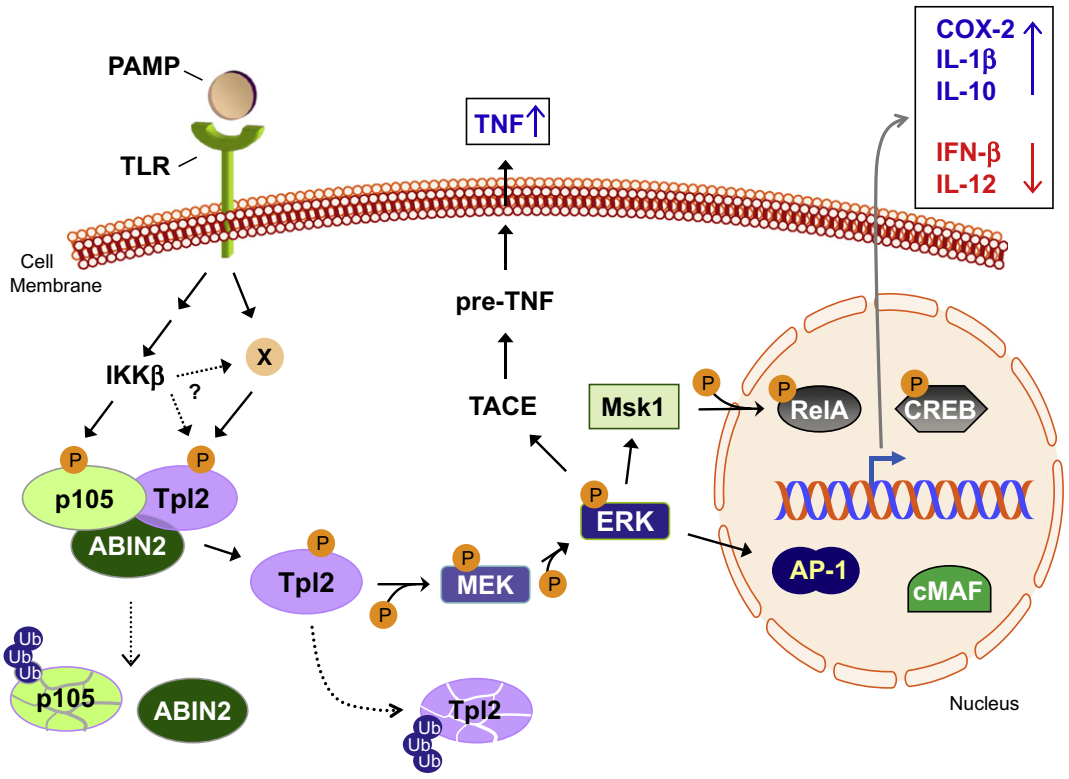

Fig. 2. Schematic representation of known components of the signaling cascade that lead to Tpl2 activation downstream of Toll-like receptors (TLRs) and its functional outcome. At steady state, Tpl2 associates with p105 NF-κB1 and ABIN2 and is inactive towards its main downstream substrate MEK, the ERK kinase. Molecules associated with group of pathogens termed PAMPs (pathogen-associated molecular patterns) are recognized by TLRs, stimulating intracellular signal transduction. The PAMP-induced activation of IκB kinase β (IKKβ) mediates the phosphorylation of p105 NF-κB1 and its subsequent poly-ubiquitination (Ub) and proteasomal degradation, releasing Tpl2 from the complex. Tpl2 is phosphorylated at Thr^{290} and Ser^{400} by as yet unknown kinase(s) (labeled as X in the figure) or through autophosphorylation at Ser^{62} while in complex with NF-κB1 (see also Figure 1A). The Thr^{290} phosphorylation is required for its release from p105 NF-κB1. Once liberated from the complex, Tpl2 is active towards MEK but unstable and undergoes proteolysis by the proteasome thus restricting the duration of MEK activation. MEK in turn phosphorylates ERK resulting in activation of various transcription factors that may negatively or positively influence transcription of pro-inflammatory genes. ERK also mediates the phosphorylation of other kinases, such as Msk1 which contributes to the activation of the transcription factors RelA (p65 NF-κB) and CREB by phosphorylating them at Ser276 and Ser133, respectively. In addition, ERK is responsible for the post-transcriptional regulation of TNF synthesis. Other pro-inflammatory cytokines, such as TNF and IL-1β activate Tpl2 also through the aforementioned IKKβ controlled NF-κB1 regulatory pathway.

suggesting that Tpl2 may operate in different tissues to regulate the inflammatory response [22]. Furthermore, in a mechanically-induced ischaemia–reperfusion injury model, *Tpl2*$^{-/-}$ tubular epithelial cells were more resistant to apoptosis indicating a role for Tpl2 in the determination of cellular death/survival ratio in an inflammatory microenvironment [23].

Further testimony to the pro-inflammatory role of Tpl2/Cot comes from studies of the atheroprotective apolipoprotein E (apoE). During inflammation, expression of apoE in macrophages is reduced leading to enhanced atheromatous plaque development. One of the molecular pathways involved in this outcome consists of the Tpl2-MEK-ERK cascade which transcriptionally represses *apoE* [24]. As atherogenesis is considered to entail both a lipid disorder and an inflammatory process, further studies will be required to define the physiological *in vivo* role of Tpl2 in atherosclerosis. *In vitro* studies also implicate Tpl2 in cytokine signaling in adipocytes, raising the possibility that it may contribute to adipose tissue dysfunction characteristic of obesity and diabetes [25].

However, in certain disease models Tpl2 deficiency exacerbates the inflammatory response. Thus, in a mouse model of ovalbumin-induced bronchoalveolar inflammation, *Tpl2* ablation leads to increase in IgE levels and severe asthma-like phenotype because of the Th2 polarization of the T cell response [18]. Therefore, the outcome of Tpl2 deficiency may depend on the specific type of immune response involved. Given that *Tpl2* ablation results in reduced production of the pro-inflammatory Th17 cytokine IL-23 in LPS-stimulated macrophages [4], it would be of interest to explore the role of Tpl2 in autoimmune diseases such as rheumatoid arthritis and systemic lupus erythematosus where Th17 cells play an important regulatory role.

2.4. The function of Tpl2 in cancer

Early studies identified the Tpl2 gene as target of provirus insertion in MoMuLV – induced T-cell lymphomas and MMTV – induced mammary adenocarcinomas [26,27]. In both cases, a C-terminus deletion occurred as a consequence of the provirus insertion in its last intron (Fig. 1).

Please cite this article in press as: M. Vougioukalaki et al., Tpl2 kinase signal transduction in inflammation and cancer, Cancer Lett. (2011), doi:10.1016/j.canlet.2011.02.004

A similarly altered *Tpl2* was described in a screen for transforming genes from a human thyroid carcinoma cell line [28]. Further studies showed that over-expression of truncated, C-terminus-deleted Tpl2 (Tpl2ΔC) associates with lymphomagenesis in mice [29] and cell cycle entry of T cells *in vitro* [30,31]. As the over-expression of wild-type Tpl2 did not exert similar oncogenic effects *in vivo*, it was proposed that Tpl2 is a proto-oncogene activated by C-terminal truncation [29].

Nevertheless, mutations in *Tpl2* are rarely observed in humans [32,33]. Our inspection of the Sanger Institute Catalogue of Somatic Mutations in Cancer (COSMIC) database (www.sanger.ac.uk/genetics/CGP/cosmic/) identified only 4 mutations among 489 tumor samples analysed (Fig. 1). Whilst elevated levels of Tpl2 have been reported in human gastric/colon adenocarcinomas [34], large granular T cell neoplasias [35], breast cancer [36,37] and Epstein–Barr virus (EBV)-related nasopharyngeal carcinoma and Hodgkin's disease [38], a detailed evaluation of *Tpl2* expression and function in human malignancy and normal tissue is still missing and the physiological role of Tpl2 in carcinogenesis remains enigmatic. Our inspection of transcriptome profiles registered in the Oncomine database (http://www.oncomine.org) reveals that Tpl2 (MAP3K8) mRNA levels are elevated in some and reduced in other cancer types (Table 2). Elevated Tpl2 expression and catalytic activity has been recently implicated in androgen depletion-independent prostate growth by constitutively engaging the MEK/ERK and NF-κB pathways [39]. In contrast, human melanomas carrying activating B-Raf mutations express reduced levels of Tpl2 [40]. Interestingly, the over-expression of Tpl2 as a result of copy number gains in melanoma cells carrying mutated B-Raf, associates with resistance to the Raf kinase inhibitor PLX4720 [40]. An RNA interference screening approach also identified Tpl2 as a regulator of apoptosis but showed that Tpl2 associates with sensitivity to TRAIL-induced cell death as the knock-down of Tpl2 decreased caspase-3 activation in human breast cancer cells [41]. Therefore, Tpl2 may impact on oncogenic events including the cellular response to therapy and immune control of cancer growth.

Tpl2 has also been studied in the context of virus-related malignancies. Thus, Tpl2 is activated by the viral product Tax in HTLV-provoked T-cell lymphomas [42] and by the oncogenic latent membrane protein-1 (LMP-1) of EBV [38] and functions as positive regulator of murine gammaherpesvirus 68 (MHV-68) lytic gene expression and replication [43].

Whereas the aforementioned studies indicate that Tpl2 may have a positive role in tumor growth, in some cases Tpl2 may function as tumor suppressor. Thus, $Tpl2^{-/-}$ mice bred onto an MHC Class I-restricted T-cell antigen receptor (TCR) transgenic background develop hyper responsiveness of CD8+ T lymphocytes and T-cell lymphomas because of defective induction of CTLA4, a negative regulator of T cell responses [44]. Furthermore, $Tpl2^{-/-}$ mice display increased incidence of skin tumors in a two-stage skin carcinogenesis model, which correlates with increased inflammation [45].

3. Tpl2-mediated signal transduction

3.1. Tpl2 is a potent kinase with broad range substrate specificity

Early studies aiming to define the biological role of Tpl2 revealed its wide range of substrate specificity. When over-expressed, Tpl2 as well as the oncogenic Tpl2ΔC mutant are able to engage a plethora of signaling pathways and to act in concert with other kinases and signaling molecules to influence cell survival and proliferation. The predominant pathway that is activated by ectopic expression of Tpl2 is the one leading to activation of ERK1 and ERK2 with MEK being its direct substrate [29,46]. However, Tpl2 can also stimulate the activation of JNK and to a lesser extent p38γ and ERK5 by directly phosphorylating their upstream kinases MKK4, MKK6 and MEK5, respectively [29,46] [47].

Tpl2 over-expression also triggers the activation of the transcription factors NFAT and NF-κB, potentiating TCR – mediated transcriptional responses. Thus, Tpl2 can lead to phosphorylation of NFATp through MEK, PKCζ and calcineurin-dependent mechanisms [31,48,49]. Moreover,

Table 2
Inspection of transcriptome profiles registered in the Oncomine database (http://www.oncomine.org) indicates that Tpl2 (MAP3K8) expression is differentially expressed in certain malignancies compared to normal tissue.

Cancer type	Sample no. tumor/normal	Fold change	Reference of transcriptome profile data
Classic meduloblastoma	46/4	3.733	[74]
Clear cell renal cell carcinoma	26/5	3.08	[75]
Gastric intestinal type adenocarcinoma	26/31	2.435	[76]
Testicular seminoma	16/20	2.247	[77]
Hereditary clear cell renal cell carcinoma	32/11	1.977	[78]
Hepatocellular carcinoma	101/74	1.572	[79]
Glioblastoma	84/3	−7.807	[80]
Burkitt's lymphoma	127/58	−6.335	[81]
Chronic lymphocytic leukemia	34/58	−2.949	
Lung adenocarcinoma	86/10	−3.723	[82]
T-cell acute lymphoblastic leukemia	11/6	−3.152	[83]
B-cell acute lymphoblastic leukemia	87/6	−2.942	
Acute myeloid leukemia	23/6	−1.947	
Lung adenocarcinoma	31/31	−3.038	[84]
Superficial bladder cancer	28/48	−2.449	[85]

Please cite this article in press as: M. Vougioukalaki et al., Tpl2 kinase signal transduction in inflammation and cancer, Cancer Lett. (2011), doi:10.1016/j.canlet.2011.02.004

ectopically expressed Tpl2 was found in a higher order complex containing NF-κB inducing kinase (NIK) and IκB kinase-α (IKKα) and proposed to directly activate NIK in T cells, leading to NF-κB activation [50].

Tpl2 has recently been implicated in the regulation of the transcription factors c-Fos and p53. Specifically, DNA damage induced by UVB has been reported to stimulate Tpl2 phosphorylation and activation causing its translocation to the nucleus. Nuclear Tpl2 phosphorylates histone H3 at Ser10 and induces *c-fos* transcriptional activation [51]. In cells stimulated with EGF, overexpressed Tpl2 mediates the interaction between Protein Phosphatase 2A and p53, thereby inhibiting the phosphorylation of p53 at Ser15 which is important for its stabilization and transcriptional activity [52]. These signaling properties are consistent with the functional role of Tpl2 in promoting cell proliferation and transformation. Whether these observations are of physiological relevance and the overexpression of Tpl2 observed in certain tumor types (see Table 2) suffices to activate these signaling pathways remains to be determined. This possibility is however supported by the reported link between naturally occurring high levels of Tpl2 expression and ERK phosphorylation in melanoma cell lines [52].

In comparison to wild-type Tpl2, expression of Tpl2ΔC associates with elevated catalytic activity and signaling capacity [29]. At least 3 mechanisms have been proposed to explain this phenomenon. First, the C-terminus deletion removes the intermolecular interaction between the C-terminal tail and the kinase domain of Tpl2, thus increasing its catalytic activity [29]. Second, the truncated protein lacks an amino-acid sequence ('degron'; aa 435–457) that targets wild-type Tpl2 for proteasomal degradation [53]. Finally, the C – terminus of Tpl2 is important for the efficient interaction with other proteins that regulate its stability and kinase activity. To date, such a regulatory role has been ascribed to p50 NF-κB precursor NF-κB1/p105, which functions to sequester Tpl2 from its substrates [54,55] (see below).

3.2. The physiological role of Tpl2 kinase in signal transduction

The phenotypic consequences of *Tpl2* ablation under acute or chronic inflammatory conditions have revealed an important physiological role for Tpl2 in ERK signaling downstream of a plethora of receptors involved in innate and adaptive immunity including TLRs, TNFR1, CD40 and the IL-1 receptor [1,8,9,11,19]. In addition to ERK, Tpl2 has been shown to contribute to JNK activation in TNF-stimulated MEFs by acting upstream of MKK4 kinase and to be required for NF-κB transactivation by mediating the Msk1 dependent phosphorylation of the RelA (p65) NF-κB subunit at Ser^{276} [9].

Tpl2 is activated upon triggering of Receptor Activator of Nuclear κB (RANK) in macrophages, contributing to ERK-mediated c-Fos and NFATc1 expression that stimulate RANKL- induced osteoclastogenesis [56]. Furthermore, proteinase-activated receptor 1 (PAR1) activates Tpl2 which engages a Rac1 and focal adhesion kinase (FAK)-dependent pathway to transduce ERK and JNK1 activation signals and to promote cell migration [57]. The intriguing finding that Tpl2 is activated upon PAR1 stimulation by proteinases produced by tumor cells raises the possibility that it may act downstream of other G-protein coupled receptors and broadens the reach of biological phenomena under Tpl2 control.

3.3. Regulation of Tpl2 activity through interaction with p105 NF-κB1 and ABIN2

Many aspects of Tpl2 signaling remain enigmatic. A major breakthrough in understanding the mechanism of Tpl2 regulation came from studies implicating the p50 precursor protein NF-κB1/p105 in Tpl2 stability [54,55]. In steady state conditions and irrespective of the cell type, the entire pool of Tpl2 associates with p105 [58]. NF-κB1 binds to and masks the degron sequence of Tpl2 preventing its proteasomal degradation. In the absence of this interaction, Tpl2 expression is thus attenuated. NF-κB1 also binds to the kinase domain of Tpl2 preventing access to MEK, the ERK kinase [54,55]. Indeed, in *nfkb1*$^{-/-}$ macrophages Tpl2 levels and TLR4 signaling to ERK, as well as CREB phosphorylation and COX-2 expression are diminished [54], similar to *Tpl2*$^{-/-}$ macrophages [2]. Therefore, NF-κB1-associated Tpl2 is stable but unable to phosphorylate MEK (Fig. 2).

The steps leading to Tpl2 activation have mostly been studied in the context of TLR4 signaling. An important aspect of Tpl2 activation is its interplay with upstream components of the NF-κB pathway, such as the IκB kinase β (IKKβ, also known as IKK2). Small molecule inhibitors and genetic studies in IKKβ-null fibroblasts have demonstrated that IKK activity is required for the activation of the Tpl2-ERK axis. This has been attributed to the IKKβ-mediated phosphorylation of p105 NF-κB1 at Ser^{927} and Ser^{932} which flags p105 for Lys^{48}-mediated poly-ubiquitination and proteasomal degradation. The stimulus-induced NF-κB1 proteolysis thus liberates Tpl2 from the p105 complex [59,60] (Fig. 2). The released Tpl2 is active towards MEK1 but unstable and is targeted for proteasome-mediated degradation, thus restricting prolonged activation of ERK signaling [54,61].

In addition to MEK, p105 NF-κB1 appears to be recipient of Tpl2 signals. Early studies demonstrated that overexpressed Tpl2 induces p105 proteolysis [58]. More recently, mutations in the Tpl2 catalytic loop which influence its p105 binding affinity were found to affect the rate of LPS-induced p105 degradation [61]. Indeed, Tpl2 in complex with p105 is catalytically active [61,62] and biochemical evidence suggests that it phosphorylates p105 NF-κB1 at a region distinct from that containing IKK phosphorylation sites [63]. The biological significance of this modification is still unclear but it is hypothesized that NF-κB1 may exert its inhibitory function on Tpl2 by also serving as competitive substrate [63]. These observations also raise the possibility that Tpl2 may phosphorylate additional substrates when complexed with NF-κB1. Identifying such Tpl2 targets is likely to broaden our understanding of Tpl2 function.

The Tpl2-p105 complex also associates with ABIN2 (A20 binding inhibitor of NFκB-2), an A20-interacting protein [64]. Studies in *tnip2*$^{-/-}$ (ABIN-2 null) mice showed that ABIN2 is important for stabilizing Tpl2 thereby influencing

Please cite this article in press as: M. Vougioukalaki et al., Tpl2 kinase signal transduction in inflammation and cancer, Cancer Lett. (2011), doi:10.1016/j.canlet.2011.02.004

ERK signals downstream of TLRs and cytokine receptors in hemopoietic cells [65]. Intriguingly, unlike *nfkb1*$^{-/-}$ cells where both ABIN2 and Tpl2 are absent, p105 NF-κB1 protein levels are normal in ABIN2 null mice [64]. The small amount of Tpl2 present in *tnip2*$^{-/-}$ cells can still be activated by LPS suggesting that ABIN2 is not however required for activation of Tpl2.

3.4. Regulation of Tpl2 activity through phosphorylation

Despite its essential role, IKKβ activation is *per se* insufficient to induce Tpl2 activity. As discussed above, the Tpl2 activation signals are stimulus and cell context specific. In contrast, a large number of pro-inflammatory stimuli or Pathogen-Associated Molecular Patterns (PAMP) activates the IKK/NF-κB pathway. It is thus conceivable that stimulation of the Tpl2 - ERK pathway requires engagement of additional signaling components. Several lines of biochemical evidence also support the requirement of multiple events that coordinate Tpl2 activation. For example, TNF-induced Tpl2 activation requires RIP1 and TRAF2 [9,66], adaptor molecules that link TNF receptor 1 to downstream signaling. However, despite the obligatory role of RIP1 kinase activity in TNF-induced ERK activation, it is dispensable for IKK/NF-κB signal transduction [67,68]. Moreover, whereas the over-expression of TRAF2 induces NF-κB signaling it does not suffice for Tpl2 and ERK activation [66].

Which additional signals are required to activate Tpl2 ? Similar to other MAP3 kinases, Tpl2 is subject to phosphorylation. Following LPS or IL-1 stimulation, Tpl2 is phosphorylated at Thr^{290}, Ser^{400} and Ser^{62} [11,62,69]. Phosphorylation at Thr^{290} and Ser^{400} are stimulus-induced and are necessary although not sufficient for Tpl2 activation, as evidenced by the fact that expression of phosphomimetic mutants T290D and S400E only partially restores LPS- induced ERK activation in *Tpl2*$^{-/-}$ macrophages [62,69]. It is therefore likely that coordination of these phosphorylation events, mediated by as yet unknown kinase(s), is necessary for full activation of Tpl2.

Both Thr^{290} and Ser^{400} phosphorylations take place prior to the dissociation of the catalytic subunit from NF-κB1/ABIN2. The phosphorylation at Thr^{290} is required for its release from p105 NF-κB1 and has been proposed to be mediated by IKKβ-dependent signals by some [69] but not other investigators [11]. Moreover, it has been suggested that Thr^{290} is autophosphorylated following LPS or IL-1 stimulation [6,70]. The way by which Ser^{400} phosphorylation contributes to kinase activation is still unclear. As this residue is within the C-terminus of Tpl2, its phosphorylation is proposed to induce a conformational change which releases the inhibitory intermolecular interaction between the C-terminal tail and the kinase domain of Tpl2 [62] (Fig. 1). Ser^{62} becomes autophosphorylated following IL-1 stimulation and has been suggested to contribute to maximal Tpl2 activation [11].

4. Concluding remarks

Tpl2 is a MAP3 kinase at the crossroad of various pro-inflammatory and oncogenic signals. Whilst the mechanism of its activation is still unclear, an interesting interplay with positive (IKKβ) and negative (p105) regulators of the NF-κB pathway emerges which may explain some of the stimulus and cell-specific effects of *Tpl2* ablation. It also generates important questions that are relevant to and bridge the NF-κB and MAPK research fields. With hindsight, it would be important to define the relative contribution of the Tpl2 – MEK – ERK axis to the pleiotropic phenotypic consequences of IKKβ ablation in inflammation and cancer [71] and to compare the functional outcomes of *Tpl2 vesrus nf-κb1* deficiency.

The identity of the kinases that mediate Tpl2 phosphorylation remains unknown and is an area of intense investigations. A src-like tyrosine kinase activity has been implicated in IL-1 [72] but not TNF-induced Tpl2 activation [66], suggesting the utilization of different kinases upstream of Tpl2 in a receptor-dependent manner. The complexity of Tpl2 kinase regulation is further highlighted by a recent study showing that the extracellular nutrient arginine positively regulates the LPS-mediated phosphorylation and activation of Tpl2 [70]. Identifying the mechanism underlying this effect may provide clues about the regulation of Tpl2.

The diverse and often contradictory *in vivo* effects of Tpl2 on immune cell function and carcinogenesis underscore the need to develop cell and tissue-specific knock-out mice to precisely dissect the influence of Tpl2 on immune responses and clarify the potential of targeting Tpl2 for the treatment of inflammatory diseases. Given the impact of chronic inflammation on cancer initiation and progression, it would also be of interest to establish the influence of Tpl2 on malignancies associated with deregulated immune function.

Conflicts of interest

None declared.

Acknowledgments

This work was supported by the European Commission research program *INFLA-CARE* (EC contract number 223151) to A.G.E.

References

[1] C.D. Dumitru, J.D. Ceci, C. Tsatsanis, D. Kontoyiannis, K. Stamatakis, J.H. Lin, C. Patriotis, N.A. Jenkins, N.G. Copeland, G. Kollias, P.N. Tsichlis, TNF-alpha induction by LPS is regulated posttranscriptionally via a Tpl2/ERK-dependent pathway, Cell 103 (2000) 1071–1083.
[2] A.G. Eliopoulos, C.D. Dumitru, C.-C. Wang, J. Cho, P.N. Tsichlis, Induction of COX-2 by LPS in macrophages is regulated by Tpl2-dependent CREB activation signals, EMBO J. 21 (2002) 4831–4840.
[3] J.P. Hall, Y. Kurdi, S. Hsu, J. Cuozzo, J. Liu, J.B. Telliez, K.J. Seidl, A. Winkler, Y. Hu, N. Green, G.R. Askew, S. Tam, J.D. Clark, L.L. Lin, Pharmacologic inhibition of Tpl2 blocks inflammatory responses in primary human monocytes, synoviocytes, and blood, J. Biol. Chem. 282 (2007) 33295–33304.
[4] K. Kakimoto, T. Musikacharoen, N. Chiba, K. Bandow, T. Ohnishi, T. Matsuguchi, Cot/Tpl2 regulates IL-23 p19 expression in LPS-stimulated macrophages through ERK activation, J. Physiol. Biochem. 66 (2010) 47–53.
[5] L.A. Mielke, K.L. Elkins, L. Wei, R. Starr, P.N. Tsichlis, J.J. O'Shea, W.T. Watford, Tumor progression locus 2 (Map3k8) is critical for host defense against Listeria monocytogenes and IL-1 beta production, J. Immunol. 183 (2009) 7984–7993.

[6] S. Rousseau, M. Papoutsopoulou, A. Symons, D. Cook, J.M. Lucocq, A.R. Prescott, A. O'Garra, S.C. Ley, P. Cohen, TPL2-mediated activation of ERK1 and ERK2 regulates the processing of pre-TNF alpha in LPS-stimulated macrophages, J. Cell Sci. 121 (2008) 149–154.
[7] N. Xiao, C. Eidenschenk, P. Krebs, K. Brandl, A.L. Blasius, Y. Xia, K. Khovananth, N.G. Smart, B. Beutler, The Tpl2 mutation Sluggish impairs type I IFN production and increases susceptibility to group B streptococcal disease, J. Immunol. 183 (2009) 7975–7983.
[8] A.G. Eliopoulos, C.C. Wang, C.D. Dumitru, P.N. Tsichlis, Tpl2 transduces CD40 and TNF signals that activate ERK and regulates IgE induction by CD40, Embo J. 22 (2003) 3855–3864.
[9] S. Das, J. Cho, I. Lambertz, M.A. Kelliher, A.G. Eliopoulos, K. Du, P.N. Tsichlis, Tpl2/cot signals activate ERK, JNK, and NF-kappaB in a cell-type and stimulus-specific manner, J. Biol. Chem. 280 (2005) 23748–23757.
[10] A. Banerjee, R. Gugasyan, M. McMahon, S. Gerondakis, Diverse Toll-like receptors utilize Tpl2 to activate extracellular signal-regulated kinase (ERK) in hemopoietic cells, Proc. Natl. Acad. Sci. USA 103 (2006) 3274–3279.
[11] M.J. Stafford, N.A. Morrice, M.W. Peggie, P. Cohen, Interleukin-1 stimulated activation of the COT catalytic subunit through the phosphorylation of Thr290 and Ser62, FEBS Lett. 580 (2006) 4010–4014.
[12] K. Cusack, H. Allen, A. Bischoff, A. Clabbers, R. Dixon, S. Fix-Stenzel, M. Friedman, Y. Gaumont, D. George, T. Gordon, P. Grongsaard, B. Janssen, Y. Jia, M. Moskey, C. Quinn, A. Salmeron, C. Thomas, G. Wallace, N. Wishart, Z. Yu, Identification of a selective thieno[2, 3-c]pyridine inhibitor of COT kinase and TNF-alpha production, Bioorg. Med. Chem. Lett. 19 (2009) 1722–1725.
[13] K. Sugimoto, M. Ohata, J. Miyoshi, H. Ishizaki, N. Tsuboi, A. Masuda, Y. Yoshikai, M. Takamoto, K. Sugane, S. Matsuo, Y. Shimada, T. Matsuguchi, A serine/threonine kinase, Cot/Tpl2, modulates bacterial DNA-induced IL-12 production and Th cell differentiation, J. Clin. Invest. 114 (2004) 857–866.
[14] F. Kaiser, D. Cook, S. Papoutsopoulou, R. Rajsbaum, X. Wu, H.T. Yang, S. Grant, P. Ricciardi-Castagnoli, P.N. Tsichlis, S.C. Ley, A. O'Garra, TPL-2 negatively regulates interferon-beta production in macrophages and myeloid dendritic cells, J. Exp. Med. 206 (2009) 1863–1871.
[15] V. Zacharioudaki, A. Androulidaki, A. Arranz, G. Vrentzos, A.N. Margioris, C. Tsatsanis, Adiponectin promotes endotoxin tolerance in macrophages by inducing IRAK-M expression, J. Immunol. 182 (2009) 6444–6451.
[16] A. Makris, C. Patriotis, S.E. Bear, P.N. Tsichlis, Structure of a Moloney murine leukemia virus–virus-like 30 recombinant: implications for transduction of the c-Ha-ras proto-oncogene, J. Virol. 67 (1993) 1286–1291.
[17] W.T. Watford, B.D. Hissong, L.R. Durant, H. Yamane, L.M. Muul, Y. Kanno, C.M. Tato, H.L. Ramos, A.E. Berger, L. Mielke, M. Pesu, B. Solomon, D.M. Frucht, W.E. Paul, A. Sher, D. Jankovic, P.N. Tsichlis, J.J. O'Shea, Tpl2 kinase regulates T cell interferon-gamma production and host resistance to Toxoplasma gondii, J. Exp. Med. 205 (2008) 2803–2812.
[18] W.T. Watford, C.C. Wang, C. Tsatsanis, L.A. Mielke, A.G. Eliopoulos, C. Daskalakis, N. Charles, S. Odom, J. Rivera, J. O'Shea, P.N. Tsichlis, Ablation of tumor progression locus 2 promotes a type 2 Th cell response in Ovalbumin-immunized mice, J. Immunol. 184 (2010) 105–113.
[19] A. Banerjee, R. Grumont, R. Gugasyan, C. White, A. Strasser, S. Gerondakis, NF-kappaB1 and c-Rel cooperate to promote the survival of TLR4-activated B cells by neutralizing Bim via distinct mechanisms, Blood 112 (2008) 5063–5073.
[20] D. Kontoyiannis, G. Boulougouris, M. Manoloukos, M. Armaka, M. Apostolaki, T. Pizarro, A. Kotlyarov, I. Forster, R. Flavell, M. Gaestel, P. Tsichlis, F. Cominelli, G. Kollias, Genetic dissection of the cellular pathways and signaling mechanisms in modeled tumor necrosis factor-induced Crohn's-like inflammatory bowel disease, J. Exp. Med. 196 (2002) 1563–1574.
[21] T. Ohnishi, A. Okamoto, K. Kakimoto, K. Bandow, N. Chiba, T. Matsuguchi, Involvement of Cot/Tp12 in bone loss during periodontitis, J. Dent. Res. 89 (2010) 192–197.
[22] G.J. Van Acker, G. Perides, E.R. Weiss, S. Das, P.N. Tsichlis, M.L. Steer, Tumor progression locus-2 is a critical regulator of pancreatic and lung inflammation during acute pancreatitis, J. Biol. Chem. 282 (2007) 22140–22149.
[23] T. Yaomura, N. Tsuboi, Y. Urahama, A. Hobo, K. Sugimoto, J. Miyoshi, T. Matsuguchi, K. Reiji, S. Matsuo, Y. Yuzawa, Serine/threonine kinase, Cot/Tpl2, regulates renal cell apoptosis in ischaemia/reperfusion injury, Nephrology (Carlton) 13 (2008) 397–404.
[24] A.V. Gafencu, M.R. Robciuc, E. Fuior, V.I. Zannis, D. Kardassis, M. Simionescu, Inflammatory signaling pathways regulating ApoE gene expression in macrophages, J. Biol. Chem. 282 (2007) 21776–21785.
[25] J. Jager, T. Gremeaux, T. Gonzalez, S. Bonnafous, C. Debard, M. Laville, H. Vidal, A. Tran, P. Gual, Y. Le Marchand-Brustel, M. Cormont, J.F. Tanti, Tpl2 kinase is upregulated in adipose tissue in obesity and may mediate interleukin-1beta and tumor necrosis factor-{alpha} effects on extracellular signal-regulated kinase activation and lipolysis, Diabetes 59 (2009) 61–70.
[26] C. Patriotis, A. Makris, S.E. Bear, P.N. Tsichlis, Tumor progression locus 2 (Tpl-2) encodes a protein kinase involved in the progression of rodent T-cell lymphomas and in T-cell activation, Proc. Natl. Acad. Sci. USA 90 (1993) 2251–2255.
[27] K.M. Erny, J. Peli, J.F. Lambert, V. Muller, H. Diggelmann, Involvement of the Tpl-2/cot oncogene in MMTV tumorigenesis, Oncogene 13 (1996) 2015–2020.
[28] J. Miyoshi, T. Higashi, H. Mukai, T. Ohuchi, T. Kakunaga, Structure and transforming potential of the human cot oncogene encoding a putative protein kinase, Mol. Cell Biol. 11 (1991) 4088–4096.
[29] J.D. Ceci, C.P. Patriotis, C. Tsatsanis, A.M. Makris, R. Kovatch, D.A. Swing, N.A. Jenkins, P.N. Tsichlis, N.G. Copeland, Tpl-2 is an oncogenic kinase that is activated by carboxy-terminal truncation, Genes Dev. 11 (1997) 688–700.
[30] A. Velasco-Sampayo, S. Alemany, P27kip protein levels and E2F activity are targets of Cot kinase during G1 phase progression in T cells, J. Immunol. 166 (2001) 6084–6090.
[31] C. Tsatsanis, C. Patriotis, P.N. Tsichlis, Tpl-2 induces IL-2 expression in T cell lines by triggering multiple signaling pathways that activate NFAT and NF-κB, Oncogene 17 (1998) 2609–2618.
[32] A.M. Clark, S.H. Reynolds, M. Anderson, J.S. Wiest, Mutational activation of the MAP3K8 protooncogene in lung cancer, Genes Chromosomes Canc. 41 (2004) 99–108.
[33] S. Shirali, R.A. Hamoudi, A. Bench, M. Scott, S.C. Ley, M.Q. Du, TPL-2 MEK kinase is not targeted by mutation in diffuse large B cell lymphoma and myeloid leukemia, Leuk. Res. 31 (2007) 1604–1607.
[34] R. Ohara, S. Hirota, H. Onoue, S. Nomura, Y. Kitamura, K. Toyoshima, Identification of the cells expressing COT proto-oncogene messenger RNA, J. Cell. Sci. 108 (1995) 97–103.
[35] A.V. Christoforidou, H.A. Papadaki, A.N. Margioris, G.D. Eliopoulos, C. Tsatsanis, Expression of the Tpl2/Cot oncogene in human T-cell neoplasias, Mol. Canc. 3 (2004) 34.
[36] G. Sourvinos, C. Tsatsanis, D.A. Spandidos, Over-expression of the Tpl-2/Cot oncogene in human breast cancer, Oncogene 18 (1999) 4968–4973.
[37] Z. Krcova, J. Ehrmann, V. Krejci, A. Eliopoulos, Z. Kolar, Tpl-2/Cot and COX-2 in breast cancer, Biomed. Pap. Med. Fac. Univ. Palacky Olomouc Czech Repub. 152 (2008) 21–25.
[38] A.G. Eliopoulos, C. Davies, S.S. Blake, P. Murray, S. Najafipour, P.N. Tsichlis, L.S. Young, The oncogenic protein kinase Tpl-2/Cot contributes to Epstein–Barr virus-encoded latent infection membrane protein 1-induced NF-kappaB signaling downstream of TRAF2, J. Virol. 76 (2002) 4567–4579.
[39] J.H. Jeong, A. Bhatia, Z. Toth, S. Oh, K.S. Inn, C.P. Liao, P. Roy-Burman, J. Melamed, G.A. Coetzee, J.U. Jung, TPL2/COT/MAP3K8 (TPL2) Activation Promotes Androgen Depletion-Independent (ADI) Prostate Cancer Growth, PLoS One 6 (2011) e16205.
[40] C.M. Johannessen, J.S. Boehm, S.Y. Kim, S.R. Thomas, L. Wardwell, L.A. Johnson, C.M. Emery, N. Stransky, A.P. Cogdill, J. Barretina, G. Caponigro, H. Hieronymus, R.R. Murray, K. Salehi-Ashtiani, D.E. Hill, M. Vidal, J.J. Zhao, X. Yang, O. Alkan, S. Kim, J.L. Harris, C.J. Wilson, V.E. Myer, P.M. Finan, D.E. Root, T.M. Roberts, T. Golub, K.T. Flaherty, R. Dummer, B.L. Weber, W.R. Sellers, R. Schlegel, J.A. Wargo, W.C. Hahn, L.A. Garraway, COT drives resistance to RAF inhibition through MAP kinase pathway reactivation, Nature 468 (2010) 968–972.
[41] D. Ovcharenko, K. Kelnar, C. Johnson, N. Leng, D. Brown, Genome-scale microRNA and small interfering RNA screens identify small RNA modulators of TRAIL-induced apoptosis pathway, Cancer Res. 67 (2007) 10782–10788.
[42] G. Babu, M. Waterfield, M. Chang, X. Wu, S.C. Sun, Deregulated activation of oncoprotein kinase Tpl2/Cot in HTLV-I-transformed T cells, J. Biol. Chem. 281 (2006) 14041–14047.
[43] X. Li, J. Feng, S. Chen, L. Peng, W.W. He, J. Qi, H. Deng, R. Sun, Tpl2/AP-1 enhances murine gammaherpesvirus 68 lytic replication, J. Virol. 84 (2009) 1881–1890.
[44] C. Tsatsanis, K. Vaporidi, V. Zacharioudaki, A. Androulidaki, Y. Sykulev, A.N. Margioris, P.N. Tsichlis, Tpl2 and ERK transduce antiproliferative T cell receptor signals and inhibit transformation of chronically stimulated T cells, Proc. Natl. Acad. Sci. USA 105 (2008) 2987–2992.

Please cite this article in press as: M. Vougioukalaki et al., Tpl2 kinase signal transduction in inflammation and cancer, Cancer Lett. (2011), doi:10.1016/j.canlet.2011.02.004

[45] K.L. Decicco-Skinner, E.L. Trovato, J.K. Simmons, P.K. Lepage, J.S. Wiest, Loss of tumor progression locus 2 (tpl2) enhances tumorigenesis and inflammation in two-stage skin carcinogenesis, Oncogene 30 (2011) 389–397.
[46] A. Salmeron, T.B. Ahmad, G.W. Carlile, D. Pappin, R.P. Narsimhan, S.C. Ley, Activation of MEK-1 and SEK-1 by Tpl-2 proto-oncoprotein, a novel MAP kinase kinase kinase, EMBO J. 15 (1996) 817–826.
[47] M. Chiariello, M.J. Marinissen, J.S. Gutkind, Multiple mitogen-activated protein kinase signaling pathways connect the cot oncoprotein to the c-jun promoter and to cellular transformation, Mol. Cell Biol. 20 (2000) 1747–1758.
[48] C. Tsatsanis, C. Patriotis, S.E. Bear, P.N. Tsichlis, The Tpl-2 protooncoprotein activates the nuclear factor of activated T cells and induces interleukin 2 expression in T cells, Proc. Natl. Acad. Sci. USA 95 (1998) 3827–3832.
[49] E. Gomez-Casero, B. San-Antonio, M.A. Iniguez, M. Fresno, Cot/Tpl2 and PKCzeta cooperate in the regulation of the transcriptional activity of NFATc2 through the phosphorylation of its amino-terminal domain, Cell Signal 19 (2007) 1652–1661.
[50] X. Lin, E.T. Cunningham, Y. Mu, R. Geleziunas, W.C. Greene, The proto-oncogene Cot kinase participates in CD3/CD28 induction of NF-κB acting through the NF-κB-inducing kinase and IκB kinases, Immunity 10 (1999) 271–280.
[51] H.S. Choi, B.S. Kang, J.H. Shim, Y.Y. Cho, B.Y. Choi, A.M. Bode, Z. Dong, Cot, a novel kinase of histone H3, induces cellular transformation through up-regulation of c-fos transcriptional activity, Faseb J. 22 (2008) 113–126.
[52] P. Khanal, K.Y. Lee, K.W. Kang, B.S. Kang, H.S. Choi, Tpl-2 kinase downregulates the activity of p53 and enhances signaling pathways leading to activation of activator protein 1 induced by EGF, Carcinogenesis 30 (2009) 682–689.
[53] M.L. Gandara, P. Lopez, R. Hernando, J.G. Castano, S. Alemany, The COOH-terminal domain of wild-type Cot regulates its stability and kinase specific activity, Mol. Cell Biol. 23 (2003) 7377–7390.
[54] M.R. Waterfield, M. Zhang, L.P. Norman, S.C. Sun, NF-kappaB1/p105 Regulates Lipopolysaccharide-Stimulated MAP Kinase Signaling by Governing the Stability and Function of the Tpl2 Kinase, Mol. Cell 11 (2003) 685–694.
[55] S. Beinke, J. Deka, V. Lang, M.P. Belich, P.A. Walker, S. Howell, S.J. Smerdon, S.J. Gamblin, S.C. Ley, NF-kappaB1 p105 negatively regulates TPL-2 MEK kinase activity, Mol. Cell Biol. 23 (2003) 4739–4752.
[56] K. Hirata, H. Taki, K. Shinoda, H. Hounoki, T. Miyahara, K. Tobe, H. Ogawa, H. Mori, and E. Sugiyama, Inhibition of tumor progression locus 2 protein kinase suppresses receptor activator of nuclear factor-kappaB ligand-induced osteoclastogenesis through down-regulation of the c-Fos and nuclear factor of activated T cells c1 genes. Biol. Pharm. Bull. vol. 33, pp. 133–137.
[57] M. Hatziapostolou, C. Polytarchou, D. Panutsopulos, L. Covic, P.N. Tsichlis, Proteinase-activated receptor-1-triggered activation of tumor progression locus-2 promotes actin cytoskeleton reorganization and cell migration, Cancer Res. 68 (2008) 1851–1861.
[58] M.P. Belich, A. Salmeron, L.H. Johnston, S.C. Ley, Tpl-2 kinase regulates the proteolysis of the NF-κB-inhibitory protein NF-κB1 p105, Nature 397 (1999) 363–368.
[59] S. Beinke, M.J. Robinson, M. Hugunin, S.C. Ley, Lipopolysaccharide activation of the TPL-2/MEK/extracellular signal-regulated kinase mitogen-activated protein kinase cascade is regulated by IkappaB kinase-induced proteolysis of NF-kappaB1 p105, Mol. Cell Biol. 24 (2004) 9658–9667.
[60] M. Waterfield, W. Jin, W. Reiley, M. Zhang, S.C. Sun, IkappaB kinase is an essential component of the Tpl2 signaling pathway, Mol. Cell Biol. 24 (2004) 6040–6048.
[61] J. Cho, P.N. Tsichlis, Phosphorylation at Thr-290 regulates Tpl2 binding to NF-kappaB1/p105 and Tpl2 activation and degradation by lipopolysaccharide, Proc. Natl. Acad. Sci. USA 102 (2005) 2350–2355.
[62] M.J. Robinson, S. Beinke, A. Kouroumalis, P.N. Tsichlis, S.C. Ley, Phosphorylation of TPL-2 on serine 400 is essential for lipopolysaccharide activation of extracellular signal-regulated kinase in macrophages, Mol. Cell Biol. 27 (2007) 7355–7364.
[63] G.R. Babu, W. Jin, L. Norman, M. Waterfield, M. Chang, X. Wu, M. Zhang, S.C. Sun, Phosphorylation of NF-kappaB1/p105 by oncoprotein kinase Tpl2: implications for a novel mechanism of Tpl2 regulation, Biochim. Biophys. Acta 1763 (2006) 174–181.
[64] V. Lang, A. Symons, S.J. Watton, J. Janzen, Y. Soneji, S. Beinke, S. Howell, S.C. Ley, ABIN-2 forms a ternary complex with TPL-2 and NF-kappa B1 p105 and is essential for TPL-2 protein stability, Mol. Cell Biol. 24 (2004) 5235–5248.
[65] S. Papoutsopoulou, A. Symons, T. Tharmalingham, M.P. Belich, F. Kaiser, D. Kioussis, A. O'Garra, V. Tybulewicz, S.C. Ley, ABIN-2 is required for optimal activation of Erk MAP kinase in innate immune responses, Nat. Immunol. 7 (2006) 606–615.
[66] A.G. Eliopoulos, S. Das, P.N. Tsichlis, The tyrosine kinase Syk regulates TPL2 activation signals, J. Biol. Chem. 281 (2006) 1371–1380.
[67] A. Devin, Y. Lin, Z.G. Liu, The role of the death-domain kinase RIP in tumour-necrosis-factor-induced activation of mitogen-activated protein kinases, EMBO Rep. 4 (2003) 623–627.
[68] A. Devin, A. Cook, Y. Lin, Y. Rodriguez, M. Kelliher, Z. Liu, The distinct roles of TRAF2 and RIP in IKK activation by TNF-R1: TRAF2 recruits IKK to TNF-R1 while RIP mediates IKK activation, Immunity 12 (2000) 419–429.
[69] J. Cho, M. Melnick, G.P. Solidakis, P.N. Tsichlis, Tpl2 (tumor progression locus 2) phosphorylation at Thr290 is induced by lipopolysaccharide via an Ikappa-B Kinase-beta-dependent pathway and is required for Tpl2 activation by external signals, J. Biol. Chem. 280 (2005) 20442–20448.
[70] V. Mieulet, L. Yan, C. Choisy, K. Sully, J. Procter, A. Kouroumalis, S. Krywawych, M. Pende, S.C. Ley, C. Moinard, R.F. Lamb, TPL-2-mediated activation of MAPK downstream of TLR4 signaling is coupled to arginine availability, Sci. Signal 3 (2010) ra61.
[71] H. Hacker, M. Karin, Regulation and function of IKK and IKK-related kinases, Sci. STKE 2006 (2006) 13.
[72] C. Rodriguez, M. Pozo, E. Nieto, M. Fernandez, S. Alemany, TRAF6 and Src kinase activity regulates Cot activation by IL-1, Cell Signal 18 (2006) 1376–1385.
[73] T.M. Black, C.L. Andrews, G. Kilili, M. Ivan, P.N. Tsichlis, P. Vouros, Characterization of phosphorylation sites on Tpl2 using IMAC enrichment and a linear ion trap mass spectrometer, J. Proteome. Res. 6 (2007) 2269–2276.
[74] S.L. Pomeroy, P. Tamayo, M. Gaasenbeek, L.M. Sturla, M. Angelo, M.E. McLaughlin, J.Y. Kim, L.C. Goumnerova, P.M. Black, C. Lau, J.C. Allen, D. Zagzag, J.M. Olson, T. Curran, C. Wetmore, J.A. Biegel, T. Poggio, S. Mukherjee, R. Rifkin, A. Califano, G. Stolovitzky, D.N. Louis, J.P. Mesirov, E.S. Lander, T.R. Golub, Prediction of central nervous system embryonal tumour outcome based on gene expression, Nature 415 (2002) 436–442.
[75] M.V. Yusenko, R.P. Kuiper, T. Boethe, B. Ljungberg, A.G. van Kessel, G. Kovacs, High-resolution DNA copy number and gene expression analyses distinguish chromophobe renal cell carcinomas and renal oncocytomas, BMC Cancer 9 (2009) 152.
[76] M. D'Errico, E. de Rinaldis, M.F. Blasi, V. Viti, M. Falchetti, A. Calcagnile, F. Sera, C. Saieva, L. Ottini, D. Palli, F. Palombo, A. Giuliani, E. Dogliotti, Genome-wide expression profile of sporadic gastric cancers with microsatellite instability, Eur. J. Cancer 45 (2009) 461–469.
[77] J.M. Sperger, X. Chen, J.S. Draper, J.E. Antosiewicz, C.H. Chon, S.B. Jones, J.D. Brooks, P.W. Andrews, P.O. Brown, J.A. Thomson, Gene expression patterns in human embryonic stem cells and human pluripotent germ cell tumors, Proc. Natl. Acad. Sci. USA 100 (2003) 13350–13355.
[78] R. Beroukhim, J.P. Brunet, A. Di Napoli, K.D. Mertz, A. Seeley, M.M. Pires, D. Linhart, R.A. Worrell, H. Moch, M.A. Rubin, W.R. Sellers, M. Meyerson, W.M. Linehan, W.G. Kaelin, Jr., S. Signoretti, Patterns of gene expression and copy-number alterations in von-hippel lindau disease-associated and sporadic clear cell carcinoma of the kidney, Cancer Res. 69 (2009) 4674–4681.
[79] X. Chen, S.T. Cheung, S. So, S.T. Fan, C. Barry, J. Higgins, K.M. Lai, J. Ji, S. Dudoit, I.O. Ng, M. Van De Rijn, D. Botstein, P.O. Brown, Gene expression patterns in human liver cancers, Mol. Biol. Cell 13 (2002) 1929–1939.
[80] J. Lee, S. Kotliarova, Y. Kotliarov, A. Li, Q. Su, N.M. Donin, S. Pastorino, B.W. Purow, N. Christopher, W. Zhang, J.K. Park, H.A. Fine, Tumor stem cells derived from glioblastomas cultured in bFGF and EGF more closely mirror the phenotype and genotype of primary tumors than do serum-cultured cell lines, Cancer Cell 9 (2006) 391–403.
[81] K. Basso, A.A. Margolin, G. Stolovitzky, U. Klein, R. Dalla-Favera, A. Califano, Reverse engineering of regulatory networks in human B cells, Nat. Genet. 37 (2005) 382–390.
[82] D.G. Beer, S.L. Kardia, C.C. Huang, T.J. Giordano, A.M. Levin, D.E. Misek, L. Lin, G. Chen, T.G. Gharib, D.G. Thomas, M.L. Lizyness, R. Kuick, S. Hayasaka, J.M. Taylor, M.D. Iannettoni, M.B. Orringer, S. Hanash, Gene-expression profiles predict survival of patients with lung adenocarcinoma, Nat. Med. 8 (2002) 816–824.
[83] K.C. Anderson, R.A. Kyle, S.V. Rajkumar, A.K. Stewart, D. Weber, P. Richardson, A.F.P.o.C.E.i.M. Myeloma, Clinically relevant end points and new drug approvals for myeloma, Leukemia 22 (2008) 231–239.

Please cite this article in press as: M. Vougioukalaki et al., Tpl2 kinase signal transduction in inflammation and cancer, Cancer Lett. (2011), doi:10.1016/j.canlet.2011.02.004

[84] L.J. Su, C.W. Chang, Y.C. Wu, K.C. Chen, C.J. Lin, S.C. Liang, C.H. Lin, J. Whang-Peng, S.L. Hsu, C.H. Chen, C.Y. Huang, Selection of DDX5 as a novel internal control for Q-RT-PCR from microarray data using a block bootstrap re-sampling scheme, BMC Genomics 8 (2007) 140.

[85] M. Sanchez-Carbayo, N.D. Socci, J. Lozano, F. Saint, C. Cordon-Cardo, Defining molecular profiles of poor outcome in patients with invasive bladder cancer using oligonucleotide microarrays, J. Clin. Oncol. 24 (2006) 778–789.

Please cite this article in press as: M. Vougioukalaki et al., Tpl2 kinase signal transduction in inflammation and cancer, Cancer Lett. (2011), doi:10.1016/j.canlet.2011.02.004